USGS
science for a changing world

Quaternary Magmatism in the Cascades—Geologic Perspectives

Professional Paper 1744

U.S. Department of the Interior
U.S. Geological Survey

This page intentionally left blank

Quaternary Magmatism in the Cascades—Geologic Perspectives

By Wes Hildreth

Professional Paper 1744

U.S. Department of the Interior
U.S. Geological Survey

U.S. Department of the Interior
DIRK KEMPTHORNE, Secretary

U.S. Geological Survey
Mark D. Myers, Director

U.S. Geological Survey, Reston, Virginia 2007

This report and any updates to it are available online at:
http://pubs.usgs.gov/pp/pp1744/

For product and ordering information:
World Wide Web: http://www.usgs.gov/pubprod
Telephone: 1-888-ASK-USGS

For more information on the USGS—the Federal source for science about the Earth,
its natural and living resources, natural hazards, and the environment:
World Wide Web: http://www.usgs.gov
Telephone: 1-888-ASK-USGS

Cataloging-in-publication data are on file with the Library of Congress (http://www.loc.gov/).

Produced in the Western Region, Menlo Park, California
Manuscript approved for publication, July 19, 2007
Text edited by James W. Hendley II
Layout and design by Judy Weathers

Cover—Distributed arc volcanoes in the Cascades of central Oregon. At least 23 separate vents are discernible in this southwestward view from low on the southern slope of South Sister. Vent belt in this continuous reach of the north-south arc is about 40 km wide, east to west. The numerous small volcanoes here consist predominantly of basaltic andesite, but many are basaltic, a few are dacitic, and (in contrast to most of the arc) several dozen are rhyolitic. In foreground, Rock Mesa rhyolite coulee and an adjacent rhyolite dome, both about 2,200 years old, each contain 73.5 percent SiO_2. Partly bare cone just beyond the rhyolite flow is early postglacial LeConte Crater, a scoria cone at the source of an extensive apron of mafic lava flows (54.5% SiO_2). The Cascade arc includes more than 2,300 Quaternary volcanoes, at least 2,050 of them independent but fewer than 30 of them the andesite-dacite or mafic stratovolcanoes conventionally thought to represent the arc. (Photograph by author taken in July 2001.

Frontispiece—Burney Mountain, 37 km north-northwest of Lassen Peak, is by far the largest of ~340 Quaternary lava domes recognized in the Cascades. The middle Pleistocene composite dacite dome has a volume of ~9 km^3, which is more than three times as large as Lassen Peak or (Shasta) Black Butte (each ~2.5 km^3) and exceeds the amount of dacite erupted from such andesite-dacite stratovolcanoes as Mount Adams or Mount Baker. Along with 110 shield volcanoes and ~1,850 monogenetic (mostly mafic) vents, individual lava domes greatly outnumber the 30-odd Quaternary stratovolcanoes and major silicic complexes in the Cascades. Relief visible in the image is ~850 m. (Photograph by L.J.P. Muffler, taken in May 1981 from near the summit of Doyle Butte, 4 km northeast of the summit of Burney Mountain.)

Foreword

The Cascade magmatic arc is a belt of Quaternary volcanoes that extends 1,250 km from Lassen Peak in northern California to Meager Mountain in Canada, above the subduction zone where the Juan de Fuca Plate plunges beneath the North American Plate. This Professional Paper presents a synthesis of the entire volcanic arc, addressing all 2,300 known Quaternary volcanoes, not just the 30 or so visually prominent peaks that comprise the volcanic skyline.

Study of Cascade volcanoes goes back to the geological explorers of the late 19th century and the seminal investigations of Howel Williams in the 1920s and 1930s. However, major progress and application of modern scientific methods and instrumentation began only in the 1970s with the advent of systematic geological, geophysical, and geochemical studies of the entire arc. Initial stimulus from the USGS Geothermal Research Program was enhanced by the USGS Volcano Hazards Program following the 1980 eruption of Mount St. Helens. Together, these two USGS Programs have provided more than three decades of stable funding, staffing, and analytical support. This Professional Paper summarizes the resultant USGS data sets and integrates them with the parallel contributions of other investigators. The product is based upon an all-encompassing and definitive geological database, including chemical and isotopic analyses to characterize the rocks and geochronology to provide the critical time constraints.

Until now, this massive amount of data has not been summarized, and a systematic and uniform interpretation firmly grounded in geological fact has been lacking. Herein lies the primary utility of this Cascade volume. It not only will be the mandatory starting point for new workers, but also will provide essential geological context to broaden the perspectives of current investigators of specific Cascade volcanoes.

Wes Hildreth's insightful understanding of volcanic processes and his uncompromising scientific integrity make him uniquely qualified to present this synthesis. During more than three decades of volcanological studies, he has carried out comprehensive investigations of Mount Adams, Mount Baker, the Three Sisters, and the Simcoe Mountains Volcanic Field. He also brings a broad experience in other volcanic arcs, having conducted integrated field and laboratory investigations at several major volcanic centers in the Andes and the Aleutian arcs. His expertise and perspective have been further enhanced by in-depth petrologic studies of caldera environments, primarily in Long Valley, California, and Yellowstone. On the basis of all these field and laboratory investigations and exhaustive literature searches, he has published three definitive petrologic syntheses addressing the passage and transformation of basaltic magmas from their mantle sources through the crust to form the many types of volcanic manifestations at the Earth's surface.

A major strength of this Professional Paper is that it adheres to data first and foremost, and only then correlates these data with relevant theories. Petrological and geophysical interpretation is left to the later sections of the volume, and even there is never allowed to stray from the pertinent databases. Hildreth's interpretations are not just idle speculations, but are carefully reasoned inferences firmly based on his thorough evaluation of the observational geological data.

Professional Paper 1744 should not be skimmed lightly, in the hope that the salient points will quickly rub off. Instead, every section, indeed every paragraph, presents scholarly observations and insightful interpretations that demand careful and thoughtful study. This volume will influence and guide the course of Cascade investigations for decades to come.

Patrick Muffler
Western Regional Geologist, retired

Contents

Figures

Tables

Quaternary Magmatism in the Cascades—Geologic Perspectives

By Wes Hildreth

Introduction

The geologic view of Cascade magmatism presented here is meant to complement flourishing geochemical and geophysical investigations of convergent-margin processes. Advances in understanding the behavior of arc volcanoes and the tectonic, thermal, and petrologic processes that contribute to arc magmatism have been substantial. Geophysical and geochemical models have clarified much (Gill, 1981; Takahashi, 1986; Jarrard, 1986; Hildreth and Moorbath, 1988; Tatsumi, 1991; Peacock, 1991, 1996, 2003; Davies and Stephenson, 1992; Gill and Condomines, 1992; Woodhead and others, 1993; Pearce and Parkinson, 1993; Stolper and Newman, 1994; Zhao and others, 1994; Kay and Kay, 1994; Pearce and Peate, 1995; Kirby and others, 1996; Luhr, 1997; Plank and Langmuir, 1998; Sisson and Bronto, 1998; Schmidt and Poli, 1998; Grove and others, 2002; Hacker and others, 2003; Hildreth, Fierstein, and others, 2004), but the geophysical insights are limited by heterogeneities on all scales at inaccessible depths, and the geochemical insights are blurred by polybaric fractionation, reaction during ascent, and mixing of magmatic contributions from varied source rocks that partially melt at many depths.

Geologic input has been comparatively neglected. One still encounters, for example, convergent-margin models in which a magmatic arc is rendered as one or two single-file chains of evenly spaced stratovolcanoes. The distribution, storage, ascent, and eruption of arc magmas are, of course, much more complex, resulting in an awesome variety of compositions and regional patterns—widely disregarded in modeling. Such patterns provide information about the spatial availability of sub-arc magma, its occasional concentration in large chambers, and the relative penetrability by magma of geologically contrasting segments of the arc crust. Providing reliable data, however, for all the volcanoes in a chosen time interval, outlining their distribution, their compositional ranges and affinities, and the time-volume-compositional evolution of each center, requires authentic geologic mapping, petrography and petrochemistry, and integration of map-based stratigraphy with detailed geochronology—all of which are labor-intensive and time-consuming. Recent advances along these lines in the Cascade arc, stimulated principally by the U.S. Geological Survey (USGS) Volcano Hazards and Geothermal Research Programs, make possible this progress report and analysis. Opportunities now exist to treat the time-space distribution of eruptive centers more systematically, to examine how such data clarify or delimit the nature of sub-arc processes, and to integrate such information into better geophysical-geochemical models of arc magmatism.

The subject transcends the academic. Volcanic chains on populous continental margins are of growing importance, economically and existentially, to expanding civilizations. In the Cascades (fig. 1), no fewer than 12 U.S. volcanic centers (Lassen, Shasta, Medicine Lake, Mazama, South Sister, Newberry, Hood, Adams, St. Helens, Rainier, Glacier Peak, and Baker) are rated as “high threat” or “very high threat” volcanoes in the framework for a National Volcano Early Warning System (Ewert and others, 2005), and the three large Canadian centers (Garibaldi, Cayley, and Meager) should be as well.

I first give an explanation of methodology and terminology and then provide a north-to-south summary of what is known of the eruptive history and vent distribution of Cascade volcanoes. These basic data are then discussed from the points of view of vent-distribution patterns, volumetric eruption rates, parental and derivative magmas, and the tectonic framework that modulates the magmatism.

Terminology and Limitations

The Cascade magmatic arc includes more than 2,300 Quaternary volcanoes (table 1). Amplification of this observation at the outset serves to introduce the conventions and definitions adopted in this paper. “Volcanoes” are simply sites of emission of volcanic products (and the distinction between independent and redundant vents is addressed below). Nearly all Cascadian volcanoes are magmatic or phreatomagmatic, and most constructed positive landforms (cones, rings, shields, domes) around their vents. Fewer than 30 of the 2,300 are the high peaks (mostly andesite-dacite or mafic stratovolcanoes) that provide the popular image of the Cascades. Most mafic magmas, however, which tend to retain more information about subcrustal or deep-crustal processes, produce small shields or scoria cones that are independent of the large centers and are far more numerous.

Owing to the emphasis placed here on volcano distribution, analysis is limited (by and large) to the last million years. The Cascade arc has been magmatically active since the

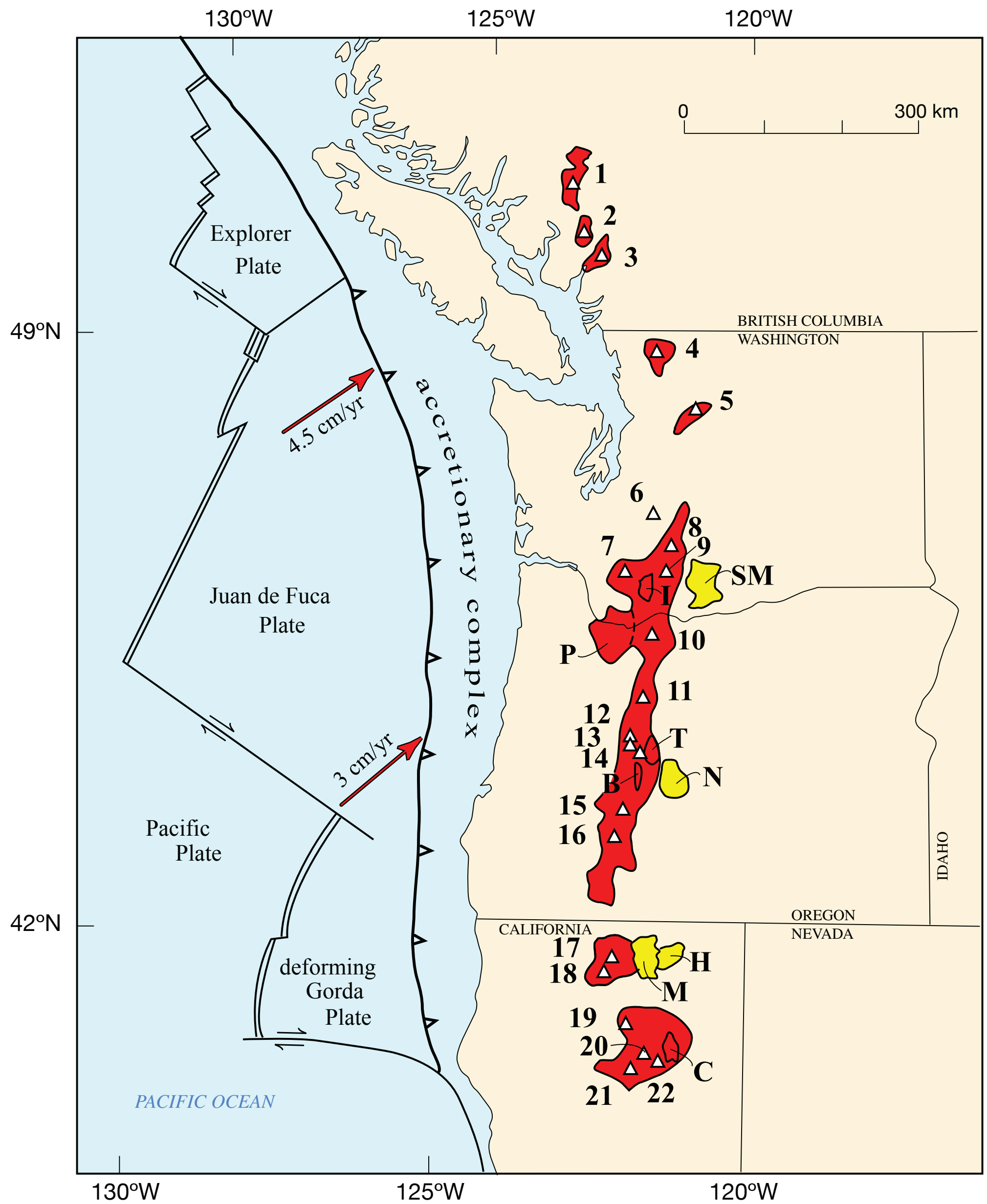

Figure 1. Quaternary Cascades volcanic arc. Red areas encompass more than 2,300 vents for more than 2,000 independent volcanoes of Quaternary age, as elaborated in figures 3, 8, 14, 15, and 21 and discussed in the text. Despite continuity of subduction beneath the 1,250-km-long arc, the several gaps in the vent belt are real, containing no or few Quaternary volcanoes. Compositionally evolved major centers are indicated by numbered triangles: **1**, Mount Meager; **2**, Mount Cayley; **3**, Mount Garibaldi; **4**, Mount Baker; **5**, Glacier Peak; **6**, Mount Rainier; **7**, Mount St. Helens; **8**, Goat Rocks; **9**, Mount Adams; **10**, Mount Hood; **11**, Mount Jefferson; **12**, Middle Sister; **13**, South Sister; **14**, Broken Top; **15**, Cappy Mountain; **16**, Mount Mazama (Crater Lake); **17**, Rainbow Mountain; **18**, Mount Shasta; **19**, Snow Mountain; **20**, Lassen volcanic center; **21**, Maidu volcanic center; and **22**, Dittmar volcanic center. Within the arc vent belt, five distributed volcanic fields are enclosed and indicated from north to south as follows: **I**, Indian Heaven; **P**, Portland (Boring); **T**, Tumalo; **B**, Bachelor chain; and **C**, Caribou. Vent zones for four extensive rear-arc volcanic fields just east of the Cascades are enclosed and identified as follows: **SM**, Simcoe Mountains; **N**, Newberry; **M**, Medicine Lake; and **H**, Hackamore. Mafic stratocones, including such large ones as North Sister, Diamond Peak, Mount Thielsen, and Mount McLoughlin, are shown on figures 14 and 15, not here. Red arrows offshore indicate (latitudinally varied) plate-convergence rate.

Eocene, but documentation of pre-Quaternary volcanic vents is far from complete. Many Tertiary vents are recognized (Luedke and others, 1983; Smith, 1993; Sherrod and Smith, 2000), but owing to erosion and burial, most are not. Restricting consideration to the Quaternary assures that most vents are accounted for and avoids unresolved questions about secular migration of the arc. The beginning of the Quaternary is variously placed at 1.65, 1.8, or 2.6 Ma (Richmond and Fullerton, 1985; Morrison and Kukla, 1998; Ogg, 2004; Pillans, 2004), and the boundaries between early, middle, and late Pleistocene are now generally agreed to be ~780 ka and ~126 ka (Gradstein and others, 2004). As a practical matter, most Quaternary vents recognized in the Cascades (table 1) are younger than ~1 Ma, ranging from perhaps 75 percent of those in California to >90 percent in Washington and British Columbia. Delineation and dating of Quaternary volcanoes older than 1 Ma is incomplete (owing to erosion and burial) and latitudinally very uneven (owing to progressively more severe glacial erosion northward).

Quaternary volcanoes of the “Cascade magmatic arc” are distributed from southwestern British Columbia to northern California (50.9° to 40.3°N), specifically from ~30 km north of Mount Meager to ~25 km south of Lassen Peak (fig. 1). The Garibaldi Volcanic Belt (Mount Meager to Glacier Peak) is thus included, but the sketchily known Franklin Glacier and Silverthrone volcanic fields (Green and others, 1988), far to the northwest and ambiguous in their affinity, are not.

Treated somewhat separately in this analysis are three major rear-arc complexes adjacent to but inboard of the north-south arc belt (fig. 1). Each of these is a “central volcano” in the sense of Walker (1993), characterized by a large mafic shield, a central rhyolite complex, and a peripheral field of hundreds of (compositionally varied) monogenetic vents, many of them independent of the centered magma-supply system. These are the Simcoe Mountains Volcanic Field, partly Pliocene but overlapped by a Quaternary field of monogenetic intraplate alkali-basalt scoria cones and shields (Uto and others, 1991; Hildreth and Fierstein, work in progress), and the Newberry and Medicine Lake Volcanic Fields, each centered on a great mafic shield-form edifice in the transition between the Cascade arc and the Basin and Range Province, and each marked by a caldera, numerous peripheral vents, and abundant low-K tholeiitic basalt.

The Quaternary Cascade arc extends 1,250 km north-south, and its belt of vents ranges in width from less than 25 km to more than 100 km. Elevation of the pre-Quaternary basement beneath the volcanic chain (which commonly forms drainage divides and provides interior rainshadows) ranges from 1,200 to 1,500 m in much of Oregon to more than 2,000 m in northern Washington. Among the major cones, a dozen exceed 3,000 m in elevation but only Rainier and Shasta exceed 4,000 m.

Arc plutons are a fundamental component of any magmatic arc, but only one pluton of Quaternary age is so far exposed in the Cascades (Hildreth and others, 2003). Nevertheless, many are likely to be at various stages of growth and consolidation, so I present below inferences relevant to Quaternary intracrustal magmatic processes, drawn in part from Cascade plutons of Tertiary age and from Quaternary granitoid ejecta brought up in explosive eruptions.

Not synonymous with the Cascade magmatic arc, the “Cascade Range” is the mountainous physiographic province limited by convention to the United States. It is a composite terrain that, in addition to constructional topography provided unevenly by Quaternary volcanoes, consists of rugged topography cut on Mesozoic or Tertiary batholiths and on Mesozoic and older metamorphic rocks, as well as on Tertiary volcanic-arc assemblages.

Volcanic-rock nomenclature in this paper is kept simple, principally based on SiO_2 contents—basalt has 47-52%, basaltic andesite 52-57%, andesite 57-63%, dacite 63-68%, rhyodacite 68-72%, and rhyolite >72% SiO_2. For reasons of convenience or uncertainty, I commonly use the terms “mafic” to lump basaltic andesite with basalt, “intermediate” for andesite-dacite, and “silicic” to cover the range of rhyodacite and rhyolite. Compositional varieties of Cascade basalt are discussed in a later section, but the acronym “HAOT” (Hart and others, 1984) will be used repeatedly for MORB-like low-potassium high-alumina olivine tholeiite, which has fed many low-viscosity lava flows within the Cascades from Washington to Lassen as well as more widely in the adjoining Basin and Range Province. I employ the simple term “arc basalt” for the common calcalkaline to weakly tholeiitic basalts that carry the familiar geochemical signature of slab-derived contributions (the “subduction component”); and I use the term“intraplate basalt” for those carrying the so-called OIB trace-element pattern—not uncommon in parts of the Cascades but typically mildly alkalic where found there.

Volcanoes and Vents

Ambiguities arise in counting volcanoes (table 1). Some eruptions issue from more than one vent, as when a chain of domes or cinder cones is fed concurrently by a single dike system. Other eruptions issue from flank vents of large cones and shields, representing lateral breakouts of magma from a central conduit system that intermittently feeds a main summit vent. Should domes, flows, and conelets erupted from such flank vents or along fissure alignments be counted as separate volcanoes? Ideally, probably not, if the aim (as here) is to delineate the extent and variety of magma available beneath the region. Without detailed study, however, there may be little justification for assuming that adjacent or aligned volcanoes erupted concurrently or are magmatically related (Conway and others, 1997). Documented examples in the Cascades are surprisingly few (for example, Scott, 1987; Gardner, 1994; Muffler and others, 1994; Hildreth and Fierstein, 1995). Moreover, the notion of so-called “parasitic” flank vents has been overextended and widely misapplied (Hildreth and Lanphere, 1994). Cinder cones peripheral to arc shields and stratocones typically exhibit compositional contrasts, usually less evolved, and most of them probably have independent conduits from the deep crust or mantle. This is in noteworthy contrast to large oceanic shields, where many flank vents are indeed fed laterally by dikes issuing from a central conduit system (for example, Eaton and Murata, 1960; Dieterich, 1988; Chadwick and Howard, 1991).

More troublesome sources of error in reckoning the number and distribution of Quaternary volcanoes are concealment by younger lavas and obliteration by glacial erosion (which increases in severity northward along the arc). At Mount Adams, for example, at least 30 vents for discrete units of mafic lava (cropping out around the periphery) are covered either by till or, in greater measure, by an apron of andesitic lava flows that extends as far as 17 km radially from the stratocone's summit (Hildreth and Fierstein, 1995). Likewise, mapping of the Mount Bachelor volcanic chain (Scott and Gardner, 1992; Gardner, 1994) illustrated that, for mafic shield alignments as well, many independent vents can be wholly buried by compositionally distinguishable products of nearby vents that may be only thousands or hundreds of years younger. Recent mapping of the glaciated district around Mount Baker raised the number of recognized Quaternary vents from 4 to 25, but mapping of ~110 dikes suggests that there had been many more (Hildreth and others, 2003). Owing to the climatic gradient along the arc, a middle Quaternary lava-cone that would be colluvium-mantled but largely intact in California might be sculpted to ridgecrest remnants in Oregon and glacially reduced to a plug or dikes in northern Washington or British Columbia (fig. 2).

Along-arc comparability of the vent-distribution data summarized in table 1 thus requires identification of eroded vent remnants, judicious counting of concealed vents for plausibly independent eruptive units, and consistency in dealing with the vent-redundancy problems. Available data are too uneven regionally to discriminate redundancy with adequate consistency, so table 1 simply records all known Quaternary vents, although I have kept track separately of all identified and probable cases of redundancy (as discussed below in the section entitled "Vent Redundancy"). Inclusion of (1) authentic flank vents, (2) aligned cinder cones and domes that could have erupted concurrently, and (3) lava domes clustered above shallow magma reservoirs no doubt inflates the vent total but, I think, by no more than 290 (~12%). There are compensating factors: Stratovolcanoes can add flank vents but they also bury independent peripheral vents, and caldera-forming reservoirs concentrate clusters of vents but also destroy many of them during collapse. Moreover, additional vents will no doubt be recognized as geologic mapping becomes more uniformly detailed. Mapping of the Quaternary Cascades is already fairly advanced, however, and it seems unlikely that future additions to table 1 would exceed a few hundred vents, most of which would probably be of early Quaternary age.

A total of 3,416 Quaternary vents is given in table 1. Among these, nearly 1,100 are rear-arc volcanoes customarily associated with the Cascades. Of the 2,339 counted for the Cascade magmatic arc itself, more than 200 are forearc volcanoes distributed well seaward of the arc's main axial belt. This is as accurate a tally of sites of magmatic emission as current data avail, although more uniformly detailed mapping will no doubt eventually add dozens (if not hundreds) more. Nearly 90 percent of the vents identified are independent volcanoes in the sense that each possesses its own conduit system stemming from a melting source or magma reservoir in the crust or the mantle.

Distribution of Quaternary Cascade Volcanoes

At first glance, the Quaternary Cascade arc (fig. 1) consists dually of a broad north-trending swath of myriad close-set vents (the Lassen region to Mount Rainier) and a narrow NNW-trending chain of well-separated vent clusters (the Garibaldi Volcanic Belt). Guffanti and Weaver (1988) combined a seismicity-based subduction model with the (5 to 0 Ma) vent-distribution data compiled by Luedke and others (1983) to define five plausible Cascade arc segments: (1) The Garibaldi Volcanic Belt, (2) Mount Rainier to Mount Hood, (3) the rest of the Oregon Cascades, (4) the Mount Shasta region, and (5) the Lassen region. Although the extent to which the segments of Guffanti and Weaver (1988) reflect lower-plate processes remains nebulous (and indeed differential lithospheric extension and block rotation may be more important), I concur with their primary utilization of regional vent distribution and their deemphasis of the stratovolcano alignments conventionally employed in segment models. In table 1 and several vent-distribution maps (see below: figs. 3, 8, 14, 15, and 21), the Quaternary vent pattern is subdivided still more finely, principally for sharpening analysis and discussion, taking into account several local changes in vent density, alignment, or distribution. These subdivisions are not "segments," in the sense of reflecting some inferred or postulated relationship to either crustal tectonics or subduction geometry, but are simply volcanic fields or empirically coherent tracts of convenience—several having diffuse boundaries. For 34 of the larger edifices in the Cascades, some basic physical data are summarized in table 2.

Garibaldi Volcanic Belt

It is clear from the vent-distribution maps that little of the Cascade arc conforms to the stereotyped festoon of solitary stratovolcanoes. Even the Garibaldi Volcanic Belt (GVB; Glacier Peak to Mount Meager and Bridge River), although closer to the stereotypical image and often referred to as a "chain of isolated stratovolcanoes," is not that at all (fig. 3). Of the five major volcanoes in the GVB, four are silicic dome complexes with stubby ice-contact lava flows surrounded by predominantly pyroclastic aprons; and the one that really is an andesitic stratovolcano (Mount Baker) is a modest young cone on the margin of an early Quaternary caldera filled by rhyodacitic ignimbrite and lava domes (Kulshan Caldera; Hildreth, 1996;

Figure 2. Examples of contrasting degrees of erosion of Cascade volcanoes near opposite ends of the arc. ***A***, Pleistocene andesitic cones in the Lassen segment, California. View is southward up Hat Creek Valley, floored by the 24-ka Hat Creek Basalt (HAOT), toward snowclad Lassen Peak and Chaos Crags, 37 km away on the far skyline. In middle distance (15-17 km away), three cones of pyroxene andesite are, left to right, Sugarloaf Peak (2,000 m), Wilcox Peak (1,970 m), and (faulted) Logan Mountain (2,210 m). Sugarloaf and Wilcox each rise ~800 m, and Logan 1050 m, above the valley floor. Sugarloaf is of late Pleistocene age, and the other two are probably of middle Pleistocene age. (Photograph by author taken in summer 1995.) ***B,*** Mount Cayley (2,377 m) on central skyline, rising above glacially incised crystalline basement rocks of the Coast Plutonic Complex, British Columbia. View is westward 25 km from Whistler Mountain. Bicolored pyramid on central skyline is Mount Cayley, a multistage edifice dominated by dacitic lavas, pyroclastic deposits, and a summit-forming dacite intrusion. Crags to its left are Vulcan's Thumb and Pyroclastic Peak (see fig. 6), also parts of the Cayley cluster. Powder Mountain icefield forms right skyline. Canyon of Brandywine Creek at left descends to join the Cheakamus River (foreground) at ~425 m elevation. Although much of Mount Cayley is thought to be middle Pleistocene or older, it may also have erupted in the late Pleistocene, as lavas on its south flank descend 1,500 m down the floor of an adjacent canyon (Souther, 1980), and several subglacial flank vents erupted during the last main glacial interval (Kelman and others, 2002). (Photograph by author taken in August 1997.)

Table 1. Distribution and spatial density of Quaternary vents.

[Areas estimated are defined by vent fields, not by lavas or other outflow deposits. For example, Medicine Lake lavas cover an area greater than 2000 km^2 (Donnelly-Nolan and others, 2003), but all or nearly all of the vents are within an area of 1,700 km^2, the area used here for vent-density calculation. HAOT is high-alumina olivine tholeiite, as elaborated in the text]

Vents	Area (km^2)	Area (km^2) per vent	Region
23	160	7	Basalts of Salal Creek to Bridge River upland
24	250	10	Meager Creek Volcanic Field (Lillooet R. to Elaho R.)
21	100	5	Mt. Cayley Volcanic Field (Tricouni to Crucible dome)
10	90	9	Garibaldi Lake Volcanic Field (The Table to Loggers Lake)
16	240	15	Mt. Garibaldi area (Watts Point to Glacier Pikes)
25	220	9	Mt. Baker and Kulshan Caldera
8	—	—	Glacier Peak to Skykomish River
127			**Garibaldi Volcanic Belt total** (fig. 3)
6	—	—	Greenwater to Mt. Rainier
30	570	19	Bumping Lake to Goat Rocks, axial
121	1,150	9	Mt. Adams Volcanic Field (Walupt Lake to Guler Mtn)
15	250	17	Gilmer shield to Underwood Mtn, axial
40	1,200	30	Mt. Defiance to Mt. Hood to Barlow Pass, axial
52	300	6	Indian Heaven Volcanic Field
61	1,850	30	Forearc: Battle Ground to Mount St. Helens to Blue Lake
87	2,500	32	Forearc: Portland to Wind River (53 in Oregon; 34 in Washington)
412			**Rainier to Hood segment total** (fig. 8)
176	1,150	7	Frog Lake Buttes to South Cinder Peak (I, fig. 14)
466	3,250	7	South Cinder Peak to Crane Prairie Reservoir (II, fig. 14)
118	1,850	16	Crane Prairie Reservoir to Cowhorn Mtn (III, fig. 14)
86	1,225	14	Cowhorn Mtn to Timber Crater (IV, fig. 15)
175	1,100	6	Mt. Mazama area (Timber Crater to Big Bunchgrass)(V, fig. 15)
33	925	28	Mt. McLoughlin area (Pelican Butte to Aspen Lake)(VI, fig. 15)
1,054			**Oregon segment total** (figs. 14, 15)
3	—	—	Copco cones (HAOT in Oregon-Shasta Gap)
32	460	14	Mt. Shasta area (west of Cascade axis)
223	2,070	9	Cascade axis (and east to Sharp Mtn and Doe Peak; fig. 21)
225			**Shasta segment total** (fig. 21)
12	—	—	Brushy Butte and Timbered Crater (HAOT in Shasta-Lassen Gap)
43	1,000	23	Lassen forearc
250	2,200	9	Cascade axis (west of Caribou Volcanic Field and Butte Creek Rim
112	300	3	Caribou Volcanic Field
71	2,100	30	Diffuse backarc (east of Caribou Volcanic Field and Butte Creek Rim)
476			**Lassen segment total** (fig. 21)
2,339	**TOTAL — CASCADE ARC (proper)**		
			Adjacent rear-arc volcanic fields
35	360	10	Simcoe Mountains Volcanic Field (not including ~150 Pliocene vents)
>450	1,630	<4	Newberry Volcanic Field
580	1,700	3	Medicine Lake Volcanic Field
12	500	40	Hackamore Volcanic Field (Basin and Range HAOT)
1,077			**Rear-arc total**
3,416			**GRAND TOTAL—CASCADIAN QUATERNARY VENTS**

Note: Principal data sources are compilations by Blakely and others (1997), Guffanti and others (1990, 1996), Luedke and others (1983), Scott (1987), Sherrod and Smith (2000), Sherrod and others (2004), and Smith (1993), as well as area studies by Bacon (1990), Bacon and Nathenson (1996), Clynne and Muffler (1990, in press), Conrey (1991), Donnelly-Nolan (in press), Green and others (1988), Hammond and Korosec (1983), Hildreth and Fierstein (1995), Hildreth and others (2003), Hildreth, Lanphere and others, 2004), Lawrence and others (1984), MacLeod and Sherrod (1992), Read (1990), Roddick and Souther (1987), Scott and Gardner (1992), Smith (1988), Stasiuk and Russell (1989), Taylor (1978, 1987), Uto and others (1991), and author's work in progress. See also references for tables 6 through 8.

Table 2. Elevation, relief, and volume of selected Cascade edifices.

[Listed north to south. **Proximal relief** is difference between summit elevation and that of highest exposure of older rocks overlain by the edifice. **Draping relief** is difference between summit elevation and that of lowest distal lavas of the edifice (not including distal pyroclastic or debris flows). **Volume** and **Composition** refer to the present-day main cone only, not including peripheral vents; M, mafic; A, andesite; D, dacite; R, Rhyodacite and Rhyolite. See text for discussion of eruptive volumes estimated, which are generally much larger than those preserved.]

Edifice	Summit elevation (m)	Highest older rocks (m)	Proximal relief (m)	Draping relief (m)	Main Edifice	
					Composition	Volume (km^3)
Meager	2,679	1,980	700	2,100	D>A>R	20
Cayley	2,377	1,830	550	2,070	D>A	15
Garibaldi	2,678	1,375	1,300	2,375	D>A>R	20
Baker	3,286	2,315	970	2,675	A	15
Glacier Peak	3,213	2,410	800	2,330	D>A	30
Rainier	4,392	2,332	2,060	3,510	A>D	130
Goat Rocks	2,494*	2,200	300	1,520	A>D	40
Adams	3,742	1,440	2,300	3,300	A>D	210
St. Helens	2,950	1,540	1,410	2,270	D>A>M	25
Hood	3,425	1,650	1,775	2,790	A>D	50-70
Olallie Butte	2,199	1,490	710	835	M	5
Jefferson	3,199	1,710	1,490	2,100	A>D	20
Three Fingered Jack	2,390*	1,790	400	1,400	M	10
Washington	2,376*	1,550	825	1,025	M	15
Belknap shield	2,095	1,680	415	1,350	M	10
Black Butte OR	1,962	1,200	760	960	M	10
Black Crater	2,210	1,900	310	930	M	7
North Sister	3,074	1,680	1,400	1,565	M	15
Middle Sister	3,062	2,560	500	1,940	A>D~M	12
South Sister	3,157	1,980	1,175	1,500	A~R~D	20
Broken Top	2,800*	2,040	760	1,800	M>D~R	10
Bachelor	2,763	1,950	815	1,270	M	25
Maiden Peak	2,383	1,700	680	900	M	12
Diamond Peak	2,665*	2,050	615	1,815	M>A	15
Odell Butte	2,143	none	760	760	M	7
Cappy Mountain	2,252*	~1,650?	600	730	A>R>D	25
Thielsen	2,799*	2,200	600	1,220	M	10
Bailey	2,549	1,850	700	1,300	M>A	15
Mazama	3,700?	2,145	1,550	2,250	A>D~R	120
McLoughlin	2,894	1,770	1,125	2,040	M	13
Shasta	4,316	1585	2,730	3,420	A~D	450
Magee	2,646*	1,805	840	1,050	M~A>R	10
Lassen Peak	3,187	2,680	500	1,050	D	2.5
Brokeoff	2,815*	2,225	590	1,470	A~D	50

* Means that the original elevation of an eroded edifice was >100 m higher. St. Helens and Mazama summit elevation estimates are pre-collapse.

Hildreth, Lanphere, and others, 2004). Glacier Peak, Mount Garibaldi, and Mount Cayley are dominantly dacitic; rhyodacite is also common at Garibaldi and Cayley and abundant at Mount Meager; high-silica rhyolite (>75% SiO_2) is uniquely present at Garibaldi; and subordinate andesite erupted at all four, apparently relatively early in the development of each center (Matthews, 1952a, 1957; Tabor and Crowder, 1969; Green and others, 1988; Stasiuk and Russell, 1989; Green, 1990; Read, 1990; Souther and Yorath, 1991).

Eruptive volumes and production rates in the GVB have not been reconstructed with much accuracy, owing to (1) difficult access, (2) severe recurrent glacial erosion of all five long-lived centers, (3) sparsity of precise geochronologic and detailed stratigraphic data for most centers, (4) predominance of glassy rocks, chilled by snow and ice, rendering precise dating difficult, and (5) unknown proportions of silicic fallout and fragmental flows deposited directly on, within, or against glaciers and removed by advances of the Cordilleran ice sheet.

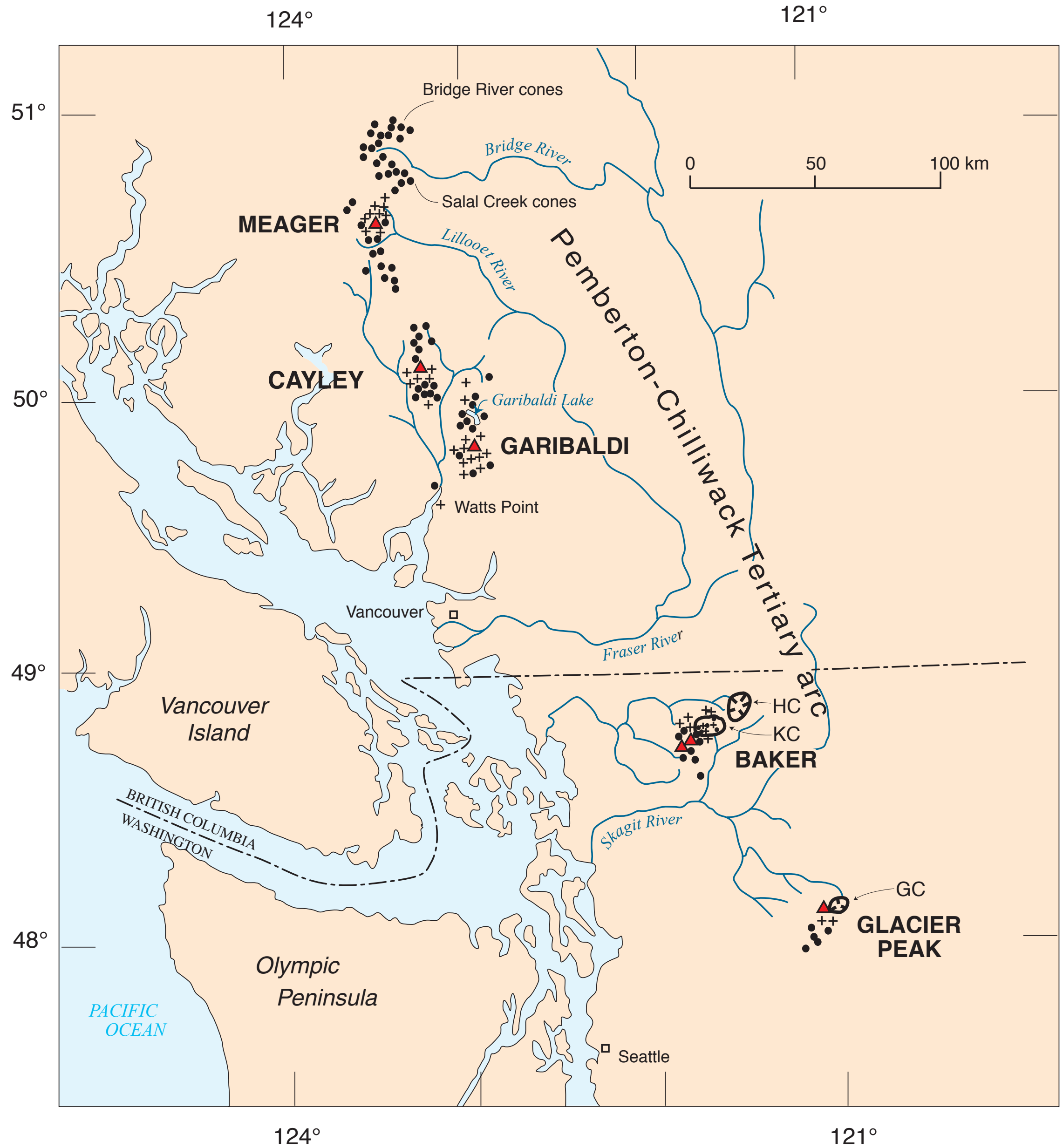

Figure 3. Garibaldi Volcanic Belt in southwest British Columbia and northwest Washington, showing distribution of 127 Quaternary volcanic vents. Dots represent volcanoes of basaltic to andesitic composition; crosses represent volcanoes of dacitic to rhyolitic composition; and triangles represent major edifices. Ovoids depict calderas: KC, 1.15-Ma Kulshan Caldera; HC, 3.7-Ma Hannegan caldera; GC, inferred Gamma Ridge Caldera, probably early Pleistocene. Axis of deeply eroded Tertiary magmatic arc inboard of the Quaternary arc is shown as Pemberton-Chilliwack belt.

Mount Baker

The Mount Baker locus (fig. 4) is probably the most productive (~160±50 km^3; fig. 18 of Hildreth and others, 2003), having erupted more than 80 km^3 of early Quaternary rhyodacite from Kulshan Caldera, about 30 km^3 of andesite from Black Buttes stratovolcano (500-300 ka), at least 15 km^3 of andesite from the active cone (Mount Baker), and more than 10 km^3 (possibly much more) from several peripheral vents now glacially ravaged. Detailed mapping and compositional data, volume estimates for 77 mapped eruptive units, and high-precision K-Ar and $^{40}Ar/^{39}Ar$ dating established an eruptive chronology (1.3 Ma to Holocene) and time-volume-composition relations for the whole Mount Baker Volcanic Field (Hildreth and others, 2003; Hildreth, Lanphere, and others, 2004). Nonetheless, the lost eruptive volume represented by ~110 mapped Quaternary dikes, most of them cutting glaciated basement rocks or intracaldera tuff, remains poorly known. The towering andesitic edifice of Mount Baker, highest peak in the North Cascades at 3,286 m, was built largely in the interval 40 to 12 ka, although it overlies a few (apparently confocal) glaciated andesite remnants as old as 100 ka. Its icecap, an acid-altered region around its steaming crater, and its steep peripheral valleys, which drain to the populous Puget Lowland, make the cone a significant debris-flow hazard. The youngest magmatic eruptions were the basaltic scoria cone and zoned lava-flow apron (Green, 1988) from the peripheral Schreibers Meadow vent (9.8 ka) and a subplinian shower of andesitic ash from Mount Baker's summit at 6.5 ka (Hildreth and others, 2003).

Glacier Peak

The volume of Glacier Peak (3,213 m) inferred from the late Pleistocene and Holocene deposits exposed is ~30 km^3 (Tabor and Crowder, 1969; Beget, 1982a,b; Sherrod and Smith, 1990), but the eruptive volume is likely to have been at

Figure 4. Kulshan Caldera and ice-clad Mount Baker (3,285 m), fumarolically active andesitic stratocone, viewed southwestward from Table Mountain. The cone has had only one documented magmatic eruption in the Holocene, a 6.5-ka subplinian shower of andesitic ash. Pale gray and tan deposits flooring middleground bowl are ash-rich sedimentary strata that rest on white intracaldera ignimbrite of Kulshan Caldera (1.15 Ma). Dark ridge at right and crag at center (below Mount Baker) are andesite lavas, 500 ka and 300 ka, respectively, that overlie the caldera fill. Rugged ridges at left include three postcaldera rhyodacite domes (1.13-1.01 Ma). Ice-filled Carmelo Crater on the summit is breached to north (right) by glacial outflow. Partway down the south (left) slope of Mount Baker, Sherman Peak forms south wall of steaming Sherman Crater. Relief visible in image is 1,900 m. (Photograph by author taken in summer 1995.)

least twice that much. The edifice is principally a dacite lava dome-and-flow complex (fig. 5), but it is surrounded by an enormous pyroclastic apron, tongues of which extended 100 km to Puget Sound. Moreover, remnants of an early Quaternary (2.0-1.6 Ma) intracaldera fill appear to be present at Gamma Ridge on the east flank (Tabor and Crowder, 1969; Tabor and others, 2002). By analogy with Kulshan Caldera near Mount Baker (Hildreth, 1996; Hildreth, Lanphere, and others, 2004), more than half of the caldera-forming eruptive volume is likely to have been eroded away.

Several episodes of postglacial eruptive activity have been identified at Glacier Peak. Two plinian eruptions (~13 ka) each released ~2 km^3 of magma as downwind fallout (Porter, 1978; Gardner and others, 1998), along with much larger volumes as pyroclastic flows (Beget, 1982a). Several substantial pyroclastic eruptions in the middle and late Holocene also produced major pyroclastic-flow and debris-flow deposits, although the fall deposits accompanying these events were thin and of modest volume (Beget, 1982a,b; Foit and others, 2004). Little is known, however, of the earlier eruptive history, which apparently dates from the middle Pleistocene, because much of the record has been glacially ravaged and buried proximally by the young dome complex. Reconnaisance K-Ar dating by M.A. Lanphere (Tabor and others, 2002) identified numerous late and middle Pleistocene lavas, the oldest about 600 ka. Magnetically reversed lavas (>780 ka) were nowhere found by Tabor and Crowder (1969). Steeply glaciated radial ridges are mantled by the 13-ka pumice-fall deposits up to about 2,500 m, and the large Disappointment Peak dacite dome (~1 km south of the summit) appears likewise to be older than 13 ka (Beget, 1982a). The summit and much of the upper 700 m of the edifice, however, apparently represent a younger dome cluster, probably sources for the thick middle and late Holocene parts of the valley-filling pyroclastic apron.

Mount Garibaldi

Similar uncertainties exist concerning the eruptive histories and volumes of the ice-clad Garibaldi, Cayley, and Meager volcanic centers. Surviving products of the Mount Garibaldi (2,678 m) dome complex (56-77% SiO_2) sum to only 16 to 20 km^3 (Matthews, 1952a, 1957, 1958), but they represent many episodes of activity spread across the long interval from about 670 ka to Holocene (Green and others, 1988; Green, 1990),

Figure 5. Glacier Peak (3,213 m) viewed northeastward from White Chuck cinder cone, 7 km southwest of summit. Disappointment Peak dome (2,973 m) forms shoulder 700 m right (south) of summit dome. Pale bare apron is mostly dacite lava flows, veneered by dacitic pyroclastic deposits that thicken into canyons below (not visible here). Darker rocks of steep lower walls and foreground ridge are Mesozoic schists and Miocene granitoids. Relief visible in image is about 1,700 m. (Photograph by author taken in August 1988.)

during which the edifice was probably torn down several times. The pyroclastic apron is large, deeply eroded, and little studied. Andesite-dacite lavas and their pyroclastic accompaniments from several vents first filled paleovalleys having as much as 1.8 km of relief glacially incised into the Coast Plutonic Complex basement. Several dacite domes and derivative pyroclastic material next built the main edifice (~260-200 ka), draping relief cut in the older assemblage. A deeply eroded obsidian dome remnant at Lava Peak (77% SiO_2) is the only Quaternary high-silica rhyolite identified anywhere in the Cascades north of the Three Sisters. The south summit of Mount Garibaldi (Atwell Peak), a large dome of hornblende-biotite rhyodacite that shed a major pyroclastic apron, may postdate the Last Glacial Maximum (LGM; 21-18 ka), as may the Glacier Pikes hornblende-dacite dome a few kilometers north of the summit. Of the several glacially sculpted (still ice-clad) summits, the hornblende-biotite dacite Dalton Dome may be the youngest. The only unit unequivocally postglacial is the 18-km-long Ring Creek lava flow (~4.5 km^3) of hornblende-biotite dacite (63-65% SiO_2) that erupted at Opal Cone on the southeast flank at ~10 ka (Brooks and Friele, 1992).

A small but independent locus of intermediate magmatism, 25 km southwest of Mount Garibaldi at the head of Howe Sound near the town of Squamish (Green, 1994b), includes the only known eruptive sites between Garibaldi and Mount Baker. Facing each other across the sound are the 200-m-thick **Watts Point** pile of dacite lavas and breccias (63-65% SiO_2) cut by thick dikes, and the 300-m-thick **Monmouth Creek** pile of hornblende andesite-dacite lavas and breccias (57-64% SiO_2), likewise cut by several dikes, which support pinnacles that tower above the complex (called "The Castle" by Mathews, 1958). Both are glacially devastated and the original volumes impossible to reconstruct. The Watts Point center is dated at about 100 ka (Green and others, 1988) and may have been erupted subglacially (Bye and others, 2000).

Garibaldi Lake Volcanic Field

The Garibaldi Lake Volcanic Field, which extends 20 km northward from the north toe of Mount Garibaldi, is a scattering of small, compositionally diverse (alkali basalt to dacite) volcanoes (Mathews, 1952a, 1957, 1958; Green, 1981, 1982, 1990; Green and others, 1988; Waddell and Green, 1993). Excluding vents on Mount Garibaldi itself, the field has at least 14 distributed vents, including three that erupted dacite, eight andesite, two basaltic andesite, and one alkali basalt and hawaiite. At least four valley-floor basalts (49-51% SiO_2) that flowed south into the volcanic field from unidentified vents more than 28 km farther up the Cheakamus River enclose sediment radiocarbon dated at 34.2 ka. The largest edifice in the field is the andesitic multivent Mount Price-Clinker Peak complex (~4 km^3; Mathews, 1958), from which two 7-km-long lava tongues distally abutted the Cheakamus valley glacier during post-LGM ice recession (Mathews, 1952b). Many units in the volcanic field exhibit ice-contact features or were erupted subglacially. The Table, a 300-m-thick multitiered pile of hornblende andesite lavas, melted out its own intraglacial cavity (Mathews, 1951), possibly also during the post-LGM deglaciation.
A few volcanic remnants in the field are early Pleistocene (as old as ~1.2 Ma), but most appear to be late Pleistocene (Green and others, 1988).

Mount Cayley

Mount Cayley (2,377 m), at least as old as middle Pleistocene, today represents 15 to 20 km^3 of glacially eroded crags (fig. 2), clearly only a modest fraction of its total output of silicic eruptive products (Souther, 1980; Souther and Dellechaie, 1984; Green and others, 1988). Three precipitous summits (Mount Cayley, Wizard Peak, and Pyroclastic Peak; fig. 6) are sculpted from a multivent andesite-to-rhyodacite edifice (57-69% SiO_2) that has nearly 2 km of relief, rests on ruggedly eroded granitoid basement, and consists of domes, shallow intrusions, lava flows, and voluminous breccias and tuffs, cut by numerous dikes and sills. The complex was divided by Souther (1980) into three unconformable eruptive sequences, but alteration and ice-contact chilling have made precise geochronology difficult (and some published dates should be considered suspect). Off-edifice peripheral vents range from the biotite+quartz-bearing dacite lava flows and craggy intrusion of Mount Fee (65-68% SiO_2), through a north-trending chain of pyroxene- or hornblende-bearing andesite/dacite domes and tuyas, to a southeastern cluster of six olivine-bearing andesitic domes at Ember Ridge (Green and others, 1988; Kelman and others, 2002). Among the youngest units may be a pair of biotite-dacite domes at the east and southeast margins of the Cayley edifice and a 5-km-long valley-filling lava tongue related to one of them. That lava flows from both Mount Cayley and Mount Fee extend down the floors of present-day tributary drainages nearly to adjacent canyon bottoms suggests that each remained active well into the late Pleistocene. Because the precipitous Cayley complex is rich in coarse proximal pyroclastic deposits, some of them hydrothermally altered, it is especially prone to slope failure and debris avalanches (Clague and Souther, 1982; Evans and Brooks, 1991).

Mount Meager

Mount Meager (fig. 7) likewise had numerous eruptive phases (58-70% SiO_2) during a lifetime that could be as long as 2.2 Myr (Read, 1978, 1990; Green and others, 1988; Stasiuk and Russell, 1989, 1990). At the south end of the compound 9x13-km edifice, basal andesite-dacite lavas and pyroclastic deposits (~2 Ma) rest on ruggedly eroded Mesozoic batholithic basement and are draped by a 500-m-thick pile of altered rhyodacite tuffs, lavas, and shallow intrusions (~2 to 1 Ma) that suggest a vent complex south of Pylon Peak. These are overlain by a large pile of silicic andesite and dacite (~1 to 0.5 Ma) as thick as 1,200 m, centered at "The Devasta-

Figure 6. Mount Cayley cluster viewed toward the northwest. Spire at left is Vulcan’s Thumb, and three main summits (from left to right) are Pyroclastic Peak, Mount Cayley, and Wizard Peak (Souther, 1980). Relief visible in image is about 900 m. (Photograph by Paul Cordy; courtesy of Professor J.K. Russell.)

Figure 7. Mount Meager complex viewed toward the west. Capricorn Mountain and Capricorn Glacier at left. Two high summits are Mount Meager at center and Plinth Peak to its right. Relief visible in image is about 1,800 m. (Photograph courtesy of Professor J.K. Russell.)

tor" and distributed radially around the compound edifice. This part of the edifice is in turn overlapped on the north by a late Pleistocene complex ≤150 ka) of biotite-quartz (± hornblende) rhyodacite that forms four additional ice-clad summits (Capricorn, Job, Meager, and Plinth) and consists of numerous domes, felsic intrusions, lava flows, and steeply dipping pyroclastic aprons. Although basement rocks are exposed locally as high as 1,800 m, products of the Meager edifice drape them to elevations as low as 600 m from the 2,679-m peak. The severely glaciated complex that survives today is a composite of deeply eroded remnants of many episodes and has a total estimated volume of ~20 km^3. Some 2 to 3 km^3 of rhyodacite magma was released in the only known Holocene eruption, the 2.4-ka Bridge River plinian fall (identified as far downwind as Alberta) and an accompanying 9-km-long valley-filling pyroclastic-flow and lava-flow assemblage (Nasmith and others 1967; Stasiuk and Russell, 1990; Read, 1990; Stasiuk and others, 1996; the Pebble Creek Formation of Hickson and others, 1999). Because of their longevities and repeated ravaging by the Cordilleran ice sheet, it should be no surprise if Mount Meager and each of the other principal GVB centers are ultimately shown to have been as productive as comparably explosive and silicic Mount St. Helens (which has produced an eruptive volume of at least 75±15 km^3).

Garibaldi Volcanic Belt—Overview

Mafic andesite and basalt issued from independent (mostly monogenetic) vents peripheral to all five principal GVB centers. At least four basaltic vents are scattered just south of Glacier Peak (Tabor and Crowder. 1969), the White Chuck scoria cone being the northernmost vent for HAOT-like magma in the Cascades (Green and Sinha, 2005). Six basaltic vents of many ages (716 to 9.8 ka) are mapped around Mount Baker (Hildreth and others, 2003). Relatively young mafic and andesitic lavas crop out adjacent to the glacial valleys at the south and southeast base of Mount Garibaldi (Green and others, 1988). The Garibaldi Lake Volcanic Field contains vents for basaltic andesites and for both alkaline and subalkaline basalts. A chain of small, subglacially erupted, andesitic volcanoes extends 25 km north-south through Mount Cayley (Souther, 1980; Green and others, 1988), and basaltic andesite erupted near both Crucible Dome (Ring Mountain) to the north and Tricouni Peak to the south (Kelman and others, 2002). Numerous vents for varied basalts, alkaline and subalkaline, are dispersed to the north, south, and west around Mount Meager (Stasiuk and Russell, 1989; Read, 1990; Green and Sinha, 2005), including a 25-km-long set of young basalts (51% SiO_2) that flowed south down the floor of the Elaho River valley.

Extending 35 km north from Mount Meager along Salal Creek to north of Bridge River, a field of at least 20 scattered mafic monogenetic volcanoes (46-51% SiO_2) terminates the Quaternary GVB. Although one or two may be postglacial, most are plugs, necks, dikes, tuyas, lava-flow remnants, and parts of small cones and shields, badly eroded and showing ice-contact features. Often called collectively the "Bridge River Cones," all or most consist of alkali basalt, hawaiite, or basanite (Lawrence and others, 1984; Roddick and Souther, 1987; Souther, 1990; Green and Sinha, 2005).

The GVB has at least 127 known vents (fig. 3; table 1), is 375 km long, trends N35˚W in the south but N20˚W in the north, suggesting internal segmentation (Green and Harry, 1999), and exhibits very uneven spacing of its five main centers—the maximum being 147 km (Baker to Garibaldi), the minimum 35 km (Garibaldi to Cayley). Extensive ice cover and the large number of dikes that cut both basement rocks and glacially scoured early edifice deposits suggest that unrecognized (or obliterated) vents are more numerous in the GVB than farther south in the Cascades and that GVB eruptive volumes are likely to be correspondingly underestimated. True basalts (47-52% SiO_2) erupted within 10 km of all five main GVB centers during late Pleistocene or Holocene time (Green and Sinha, 2005). Extraordinarily for the Cascades, however, as much as 75 percent of the eruptive volume of the GVB is dacite and rhyodacite.

Mount Rainier to Mount Hood Segment

The contrast between the Garibaldi Volcanic Belt (fig. 3) and the broad region of Quaternary volcanism in southern Washington and northernmost Oregon (fig. 8) could scarcely be greater. A virtually continuous array of at least 150 Quaternary volcanic vents extends 170 km along the main Cascade axis from Mount Hood (45˚22'N) to Bumping Lake (46˚54'N) (Luedke and others, 1983; Smith, 1993). Trending N10˚E and having no vent-free gap longer than 10 km, this axial belt includes Mount Hood, Mount Defiance, Underwood Mountain, Gilmer shield, King Mountain, Mount Adams, Goat Rocks, Hogback Mountain, and Tumac Mountain; it ends abruptly against a 120-km-long gap that separates it from the next Quaternary vent cluster just south of Glacier Peak. In addition, a broad forearc region includes Mount Rainier, Mount St. Helens, and scatterings of mafic shields and monogenetic vents that, near Portland, reach halfway to the Pacific coast. East of the Cascade axis, the rear-arc Simcoe Mountains have at least 35 cinder cones and maars of Quaternary age (largely hawaiite and alkali basalt), which augment a more extensive Pliocene volcanic field (subalkaline and alkaline) arrayed around a rhyolite-cored mafic shield volcano (Sheppard, 1967; Uto and others, 1991; Hildreth and Fierstein, work in progress). Whereas the widest array of Quaternary vents across the Garibaldi Volcanic Belt is less than 25 km, the Quaternary volcanic zone of southern Washington stretches 160 km west to east (Portland to Goldendale) and would still be 110 km wide if the intraplate Simcoe Mountains Volcanic Field were excluded (fig. 8).

Cascade Axis

The axial belt (fig. 8) includes four andesite-dacite centers, one modest (Jennies Butte) and three large (Goat Rocks,

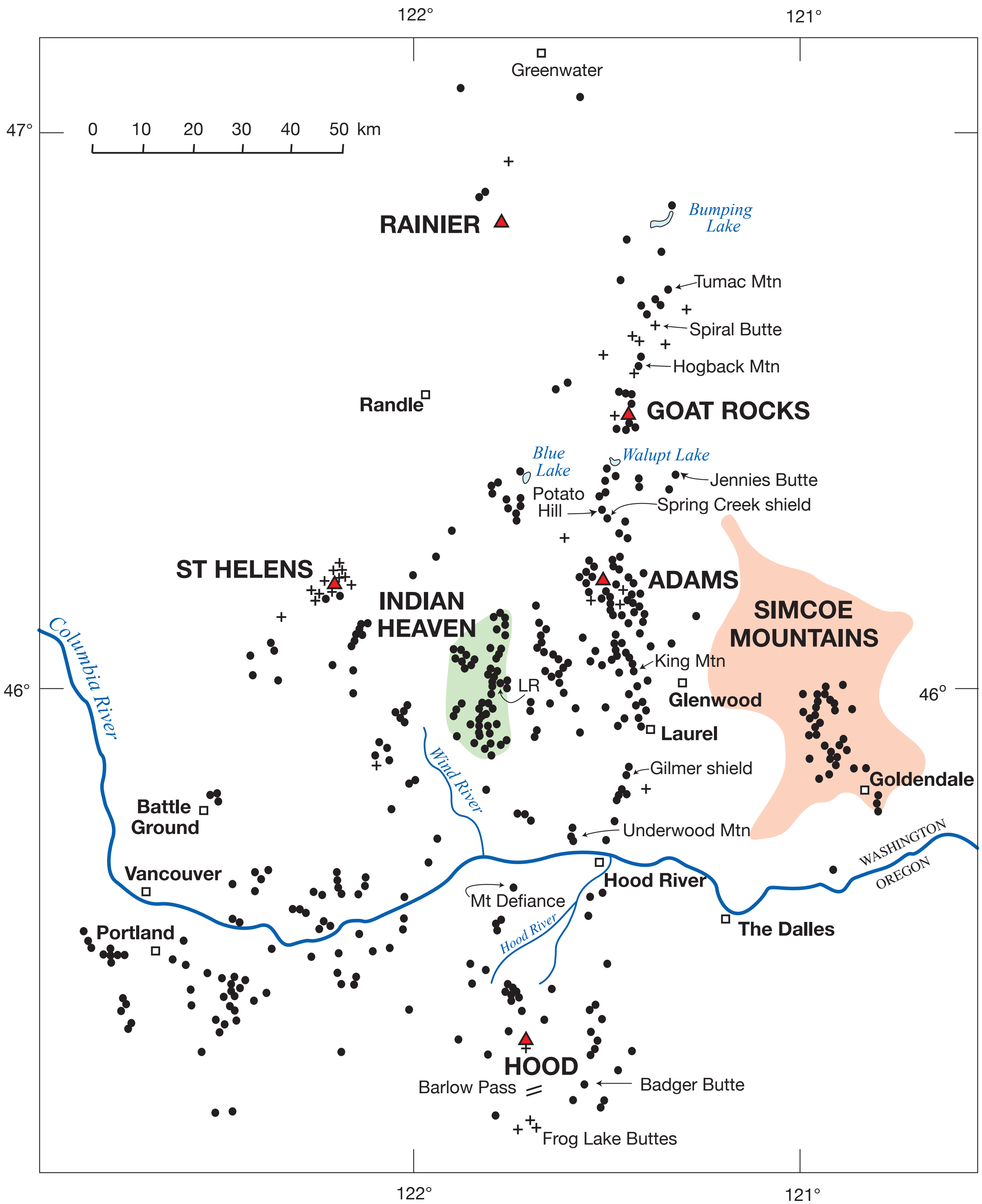

Figure 8. Rainier-to-Hood segment of the Cascade arc, showing distribution of 412 Quaternary volcanic vents, 319 of them in Washington and 93 in Oregon. Two colored fields depict limits of vent distributions that define Indian Heaven Volcanic Field (middle Pleistocene and younger) and Simcoe Mountains Volcanic Field (4.5-0.6 Ma), within which only the ~35 Quaternary vents are indicated. LR, Lemei Rock shield. Dots represent volcanoes of basaltic to andesitic composition; crosses, those of dacitic to rhyolitic composition; and triangles, major edifices.

Adams, Hood), as well as ~15 basaltic shields, and at least 130 lesser (mostly monogenetic) Quaternary volcanoes, among which basalt predominates over basaltic andesite (proportions opposite those in the Oregon Cascades). Quaternary dacites and andesites from vents independent of the stratovolcanoes are few, modest, and largely concentrated along the 35-km-long axial strip north of Goat Rocks (Clayton, 1980; Smith, 1993). Quaternary rhyolites are absent.

Goat Rocks

The Goat Rocks stratovolcano complex (fig. 9) has been glacially reduced to ridge-forming remnants of radially dipping stacks of andesite (mostly 58-62% SiO_2) that surround altered cores laced with plugs and dikes (Swanson and Clayton, 1983; Swanson and others, 1989). The eruptive volume of the edifice was estimated by G.A. Clayton (Smith, 1993) to have been about 60 km^3, which seems conservative in view of the extent and thickness of the remnants, which represent products of a cluster of vents (Swanson and Clayton, 1983; Smith, 1993). The Goat Rocks may well have been as voluminous as present-day Mount Hood, likewise an andesite-dominated center. Like the Mount Baker locus, the Goat Rocks edifice was a high andesitic cone cluster built at the margin of an older silicic complex—in this case the rhyolite complex of Devils Horns (~3.2 Ma; Swanson and Clayton, 1983), a pile of ignimbrite, lavas, and (caldera-collapse) breccias, exposed for more than 900 m vertically and evidently representing the fill within a caldera roughly 5×8 km in area (Smith, 1993). How long after the Pliocene rhyolitic episode the Goat Rocks cone began its growth is not well established, but parts of the andesitic edifice are certainly of early Quaternary age and younger. Intracanyon lava flows from the Goat Rocks center include the 80-km-long Tieton Andesite (59-60% SiO_2; perhaps the longest andesitic flow in the world), which erupted at ~1.0 Ma (Ellingson, 1972; Swanson, 1978; Hammond, 1980). The youngest major vent for pyroxene andesite dates from ~0.7 Ma, and intracanyon flows of hornblende andesite issued still later from vents near the volcano's core during the middle (and perhaps late) Pleistocene (Clayton, 1983; Swanson and others, 1989).

Although mid-Pleistocene waning of central activity at Goat Rocks was roughly concurrent with the beginning of andesitic cone growth at modern Mount Rainier 40 km to the northwest, the axis of Cascade magmatism did not shift. Along-axis eruptions of basalt and basaltic andesite took place before, during, and after construction of the Goat Rocks

Figure 9. Goat Rocks volcanic cluster viewed northwestward from Jennies Butte (with ice-clad Mount Rainier far behind, 60 km distant). In foreground, uppermost Klickitat River canyon heads on Cispus Pass. At right, Klickton Divide culminates in pyramidal Gilbert Peak (2,494 m), which stands above the cliffy Goat Rocks (proper). In distance, left of center, Ives Peak and Old Snowy Mountain mark the Pacific crest divide. All the named peaks are broadly andesitic and are thought to be early Quaternary. The Pliocene Devils Horns rhyolitic complex is out of view to the right, 4 km northeast of Gilbert Peak. Relief visible in image is about 1,200 m. (Photograph by author taken in August 2001.)

stratocone. About 20 post-Goat Rocks mafic and andesitic volcanoes have erupted along or near the Cascade crest, north and south of the Goat Rocks center (from Tumac Mountain to Jennies Butte and Potato Hill), several of them as recently as 30 to 15 ka (Ellingson, 1972; Swanson and others, 1989, Swanson, 1990; Smith, 1993; Hildreth and Fierstein, 1997). Moreover, while Mount Rainier was growing in virtual isolation 30 km to the west, as many as ten additional middle and late Pleistocene vents along the Cascade axis between Goat Rocks and Bumping Lake contemporaneously produced hornblende andesite and dacite (Clayton, 1980; Smith, 1993).

Mount Adams

Mount Adams (3,742 m), an active 200-km^3 andesite-dacite stratovolcano (fig. 10) and the most voluminous Quaternary volcano in Washington, lies on the Cascade axis 35 km south of Goat Rocks and 90 km north of Mount Hood. The great cone stands near the center of a 1,250-km^2 coeval volcanic field that contains at least 120 separate vents (fig. 8). About 25 of these, all within 6 km of the summit, are considered flank vents because they erupted andesite and dacite similar to that from the stratocone's central vent complex. The rest, however, are peripheral eruptive centers that probably (on compositional and spatial grounds) have independent conduits from magma reservoirs in the deep crust or mantle. Distributed on all sides of Mount Adams, between 5 and 25 km from its summit, the majority of these peripheral volcanoes are basaltic; others consist of basaltic andesite, but only eight nonflank vents (6 km or more from the summit) ever produced andesite or dacite. The greatest concentration of peripheral vents defines a north-trending (355^{o}) belt only 6 to 7 km wide but more than 50 km long that includes several shields, numerous scoria cones, and the multivent stratovolcano itself.

Detailed mapping and compositional data, volume estimates for 124 mapped eruptive units, and high-precision K-Ar dating have established the eruptive chronology and time-volume-composition relations for the whole volcanic field—strato-

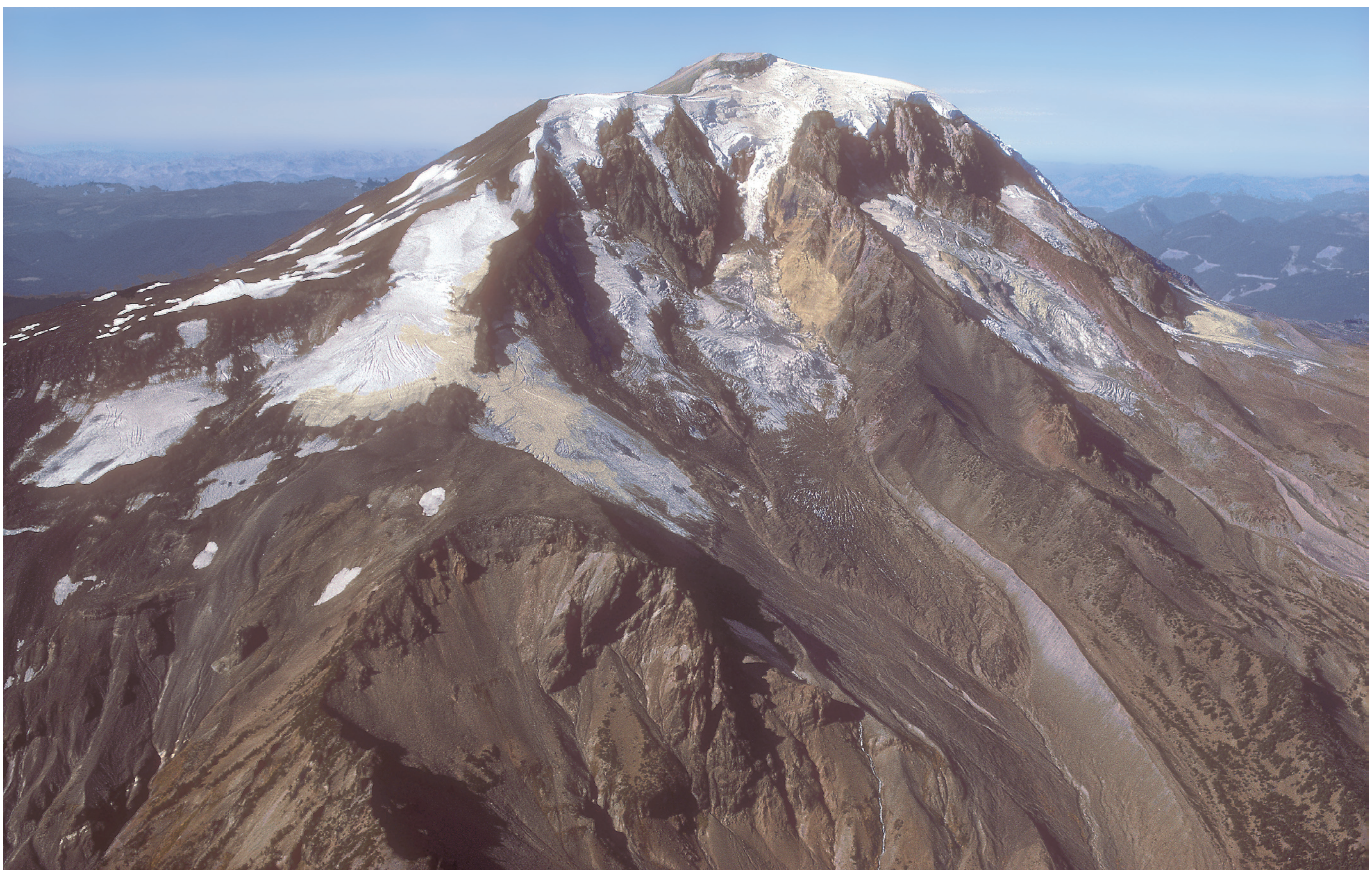

Figure 10. Upper half of Mount Adams (3,742 m) viewed northwestward from the air. Mazama Glacier at left; Battlement Ridge at center, flanked by debris-covered Klickitat and Rusk Glaciers. Black-over-brown unconformity at lower left places 33±14 ka lavas from South Summit (snow-topped shelf to left of summit) atop the dike-laced 500-ka lavas of a large predecessor edifice (Hellroaring Volcano). Small ejecta cone at summit, partly agglutinated, is dated at 15±8 ka. Black knob standing against the summit icecap at top of Battlement Ridge is "The Castle" (255 m lower than the summit), which is also visible in figure 24 (where seen from the north). Relief visible in image is about 1900 m. Image taken in 1987, a year of unusually strong summer melt-off.
(Copyrighted photograph by and courtesy of Darryl Lloyd.)

cone and periphery (Hildreth and Lanphere, 1994; Hildreth and Fierstein, 1995, 1997). Eruption of basalt began about 940 ka, and inception of the stratocone near the center of the distributed volcanic field took place about 520 ka. Although the cone grew principally in three episodes centered at 500, 450, and 50-30 ka, it remained recurrently active between pulses, never really shutting down. Andesite-dacite activity in the focal region and dominantly basaltic activity around the periphery have coexisted for 520 kyr, and their products are interstratified. During the 520-kyr lifetime of the stratovolcano, basalt erupted many times within 5 to 10 km of its summit, but only once (at 63±14 ka) did basalt penetrate the andesitic focus itself and erupt centrally. Vents for calcalkaline, arc-tholeiitic, arc-alkaline, intraplate-alkaline, low-K HAOT, and ocean-island-type basalts are mutually interspersed and lie within 5 to 25 km of the central conduit system for the coeval andesite stratovolcano (Hildreth and Fierstein, 1995). Substantial shields adjacent to Mount Adams include Goat Butte (~159 ka) and King Mountain (100-160 ka), both arc basalt; Lemei Rock (~22 ka) and Spring Creek (late Pleistocene), both HAOT; and Smith Butte (14 ka), alkali basalt. The cumulative eruptive volume of the volcanic field is 315 ± 84 km^3, of which ~85 percent issued focally from central or proximal-flank vents. Of the total eruptive volume, basalt constitutes 9 to 15 percent, dacite only 1 to 2 percent, and andesite plus basaltic andesite 84 to 89 percent (Hildreth and Lanphere, 1994).

Mount Hood

Mount Hood (3,425 m) is another active andesite-dacite stratovolcano on the Cascade axis. The present cone has been active since the middle Pleistocene (~0.5 Ma), but it overlaps remnants of at least two early Pleistocene centers (Scott and others, 1997; Keith and others, 1985; Swanson and others, 1989; Wise, 1968, 1969). These include the mafic-to-andesitic Sandy Glacier Volcano (~1.3 Ma) beneath the west flank of Mount Hood (fig. 11) and the buried source(s) of andesitic lava flows (1.5-0.8 Ma) that crop out beneath products of the modern cone to the southeast, northeast, and near Vista Ridge to the northwest. There may have been an interval of low productivity (0.8-0.5 Ma) prior to inception of the modern cone ~500 ka.

Present-day volume of Mount Hood was estimated by Sherrod and Smith (1990) to be ~50 km^3, but, taking into account recurrent glacial erosion, an eruptive volume of 70 to 100 km^3 is likely for the Quaternary locus. Compared to Mount Adams where products of central and proximal-flank vents range continuously from 52 to 68 percent SiO_2, Mount Hood is compositionally intermediate, 57 to 64 percent SiO_2 (Wise, 1969; White, 1980; Scott and others, 1997). Although the stratocone consists mostly of phenocryst-rich andesite, low-silica dacite (63 to 64% SiO_2) erupted sporadically throughout its construction (White, 1980) and dominated products of the last 50 kyr, which have largely been summit domes and derivative block-and-ash flows that built extensive radial fans (Crandell, 1980; Scott and others, 1997). Despite the importance of dacitic pyroclastic activity, no widespread fall units are known to have erupted from Mount Hood. Concurrent with the central andesite-dacite activity, basaltic andesite (55-58% SiO_2) erupted from several peripheral vents nearby, including the prominent Cloud Cap (~424 ka) and Pinnacle (~128 ka) centers, respectively only 5 km northeast and north of Mount Hood's summit (Scott and others, 1997). True basalt is not known to have erupted at Mount Hood, nor anywhere in its near periphery since the early Pleistocene.

Within a 25-km radius, an additional 40 to 45 peripheral volcanoes of Quaternary age (and many more of Tertiary age) surround Mount Hood on all sides (fig. 8; Sherrod and Scott, 1995; Sherrod and Smith, 2000). Most consist of basaltic andesite, a few are andesitic or basaltic, and all are modest in volume. Among the larger ones are the mafic shields of Lost Lake Butte to the northwest, Aschoff Butte to the west, Grasshopper Point to the southeast, and Fir Mountain to the northeast, as well as andesitic Badger Butte to the southeast. The youngest peripheral vent (7.7 ka), near Parkdale (12 km northeast of Mount Hood's summit), produced a basaltic andesite lava tongue that flowed 6 km down the Hood River Valley.

Farther north, the axial strip stretching between Mount Hood's peripheral array and the King Mountain-Mount Adams vent corridor is an area of relatively reduced vent density. This 40-km-long reach (Hood River Valley to Laurel; fig. 8) contains only about 20 Quaternary vents, but among them are substantial mafic shields at Gilmer, Underwood Mountain, and Mount Defiance, the latter in part andesitic.

Forearc

West of the Quaternary axis lie four extraordinary components of the volcanic Cascades: Two major foci at Mount Rainier and Mount St. Helens, a concentration of about 50 mafic vents making up the Indian Heaven Volcanic Field, and a diffuse scattering of compositionally varied forearc volcanoes in the Portland region (fig. 8). The term "forearc" is used in a straightforward geographic sense (fig. 8) with no compositional implications.

Mount Rainier

Mount Rainier (4,392 m), the highest peak in the Cascades and second most voluminous stratocone in Washington, stands in splendid isolation 35 km west of the northern terminus of the continuous Cascade axis (fig. 8). The great cone consists of eruptive products of exclusively normal magnetic polarity, mostly of pyroxene andesite-dacite in the range 59 to 65 percent SiO_2, with minor amphibole in some dacites. Its growth has been fed largely by a persistent east-west summit-vent alignment from which radial dikes have occasionally produced voluminous flank effusions from vents partway up the edifice (Fiske and others, 1963; Sisson, 1995; Sisson and Lanphere, 2000). Some 140 to 200 km^3 of rapidly erodable material has issued from a conduit system fixed beneath the cone for ~500 kyr (Fiske and others, 1963, 1964; Luedke and others, 1983; Swanson and others, 1989; Lanphere and Sisson, 1995).

Figure 11. West face of Mount Hood (3,425 m) viewed eastward up Muddy Fork of Sandy River. Sandy Glacier at center; Reid Glacier at upper right, below Illumination Rock (2,909 m) on right skyline. Darker cliffs beneath the glaciers are mafic-to-andesitic lavas and fragmental deposits of the early Pleistocene Sandy Glacier Volcano (~1.2±0.1 Ma) that dip eastward beneath Mount Hood and are cut by numerous dikes. Above the leftward-sloping unconformity, Mount Hood lavas supporting the glacier shelves are middle Pleistocene (~450-130 ka), whereas the summit consists largely of dacite domes younger than 50 ka (Scott and others, 1997). Relief visible in image is 2,200 m. (Photograph by W.E. Scott taken from Bald Mountain in August 1990.)

Mount Rainier is unusual among Cascade stratocones in having so few peripheral vents around it. Leaving aside the high dikes radial to the summit vent system, the only ones identified are a pair of basaltic-andesite vents (~105 ka; Lanphere and Sisson, 1995; McKenna, 1994) on the northwest flank (fig. 54 of Fiske and others, 1963), the hornblende-dacite lava of Bee Flat (~130 ka; 11 km north of the summit), and two much older vents for mafic lavas (48-53% SiO_2; Reiners and others, 2000) near Greenwater, 30 km to the north (fig. 8). Basaltic andesite is nonetheless common as chilled enclaves in the intermediate lavas of the edifice and is probably the main parent magma that feeds into Rainier's mid-to-upper crustal reservoir (Sisson and others, 2001). Petrologic studies suggest upper-crustal magma storage, differentiation, and recharge in complex multilevel reservoirs, commonly resulting in mixed or zoned eruptions (Venezky and Rutherford, 1997; Stockstill and others, 2002).

The Rainier edifice is constructed principally of stacks of lava flows and of fragmental deposits derived from them. Large tephra eruptions have been rare, although remnants of two substantial pumice falls (~380 ka and 190 ka), each likely to have exceeded 1 km^3 in volume, have been recognized (Sisson and Lanphere, 2000). In postglacial time, at least 10 pumiceous tephra falls of limited volume (0.001 to 0.1 km^3) erupted from Mount Rainier (Mullineaux, 1974), and as many as 25 layers of poorly vesicular (lithic) fallout identified by Vallance and Donoghue (2000) were deposited locally by phreatomagmatic eruptions or by ash clouds rising from the block-and-ash flows that have swept down nearly every radial valley. At least ten of these fall layers are younger than 2.6 ka, four may be younger than 2.2 ka, and most may have been accompanied by debris flows. Because Mount Rainier was built upon a high basement terrain already deeply dissected, however, it failed to construct a ring plain of fragmental deposits like those around Mount Shasta, St. Helens, and Glacier Peak. Block-and-ash pyroclastic flows and debris flows from Mount Rainier have been abundant but tend to be funneled into the many radial canyons, where they are readily eroded and reworked as alluvium. Because of its elevation (4,392 m), relief, hydrothermal alteration, icecap, glacier-fed radial valleys, and proximity to encroaching suburbs of the Seattle-Tacoma metropolis, Mount Rainier is the most threatening volcano in the Cascades, owing less to eruption itself than to its potential for sector collapse, magma-water-ice interaction, and downvalley debris flows (Crandell, 1971; Scott and others, 1995; Vallance and Scott, 1997).

Several mid-Pleistocene andesite-dacite lava flows are of large volume (3 to 9 km^3) and as thick as 350 m (Sisson and others, 2001; Stockstill and others, 2002). Extending from flank vents high on the edifice, some are as long as 15 to 22 km and are preserved as an array of great radial ridges (Lescinsky and Sisson, 1998). Episodes of elevated eruptive output have been identified for the intervals 500 to 420 ka and 280 to 190 ka; and productivity has again been fairly high since ~40 ka (~0.4 ± 0.1 km^3/kyr), including refilling of the amphitheater left by a major flank collapse at 5.6 ka (Vallance and Scott, 1997; Sisson and Lanphere, 2000).

A large predecessor volcano marked by hornblende-rich andesite grew during the interval 1.3 to 1.0 Ma on or near the site of the present edifice, but it was largely eroded away prior to inception of Mount Rainier ~500 ka; remnants survive east of the modern volcano but principally as fluvial gravel and mudflow deposits of the Lily Creek Formation, 25 to 35 km northwest of it (Crandell, 1963; Sisson and Lanphere, 2000).

Mount St. Helens

Mount St. Helens is a predominantly dacitic forearc volcano 50 km west of the Cascade axis (fig. 8). One of the most active young centers in the Cascades, it has erupted at least 75±15 km^3 of magma—more than half of it in the last 28 kyr. At least 90 percent of its products are dacite (along with minor rhyodacite), mostly emplaced fragmentally as fallout, pyroclastic flows, and derivative debris flows (Crandell, 1987; Scott, 1988, 1989; Mullineaux, 1996). The largest single eruption recognized took place ~3.5 ka, issuing ~4 km^3 of magma as plinian fallout and pyroclastic flows. Andesite and basalt are mainly limited to the young composite stratocone, which was constructed during the last 2.5 kyr, laced with dacite domes (fig. 12), and eviscerated by sector collapse in 1980 (Lipman and Mullineaux, 1981; Hopson and Melson, 1990). Partly concealed by the young cone are remnants of episodically emplaced dacite dome complexes as old as 28 ka, sources of a stratigraphically complex fragmental apron that has permitted exceptionally detailed documentation and age-calibration of the volcano's eruptive history (Mullineaux and Crandell, 1962, 1981; Hyde, 1975; Crandell, 1987; Hopson and Melson, 1990; Mullineaux, 1996). It was long thought that the earliest activity at Mount St. Helens was about 40 to 50 ka, but recent fieldwork and dating has identified remnants of dacite domes and fragmental deposits from at least two older episodes at 300 to 250 ka and 160 to 35 ka (Clynne and others, 2005, in press). Extending as far as 10 km southwest of the modern edifice, these older dome clusters were ravaged by glacial erosion and by a late Pleistocene debris avalanche larger than that of 1980. In addition to the amphiboles and pyroxenes typical of younger St. Helens dacites, the products of these early episodes (preserved as fallout, domes, fragmental flows, and avalanche deposits) commonly also contain quartz and biotite phenocrysts, both of which are rare elsewhere in the Cascades. Most rocks of all ages at Mount St. Helens are distinctively phenocryst-rich, carrying 20 to 40 percent plagioclase, and most products of the volcano are notably rich in Na.

Mount St. Helens dacites provide one of the clearest examples in the Cascades of focused intracrustal melting (Hildreth, 1981a; Halliday and others, 1983; Smith and Leeman, 1987, 1993; Dawes, 1994; Green, 1994a; Conrey, 2002). Extensive partial melting of deep young mafic crust results in extraction of voluminous dacitic magma, entrapment of most batches of the mantle-derived basalt that promotes the melting, and repeated replenishment-mixing that maintains a zoned or heterogeneous reservoir and produces the hybrid andesite intermittently permitted to erupt (Hopson and Melson, 1990; Smith and Leeman, 1993). Petrologic studies suggest upper-crustal magma reservoirs at 6 to 12 km depth (Pallister and others, 1992), with water-rich cummingtonite dacites at temperatures <800°C and hornblende-hypersthene dacites at 850 to 920°C with lower water contents (3 to 5 wt%) (Rutherford and others, 1985; Geschwind and Rutherford. 1992; Gardner and others, 1995). Gabbroic inclusions, many of them carrying interstitial glass, are common in St. Helens dacites (Heliker, 1995); some are probably partially melted fragments of Tertiary plutonic rocks (M.A. Clynne, work in progress), and some may be cumulates related to the mafic magmas that began penetrating the shallow dacitic reservoir during the last 2,500 years.

In considering the complex distribution of volcanoes within this segment of the Cascades, it should be kept in mind that during the early eruptive histories of nearby Rainier, Adams, Hood, and Indian Heaven, Mount St. Helens had not yet come into existence; and, although its eruptive activity may have started around 300 ka, its output rate remained low until after 28 ka (Clynne and others, 2005, in press).

Indian Heaven Volcanic Field

Indian Heaven (fig. 13), centered 30 km southwest of Mount Adams, is a 450-km^2 volcanic field consisting principally of coalescing mafic shields and a scattering of cinder cones and tuyas (Hammond and Korosec, 1983; Korosec, 1989). Although vents are also dispersed some 20 km east to west, about half of the 50 known vents (including the most productive ones) define a 30-km-long constructional highland (fig. 13) that trends N10°E, roughly parallel to (but 15-20 km west of) the Cascade axis of southern Washington and northern Oregon (fig. 8). Eruptive activity extended from middle Pleistocene to Holocene, the latest eruption (9 ka) being that of Big Lava Bed (0.9 km^3) at the south end of the field. Contrary to older estimates of far greater longevity, virtually all Indian Heaven units exposed have been shown to be normally polarized (Mitchell and others, 1989), thus younger than 780 ka, the only exception recognized being the lowest lavas in the eroded core of Gifford Peak (Korosec, 1989). The volcanic field has an eruptive volume of 60 to 80 km^3, at least 80 percent of which is true basalt, making Indian Heaven the most voluminous field of Quaternary basalt anywhere in the Cascades north of the Newberry Volcanic Field in central Oregon. Indian Heaven basalts include low-K HAOT, calcalkaline, shoshonitic, and alkaline intraplate varieties. Subor-

Figure 12. North side of Mount St. Helens (2,950 m) in 1972, before it was wrecked by the sector collapse and ensuing eruption of 18 May 1980. The elegant cone had been constructed by central eruptions of andesitic (and fewer mafic) lavas only during the last 2,500 years, succeeding what had long been a dacite domefield. Several dacite domes continued to be emplaced during late Holocene growth of the cone; those visible in this image are Dogs Head dome on left skyline; Sugar Bowl dome directly below it; Goat Rocks dome right of center, halfway up; and West dome on right skyline. The Summit dome, exposed as the thin dogleg cleaver (The Boot) extending to the central skyline, was emplaced in the 17th Century. Goat Rocks dome and the fan of pyroclastic deposits and leveed andesitic lava flows below it were emplaced in the 19th Century, representing the last pre-1980 eruptive episode. The two midslope (andesitic) cleavers between Dogs Head and Goat Rocks domes were called the Big and Little Lizards. Relief visible in image 1,850 m. (Copyrighted photograph by and courtesy of Darryl Lloyd; taken in 1972.)

dinate basaltic andesite and sparse andesite (as much as 59% SiO_2) erupted from several vents along the crest, but dacite is lacking (Hammond and Korosec, 1983; Smith, 1984; Leeman and others, 1990, 2005; Hildreth and Fierstein, 1995). In some respects, Indian Heaven is the "inverse" of nearby Mount St. Helens, in that voluminous basalt has passed through the crust in numerous conduits without engendering crustal melting on a large scale.

Diffuse Forearc Volcanism

Distributed forearc volcanism is as well developed in this arc segment as anywhere in the world, certainly more strikingly than elsewhere in the Quaternary Cascades. Scattered as far as 90 km west of the Cascade axis, the abundant forearc volcanoes provide perhaps the strongest volcanological rationale for postulating a segment boundary at the southern limit of their distribution (fig. 8). Radiometric dating indicates sporadic but persistent activity ranging from about 2.5 Ma to as young as 57 ka (Conrey and others, 1996; R.C. Evarts, work in progress, 2007). Most of the nearly 150 forearc vents can be lumped broadly into three main areal groups:
(1) a large region of at least 60 scattered vents extends east-west on both sides of the Columbia River and through the city of Portland (Allen, 1975; Conrey and others, 1996); (2) southwest of Indian Heaven, a southeast-trending 40-km-long diffuse belt of at least 22 vents includes Marble Mountain, Bare Mountain, West Crater, and Trout Creek Hill and has had at least three postglacial eruptions (Wise, 1970; Hammond, 1990); and (3) a northeast-trending diffuse zone of about 30 small volcanoes extends 90 km from Battle Ground maar (past the Mount St. Helens vent cluster) to an array of basaltic vents near the Cispus River and Blue Lake (Swanson and others, 1989; Swanson, 1994, 1996; Evarts and Swanson, 1994).

A few of these 150 scattered forearc volcanoes are small shields, thus perhaps polygenetic, but most are monogenetic cones and lava flows. Although many consist of basaltic andesite and a few are andesitic (Swanson, 1989; Smith, 1993; Conrey and others, 1996; Leeman and others, 2005), most are basaltic—including HAOT, alkaline, calcalkaline, shoshonitic, and intraplate varieties. Tumtum Mountain, a small rhyodacite dome (68-70% SiO_2), which stands alone 32 km southwest of Mount St. Helens, was formerly thought to be Pleistocene (Mundorff and Eggers, 1988) but is now dated as Miocene (R.C. Evarts, work in progress).

Contrasts with Garibaldi Volcanic Belt

As defined by vent distribution, the across-arc width of the Quaternary volcanic region of southern Washington and northernmost Oregon is 5 to 10 times greater than the GVB (figs. 3, 8). The number of Quaternary volcanoes is correspondingly greater, with 127 vents identified in the 375-km-long GVB segment and 412 in the 190-km-long Rainier-to-Hood segment (table 1). The trend of the GVB roughly parallels the strike of the subducting plate, but any lower-plate influence on volcano distribution in southern Washington is obscure at best. Two stratocones, a concentrated basaltic volcanic field, and 150 scattered forearc volcanoes lie west of the broad and continuous Hood-Adams-Goat Rocks-Tumac Mountain axis, whereas virtually no vents lie significantly seaward of the narrow and discontinuous GVB axis. Vent alignments and elongate zones of high vent density are locally conspicuous in southern Washington, suggesting the influence of upper-crustal stress field and structure on magma transport. Such trends are close to northerly in the Mount Adams, Indian Heaven, and central Simcoe Mountains Volcanic Fields but N35°E near Mount St. Helens and N35°W for Quaternary cinder cones in the southern Simcoe Mountains.

Dacite and rhyodacite are the principal eruptive products of the GVB, but in the Rainier-to-Hood segment Quaternary rhyodacite is almost absent and dacite is dominant only at Mount St. Helens. Eruptive volumes are hard to compare, owing principally to the greater severity of glacial erosion and the prevalence of explosive silicic volcanism in the GVB. At least two-thirds of the material erupted by Mount St. Helens was dispersed as fallout or deposited beyond the stratocone as pyroclastic and debris flows. The same is likely for all five major GVB centers, where fallout and fragmental flows would commonly have been deposited on the Cordilleran ice sheet or removed by its next advance. More than half (perhaps two-thirds) of the Quaternary material erupted from the Mount Baker-Kulshan Caldera locus has been stripped (Hildreth, 1996). Farther south, I estimate that the preserved edifice of Mount Adams represents 50 to 70 percent of the volume erupted, and comparable surviving fractions seem reasonable

Figure 13. Indian Heaven Volcanic Field, viewed southwestward from ~1,850 m elevation on southwest slope of Mount Adams (~1 km east of Horseshoe Meadow). The three skyline peaks with traces of snow are (left to right) Lemei Rock shield (also called Lake Wapiki volcano; 1,806 m), Bird Mountain (1,739 m), and Sawtooth Mountain (1,632 m); to the left of Lemei Rock are Berry Mountain (1,525 m) and (at left edge) Red Mountain (1,513 m); all five consist of middle or late Pleistocene basalt and belong to the north-trending vent zone that dominates the volcanic field (fig. 8). East Crater and Gifford Peak, additional members of the alignment, are hidden by Lemei Rock. Broad swell in middle distance is called Sleeping Beauty; it consists of Tertiary intermediate volcanic and sedimentary rocks and is marked by a prominent intrusive plug (at left end), four fine examples of clearcuts, and several inconspicuous Pleistocene scoria cones marginal to the Indian Heaven field (Hildreth and Fierstein, 1995). Forested foreground is Stagman Ridge, which consists of lavas from Mount Adams and is separated from Sleeping Beauty by the canyon of the White Salmon River. Relief visible in image is ~800 m. (Copyrighted photograph by and courtesy of Darryl Lloyd; taken in 1970.)

for Hood and Rainier. Sherrod and Smith (1990) tabulated present-day volumes of 651 km^3 for Quaternary products of the Rainier-to-Hood segment and 194 km^3 for the GVB, a ratio of 3.4 to 1. The ratio of eruptive volumes may have been smaller than 2 to 1 and perhaps close to unity.

Oregon Cascades Segment

At least 1,054 Quaternary volcanoes (table 1) define an uninterrupted vent belt 25 to 50 km wide that straddles the Cascade crest for 340 km south of Mount Hood (figs. 14, 15). An additional 450 (or more) Quaternary vents are present on the great Newberry edifice just east of the Cascades. The continuous axial belt ends 30 km north of the California border, where a 64-km gap (containing many Tertiary but hardly any Quaternary volcanoes) separates it from the Quaternary volcanic region around Mount Shasta. The north end of the Oregon segment is placed at Frog Lake Buttes (~17 km south of Mount Hood), within a limited stretch of the Cascade axis where few centers are younger than early Quaternary and seaward of which the region of widespread forearc volcanism terminates (Sherrod and Smith, 2000). In contrast to the Portland region, in all of Oregon south of 45˚15'N only about ten Quaternary forearc volcanoes have been recognized (compare fig. 8 with figs. 14, 15; Sherrod, 1990a; White, 1992). About midway along the Oregon segment, with no discontinuity or change in width, there is a slight right-stepping dogleg in the Quaternary vent belt (fig. 14), from north-south in northern (and southern) Oregon to N15-20°E for the 40-km reach south of Crane Prairie Reservoir (43°46'N).

For a convergent-margin volcanic belt, the density of Quaternary volcanoes in the Oregon Cascades is extraordinary (1,054 vents in ~9500 km^2; table 1). The only comparably extensive areas with such concentrations of Quaternary arc volcanoes are in Michoacán (Mexico) (Hasenaka and Carmichael, 1985; Hasenaka, 1994), southern Washington and northern California (table 1), and a few short reaches of the Chilean Andes (Moreno-Roa, 1976; Servicio Nacional de Geología y Minería, 1982).

Most of the Oregon Cascade volcanoes are scoria cones, small shields, and fissure-fed lava fields, the great majority composed of basaltic andesite. Basalt and andesite are common as well but subordinate. More than 50 of the Oregon volcanoes are substantial shields 3 to 10 km across that exhibit a range of profiles from gentle to steep. Steeper shields grade to lava cones and, with increasing accumulation of fragmental ejecta at the core, into mafic composite stratovolcanoes. Stratocones consisting principally of basaltic andesite are common in this segment, including Mounts McLoughlin, Thielsen, Bachelor, and Washington, Three Fingered Jack, Black Butte, Black Crater, and North Sister. Stratocones that likewise contain substantial basaltic andesite but also extend to andesitic or more silicic products include Broken Top, Middle Sister, Diamond Peak, and Mount Bailey. Major stratocones made up predominantly of andesite and more silicic material are Mount Jefferson, South Sister, Cappy Mountain (Williams, 1957), and Mount Mazama (as well as Mount Hood, just north of the segment).

Lesser andesitic centers, uncommon in Oregon, include Badger Butte and Frog Lake Buttes in the north (fig. 14), Brown Mountain and Pelican Butte in the south (fig. 15), Crater Butte at 43˚30'N, and minor clusters near Santiam Pass (44˚25'N) and south and west of Summit Butte (45˚N) (Sherrod and Smith, 2000; Webster, 1992). Isolated dacite volcanoes are fewer still, limited to Frog Lake Buttes, dome clusters near Mount Jefferson, First Creek (southeast of Three Fingered Jack), Bench Mark Butte, three tiny domes near Wickiup Reservoir, Mule Peak, and flows near Salt Creek (fig. 14) west of Maiden Peak (Taylor and others, 1987; Sherrod, 1991; Conrey, 1991; Sherrod and Scott, 1995; Sherrod and Smith, 2000). As in Washington, most dacite erupted from the flanks or summits of large stratovolcanoes.

Quaternary rhyodacites (and minor rhyolite) are important in the Oregon segment, much less so than in the Garibaldi Volcanic Belt but far more so than in southern Washington. Such evolved products are restricted, however, to a few major centers—Mount Jefferson, Tumalo, Three Sisters, Cappy Mountain (Burn and Clover Buttes), and Mount Mazama (Taylor and others, 1987; Scott, 1987; Bacon and Druitt, 1988; Conrey, 1991; Hill, 1991; Nakada and others, 1994; Sherrod and Smith, 2000). In contrast to the arc itself, rhyolites are numerous in the rear-arc Newberry Volcanic Field and elsewhere across much of the Oregon Basin and Range Province.

For convenience of discussion, the Oregon segment is here divided into six reaches or subsegments (figs. 14, 15) designated I to VI from north to south.

Jefferson Reach (I)

The northern 75 km of the Oregon segment (fig. 14), from Frog Lake Buttes (45˚13'N) to South Cinder Peak (44˚34'N), contains at least 175 Quaternary volcanoes but is the narrowest stretch of the Quaternary vent zone anywhere south of Mount Rainier. Only 25 km wide, this reach contrasts drastically with the adjacent region to the north, where Quaternary volcanoes are scattered from east of Mount Hood to west of Portland, 105 km from east to west. The northernmost 30 km of this narrow axial reach is also atypical (for the Oregon Cascades) in having few centers younger than early Pleistocene and in having several minor andesitic and dacitic volcanoes scattered within the dominating array of mafic shields (Sherrod and Smith, 2000). Just south of the andesite-dacite dome cluster at Frog Lake Buttes, the axis is dominated by an array of coalescing basaltic andesite shields that include Clear Lake Butte, Mount Wilson, North Wilson, Wests Butte, and Summit Butte, among which are scattered ~20 mafic and andesite-dacite scoria cones and domes (Sherrod and Scott, 1995), few of which are likely to be younger than 500 ka. Because the Cascade crest here is atypically low (1,100-1,500 m) for Oregon, these older centers are heavily soil-mantled and only locally glaciated (Sherrod, 1990b). From Pinhead Buttes (44˚56'N) southward, however, the rest of this 75-km reach (and indeed the next 250 km of the Cascade axis) is capped by a continuous array of middle Pleistocene and younger volcanic centers, generally glaciated, among which the largest mafic shields are Sisi and Olallie Buttes (Sherrod, 1990b).

Mount Jefferson

Mount Jefferson (3,199 m), largest volcano in this reach but one of the smaller andesite-dacite stratocones in the Cascades, was built in several stages between ~280 ka and latest Pleistocene, much of it around 70 ka (Conrey, 1991). The youngest additions to the main cone may have been in the interval 30 to 20 ka (fig. 16). Glaciated remnants of distributed andesite-dacite precursors east and west of the modern edifice, however, suggest longevity of at least 1 Myr for the Jefferson andesite-dacite locus; moreover, a few other evolved loci of pre-Quaternary age are recognized within 10 km (Conrey, Hooper, and others, 2001). Present-day edifice volume was estimated to be ~14 km^3 by Sherrod and Smith (1990) or 25 km^3 by Conrey (1991), but in view of recurrent glacial erosion and dispersal of rhyodacitic plinian fallout and pyroclastic flows (Yogodzinski and others, 1983; Conrey, 1991), eruptive volume could well have been as much as 30 km^3.

Around the main cone (which is largely andesite-dacite with 58-64 percent SiO_2), and as far as 13 km north and 7 km south of it, andesite and dacite also erupted from at least 35 lesser vents, building many domes, small shields, and lava aprons. About 8 additional vents produced rhyodacite lavas and unknown volumes of pyroclastic ejecta that have been extensively stripped. North and south of this 20-km-long zone transecting Mount Jefferson, the eruptive dominance of basaltic andesite resumes, as exemplified by Olallie Butte, Three Fingered Jack, and dozens of lesser volcanic centers. Conrey (1991) emphasized the longevity of the andesite-dacite anomaly where, within a 20×8-km axial strip, mafic lavas have largely been excluded—not only during the lifetime of the Mount Jefferson edifice but throughout the Quaternary (and perhaps during much of Pliocene time as well). Conrey, Hooper, and others (2001) interpreted the strip as a long-lived focus of intracrustal melting and magma storage and provided evidence for ubiquitous mixing between mafic and silicic magmas in producing the andesites and dacites. Eruption of postglacial basaltic andesite from four monogenetic vents 6 to 12 km south of Mount Jefferson (Scott, 1977) suggests that the system remains potentially active.

Sisters Reach (II)

From South Cinder Peak (44˚34'N) to Crane Prairie Reservoir (43˚47.5'N), the next reach of the Quaternary vent zone broadens markedly, expanding abruptly to 35 km, then gradually to 45 km toward its south end—where most vents lie well east of the Cascade crest (fig. 14). This 90-km-long subsegment contains at least 466 Quaternary volcanoes. It continues the high vent density of the narrower Jefferson reach and has roughly double that of the neighboring reach to the south (table 1). Nowhere in the Cascades are vent alignments more conspicuous than in this reach, where lines of mafic volcanoes (and even chains of rhyolite vents) form several north-trending arrays (Bacon, 1985; Hughes and Taylor, 1986; Scott, 1987; Scott and Gardner, 1990, 1992). At the leading western end of the propagating crustal melting anomaly that has crossed Oregon since the mid-Miocene (MacLeod and others, 1975; Jordan and others, 2004), this reach is also extraordinary (for the Quaternary Cascades) in having numerous eruptive units of true rhyolite, which is rare elsewhere along the arc proper (though common at rear-arc centers).

Among the many mafic volcanoes, basaltic andesite is again dominant, but true basalt is more common in this reach than elsewhere in the Oregon Cascades. More than 30 mafic shields and stratocones, ranging in age from early Pleistocene to Holocene, are continuous along the entire length of the subsegment. Larger ones include Three Fingered Jack, Maxwell Butte, Hoodoo Butte, Cache Mountain, Mount Washington, Belknap Crater (fig. 17), Scott Mountain, Black Crater, Black Butte, Trout Creek Butte, North Sister, Little Brother, The Husband, Substitute Point, Sphinx Butte, The Wife, Burnt Top, and the shields of the Bachelor chain, as well as Tumalo, Koosah, Horse, Packsaddle, Williamson, Irish (30 km^3), Lookout, and Cultus Mountains (Williams, 1957; Taylor and others, 1987; Sherrod, 1990b; Sherrod and Smith, 1990, 2000).

Postglacial mafic eruptions, more common here than anywhere else in the Cascades, include a lava flow adjacent to South Cinder Peak, the Nash Crater-Lost Lake cone cluster, Sand Mountain chain, Inaccessible Cone chain, Blue Lake cone, Belknap shield complex (fig. 17), and several additional monogenetic scoria cones or chains with associated lava flows (Williams, 1957; Taylor, 1968; Black and others, 1987; Gardner, 1994; Sherrod and others, 2004). In the area of McKenzie and Santiam Passes (fig. 14), more than a dozen separate mafic eruptions are radiocarbon-bracketed between 4.5 and 1.1 ka (Sherrod and others, 2004), representing a 15-km^3 distributed mafic pulse in the late Holocene (Taylor, 1968). Moreover, just south of there, peripheral to the Three Sisters, several additional mafic units that include Sims Butte, Cayuse Crater, LeConte Crater, the Mount Bachelor chain, the Egan Cone cluster, and the Katsuk-Talapus chain may all have erupted in the interval 18 to 8 ka, during deglaciation or early postglacial time. Near the south end of the Sisters Reach, a postglacial basaltic lava flow erupted on the east flank of (much older) Sitkum Butte.

Much of the andesite and dacite in this reach erupted from central or high flank vents of four large volcanic centers—Broken Top, Middle and South Sisters, and the mid-Pleistocene Todd Lake Volcano south of Broken Top (Taylor, 1978; Taylor and others, 1987; Webster, 1992), but several small dispersed intermediate volcanoes are present as well. Isolated among the coalescing mafic volcanoes, phenocryst-poor intermediate domes include dacitic Bench Mark Butte

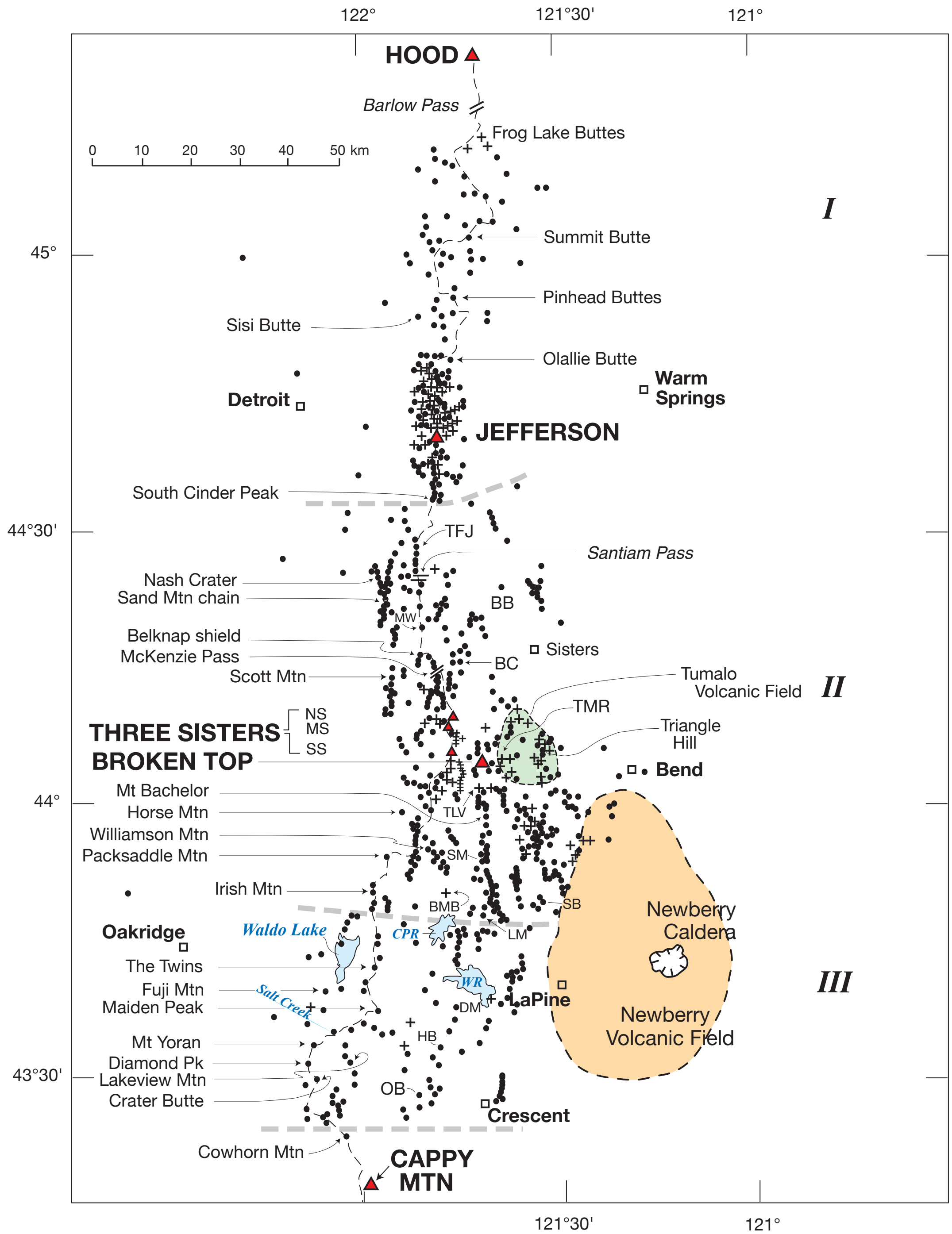

Figure 14. Northern part of Oregon segment of the Cascade arc, showing distribution of 760 Quaternary volcanic vents and subdivided into reaches (I, II, III, by gray dashed east-west lines), as discussed in text. Vent symbols as in figures 3 and 8. Axial dashed line is Cascade topographic crest. Small green ovoid encloses vents for silicic units attributed to Tumalo Volcanic Field. Large orange ovoid is generalized outline of rear-arc Newberry vent field, which encompasses at least 450 additional Quaternary vents, after MacLeod and others (1995). Note the atypical abundance of silicic vents (predominantly rhyolite) in the Cascade arc northwest of Newberry. Abbreviations from north to south: TFJ, Three Fingered Jack; BB, Black Butte; MW, Mount Washington; BC, Black Crater; TMR, Tam McArthur Rim; NS, North Sister; MS, Middle Sister; SS, South Sister; TLV, Todd Lake volcano; SM, Sheridan Mountain; BMB, Bench Mark Butte; SB, Sitkum Butte; LM, Lookout Mountain; CPR, Crane Prairie Reservoir; WR, Wickiup Reservoir; DM, Davis Mountain; HB, Hamner Butte; OB, Odell Butte.

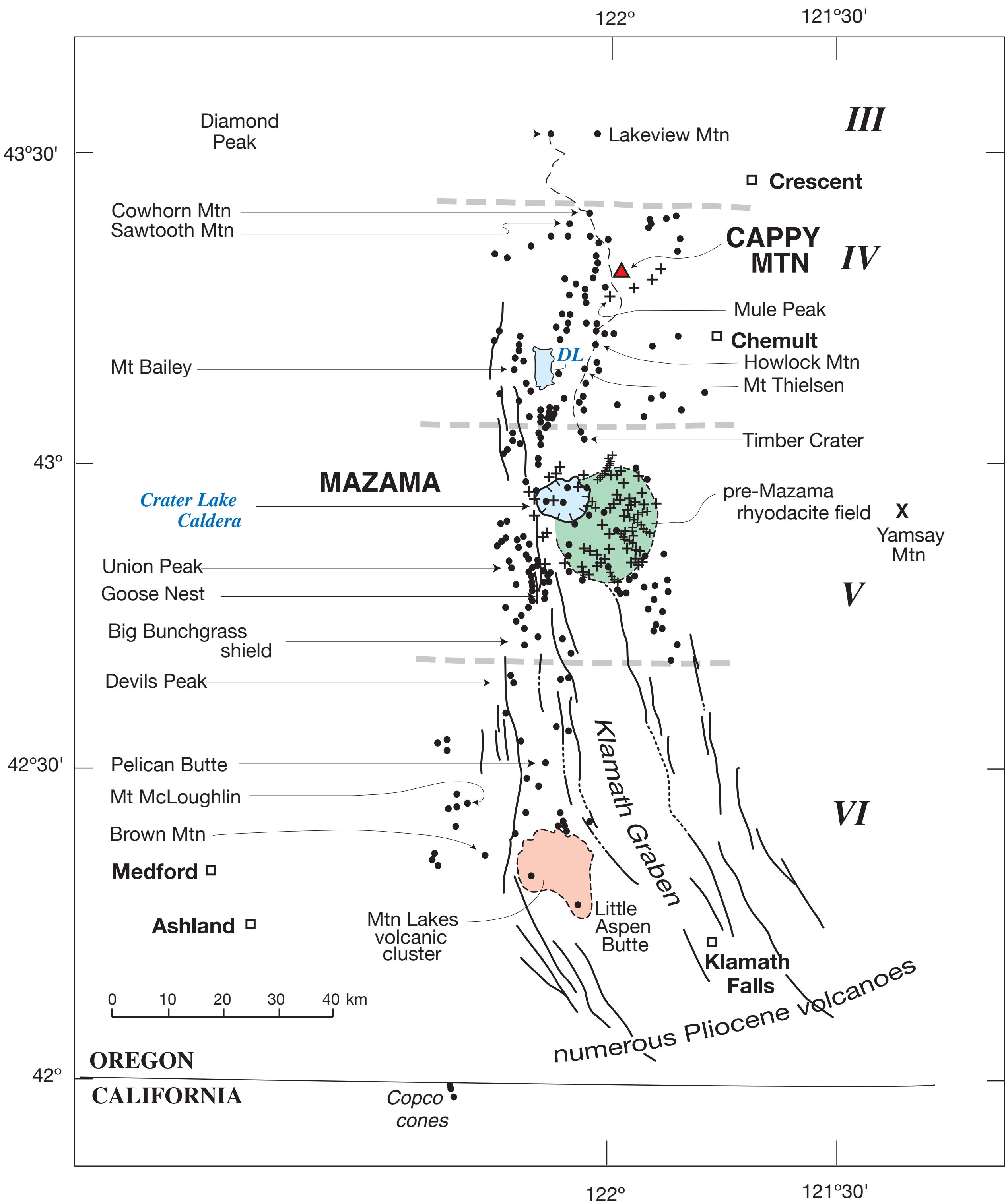

Figure 15. Southern part of Oregon segment of the Cascade arc, showing distribution of 294 Quaternary volcanic vents and subdivided into reaches (IV, V, VI, by gray dashed east-west lines), as discussed in text. Vent symbols as in figures 3 and 8. DL, Diamond Lake. Axial dashed line is Cascade topographic crest (poorly defined in Crater Lake area and southward). Green field encloses vents for mid-Pleistocene pre-Mazama rhyodacites. Yamsay Mountain is a major volcanic locus of late Tertiary age, and the Mountain Lakes volcanic cluster (pink field) may be of both Pliocene and Quaternary age. Area around and south of Klamath Falls has numerous well-preserved mafic shields and scoria cones, all or most older than 2 Ma (Sherrod and Pickthorn, 1992).

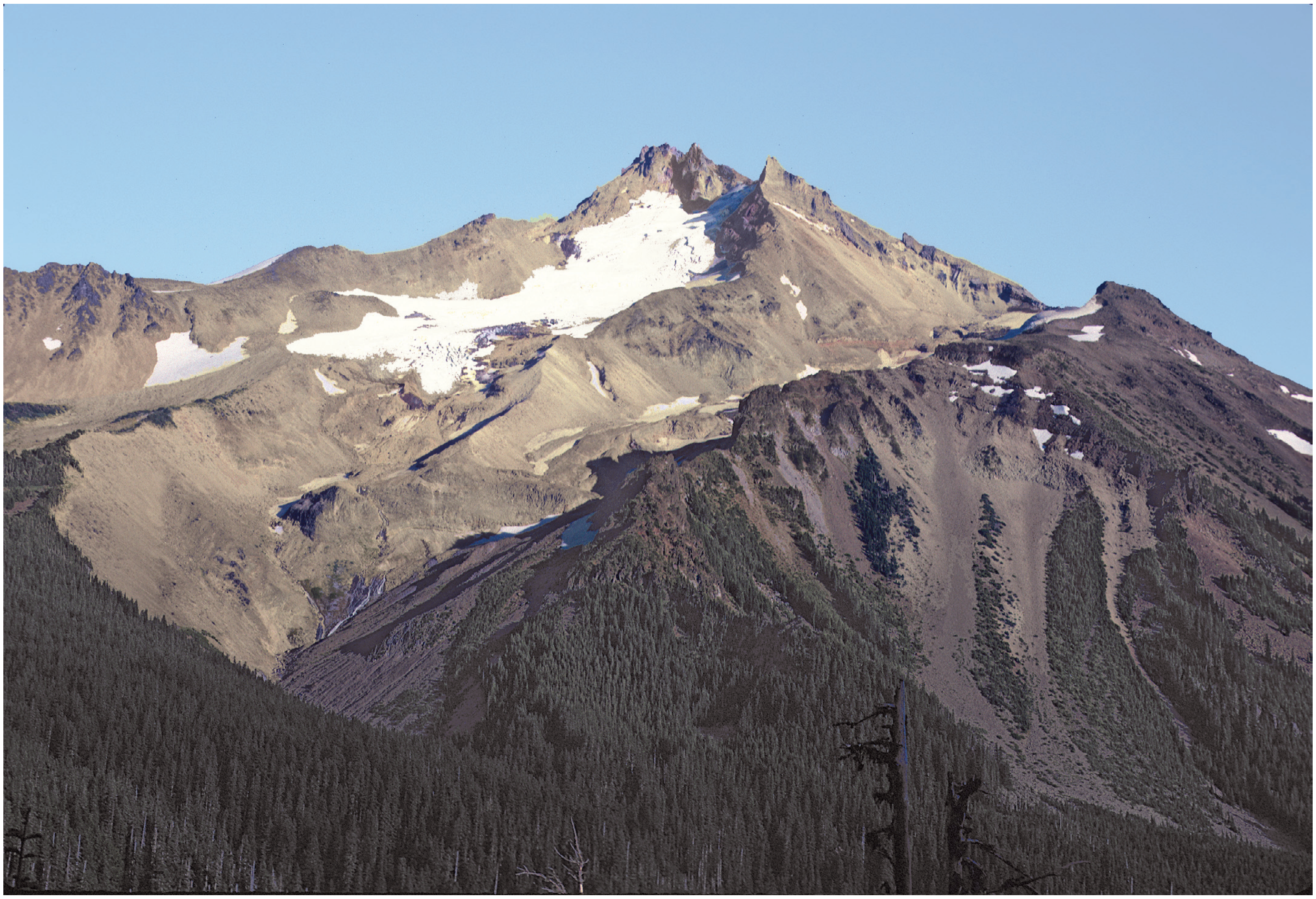

Figure 16. North face of Mount Jefferson (3,199 m) and north and northwest ridges of the edifice, viewed toward the south-southeast. Upper part of mountain is carved from thick andesite-dacite lavas younger than 70 ka and some as young as the last major glacial interval. Dome complex on far left skyline (28±9 ka) is overlain by uppermost package of summit lavas, which gave a $^{40}Ar/^{39}Ar$ age of 20.5±4 ka (R.M. Conrey, unpub. data, 2007). There have been no postglacial eruptions of the main edifice. True summit is largely hidden slightly beyond the apparently uppermost crags of the north summit. Relief visible in image is 1,500 m. (Photograph by author taken in August 1988.)

(65.5% SiO_2) in the south and andesitic Hogg Rock and Hayrick Butte (both 60% SiO_2) near Santiam Pass, all three of late Pleistocene age (Taylor, 1981; Black and others, 1987; Hill and Priest, 1992). In upper First Creek, just northeast of Santiam Pass, an early Pleistocene phenocryst-poor lava and tuff include both dacite and andesite, and several middle Pleistocene andesitic scoria cones are present in the vicinity of Triangle Hill (Sherrod and others, 2004). Kokostick Butte, a phenocryst-rich dacite coulee with several satellite vents (63% SiO_2), erupted 7 km south of South Sister at ~27 ka. The Four-in-One Cone chain of six andesitic scoria cones (56-59% SiO_2) erupted 5 km northwest of North Sister at ~1.9 ka. Finally, the Collier Cone (at the northwest toe of North Sister), one of the youngest eruptive units in the reach (~1.5 ka), released an apron of lava flows as long as 13 km that range from 56 to 65 percent SiO_2 (Schick, 1994).

The middle part of this reach contains the second most extensive field (behind Lassen) of silicic volcanic rocks in the Quaternary Cascades (fig. 14). Within a 20×25-km area extending from the Three Sisters to well east of Broken Top and Mount Bachelor, there are no fewer than 50 known or concealed eruptive sites for rhyolitic and rhyodacitic lavas and ejecta (Taylor, 1978, 1987; Taylor and others, 1987). Most of the silicic units are middle and late Pleistocene, but ~20 vents adjacent to South Sister produced Holocene rhyolite during two or three eruptive episodes at 2.3-2.0 ka (Scott, 1987). Because many of the more easterly silicic units are middle Pleistocene (Hill, 1991), still more silicic vents may be hidden by younger lavas and till. Although rhyodacite (68-72% SiO_2) is fairly common in the Cascade arc, Quaternary rhyolite (72-77% SiO_2) is rare, significant only at Mount Garibaldi, in the Lassen region, and here in the Three Sisters-Broken Top-Tumalo area. As widely noted for “bimodal” extensional volcanic fields elsewhere, the elevated proportions of true rhyolite and true basalt in the Sisters reach (at the expense of the intermediate compositions dominant in adjacent reaches)

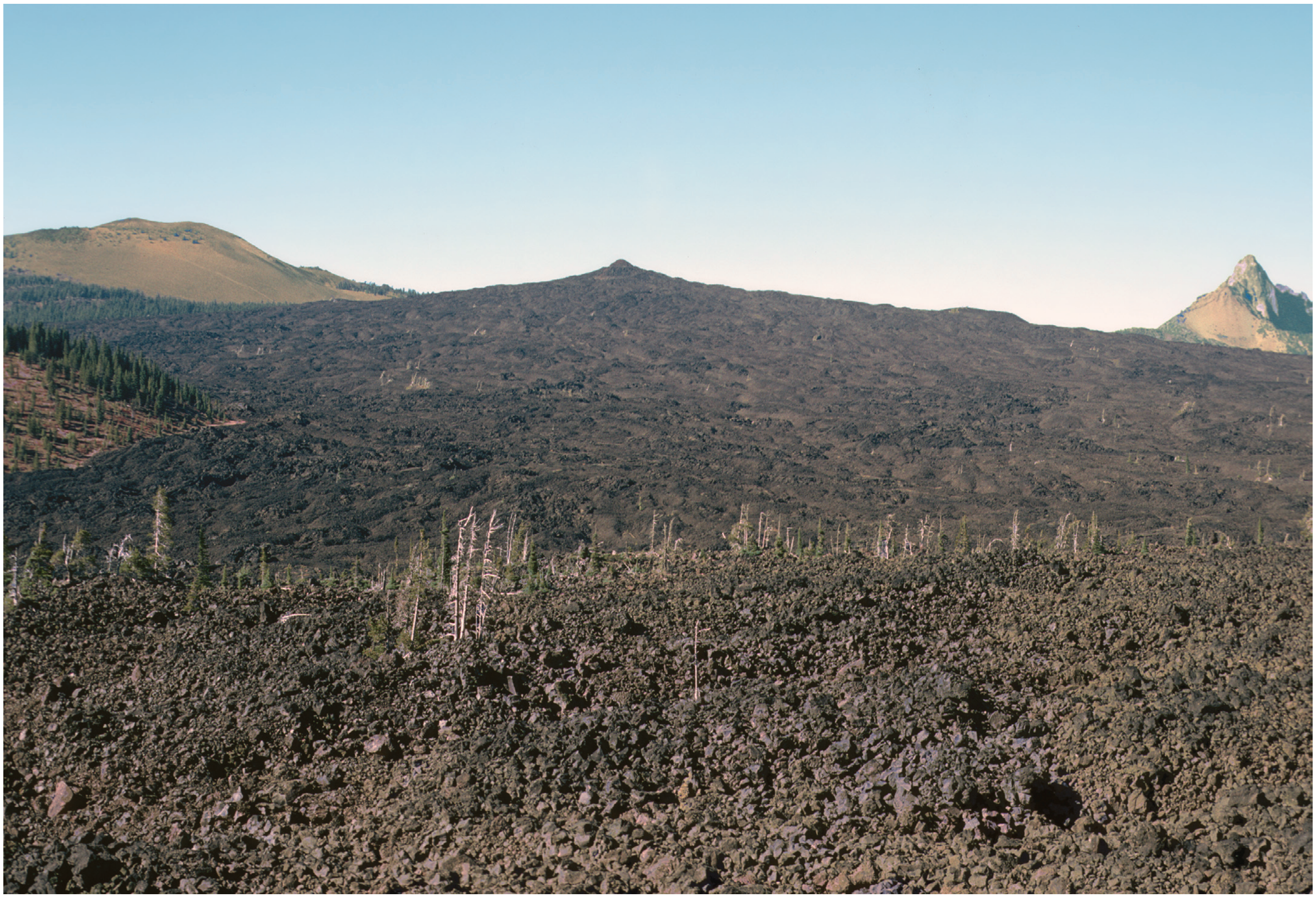

Figure 17. Little Belknap shield (~3 ka) flanked by 150-m-high Belknap Crater scoria cone on left and middle Pleistocene Mount Washington in right distance. Little Belknap is a flank shield built on the much larger Belknap shield, which had several secondary vents in addition to the summit scoria cone and was active both before and after growth of Little Belknap (from before 3 ka until about 1.3 ka). Summit of Belknap is 500 m higher than the camera and summit of Little Belknap 350 m higher. The two represent examples of shields with and without significant scoria cones, perhaps because the magma that fed Little Balknap had extensively degassed prior to shallow lateral transport to the lower flank vent. Mount Washington (2,376 m), 8 km north and nearly 800 m higher than the camera, is a glacially sculpted mafic stratocone (like North Sister, Three Fingered Jack, and Mount McLoughlin) with a broad apron of mafic lavas; its summit is part of a 400-m-wide central intrusion surrounded by an eroded collar of radially dipping lavas and ejecta cut by many dikes. (Photograph by author taken in August 1988.)

probably reflects penetration of the Cascade arc by whatever combination of mantle flow and lithosphere extension has guided rhyolitic volcanism westward across the High Lava Plains and Newberry since the Miocene (MacLeod and others, 1975; Jordan and others, 2004).

Tumalo Volcanic Field (Bend Highland)

The area containing distributed silicic lavas east of Broken Top was called the “silicic highland” by Taylor (1978, 1987) and later termed the “Tumalo volcanic center” by Hill and Taylor (1989, 1990). The 15×20-km area (fig. 14) includes andesitic and mafic scoria cones as well as numerous rhyolitic and rhyodacitic lava flows and domes. It is thought to be the source of several rhyolitic to andesitic ignimbrites and plinian fall deposits exposed near the towns of Tumalo and Bend (Taylor, 1981; Hill and Taylor, 1990; Mimura, 1992; Taylor and Ferns, 1994) that erupted between ~650 ka and ~250 ka (Sarna-Wojcicki and others, 1989; Gardner and others, 1992; Lanphere and others, 1999; Sherrod and others, 2004). Owing to extensive cover by younger mafic lavas and glacial deposits, neither the integrity of the Tumalo volcanic “center” nor its western limit is well defined. Because silicic lavas of Todd Lake Volcano and Tam MacArthur Rim, both adjacent to the Broken Top edifice (Williams, 1944; Taylor, 1978) erupted during the same time interval (Hill, 1991) as the Tumalo volcano center (as defined by Hill and Taylor, 1990), they could likewise be considered parts of an extensive mid-Pleistocene silicic volcanic field. Of the four nearby stratovolcanoes, South and Middle Sisters are now known to be wholly younger

(Fierstein and others, 2003) than the distributed activity in the "silicic highland" (Taylor, 1978, 1987, 1990a; Hill and Taylor, 1990; Sherrod and others, 2004), but the eruptive lifetimes of North Sister and Broken Top overlapped with it.

Volumes of three extensive ignimbrites, patchily but widely preserved in the periphery of the highland, are poorly known but likely to be in the range 5 to 10 km^3 each. Such volumes are near the usual threshold for caldera formation, so the Tumalo Volcanic Field might or might not contain an unrecognized filled caldera, obscured by products of younger eruptions. Following Hill and Taylor (1990), Sherrod and others (2004) suggested a 5-km-wide buried source area centered on Triangle Hill (fig. 14), whereas Conrey and others (2002) suggested a location 6 km farther west (near Tam MacArthur Rim) as a possible source for one of them. Pinning down the source vents for the three Tumalo ignimbrites (the Desert Springs, Tumalo, and Shevlin Park Tuffs) remains one of the more challenging unresolved problems in Cascades volcanology.

Broken Top

Only 5 km southeast of South Sister, Broken Top was a modest middle Pleistocene stratovolcano (eruptive volume 7-10 km^3), active in the interval from about 300 to 150 ka and long extinct. Its mafic apron lavas bank against Todd Lake Volcano (460±30 ka; Hill, 1991), and they sandwich thick rhyodacite lavas at Tam MacArthur rim (213±9 ka; Hill, 1991) and at Squaw Creek Falls (169±2 ka; USGS work in progress). Although dominantly basaltic andesite (Webster, 1992), subordinate products of Broken Top range from andesite to rhyodacite. Internal structure of the ice-sculpted edifice (fig. 18) is well exposed on cirque headwalls, radial ridges, and in a large southeast-facing amphitheatre of uncertain origin (Taylor, 1978; Grubensky and others, 1998). **Cayuse Crater** is an unrelated postglacial basaltic (50-52% SiO_2) complex of lava flows and scoria cones that erupted ~11 ka on the southwest apron of Broken Top. Like Mount Baker, Goat Rocks, and Brokeoff, Broken Top was a stratocone built at the margin of a large silicic complex.

Three Sisters

These three modest contiguous stratocones (Williams, 1944), conventionally lumped sororally, could hardly display less family resemblance. North Sister is a middle Pleistocene monotonously mafic edifice, Middle Sister a basalt-andesite-dacite cone largely built in the interval 37 to 14 ka, and South Sister a bimodal rhyolite-andesite edifice that has alternated compositional modes from 178 ka to 2 ka. For each of the three, the eruptive volume is likely to have been in the range 15 to 30 km^3, but such estimates are fairly uncertain, owing not only to glacial erosion but to doubts about the affinities and vent locations for varied apron lavas that issue from beneath bases of the two younger cones (see Taylor and others, 1987).

North Sister (3,074 m) is a glacially dissected stratocone of fairly uniform basaltic andesite (52.5-55% SiO2; Taylor, 1987; Schmidt and Grunder, 2003), sufficiently eroded to expose hundreds of dikes and sills internally. Many are zigzag or inconsistently oriented within the great pile of thin rubbly lava flows, but Schmidt (2005) observed a long-term shift from edifice-influenced radial diking toward later dominance of north-south dikes controlled by the regional stressfield. Oldest of the Three Sisters, its period of construction overlapped with that of Broken Top. A few of the distal lavas from North Sister overlie the northwesternmost remnant of the Shevlin Park Tuff, which at ~260 ka is the youngest ignimbrite of the Tumalo Volcanic Field (Lanphere and others, 1999). The oldest lava flow exposed at the south toe of North Sister yields an age of 311±23 ka (USGS work in progress), whereas higher parts of the multistage edifice may be as young as 100 ka (Schmidt and Grunder, 2003; Schmidt, 2005). It is noteworthy that so long-lived an edifice remained so compositionally monotonous (4.5-6% MgO; 0.6-0.8% K_2O) throughout its eruptive history. Much younger are late Pleistocene north-trending chains of mafic scoria cones and dike-fed agglutinate that erupted through and unconformably drape the North Sister edifice and extend ~11 km farther northward (collectively called the "Matthieu Lake fissure" by Schmidt and Grunder, 2003; Schmidt, 2005).

Middle Sister (3,062 m) is the youngest cone of the three, the present edifice having been built during the interval 37 to 14 ka, mostly 25 to 18 ka (USGS work in progress), although glaciation (persistent from late Pleistocene to the present) has sharply steepened its eastern face. The young cone has issued a range of mafic, andesitic, and dacitic lavas (52-65% SiO_2) from its central vent, as well as dacites from six flank vents (three of them high on the edifice) and andesites from three more. The largest dacite flank vent, which fills the saddle between North and Middle Sisters, built a substantial pile (informally called Prouty Point, the Black Hump, or Step Sister) of at least five coulees (64% SiO_2) dated at 27 to 18 ka. Distal mafic lavas from a buried older edifice that extend eastward beyond the limit of lavas from the modern cone yield ages of 180 to 160 ka, and a western apron of young andesite-dacite lavas (30 to 19 ka) from Middle Sister banks against glaciated mafic centers dated at 170 to 150 ka. There thus appears to have been an extended period (>100 kyr long) with little or no activity on the site prior to initiation of modern cone growth, for which eruption of the high-silica-rhyolite coulee of Obsidian Cliffs (38±2 ka) at the northwest toe of the subsequent Middle Sister edifice may have been the thermal harbinger.

South Sister (3,157 m), formerly considered the youngest stratocone in the cluster (Wozniak, 1982; Clark, 1983), began its growth well before Middle Sister. A distal dacite lava flow southeast of the cone yields an age of 178±1 ka (USGS work in progress), and an age of 93±11 ka was reported by Hill (1991) for an andesite lava flow to the northeast, although each of these units predates construction of the modern cone. During the interval 50 to 30 ka, South Sister became a rhyolite volcano consisting of numerous and varied (aphyric to phenocryst-rich) rhyolitic lava flows and domes (72-74% SiO_2) that crop out radially on the cone to eleva-

Figure 18. Broken Top mafic stratocone, inactive since 150 ka or longer, viewed northwestward. Radially dipping strata of the cone include subequal proportions of lava flows and flow breccias and of proximal agglutinate and scoria falls, nearly all having 54 to 56 percent SiO_2. Numerous mafic dikes and sills intrude the cone, and an apron of compositionally similar mafic lavas extends far outward from the cone. Skyline crags behind buttress at right are top of a central intrusion 400 m wide, also with 54 percent SiO_2. Altered core of the edifice was eviscerated by glacial erosion, probably by enlargement of an old crater (suggested by internal unconformities). Unusual orientation of the cirque, open to the southeast, might suggest sector collapse, but no avalanche deposit is recognized. Neoglacial moraine obscures small ice remnant. Orange layer on left wall is 20-m-thick dacitic pyroclastic deposit, which (along with two thinner such layers) interrupted the mafic monotony of the cone-building sequence. Relief visible in image is about 600 m. (Photograph by author taken in September 2001.)

tions within 500 m of the present summit. Around the base of the edifice, two large rhyolite domes (Kaleetan Butte and Devils Hill) at the south toe of South Sister, one near Green Lakes at the east toe, another near Chambers Lakes at the north toe, and a coulee along Squaw Creek northeast of the cone erupted during this same time interval; all five have 74 percent SiO_2. Resumption of intermediate magmatism began with radial outflow of several rhyodacite and dacite lavas in the interval 38 to 32 ka, alternating with the rhyolite eruptions, followed by construction of a broad cone of silicic andesite lavas (62-64% SiO_2), and culminating at 27±3 ka in growth of a steeply dipping summit cone of agglutinate-dominated basaltic andesite (54-57% SiO_2). Emplacement of a multiphase andesitic intrusive complex (17±2 ka) culminated in formation of a summit crater 800 m wide (fig. 19). Subsequent filling of the large crater by thick dacite lava and more than 150 m of dacitic pyroclastic ejecta, followed by draping of the summit by a final thin sheet of andesitic agglutinate (derived from the small present-day summit crater), constitute a sequence that may have extended to the very end of the Pleistocene.

After about 10,000 years of inactivity, the South Sister locus underwent yet another compositional reversal, yielding two complex but discrete rhyolitic eruptions ~2.2 and 2.0 ka (Taylor, 1978; Scott, 1987). The first episode produced the 0.5-km^3 Rock Mesa coulee and subordinate tephra and satellite domelets (altogether ~0.53 km^3; all ~73.5 percent SiO_2) at the southwest toe of the South Sister edifice. The second episode produced the dike-fed 5-km-long Devils Chain of 16 vents that

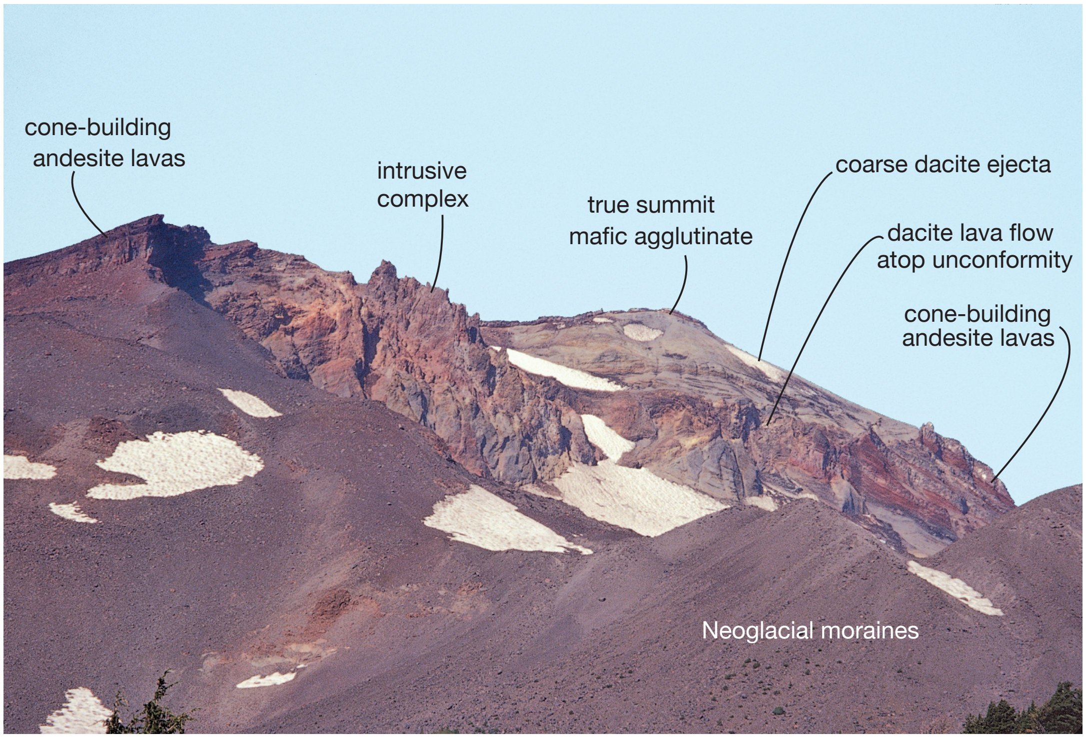

Figure 19. Northeast face of South Sister. Neoglacial moraines in foreground conceal small Prouty Glacier. At left and right, radially dipping gray-and-red lavas and ejecta define an andesitic stratocone (27±3 ka), the top of which ends abruptly at a subhorizontal unconformity. Craggy mass just left of center is an intrusive complex dated at 17±2 ka. Above central snow chute, a subhorizontal but convolutely foliated dacite lava flow at least 60-m-thick fills the paleocrater, rests on the unconformity, and banks against the intrusive complex. The dacite lava is overlain by 150 m of poorly to crudely stratified gray-to-tan phreatomagmatic dacite ejecta of different composition, capped in turn by a red-and-gray ledge of mafic-andesite agglutinate 5-to-10 m thick at the true summit. Relief visible above the lower snowfield is 290 m. (Photograph by author taken in September 2006.)

cuts both the 30-ka Devils Hill dome and the southeast flank of the South Sister edifice itself. North of a 3-km-long gap bypassing the summit, another 1.2-km-long parallel chain of four additional minor vents runs down the northern slope of the edifice and may have been fed concurrently by the same dike system (Scott, 1987). All 20 vents of the younger episode (about 0.32 km^3 altogether) produced rhyolite lava or tephra with 72.5 percent SiO_2, compositionally clearly distinguishable from rhyolite of the Rock Mesa episode. The northernmost vent of the Devils Chain proper lies at 2,400 m, well up the South Sister edifice and close to vents for several of the late Pleistocene rhyolites. That some 60 percent of the magma released during the younger episode issued from this uppermost vent (the Newberry Flow) supports the likelihood that the rhyolitic magma reservoir lies under the edifice itself (Bacon, 1985; Scott, 1987).

Taylor (1990a) proposed that a plexus of varied magma reservoirs has underlain the whole Tumalo-Broken Top-Three Sisters region. Hill (1991) advocated a wide range in the proportions of crustal and mantle contributions to intermediate magmas of the region, and he inferred lithologically distinct crustal sources for the silicic magmas around the Three Sisters vis-à-vis those in the Tumalo-Broken Top area. Bacon (1985) and Scott (1987) addressed the implications of rhyolite vent patterns for the nature, size, and depth of the silicic magma reservoir that probably still lies below South Sister. Eruption of numerous postglacial and late-glacial basaltic-to-andesitic lavas and cinder cones nearby indeed suggests that magmatism beneath the Three Sisters region remains potentially as vigorous as ever (Williams, 1944; Taylor and others,1987; Scott and Gardner, 1990)

Mount Bachelor

Mount Bachelor, a 2,763-m mafic cone-atop-shield volcano 15 km southeast of South Sister, is the largest center along a 25-km-long chain of ~50 vents that produced 40±5 km^3 of basalt and basaltic andesite (49-57% SiO_2) in a few major episodes during the interval 18 to 8 ka (Scott and others, 1989; Scott and Gardner, 1990, 1992; Gardner, 1994). Most of the vents lie along a north-south alignment marked by numerous scoria cones, but most of the magma issued effusively to build shields and lava fields. Five main eruptive episodes were defined (stratigraphically and paleomagnetically) and related to late-glacial features, suggesting that most of the material erupted between 15 ka and 12 ka and that as much as 25 km^3 of it may have erupted in less than 1,500 years.

The comprehensive study of the Bachelor chain illustrates several important processes: (1) that rapid eruptive pulses built much of the Quaternary Cascades of Oregon; (2) that the north-south vent alignments common in the Oregon Cascades are parallel to the arc and to the maximum horizontal compressive stress in the segment (Zoback and Zoback, 1980; Bacon, 1985; Scott and Gardner, 1992); (3) that eruption rates for mafic shields (on 10^3 to 10^4 year timescales) can match or exceed those for stratovolcanoes; and (4) that coeruption and mixing of independent magmatic lineages indicate complex shallow magmatic plumbing and compartmentalized reservoirs (Gardner, 1994). A comparable effusion rate for basalt zoned to basaltic andesite marked the late Holocene just north of the Three Sisters, where the 6 to 9 km^3 multivent Belknap shield was constructed in less than 1,500 years (Taylor, 1965, 1968). Only slightly older than Belknap (fig. 17), a nearby chain of scoria cones that includes Nash Crater and Sand Mountain (fig. 14) produced 2 to 3 km^3 of Holocene mafic lavas and ejecta in about 1,000 years (Taylor, 1968; Sherrod and others, 2004).

Wickiup Reach (III)

From near Crane Prairie Reservoir (43˚47.5'N) as far south as Cowhorn Mountain (43°24'N), the next 40-km reach of the Oregon Cascades (fig. 14) is distinguished by a modest (15-20 km) right-stepping offset of the Quaternary volcanic zone (Williams, 1957; Sherrod and others, 1983b; Sherrod, 1991; MacLeod and Sherrod, 1992; Sherrod and Smith, 2000). As the Cascade crest also swings west (from Maiden Peak to Diamond Peak), most of the Quaternary vents remain east of the drainage divide, as in the Mount Bachelor region to the north. The Quaternary vent belt remains 40 to 50 km wide, but it trends N15-20°E in this reach, whereas its strike is northerly for the 175 km between Mount Hood and the Bachelor chain. Although at least 118 Quaternary vents are recognized in this oblique subsegment, its vent density is only half that in the reach next north (table 1), and vent alignments are present but far less common.

Along with scattered cinder cones, middle and late Pleistocene mafic shields are numerous here. At least 15 shields are prominent (Williams, 1957), and several (for example, The Twins, Hamner Butte, Maiden Peak, Mount Yoran, and Davis, Fuji, Sawtooth, and Cowhorn Mountains) have eruptive volumes greater than 10 km^3. In general, the shields east of the Cascade crest are well-preserved, whereas most of those on or west of the crest are glacially sculpted. A few of the mafic shields (for example, Odell Butte) are unusually steep, and (with increasing amounts of fragmental material at the core) some grade from shields to modest stratocones like Mount Yoran, Lakeview Mountain, and 2,665-m Diamond Peak (~15 km^3).

Basaltic andesite greatly exceeds basalt along this reach, but products still more evolved are especially sparse. Much of the upper part of Diamond Peak and adjacent Crater Butte are andesitic (Webster, 1992), and dacitic to rhyolitic lavas and tuffs were mapped by Sherrod (1991) in Salt Creek ~10 km west of Maiden Peak. Crossing the cluster of mafic shields south of Wickiup Reservoir, a 20-km-long north-south alignment of three separate Holocene andesitic lava flows (the only postglacial eruptive units in the Wickiup Reach) may have been mutually dike fed. Also nestled among the steep shields south of Wickiup Reservoir are three small isolated andesite-dacite domes—McCool, Ranger, and Eaton Buttes (with 62.1, 63.9, and 62.6% SiO_2, respectively)—that are thought to be of early Pleistocene age (Sherrod, 1990b; MacLeod and Sherrod, 1992; Sherrod and Smith, 2000).

Thielsen Reach (IV)

From Cowhorn Mountain (43°24'N) to about 43°05'N, just north of Timber Crater, the next 40-km-long reach of the Quaternary vent zone narrows slightly to ~35 km. With only 86 Quaternary vents recognized, its vent density is similar to that of the Wickiup reach to its north but much lower than in the Mount Mazama area to its south (table 1). The belt resumes the roughly north-south trend otherwise so characteristic of the Oregon segment but interrupted by the Wickiup-Cowhorn right-stepping offset. Vent alignments are not pronounced in this subsegment, although crude arrays trending N15°E do run through Mounts Bailey and Thielsen.

As in most of the Quaternary Oregon Cascades, basalt is subordinate to basaltic andesite, which makes up numerous scoria cones, shields, and a few steep cone-atop-shield complexes that include Cowhorn, Sawtooth, and Howlock Mountains, and 2,799-m Mount Thielsen, the "lightning rod of the Cascades" (Williams, 1933, 1957; Sherrod, 1991). Like 290-ka Mount Thielsen (fig. 20), the intrusive spire of which is so starkly exposed, the other three large centers are glacially dissected and probably likewise of middle Pleistocene age. Each of the four edifices may have released as much as 15 to 20 km^3 of magma. Less eroded but comparably voluminous (~15 km^3), the Mount Bailey edifice appears to be late Pleistocene, as are ten or more scoria and lava cones along the reach. Among these smaller cones, well-preserved Red Cinder Butte, Windigo Butte, Tenas Peak, Kelsay Point, and Thirsty Point are among the youngest, probably latest Pleistocene, and Cinnamon Butte may have erupted during or after deglaciation (Sherrod and others, 1983a; Sherrod, 1990b).

Andesite is limited to Timber Crater (Bacon, 1990), parts of Mount Bailey (Barnes, 1992), and a deeply eroded middle Pleistocene stratovolcano centered on **Cappy Mountain** (43°18.5'N, 121°59'W) and adjacent Tolo Mountain. Rhyodacitic lavas (69-71% SiO_2) are mapped around the flanks of the Cappy Mountain center (at Mule Peak; Burn, Hemlock, and Clover Buttes; Williams, 1957; Sherrod and Smith, 2000). With preserved relief of 700 m and a width of 12 km, the

Figure 20. Mount Thielsen, the “lightning rod of the Cascades,” a 300-ka mafic cone, viewed eastward. Relief visible in image is 1,100 m, of which about 600 m is above timberline. Physically similar to Goosenest (fig. 22) and many steep mafic shields in the Cascades, Thielsen's interior has been unusually well exposed by glacial erosion. Several radial arêtes consist of modestly dipping stacks of scores of thin rubbly lava flows that interfinger proximally with a fragmental core facies of loose-to-agglutinated stratified ejecta that thickens and steepens inward from ~10° to as much as 35°. The pyroclastic core is laced with dikes, is widely altered hydrothermally, and is locally deformed by a composite intrusion that supports the summit spire.
(Photograph by author taken in September 2001.)

glacially devastated andesitic stratocone and its flanking silicic units represent an evolved-magma anomaly comparable in importance to Mount Jefferson or South Sister. Its eruptive volume is poorly known but may have exceeded 30 km^3.

Mazama Reach (V)

The Mazama reach of the Oregon segment, extending 40 km from Timber Crater (43°04’N) to Big Bunchgrass shield (42°42’N), contains ~175 Quaternary vents in a belt only 25 to 30 km wide (fig. 15). Although the vent belt is relatively narrow for the Cascades, vent density is unusually high (table 1), as is the proportion of silicic products erupted (Williams, 1942; Bacon and others, 1994; Bacon and Lanphere, 2006). Except close to the large Mount Mazama edifice itself (Bacon, 1985), many shields and monogenetic vents lie along north-south alignments, some in association with north-trending normal faults of the Klamath Graben system that strikes toward and past Mount Mazama (Bacon and Nathenson, 1996; Bacon and others, 1999; Bacon, 2007). Straddling the Cascade axis, Mount Mazama itself is a cluster of overlapping stratovolcanoes, by far the most voluminous Quaternary volcanic system in the Oregon Cascades, and the second largest (behind Newberry) Quaternary volcanic locus in Oregon.

Mount Mazama

Mount Mazama is a large compound edifice, active quasi-continuously since ~420 ka, built largely of andesite and dacite (55-68% SiO_2) with very minor basaltic andesite (Bacon, 1983; Bacon and Lanphere, 1990, 2006). Limited exposures of early and middle Pleistocene (1.8-0.6 Ma) volcanic precursors include as many as ten mafic and andesitic units peripheral to the edifice and several dacites and rhyodacites beneath and just southeast of it. As a silicic focus, the area developed slowly, with scattered dacites as old as 1.28 Ma and a few rhyodacites erupted during the long interval 725 to 500 ka (Bacon and Lanphere, 2006). Activity then intensified to produce a 16×24-km domefield (~20 km^3) containing as many as 40 rhyodacite lava domes and flows (470-410 ka) that directly preceded growth of the stratocone cluster (Nakada and others, 1994). Beginning with dacitic Mount Scott (420-350 ka), the andesite-dacite edifice then grew piecemeal, covering the west margin of the rhyodacite domefield. It became a cluster of contiguous and overlapping cones and shields, each active briefly or for as long as 70 kyr. Among some 50 separate components identified by Bacon (2007), the largest (~5-11 km^3 each) include Mount Scott and the andesitic edifices of Kerr Notch (340-300 ka), Applegate Peak (270-210 ka), Llao Bay

(150-100 ka), and the West Wall (~70 ka). Although andesite exceeds dacite in the compound edifice by roughly 2:1, dacite magma erupted recurrently, at least ten times during growth of the edifice. During this 400-kyr interval, however, not a single rhyodacite was produced until ~27 ka, shortly after the final eruption of dacite at ~35 ka. Subsequently, several rhyodacite eruptions took place, as the rhyodacite magma reservoir grew by an average of 2.5 km^3/kyr for ~20 kyr leading up to the caldera-forming eruption at 7.7 ka.

Surrounding and contemporaneous with growth of Mount Mazama are two substantial shields and at least 35 monogenetic vents within ~12 km of the caldera rim. The shields are mafic Union Peak (~6 km^3, ~164 ka) and andesitic Timber Crater (~9 km^3, ~137 ka). Most of the lesser peripheral vents (~300-10 ka) erupted basaltic andesite (for example, Desert Cone, Bald Crater, Red Cone, Oasis Butte, Maklaks Crater, Whitehorse Bluff, and Scoria Cone); about six produced andesite (for example, Crater Peak); but none produced dacitic or more silicic magmas, which are strictly limited to the focal edifice. Several of the youngest peripheral vents (~35-10 ka), which lie west of the edifice, erupted relatively primitive arc magmas (51-54% SiO_2) and HAOT (48-50% SiO_2), plausibly representing part of an episode of elevated thermal and material input beneath the contemporaneously accumulating rhyodacite reservoir nearby (Bacon and Lanphere, 2006).

Structural collapse at 7.7 ka during catastrophic eruption of ~50 km^3 of magma (zoned from rhyodacite to mafic cumulate mush) produced Crater Lake Caldera, which engulfed summits as much as 1 km higher than its rim (Bacon, 1983). Strata exposed on the caldera wall include andesite-dacite cone-building lavas, two small mafic shields, and dacitic pyroclastic deposits, all alternating recurrently rather than following any systematic compositional progression. Near the rim, the wall truncates some of the rhyodacite lavas that leaked from the shallow zoned reservoir during the 20-kyr interval of preclimactic magma accumulation (Williams, 1942; Bacon, 1983; Bacon and Druitt, 1988; Bacon and Lanphere, 1990, 2006; Bacon 2007). Postcaldera eruptions on the caldera floor involved four vents that released ~4 km^3 of andesite soon after collapse as well as a small rhyodacite dome emplaced ~4.8 ka (Bacon and others, 2002). Along with Kulshan Caldera adjacent to Mount Baker and Rockland Caldera at Lassen, Crater Lake is one of only three Quaternary calderas recognized in the Cascades, an anomalously small number for a continental-margin arc (Hildreth, 1996).

Precollapse volume of the Mazama edifice was roughly 112 km^3 (Bacon and Lanphere, 2006), but, considering glacial erosion, the volume erupted might well have been greater than 130 km^3. Moreover, the 50-km^3 magma volume estimated for the climactic eruption is probably an underestimate, as it takes no account of concealed intracaldera ignimbrite. A total eruptive volume since 420 ka (neglecting the pre-Mazama rhyodacite domefield and its early Pleistocene intermediate platform) may thus have been greater than 180 km^3, suggesting that Mount Mazama rivals Rainier and Lassen as the third or fourth most productive Quaternary center in the Cascades.

U-Th model ages of zircons from (variably melted) granodiorite blocks that were plucked from the walls of the magma chamber and ejected radially during the caldera-forming eruption record a 300-kyr history of freeze-thaw fluctuations during assembly of a composite pluton (Bacon, 1992, 2005; Bacon and others, 2000, 2005; Bacon and Lowenstern, 2005). Multimodal age spectra for individual blocks are interpreted as reflecting recycling of zircon antecrysts from earlier intrusions and from crystallizing stalled mush batches. The main zircon age clusters (200-50 ka) for granodiorite blocks ejected in different radial sectors correspond to K-Ar ages of dacites erupted in those sectors, suggesting assembly of many modest silicic batches crystallizing piecemeal in constructing a multiphase pluton at least as wide as the 30-km^2 subsided floor.

Other important centers in the Mazama reach are (1) the 10-km-wide andesitic Timber Crater shield just north of Mount Mazama; (2) the 7-km-wide mafic shield of Union Peak southwest of Mount Mazama, topped by a glaciated central intrusive spire comparable to that of Mount Thielsen (Williams, 1942); (3) a chain of andesitic scoria cones ~13 km south of Crater Lake that includes Goose Nest, which produced a 60-km^2 fan of lava and fragmental flows (Smith, 1983; 1988); and (4) a cluster of mafic cones around the Big Bunchgrass shield (fig. 15). Altogether, at least 80 vents in the reach erupted products ranging from HAOT to andesite (47-62% SiO_2) before or during construction of the Mazama edifice (Williams, 1942; Bacon, 1990, 2006; Bacon and others, 1994; Bacon and Lanphere, 2006). Despite an abundance of basaltic andesite cones and shields, the Mazama reach is unique in the Quaternary Cascades in having erupted almost no true basalts (<52% SiO_2, noncumulative) other than HAOT (Bacon and others, 1994). Equally remarkable is the absence of true rhyolite; although at least 75 km^3 of rhyodacite was released in more than 50 mid-Pleistocene to Holocene eruptions at or adjacent to Mount Mazama, not a single unit having >73 percent SiO_2 has been reported (Bacon and Druitt, 1988; Nakada and others, 1994; Bacon and Lanphere, 2006).

McLoughlin Reach (VI)

The 50-km-long McLoughlin reach, from Big Bunchgrass shield (42˚42’N) to Little Aspen Butte (42°17’N), contains ~33 Quaternary volcanoes in a vent zone only 15-25 km wide (fig. 15). Vent density is far lower than in the adjacent Mazama reach (table 1), and Quaternary eruptive volume (<100 km^3) is low for the Cascades. There may be a slight westerly (right-stepping) offset of the vent zone relative to the Mazama reach, but thick sedimentary fill in the Klamath Graben just east of the zone makes both the apparent shift and the width of the zone equivocal. In striking contrast to the Mazama reach, no dacitic or more silicic Quaternary volcanic rocks have erupted in this reach. Although basalts are sparse, both HAOT and arc types are present (Mertzman and others, 1992). In the number of volcanoes, basaltic andesite dominates (as everywhere in Oregon), but a few of the main centers in the reach are andesitic: (1) Pelican Butte shield, the largest Quaternary center at ~20 km^3; (2) Brown Mountain (~5 km^3), which is probably the youngest; and (3) Devils Peak (>10 km^3), a glacially dissected cone-on-shield of middle or early Pleistocene age that consists of both andesite and basaltic andesite (Smith, 1983, 1988). **Mount McLoughlin** is a towering (2,894 m) but volumetrically modest (~13 km^3) late Pleistocene stratocone built almost wholly of basaltic andesite (54-57% SiO_2; Maynard, 1974), more like Mount Bachelor or North Sister than the andesite-dacite stratovolcanoes with which it is often confused.

The glacially excavated Mountain Lakes volcanic cluster (Greylock Mountain-Whiteface Peak-Aspen Butte) is a major eruptive complex (>50 km^3) and dominantly andesitic. It has been thought to be mostly of Pliocene age (Smith, 1983; Sherrod and Smith, 2000), but several mafic and andesitic flank vents are probably Quaternary. Much of the Cascade crest in this reach is wilderness that has been studied only in reconnaissance. It should come as no surprise if detailed mapping and dating were to show that many more of the glacially dissected edifices in the Mountain Lakes, Sky Lakes, and Seven Lakes Basin areas are Quaternary.

Little Aspen Butte, a mafic shield on the south flank of the Mountain Lakes cluster, is the southernmost Quaternary volcano in Oregon. South of it, a 64-km stretch of the Cascades almost lacking in Quaternary volcanoes separates the Oregon segment from the vigorously productive volcanic region around Mount Shasta. Although the gap is rich in Pliocene mafic centers, the small Copco scoria cones on the Klamath River (Williams, 1949; Hammond, 1983) may be the only Quaternary volcanoes within it. The southern termination of the Quaternary volcanic belt in Oregon (fig. 15) coincides with an abrupt change in strike of Basin and Range faults of the Klamath Graben system, from northerly trends adjacent to the Quaternary volcanoes to northwest-southeast trends in the volcanically inactive region farther south (Walker and MacLeod, 1991; Blakely and others, 1997).

Contrasts Between Oregon and Rainier-to-Hood Segments

Scarcity of forearc volcanoes south of 45°15’N, unbroken continuity of the vent-zone axis, and narrowness of the Quaternary volcanic belt (one-third as wide as in southern Washington) distinguish the Oregon segment from the adjacent one to the north. Moreover, in contrast to the quadrilateral of stratocones in southern Washington (fig. 8), all the main stratovolcanoes of Oregon lie on or very close to the Cascade axis. Although axial vent-densities are comparable (table 1), some broad compositional differences also distinguish the segments: (1) importance of rhyodacite at several major centers in Oregon; (2) predominance of basaltic andesite among the many mafic shields, cones, and lava fields in Oregon but of true basalt among those in the Rainier-to-Hood segment; and (3) absence in the Oregon Quaternary Cascades of the mildly alkalic basalts that are scattered across southern Washington. Because the crust beneath the Oregon Cascades is thought to be younger, less mature, and less continental than beneath adjacent parts of the Washington and California Cascades, the scarcity of basalts relative to those areas is an apparent paradox.

Although eruptive volumes are hard to estimate and compare with much accuracy, a first-order contrast in volume-proportions of the stratocones vis-à-vis the surrounding mafic volcanoes nonetheless stands out between these segments. If consideration is limited to the Brunhes Normal-Polarity Chron (for the sake of better preservation and definition of the evidence), then the data of Sherrod and Smith (1990) suggest that during the last 780 kyr no more than one-third and perhaps as little as 10 percent of the material erupted along the Oregon Cascades issued from the major evolved centers; that is, 67-90 percent of the mid-Pleistocene and younger volume of the Oregon segment originated in mafic shields and cones. For the Rainier-to-Hood segment, virtually the opposite is clear—about 80 percent of the volume younger than 780 ka erupted from four andesite-dacite stratovolcanoes, whereas more than 150 mafic vents (including Indian Heaven) accounted for only ~20 percent.

The volumetrically dominant form of Quaternary volcanism of the Oregon Cascades— eruption of a nearly continuous belt of coalescing mafic shields and cones—had already been characteristic of the Oregon segment in the Pliocene, and it may have begun locally as long ago as 7 Ma (Sherrod and Smith, 2000). This long-lived mafic swath along the Oregon rangecrest, which includes the “High Cascade platform” of Taylor (1990a), has no counterpart in southern Washington, where Pliocene shields (for example, Hogback Mountain and the Simcoe Mountains shield) are few and far between. Except for the rear-arc Simcoe Mountains Volcanic Field, very little of the widespread basalt erupted in southern Washington is pre-Quaternary. In contrast to the dispersed and mostly Quaternary mafic volcanism of the Rainier-to-Hood segment, the mafic axis of the Oregon Cascades has been a stable, concentrated, and persistent eruptive belt some 25 to 50 km wide for several million years.

Shasta Segment

The Quaternary volcanic zone containing the huge Mount Shasta center is separated from the Oregon and Lassen segments by extensive gaps (figs. 1, 21) where little Quaternary volcanism has taken place. Along the arc, from **Goosenest** (41°43’N) to **Signal Butte** (41°17’N), the Quaternary Shasta segment is only 50 km long (fig. 21), no longer than the gaps north and south of it. West-to-east, however, the Quaternary vent zone is extraordinarily wide, extending without interruption for at least 120 km, from west of Mount Shasta across the Cascades and far into the Basin and Range Province, embracing the great Medicine Lake Volcanic Field (Anderson, 1941; Donnelly-Nolan, 1988) and the adjacent Hackamore basalt field (Donnelly-Nolan and others, 1996), both of which include abundant HAOT. Not counting these dense inboard arrays of Quaternary vents (table 1) as parts of the main arc belt, the

Shasta segment of the Cascades proper is still 40 to 50 km wide and contains at least 255 Quaternary vents (fig. 21).

Volcanism was even more extensive here in the Pliocene, when it was characterized principally by mafic shields and fissure-fed plateau-capping basalts that extend from the Cascades to far east of Medicine Lake and the Klamath Graben (Luedke and Smith, 1981; McKee and others, 1983; Mallin and Hart, 1991; Sherrod and Pickthorn, 1992; Sherrod and Smith, 2000; Carmichael and others, 2006). Before the Oregon-Shasta gap fell quiescent in the late Pliocene, an axial belt of mafic shields was continuous across it, extending from southern Oregon to the Eagle Rock and Willow Creek Mountain shields (fig. 21). The trend of the Cascade axial belt changes near Goosenest (fig. 21) from the north-south orientation characteristic of Oregon to the southeasterly trend typical of the adjacent part of the Basin and Range Province, passing well inboard of the subsequent site of Mount Shasta and extending as far southeast as the Black Fox Mountain mafic-shield cluster (fig. 21). Because erosion of mafic shields is relatively slow in the southern Cascades, the constructional topography established largely in the Pliocene remains the physiographic axis of the Cascades here (Williams, 1949). Since then, the active Cascade axial belt has contracted latitudinally, the enormous Medicine Lake and Mount Shasta systems have developed east and west of the axis (largely during and since the middle Pleistocene), and scores of mafic to silicic volcanoes have built an across-axis highland between them (Christiansen, 1996; Donnelly-Nolan, in press). Quaternary arc volcanism has thus been limited to an equant (50x50 km) tract of the Cascades that overlaps inland with the contemporaneous (and areally comparable) Medicine Lake Volcanic Field, which is fundamentally extensional and powered in part by HAOT (Donnelly-Nolan, 1988).

Mount Shasta

Mount Shasta (4,316 m) is by far the most voluminous stratovolcano in the Quaternary Cascades, having a diameter of 30 km, relief of 3.3 km, and an eruptive volume greater than 450 km^3. Active since ~600 ka, the central cone complex has recurrently produced silicic andesite and dacite (57-67% SiO_2; Christiansen, 1982, 1985, 1990; Grove and others, 2002). An ancestral andesite edifice (Sand Flat cone) was destroyed by sector collapse, probably between 400 and 300 ka; a remnant left in place gave a K-Ar age of 593±41 ka (Crandell, 1989). The hummocky debris avalanche deposit is one of the world's largest (~45 km^3), having flowed at least 50 km northwest of the present summit and today covering about 675 km^2. The great compound edifice present today was subsequently constructed during at least four main episodes that built four overlapping stratocones, the dome-filled craters of which are separated by only 1 to 3 km (Christiansen and others, 1977). Middle Pleistocene lava flows from the oldest of the four locally overlap the debris avalanche deposit, and their source edifice (Sargents Ridge cone, ~85-km^3) is overlapped in turn by a substantial late Pleistocene edifice (Misery Hill cone, ~60 km^3). The two youngest cones, Shastina and the modern summit edifice (Hotlum cone), together represent at least 60 km^3 of eruptive products and were built entirely during the Holocene (Miller, 1980; Christiansen and Miller, 1989; R.L. Christiansen, written commun., 2006).

In addition to central dacite domes culminating each andesite-dacite cone-building episode, at least 16 flank domes are exposed, nearly all of them likewise dacitic (Christiansen and others, 1977). A small remnant (72% SiO_2) just south of dacitic McKenzie Butte, low on the south flank, is the only unit at Mount Shasta known to have more than 67 percent SiO_2, and it may be the only Quaternary arc rhyodacite between Mazama and Lassen. Haystack dome (64% SiO_2) on the northwest has geochemical characteristics that suggest derivation by partial melting of MORB-like source rocks (Kay and others, 1993; Feeley and Hacker, 1995), perhaps part of the ophiolitic Klamath basement. Black Butte dome (65-66% SiO_2), 13 km southwest of Shasta's summit, is the largest dome exposed here (~2.5 km^3), consists of four steep extrusions of hornblende dacite, and is only ~9,500 years old (Miller, 1980). Extensive pyroclastic-flow fans from Black Butte and the dome cluster atop Shastina overlap at the west toe of Mount Shasta; both fans were emplaced ~9,500±300 years ago, the one from Black Butte being slightly younger (Miller, 1978). Another large apron of pyroclastic and debris flows, derived from the Hotlum cone (mostly 9 to 4 ka), spreads around the north and east sides of the great edifice.

The scattering of varied silicic domes as far as 10 to 15 km to the north, south, and west (but none to the east) of the summit suggests that partial melting is distributed beneath an area somewhat wider than the principal melting zone that has supplied exceptionally voluminous andesite-dacite magma to the central conduit cluster, which itself shifted less than 3 km in 600 kyr. Together with nine of the domes, several andesitic to mafic cinder and spatter cones on Shasta's north and south flanks define a narrow north-trending array of vents (fig. 21) of various ages and compositions that probably reflects regional stress or structural influence rather than local edifice control (Williams, 1932a; Christiansen and others, 1977). One of the mafic cones, Green Butte (53-54% SiO_2, $MgO > 8\%$; Anderson, 1974; Baker and others, 1994), lies only 4 km south of the summit at an elevation of 2,800 m, thus ranking among the highest mafic vents in the Cascades (Christiansen and Miller, 1989). A vent location so nearly central (on an andesite-dacite edifice) for magma so mafic suggests complex crustal plumbing and dispersed (nonintegrated) silicic magma bodies beneath Mount Shasta. Several more cinder cones north, south, and northwest of Mount Shasta (Christiansen and Miller, 1989) erupted Mg-rich basaltic andesite or basalt (Baker and others, 1994; Grove and others, 2002); some represent the most primitive magma associated with the Shasta system whereas others are hybrids (Streck and others, 2007). In addition, sheets of HAOT contemporaneous with the edifice are widespread in the lowland periphery of Mount Shasta (Williams, 1949), as well as far into the Basin and Range interior of northern California and southern Oregon (Hart and others, 1984).

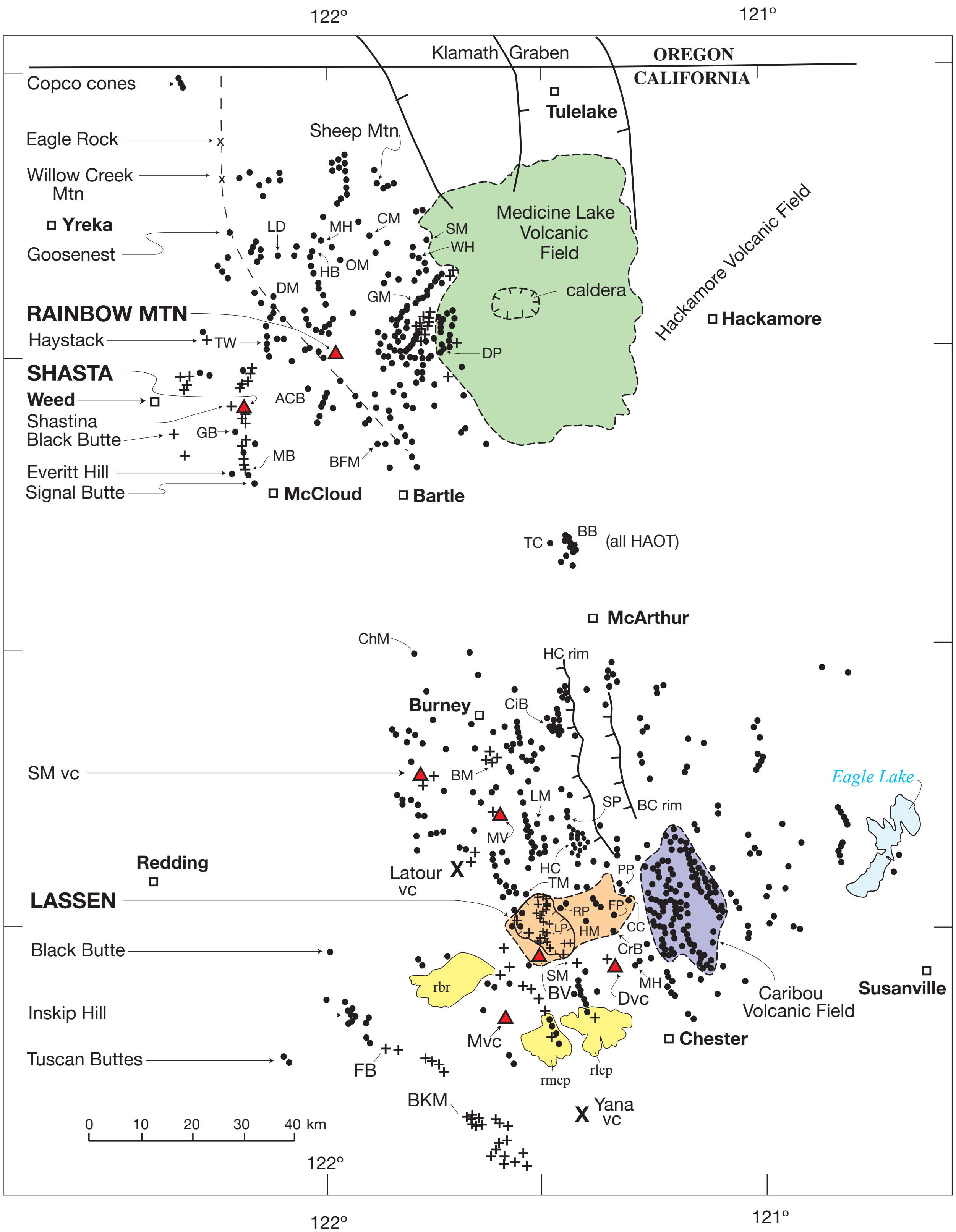

122°
121°
42°
41°30'
41°
40°30'
Klamath Graben
OREGON
CALIFORNIA
Copco cones
Eagle Rock
Willow Creek Mtn
Yreka
Goosenest
RAINBOW MTN
Haystack
SHASTA
Weed
Shastina
Black Butte
Everitt Hill
Signal Butte
Sheep Mtn
Tulelake
Medicine Lake Volcanic Field
caldera
Hackamore Volcanic Field
Hackamore
LD
MH
CM
SM
WH
HB
OM
DM
GM
TW
DP
ACB
GB
MB
BFM
McCloud
Bartle
TC
BB
(all HAOT)
McArthur
ChM
HC rim
Burney
CiB
SM vc
BM
LM
SP
BC rim
MV
Eagle Lake
Latour vc
Redding
LASSEN
HC
TM
PP
RP
FP
LP
HM
CC
CrB
Black Butte
SM
BV
Dvc
MH
rbr
Caribou Volcanic Field
Susanville
Inskip Hill
Mvc
Chester
Tuscan Buttes
FB
rmcp
rlcp
BKM
Yana vc
0 10 20 30 40 km

Elsewhere in the Shasta segment, as in the Oregon segment, a majority of the Quaternary volcanoes consist of basaltic andesite. In contrast to Oregon, however, the volumetrically dominant composition erupted during the Quaternary is andesite—owing not only to massive Mount Shasta but to Rainbow Mountain, Goosenest, and a few lesser volcanoes. Centered about 20 km northeast of Mount Shasta and predating it, the **Rainbow Mountain** center was one of the largest andesite-dacite stratovolcanoes in the Cascades during the early Pleistocene, measuring ~20 km across (R.L. Christiansen, work in progress; Guffanti and others, 1994). Called Haight Mountain volcano by Williams (1949, p. 39), the glacially dissected pile probably had an eruptive volume well in excess of 100 km^3. On the Cascade crest 35 km north of Mount Shasta, Goosenest (Williams, 1949) is a 10-km^3 late Pleistocene andesitic cone (up to 58.5% SiO_2) with ~1,400 m of relief (fig. 22). Andesite contributions (accompanied by basaltic andesite and HAOT) also make up significant parts of the early Pleistocene Deer Mountain vent complex (southeast of Goosenest; Williams, 1949) and the middle Pleistocene Garner Mountain cone and fissure-vent system (Hughes and Mertzman, 1976; Hart and others, 1979) ~25 km farther east. The Fisk Ridge to Pumice Stone Mountain alignment of about 20 vents (parallel but 8 km south of the northeast-striking Garner Mountain chain) includes a compositionally wide array of (early to late Pleistocene) HAOT, mafic and silicic andesite, dacite, and the 1.0-Ma rhyolite of Red Cap Mountain (Mertzman, 1982; Donnelly-Nolan, in press). Nonetheless, most of the many Pleistocene shields and cones scattered between Medicine Lake and Shasta consist of basaltic andesite—including Horsethief Butte, Mount Hebron, and Sheep, Cedar, Orr, and Little Deer Mountains. Likewise basaltic andesite but of Pliocene age are nearby Sharp and Wild Horse Mountains (R.L. Christiansen, work in progress). Adjacent to Mount Shasta and contemporaneous with its construction, three middle Pleistocene shields (Everitt Hill, Ash Creek Butte, and The Whaleback) each produced 5-10 km^3 of basaltic andesite. Additional mafic shields may lie buried beneath the great stratovolcano itself (Christiansen and others, 1977).

Lassen Segment

The Quaternary volcanic zone in the Lassen region (fig. 21) extends at least 110 km east-west (Eagle Lake to Inskip Hill) and 80 km north-south, from 41°N to 40°15'N, where the Quaternary Cascade arc terminates. The Lassen segment is separated from the Shasta segment by a 50-km gap having hardly any Quaternary volcanoes and relatively few of Pliocene age (Luedke and Smith, 1981; Blakely and others, 1997). Within the Lassen segment, at least 476 vents are thought to be younger than 2 Ma (table 1), and 121 more were reported by Guffanti and others (1990) for the pre-Quaternary interval 7 to 2 Ma.

A 25-km-wide swath of ~200 close-set volcanoes trending north-northwest through the Lassen volcanic center (fig. 21) constitutes the voluminous axial zone of the Quaternary Cascades. At least 17 forearc vents lie as far as 40 km southwest of the axial belt (fig. 21; Helley and others, 1981; Helley and Harwood, 1985). About 200 more Quaternary shields, cones, and fissure vents lie as far as 60 km east of the axis (Guffanti and others, 1990), either concentrated in the Caribou Volcanic Field (Guffanti and others, 1996) or scattered less densely across a wide inboard region (table 1; fig. 21). Although much of the Lassen segment is marked by Basin and Range extensional faults and associated vents for HAOT, its calcalkaline arc products (basalt to dacite) are not subordinate to HAOT except perhaps far inboard near Eagle Lake. For this reason, the expanse of Quaternary volcanoes well east of the Cascade axis in the Lassen segment is treated here as Cascadian, though its eastern portion might well be considered another rear-arc volcanic field (fig. 1). Compared to the Caribou-Eagle Lake rear-arc area, however, the Hackamore and Medicine Lake Volcanic Fields (equivalently contigu-

← **Figure 21.** Shasta and Lassen segments of the Cascade arc, showing distribution of 746 Quaternary volcanic vents. Vent symbols as in figures 3 and 8. Lassen region vent distribution from Guffanti and others (1990, 1996) and Clynne and Muffler (2007). Generalized extents of rear-arc edifice of Medicine Lake vent field (green) and adjacent Hackamore vent field (encompassing ~580 and ~12 additional Quaternary vents, respectively) are adapted from Donnelly-Nolan (1988, in press) and Donnelly-Nolan and others (1996). Also outlined are Caribou Volcanic Field (violet; enclosing ~112 Pleistocene vents), Lassen volcanic center (orange; >40 vents), and the caldera formed during the 610-ka Rockland eruption and later filled by the Lassen domefield. Major volcanic centers (vc) active in the early Quaternary include Rainbow Mountain, Snow Mountain (SMvc), Dittmar (Dvc), and Maidu (Mvc); large Yana vc and Latour vc (both indicated by X) were built during the Pliocene. The Cascade axis (dashed line), well defined only in the north, is in part marked by two well-preserved mid-Pliocene mafic shields (x), Eagle Rock and Willow Creek Mountain. Unless indicated, all other vents identified are Quaternary. Shasta segment abbreviations: ACB, Ash Creek Butte; BB, Brushy Butte; BFM, Black Fox Mountain; CM, Cedar Mountain; DM, Deer Mountain; DP, Doe Peak; GB, Green Butte; GM, Garner Mountain; HB, Horsethief Butte; LD, Little Deer Mountain; MB, McKenzie Butte; MH, Mount Hebron; OM, Orr Mountain; SM, Sharp Mountain (Pliocene); TC, Timbered Crater; TW, The Whaleback; WH, Wild Horse Mountain (Pliocene). Lassen segment abbreviations: BC, Butte Creek Rim; BM, Burney Mountain; BKM, Barkley Mountain dacite chain; BV, Brokeoff Volcano; ChM, Chalk Mountain; CiB, Cinder Butte; CrB, Crater Butte; CC, Cinder Cone; FB, Finley Butte; FP, Fairfield Peak; HC, vents for Hat Creek Basalt and nearby fault-scarp rim; HM, Hat Mountain; LM, Logan Mountain; LP, Lassen Peak; MH, Mount Harkness; MV, Magee Volcano; PP, Prospect Peak; RP, Raker Peak; SP, Sugarloaf Peak; TM, Table Mountain. Large rhyolite lava flows (in yellow) around Maidu volcanic center form Blue Ridge (rbr), Mill Creek Plateau (rmcp), and Lost Creek Plateau (rlcp).

ous behind the Shasta segment; fig. 1), appear to have still larger proportions of the HAOT and HAOT-derivative magmas, reflecting a dominance of dry decompressive (Basin and Range) mantle melting where extensional unloading has impinged on the subduction-dominated Cascade arc.

Pliocene volcanism was even more widespread, well established along what is now the Quaternary axis but extending farther inland—as far as 120 km east of Lassen Peak. Contraction of activity during the Quaternary (Guffanti and others, 1990) entailed accentuation of the north-side gap, extinction of a large Pliocene volcanic region south of 40˚15’N (principally the Yana volcanic center; fig. 21; Clynne, 1990a,b), and shrinkage of the wide volcanic region east of the axis, part of a longer-term westward migration of the eastern limit of active volcanism (Grose and McKee, 1986; Grose and others, 1990, 1992). At first glance, figure 1 seems to show a 40 to 50 km left-stepping offset between the Shasta and Lassen segments (Luedke and Smith, 1981). The offset is less profound than apparent, however, if account be taken of (1) the gap between segments, (2) the deviation (north of Mount Shasta) of the Cascade axis from a southerly to a south-southeasterly trend (fig. 21), and (3) the position of Mount Shasta itself, well west of the axis.

Mafic volcanoes predominate numerically in the Lassen segment, as they do in all parts of the Cascades south of Mount Rainier. Fewer than 20 percent of the Quaternary volcanoes here are andesitic, and fewer than 10 percent are silicic (Guffanti and others, 1990). In contrast to the Oregon and Shasta segments, where basalt is sparse and basaltic andesite far more dominant, as many as 30 percent of the ~350 Quaternary mafic vents in the Lassen segment erupted true basalt (<52% SiO_2, either calcalkaline or HAOT) (Guffanti and others, 1990; Clynne, 1993). Some 13 units of HAOT younger than ~1 Ma are exposed across the Lassen region (Clynne and Muffler, in press), and numerous older examples have been mapped just east of the Quaternary arc (Grose and others, 1990, 1992). A generally westward progression of scattered HAOT magmatism has accompanied westward advance of Basin and Range extension into the arc (Hart and others, 1984; Guffanti and others, 1990). The youngest and best-known representative is the Hat Creek Basalt (24±6 ka; 48-49% SiO_2), a 30-km-long, tube-fed lava-flow complex (~5-km^3) that erupted from a multivent fissure ~18 km north-northeast of Lassen Peak (Anderson, 1940; Anderson and Gottfried, 1971; Anderson, 1971; Muffler and others, 1994; Turrin and others, 2007).

Arc (calcalkaline) basalts are also scattered among the more numerous basaltic andesite cones and shields across the Lassen segment, although they are missing within the Lassen volcanic center itself, presumably intercepted at depth by a long-lived reservoir or crustal column of evolved magma

Figure 22. Goosenest shield viewed southward (with lower flank of Mount Shasta in left distance). Transitionally mafic-to-silicic andesite, this latest Pleistocene nonglaciated edifice shows smooth moderate slopes typical of numerous Cascade shields, as well as modest asymmetry that commonly results from growth on a preexisting slope. The summit cone of scoria and agglutinate, which rises 250 m above the shield, is not a subsequent cinder cone but, rather, the youngest part of a core facies that typically interfingers radially with the flank lavas throughout growth of such an edifice. Relief visible in image is about 1,200 m.
(Photograph by author taken in September 1991.)

(Hildreth, 1981a; Hildreth and Moorbath, 1988; Guffanti and others, 1996). At least 50 vents for relatively primitive arc basalts have been identified and their products analyzed and discussed by Clynne (1993), Borg and others (1997), and Clynne and Muffler (in press). These include Inskip Hill and Cold Creek, Soap, and Black Buttes in the forearc; parts of the compositionally varied major shields at Sifford Mountain and Mount Harkness along the arc axis; and the Swain Mountain shield and numerous scoria cones of the Caribou field east of the axis. At least a dozen vents have also been identified for primitive high-Mg basaltic andesite, most of them west of the axis (Clynne, 1993; Borg and others, 1997).

Volumetrically, however, as opposed to numbers of vents, andesitic and silicic eruptive products, taken together, exceed the Quaternary output of the more numerous mafic volcanoes in the Lassen segment. The Lassen volcanic center alone has produced more than 200 km^3 of material in the last 825 kyr (Clynne, 1984, 1990a; Clynne and Muffler, in press), ~95 percent of it andesitic or more silicic. Three additional large centers (intermediate stratovolcanoes with late-stage peripheral silicic lavas) were established nearby around 2.5 Ma and may have remained active until ~1 Ma, that is, through much of the early Quaternary (Clynne, 1990b; Guffanti and others, 1990; Clynne and Muffler, in press). These are the Snow Mountain, Dittmar, and Maidu volcanic complexes (fig. 21), centered 40 km northwest, 15 km southeast, and 18 km south-southwest, respectively, from Lassen Peak. Several lava plateaux flanking the huge Maidu complex represent by far the most voluminous occurrence of Quaternary rhyolite lava in the Cascades; the 1.2-Ma Blue Ridge flow alone (75% SiO_2), though eroded, still covers ~90 km^2 and is as thick as 150 m (Gilbert, 1969; Clynne and Muffler, in press). Eruptive volumes of these eroded centers are difficult to reconstruct, but edifice dimensions estimated by Clynne (1990b) permit crude reckoning of volumes (ignoring dispersed pyroclastic ejecta) that might reasonably be expected for such complexes: Snow Mountain >25 km^3, Dittmar >150 km^3, and Maidu >200 km^3. In addition, a middle Pleistocene stratocone, the glacially gutted Magee Volcano 25 km northwest of Lassen Peak, consists mostly of andesite and basaltic andesite (53-63% SiO_2) but produced a late-stage lava flow and plug of rhyodacite (Macdonald, 1963; Borg, 1989; Borg and Clynne, 1998). Eruptive volume of the Magee center may have been 15±5 km^3, comparable to that of South Sister.

Away from these big centers, Quaternary rhyolite and rhyodacite vents are unknown, and the only substantial occurrences of dacite are Burney Mountain (~9 km^3), a steep middle Pleistocene composite dome ~900 m high (40 km north-northwest of Lassen Peak; see Frontispiece), and the early Pleistocene coulees of Huckleberry Mountain (20 km northwest of Lassen Peak). Scattered across the segment, however, as many as 50 Quaternary cones and shields are wholly or partly andesitic, including such substantial edifices as Prospect, West Prospect, and Sugarloaf Peaks; Table, Sifford, Red Lake, Badger, and Logan Mountains; Mount Harkness shield, and several chains and clusters of lesser cones and lava fields such as Tumble Buttes, the Sugarloaf chain, and the Red Cinder chain in the Caribou Volcanic Field (Guffanti and others, 1996; Clynne and Muffler, in press)—altogether contributing some 150 to 200 km^3 of nonmafic eruptive products.

Excluding the major evolved centers, Sherrod and Smith (1990) gave what they called a conservative volume estimate of 425 km^3 for products of regional cones and shields younger than 2 Ma in the Lassen segment. At least 25 percent (and conceivably 40 percent) of this total is likely to be andesitic and the rest mafic. It is unlikely that mafic products (basalt and basaltic andesite) of the last 2 Myr, even if underestimated, could approach in volume the 700 km^3 or more of andesite-to-rhyolite magma erupted in the Lassen region during that interval.

Quaternary vent density for the axial belt (and for the Lassen segment as a whole) is similar to that of the Cascades in central Oregon (table 1), but vents are locally spaced more densely—particularly in the Lassen domefield and in the Caribou Volcanic Field (25 km east of Lassen Peak). The Lassen concentration reflects the numerous silicic lava domes that leaked recurrently from a long-lived crustal magma column under the Lassen Peak area, whereas the Caribou concentration reflects several crowded mafic-vent alignments controlled by Basin and Range extension within the arc. The 50-km^3 Caribou Volcanic Field consists of basalt to andesite (basaltic andesite predominating), and a majority of its ~140 middle and late Pleistocene cones and shields are aligned north-northwest, along or parallel to regional extensional faults (Guffanti and others, 1990, 1994, 1996; Clynne and Muffler, in press). The extraordinary vent density in the Caribou Volcanic Field (<3 km^2 per vent; table 1) is comparable to that of Medicine Lake and Newberry fields, where Basin and Range extensional faulting is likewise important. Although Basin and Range faulting has encroached into the Cascades east of Mount Shasta and south of Crater Lake as well, in the Lassen segment the faulting affects not only the eastern approaches but completely overlaps the main axial belt of the magmatic arc (Guffanti and others, 1990, 1994).

Lassen Volcanic Center

Surrounded by the distributed mafic-to-andesitic volcanic field, the 400-km^2 Lassen volcanic center (LVC) is the southernmost large active center in the Cascades. Since ~825 ka (perhaps since ~1 Ma), it has remained a major magmatic focus, recurrently one of the foremost silicic volcanic areas in the Cascades (Williams, 1929, 1932b; Clynne, 1984, 1990a; Bullen and Clynne, 1990; Clynne and Muffler, 1990, in press). The LVC consists of four main components: (1) a precaldera and caldera-forming silicic sequence (825 to 600 ka); (2) an andesite-dacite stratocone (590 to 390 ka); (3) a dacite domefield containing ~35 domes that erupted during two main episodes at 300 to 190 ka and 70 to 0 ka; and (4) a field of hybrid intermediate cones and lava flows peripheral to the domefield but contemporaneous (313 to 0 ka) with it.

The earliest phase, the “Rockland sequence”, produced a 15-km-wide ring of 15 precaldera dacite domes and lava flows (64-68% SiO_2) that surround the filled and buried caldera source of the 600-ka Rockland Tuff (>75 km^3), a silicic ignimbrite and far-flung ashfall known from Utah to the Pacific Ocean (Sarna-Wojcicki and others, 1985; Meyer and others, 1991; Lanphere and others, 2004). Unique among the domes, the youngest (Raker Peak ~600 ka) is rhyolitic (73.5% SiO_2) and compositionally similar to the dominant pumice in the ignimbrite (71-74.5% SiO_2) (Clynne and Muffler, in press). Soon after the Rockland eruption, a successor stratocone, long-lived Brokeoff Volcano (590 to 390 ka), began to grow atop the southern part of the caldera, producing ~80 km^3 of andesite and dacite (55-68%, mostly 57-63% SiO_2). The present-day amphitheatre of the gutted stratovolcano is not itself a caldera (as advocated by Williams, 1932b) but simply reflects glacial erosion of its altered core (Clynne and Muffler, 1989, in press).

Filling and obscuring of the Rockland Caldera was subsequently completed by growth of the Lassen domefield, an 8×15-km assemblage of about 35 contiguous dacite and rhyodacite (63-72% SiO_2) lavas and pyroclastic deposits emplaced in at least 20 events (Clynne, 1990a) between ~300 ka and 1.1 ka, clustering into two main episodes dated at 300-190 ka and 70-0 ka (Clynne and Muffler, 1989, in press). Youngest is the **Chaos Crags** cluster of six domes that erupted ~1,100 years ago (Crandell and others, 1974; Heiken and Eichelberger, 1980; Clynne and others, 2002; Christiansen and others, 2002). Highest point in the whole segment is **Lassen Peak** (3,187 m), which is not a stratocone (as some assume) but a 2.5-km^3 rhyodacite dome (63-70% SiO_2) more than 800 m high (Williams, 1929, 1932b), one of the youngest members of the domefield at ~27 ka (Turrin and others, 1998). Many of the postcaldera domes contain quartz phenocrysts, which are rare elsewhere in the Quaternary Cascades, in addition to biotite, hornblende, plagioclase, sparser pyroxenes, and commonly mafic enclaves.

The postcaldera Lassen domefield represents at least 50 km^3 of silicic magma (Guffanti and others, 1996), approaching the magma volume released as fallout and outflow by the caldera-forming eruption. Because neither the volume of intracaldera Rockland ignimbrite nor that of tephra dispersed by recurrent postcaldera dome-producing episodes is known, however, the nominal total of ~125 km^3 of silicic magma erupted during the last 600 kyr of activity at the LVC is likely to be an underestimate. As the nearby Maidu volcanic center (fig. 21) also produced abundant rhyolite and dacite (probably >50 km^3) during the early Pleistocene, the Lassen district volumetrically rivals and probably exceeds Mazama, Tumalo, St. Helens, Kulshan, and Meager in Quaternary eruption of silicic magma. For eruption of rhyolite alone (>72% SiO_2), the Maidu and Lassen volcanic centers are unrivalled in the Quaternary Cascades.

Peripheral to and within the Lassen domefield, ten volcanoes contemporaneous with it produced at least 10 km^3 of “hybrid andesites” (including “quartz basalts” of early investigators), interpreted by Williams (1932b, p. 373) as mixtures of mafic and dacitic magmas, a hypothesis confirmed and elaborated analytically by Clynne (1989, 1990a, 1999). The hybrids include products of such centers as Hat Mountain, Crater Butte, and Raker and Fairfield Peaks and appear to entail varied proportions of regional mafic magmas blended with rhyodacite magmas like those of the Lassen domefield. Also assigned to the hybrid group by Clynne and Muffler (in press) are the complex mid-17th century eruption of Cinder Cone (53-60% SiO_2; Clynne and others, 2000) and the small andesite-dacite mixed eruptions of May 1915, which fortuitously broke out through the top of the 27-ka Lassen Peak dome (Clynne, 1999; Christiansen and others, 2002).

Conspicuous in most of the silicic lavas of the domefield itself are chilled enclaves and blebs of mafic and andesitic magma (Williams, 1932b; Clynne, 1989, 1990a), as well as unequilibrated phenocrysts dispersed from such inclusions. Clynne (1990a) showed that dispersal, disaggregation, and mixing of such material into the resident rhyodacite magma reservoir extends the centrally eruptible compositional range down to dacite and even to silicic andesite. The ubiquity of mafic inclusions in the many domefield lavas suggests that the LVC rhyodacite reservoir is thin and susceptible to wholesale convection when injected by batches of mafic magma. Vents for more homogenized hybrid andesites are scattered from the domefield to as far as 12 km outside it (fig. 21), indicating distribution of additional silicic melt pockets well outside the focal reservoir.

California Comparisons

The Lassen and Shasta segments are rather different from the rest of the Cascades, having some features in common with other segments but each being unique in its combination of characteristics. The volcanically inactive gaps north and south of the Shasta segment provide a first-order contrast with the unbroken belt of close-set volcanoes that stretches more than 500 km from central Washington to southern Oregon. The great width of the Quaternary volcanic zone in California resembles that of southern Washington and northernmost Oregon, but it contrasts strongly with the discontinuous vent zone of the Garibaldi Volcanic Belt and with the continuous but narrower Oregon Cascades (fig. 1). In California, the main Cascade axis trends north-northwest, parallel to many sets of Basin and Range faults, in contrast to the northerly (or N10˚E) trend of the axis in Oregon and southern Washington. Shasta and Maidu are huge centers that lie west of the Cascade axis in California, but elsewhere in the Cascades the only large forearc edifices are Rainier and St. Helens. Likewise, the only thing comparable to the scattering of small forearc volcanoes southwest of Lassen is in the region around Portland and southwest Washington. Elsewhere in Oregon, only a few isolated vents of Quaternary age lie significantly west of the main belt (Sherrod, 1990a), and in the Garibaldi Volcanic Belt no forearc vents are recognized.

Clustering of the voluminous Latour (3.5 to 3.0 Ma), Yana (3.2 to 2.4 Ma), Dittmar (2.4 to 1.4 Ma), Maidu (2.4 to 1

Ma), and Lassen (1 to 0 Ma) volcanic centers within 15 to 25 km of each other is unparalleled elsewhere in the Quaternary Cascades. The volume erupted by each may have matched that of the entire Mazama cluster. For comparison, spacing is much greater among the Hood, Adams, St. Helens, Rainier, and Goat Rocks stratovolcanoes (a not dissimilar regional array of scattered major centers; figs. 1, 8), ranging from 35 to 100 km.

Counting the small volcanoes, however, Quaternary vent densities along most of the Cascade axial region are generally comparable (8-30 km^2/vent; table 1). Vent density is significantly greater around the Lassen and Mazama evolved centers, and it attains maximum values at the three extensional, predominantly mafic, foci farther inland—Caribou, Medicine Lake, and Newberry (table 1).

The major evolved foci account for 60 to 75 percent of the Quaternary eruptive volume in the Lassen segment and more than 80 percent in the Shasta segment, as compared to only 10 to 33 percent along the Oregon segment. In southern Washington, the proportion is about 80 percent and in the Garibaldi Volcanic Belt more than 98 percent. From a different perspective, however, major andesitic-to-silicic volcanic centers number only six among the more than 740 Quaternary vents in the California Cascades, only six among the more than 1050 in the Oregon segment, five among the 412 in the Hood-to-Rainier segment, and five among the 127 in the Garibaldi Volcanic Belt (tables 1, 2).

Considering compositional output more narrowly, the eruptive volume of true rhyolite in the Lassen segment (mainly Maidu and Rockland) is unapproached elsewhere in the Quaternary Cascades, that of the Tumalo-South Sister area being a distant second. Moreover, production of Quaternary rhyodacite at Lassen volcanic center is rivalled only by the Mazama/pre-Mazama, Tumalo, Jefferson, Kulshan, and Meager systems. In the Shasta segment, on the other hand, rhyolite is absent and rhyodacite nearly so. Dacite is plentiful at the major centers in both California segments. Accurate estimates are not feasible, but a total volume of dacite greater than 50 km^3 is likely at Mount Shasta and likewise at the Lassen volcanic center, where much of it may result from mixing of rhyodacitic and mafic magmas. Such volumes may exceed the amount of dacite erupted from such dacite-dominated volcanoes as Glacier Peak, Mount Cayley, and Mount Garibaldi, and they rival that of Mount St. Helens. Away from the major foci, however, Quaternary dacite is rare in the Lassen and Shasta segments, even sparser than the isolated dacite occurrences in the Cascades of Oregon and Washington. Burney Mountain, however, one such rarity in the Lassen segment, consists of ~9 km^3 of phenocryst-poor dacite, a volume surpassing the amount of dacite produced by Mount Adams or Mount Baker and rivalling the dacite output of Mounts Hood and Jefferson. Volumetrically, silicic andesite is the dominant composition at Mount Shasta, probably also at Rainbow Mountain, and therefore in the Shasta segment as a whole. Andesite is probably the leading Quaternary composition erupted in the Lassen segment as well, owing to the large contributions of the Dittmar, Maidu, and Brokeoff edifices, even though it is exceeded in volume at the Lassen volcanic center itself by still more silicic products. In the Cascades of California (as in Oregon but not in Washington), a majority of the individual Quaternary volcanoes consist, however, of basaltic andesite, reflecting the great number of shields, cones, and modest lava fields distributed regionally. The Lassen segment is distinctive, nevertheless, in that small scattered andesitic and basaltic volcanoes are also well represented; although still numerically subordinate to basaltic andesite, both are much more common than in the Oregon and Shasta segments of the arc.

Among true basalts in the California Cascades, HAOT is widespread, and its vents are widely but sparsely distributed. In the Lassen segment, arc basalt is much more common than HAOT, in both eruptive volume and number of vents (Guffanti and others, 1990), but in the Shasta segment the mafic calcalkaline rocks are virtually all basaltic andesite (>52% SiO_2). HAOT is the hallmark of extension-related magmatism in the parts of California and Oregon inland of the Cascades, and HAOT appears to be the leading parental magma at the Medicine Lake Volcanic Field and probably at Newberry, as well. As westward-encroaching Basin and Range faulting invaded the Cascades and even reached the Cascade axis, so did venting of HAOT. The volcanically inactive gaps north and south of the Shasta segment are not longstanding but are marked by Pliocene mafic shields and cones, abundant in the northern gap, sparse in the southern. Development of the quiescent gaps in the southern Cascades is a Quaternary phenomenon, concurrent with northward contraction of the arc's southern terminus, westward drift of the eastern limit of the active belt, and westward penetration of extension-related faulting and magmatism to the heart of the Cascade arc.

Contemporaneous Volcanic Fields Behind the Arc

Three large Quaternary volcanic fields conventionally associated with the Cascade arc occupy discrete areas just east of it (figs. 8, 14, 21) and, although contiguous with the arc, they exhibit tectonic and compositional features distinguishable from typical arc volcanism. All three may be regarded in part as “central volcanoes” in the sense of Walker (1993) in that significant volumes of rhyolite are intruded and erupted near the central focus of a distributed, multivent, fundamentally basaltic volcanic field in which intermediate compositions are subordinate and mostly hybrid. Each of the three has commonly been referred to as “a volcano” (for example, Newberry Volcano), a usage I regard inappropriate and volcanologically misleading. Each of the three volcanic fields consists of hundreds of volcanoes. Although some vents are indeed laterally dike-fed at shallow levels, from the central magma-supply system out onto the flanks (as on some oceanic shields), many or most peripheral vents instead have independent conduit systems from the deep crust or mantle, and only a modest fraction of the vent array is concentrated in the (rhyolite-rich) summit region of the shield.

Simcoe Mountains Volcanic Field

The Simcoe Mountains Volcanic Field extends ~45 km eastward from the (mostly younger) Mount Adams Volcanic Field in south-central Washington (fig. 8). It also extends ~75 km northwest from Goldendale as far as Jennies Butte, draping two of the preexisting east-west-trending anticlinal ridges (consisting predominantly of Miocene flood-basalt units) that form the Yakima Foldbelt (the southern of the two being the Simcoe Mountains proper). The volcanic field lies largely in the Yakama Indian Reservation, and only its southern third drapes the Simcoe Mountains Anticline (atop which the conspicuous multivent Simcoe shield was constructed). New mapping (author's work in progress) has raised the number of vents identified to 184, of which at least 35 are of early to middle Quaternary age, the remainder Pliocene. A majority of the vents occupy the trough between the anticlines. Most are basaltic scoria cones and fissure-fed lava fields, although about 10 scattered units are intermediate (53-67% SiO_2), and five rhyolites (73-75% SiO_2) are exposed near the top of the shield. Predominant among the mafic rocks (46-53% SiO_2) are intraplate (rather than arc) trace-element signatures, and most are moderately alkalic (some carrying harzburgite, dunite, or lherzolite xenoliths), although subalkaline and even a few HAOT units are also present. In the southern and central parts of the field (as roughly partitioned by the two east-west anticlines), numerous vent cones are clustered, and some are locally aligned roughly north-south or NNW; but in the northern third of the field, vents are fewer, more widely spaced, and small shields dominate. K-Ar ages determined by Uto and others (1991) range from 4.5 to 0.6 Ma, and extensive $^{40}Ar/^{39}Ar$ dating currently underway (2007) in concert with our mapping confirms that range. The Simcoe Mountains Volcanic Field covers at least 1,400 km^2, with an estimated volume of ~200 km^3, of which about half may be younger than 2 Ma and roughly 10 percent younger than 1 Ma.

Newberry Volcanic Field

The Newberry Volcanic Field in central Oregon (fig. 14) contrasts with the Simcoe field in being subalkaline, younger, and far more voluminous. Although Newberry takes the form of a great shield volcano 35×65 km across, it is a profoundly hybrid edifice. Capped by a 5×7-km late Pleistocene caldera, the edifice has a rhyolite-rich core surrounded by a gently dipping apron sprinkled with more than 400 mafic scoria cones and fissure vents along with about 20 silicic flank domes (MacLeod and others, 1995). Many more domes and cones are likely to be concealed beneath the mantle of thin mafic lavas and mafic-to-silicic pyroclastic deposits that smooths the surface and conveys a deceptive integrity to the edifice, which is in large part a distributed volcanic field that surrounds and interfingers with products of the central volcano.

The Newberry Volcanic Field occupies a tectonic singularity where the age-progressive rhyolite trend of the High Lava Plains (Walker, 1974; MacLeod and others, 1975) and the northwest prong of Basin and Range extensional faulting both impinge upon the Cascade arc (Walker and MacLeod, 1991; Jordan and others, 2004). Many vents are northeast-aligned on the south flank and northwest-aligned on the north flank, reflecting extensional fault belts that intersect beneath the edifice and probably helped instigate the major magmatic focus here. North-south elongation of the edifice and east-west elongation of the caldera may both reflect the influence of net east-west extension—on mafic dike propagation and on growth of a shallow silicic magma reservoir, respectively.

The caldera is likely to be a composite structure that resulted from two or three syneruptive subsidence events, probably related to pyroclastic deposits that crop out patchily on most flanks of the edifice (MacLeod and others, 1995). Silicic ignimbrites (~300 ka) on the east flank may be related to an early subsidence, and compositionally zoned pyroclastic deposits (75-80 ka) on the west flank may be related to a younger collapse (Donnelly-Nolan and others, 2004). The high south wall of the caldera cuts the rhyolite lava of Paulina Peak, which has been dated at 83±5 ka (Donnelly-Nolan and others, 2004). Several more late Pleistocene rhyolitic lava flows are cut by the caldera walls, and a dozen intracaldera rhyolite vents (mostly Holocene) have erupted lavas and pumice (Williams, 1935; MacLeod and Sherrod, 1988; MacLeod and others, 1995; Jensen, 2006). Recurrent intracaldera eruptions of phenocryst-poor rhyolite of similar composition (73-74% SiO_2, 790-850 ppm Ba), the latest one as recent as 1.3 ka, and the scarcity of mafic eruptions on the caldera floor support the likelihood of a shallow rhyolitic magma reservoir (MacLeod and Sherrod, 1988), as does the 600ºC/km conductive thermal gradient measured for the bottom 300 m of a 932-m-deep drillhole on the caldera floor (MacLeod and Sammel, 1982). Eruption of Little Crater and other mafic tuffs on the caldera floor, probably in the early Holocene, suggests, however, that the rhyolitic magma reservoir is modest and either distributed or transient. Relatively young mafic lavas (53.5-57% SiO_2) have also erupted nearby, in the early Holocene along the east rim and on the east flank, as well as around 7 ka from at least two vents south of the caldera and a 23-km-long chain of vents northwest of it (MacLeod and others, 1995; Donnelly-Nolan and others, 2004; Jensen, 2006). As currently understood, products erupted at Newberry are strongly bimodal, silicic andesite and dacite being sparse while basaltic andesite, basalt, and rhyolite-rhyodacite are abundant.

The Newberry edifice itself covers ~1,600 km^2, but a (vent-poor) low-gradient apron of fluid tube-fed lava flows adds another 1,000 km^2, principally in a broad thin lava field extending ~50 km northward from the toe of the edifice. Eruptive volume is at least 500 km^3—not counting lost downwind tephra, which may be substantial (Kuehn, 2002). Basaltic andesite is strongly represented among the abundant scoria cones and lava flow fields at Newberry, but at least two kinds of relatively primitive basalt (48-50% SiO_2) are also present—HAOT like that of the High Lava Plains (of eastern Oregon) and arc basalt rich in Ba and Sr (J.M. Donnelly-Nolan, work in progress).

Medicine Lake Volcanic Field

Another great edifice adjacent to but inboard of the Cascade arc is the Medicine Lake Highland (Anderson, 1941; Donnelly-Nolan, 1988, in press) in northernmost California, centered 55 km east-northeast of Mount Shasta (fig. 21). Like Newberry, it takes the form of a gently sloping central shield dotted by hundreds of scoria cones and fissure vents, topped by a caldera, and surrounded by a low-relief apron of fluid basaltic lava flows (Donnelly-Nolan and Champion, 1987; Waters and others, 1990). Also like Newberry, it occupies an area of Basin and Range faulting, where net east-west extension may have influenced both north-south elongation of the vent zone and east-west elongation of the caldera. Vents of the volcanic field encompass an area of 40×55-km (fig. 21) to which the surrounding apron of outflow lavas adds half again as much more. About 66 percent of the surface exposure is basalt, 13 percent basaltic andesite, 15 percent andesite, and only 6 percent dacite and rhyolite (Donnelly-Nolan and others, 2003). With an eruptive volume of ~600 km^3, the Medicine Lake Volcanic Field is the most voluminous Quaternary eruptive locus in or adjacent to the Cascades, approached in volume only by Newberry and Shasta.

A dozen geothermal drillcores (Donnelly-Nolan, 2006) reveal, however, that the central core of the edifice contains numerous 475-to-300-ka rhyolite lavas, which are largely concealed by the veneer of mafic and intermediate lavas that shingle off toward the apron, conveying the deceptive appearance of a simple mafic shield. Like Newberry, therefore, the Medicine Lake Volcanic Field has as its focus a “central volcano” (in the usage of Walker, 1993), a multivent mafic shield centered on a rhyolite-rich core, but its flanks and periphery are also studded by hundreds of widely distributed monogenetic vents, many of which are fed by separate conduits from separate source volumes, independent of the shield's central magma-supply system. Donnelly-Nolan (in press) further distinguished 13 rhyolitic units that crop out on the upper flanks of the edifice, many of them of middle Pleistocene age like those in the drillcores; two more are late Pleistocene, and two erupted in the late Holocene.

Although several smaller mafic shields, a few early Pleistocene rhyolites, and probably the buried source of a 1-Ma rhyolitic ignimbrite already occupied the site, construction of the present-day Medicine Lake edifice began ~500 ka (Donnelly-Nolan and Lanphere, 2005), roughly contemporaneous with initiation of Newberry and several intermediate Cascade stratocones (Baker, Rainier, Adams, Mazama, and Shasta). After 200 kyr as a bimodal (mafic-rhyolitic) center, Medicine Lake became a predominantly mafic eruptive center around 300 ka and has remained so since.

The caldera, which has rim dimensions of 7×12 km, is of uncertain origin. Only one ignimbrite is exposed on the edifice (Anderson, 1941; Donnelly-Nolan and Nolan, 1986). Dacitic in pumice composition (63-67% SiO_2), the tuff is 10 to 30 m thick in drillcores beneath the summit, crops out widely but thinly (less than 5 m) on the flanks, is dated at ~180 ka, and appears to be too small (5-10 km^3) to account for the caldera (Donnelly-Nolan, 2006). It may be that mafic magma withdrawal toward flank vents (repeatedly?) and eruption of the dacite tuff both contributed to subsidence, creating ring faults that subsequently provided conduits for a ring of andesite-dacite lavas (~100 ka) that surrounds and thus accentuates the depression (Anderson, 1941; Donnelly-Nolan, in press).

The Medicine Lake edifice has had 17 postglacial eruptions (Donnelly-Nolan and others, 1990). A sequence of eight events released ~5.3 km^3 of HAOT, basalt, and basaltic andesite ~13 ka, by far the largest being the zoned Giant Crater lava field (~4.3 km^3). After a subsequent lull, nine more events beginning at 4.4 ka produced HAOT, basalt, basaltic andesite, andesite, dacite, and rhyolite. Of the nine, the most recent (Glass Mountain) eruption (in the 11th Century) was the most voluminous (~1 km^3), as well as the most silicic (zoned up to 74.6% SiO_2) and explosive (Eichelberger, 1975; Heiken, 1978; Donnelly-Nolan and others, 1990; Grove and others, 1997).

Vent alignments are numerous and conspicuous on the Medicine Lake edifice, rivalled only by Newberry and Bachelor in their importance. Generally (but not strictly) reflecting east-west tectonic extension, most alignments strike within 30º of north, augmented by a few that are influenced by the caldera or other edifice effects or by a preexisting vent alignment that extends east-northeast from Rainbow Mountain through Garner Mountain and beneath the Medicine Lake edifice (Donnelly-Nolan and others, 1990).

Smith and Donnelly-Nolan (2005) identified 525 Quaternary vents mapped on or near the Medicine Lake edifice, noting also that vents for an additional 56 map units have been buried by younger units. They report that 20 percent of the vents released HAOT, 53 percent other basalts and/or mafic andesite, 11 percent andesite, 3 percent dacite, and 9 percent rhyodacite and rhyolite. Because many map units have multiple vents, vent redundancy is far greater here than anywhere in the Cascade arc proper, reflecting the abundance of fissure eruptions of dike-fed basaltic lavas influenced by Basin and Range extension.

Primitive magmas at Medicine Lake are predominantly HAOT, which is widespread in the Basin and Range Province of northeastern California and the High Lava Plains of Oregon but is also sprinkled sparingly along the Quaternary Cascade arc from Lassen to Goat Rocks. Thought to be produced under tectonic extension by dry decompression melting of shallow MORB-source mantle, HAOT magmas at Medicine Lake are water-poor (Sisson and Layne, 1993), as impoverished in K_2O as 0.07 percent, and have repeatedly induced upper-crustal melting, which has led to mixing, assimilation, and eruption of extensive lava flows zoned from primitive HAOT to basaltic andesite and andesite (Grove and others, 1988; Donnelly-Nolan and others, 1991; Baker and others, 1991; Bartels and others, 1991). Nonetheless, hydrous arc basalts containing 3 to 6 percent H_2O have also erupted at Medicine Lake (Wagner and others, 1995; Kinzler and others, 2000), two as recently as the 9th Century, attesting to the influence of a slab-derived fluid flux (however attenuated) that affects some domains of the mantle wedge well into the rear-arc.

The **Hackamore Volcanic Field** (fig. 21), which extends from beneath the Medicine Lake apron for at least another 25 km eastward, is a HAOT-dominated Quaternary lava field formerly lumped with the Tertiary HAOT lavas it overlies (Donnelly-Nolan and others, 1996). Covering at least 850 km^2, the field has a dozen or more vents, most of them early Quaternary, but a few are middle Quaternary and as young as ~600 ka (Donnelly-Nolan and Lanphere, 2005). Like Medicine Lake, Hackamore is a Basin and Range volcanic field, and it may be far enough inboard to be completely beyond the influence of the slab-derived fluid contributions sporadically or locally effective beneath Medicine Lake.

Characteristics of Quaternary Volcano Distribution

Types of Volcanoes

Of the 2,339 Quaternary volcanoes identified in the Cascade arc proper (table 1), only 19 are andesite-dacite stratovolcanoes in the usual sense of being steep composite cones (solitary or clustered) built up of interstratified lava flows and fragmental deposits. Ranging in eruptive volume from ~10 to 450 km^3 each, these are Baker, Rainier, Goat Rocks, Adams, St. Helens, Hood, Jefferson, Broken Top, South Sister, Middle Sister, Cappy, Mazama, Rainbow, Shasta, Snow Mountain, Magee, Maidu, Dittmar, and Brokeoff. The apparent cone height of these edifices (excluding apron deposits that extend down radial valleys cut in older rocks) ranges from 1,300 m for South and Middle Sisters, to ~2,000 m for Jefferson, Baker, and pre-1980 St. Helens, to ~2,300 m for Hood and Rainier, to 2,650 m for Adams, and 3,250 m for Mount Shasta. For more details, see table 2. Among the other major centers, Glacier Peak, Garibaldi, Cayley, and Meager are in large part well-focussed silicic dome clusters surrounded by aprons of lavas and pyroclastic flows, whereas Lassen, Kulshan, and Tumalo are distributed silicic domefields, as was the pre-Mazama rhyodacite field. Mount St. Helens added its modest intermediate-to-mafic stratovolcano to its volumetrically dominant silicic domefield only during the past 2,500 years, whereas the long-lived Mazama locus underwent alternating episodes of domefield and stratocone growth. Mount Meager may also have had an early stratocone-bulding phase. The Lassen region has produced a succession of intermediate stratovolcanoes, each culminating in peripheral eruption of rhyolite or rhyodacite.

To the list of large evolved edifices should be added at least 11 large mafic cones (predominantly basaltic andesite; all in Oregon) that are sufficiently composite, steep, and high (700 to 1,300 m relief) to qualify as stratocones. These are McLoughlin, Bailey, Thielsen (fig. 20), Odell Butte, Diamond Peak, Bachelor, North Sister, Black Crater, Black Butte (Oregon), Mount Washington (fig. 17), and Three Fingered Jack (each having an eruptive volume in the range 5-to-25 km^3). There is a morphological continuum, however, from these steep mafic cones through transitionally conical shields (such as Olallie Butte, Maiden Peak, Hamner Butte, Davis Mountain, and Goosenest (fig. 22) into a spectrum of flatter mafic shield volcanoes (fig. 17) cored or capped by a fragmental facies. Table 2 summarizes some physical dimensions of most of the major edifices in the Cascades.

At least four times more abundant than stratovolcanoes in the Cascades are shield volcanoes, the number of Quaternary shields totalling about 110 (~30 in California, ~60 in Oregon, ~20 in Washington, and none in the GVB). Most are basaltic andesite or calcalkaline basalt, but a few consist of HAOT (for example, Lemei Rock, Spring Creek) or andesite (Timber Crater, Pelican Butte, Goosenest). Some of the smaller shields (0.1-2 km^3) may be short-lived or even monogenetic, but many larger ones (2-35 km^3) are probably polygenetic, erupting recurrently for centuries or millennia. Several of the largest Cascade shields (including King Mountain, Lemei Rock, Irish Mountain, The Twins, Fuji Mountain, Mount Yoran, Cowhorn Mountain, Sawtooth Mountain, Howlock Mountain, Timber Crater, Union Peak, Pelican Butte, Whaleback, and Ash Creek Butte) have volumes in the range 7 to 35 km^3, thus rivalling or surpassing in size several of the smaller stratovolcanoes. Slope gradients of shields range greatly, from 2º for the Spring Creek shield (north of Mount Adams), which consists of fluid HAOT, to 7 to 10º for many basaltic and mafic andesitic shields like King Mountain, Trout Creek Butte, Maiden Peak, Davis Mountain, and Everitt Hill, to 15 to 20º for Odell and Black Buttes (Oregon), which would better be called cones than shields. Mount Bachelor illustrates a common ambiguity whereby a later cone (~20º) grew with apparent eruptive continuity from the same vent system atop an earlier shield (4 to 7º) of similar composition. Magma viscosity is an obvious influence, but prevalence of low-intensity eruptions of spatter and scoria that pile up proximally would also steepen shields into cones. Topographic profiles of many types of Cascade volcanoes are assembled in figure 23.

Lava domes (including equivalent stubby viscous flows) account for about 15 percent of the vents, approximately 340 such units among 2,339 Quaternary vents in the arc. Nearly all domes consist of dacite or rhyodacite, but a few are andesite (for example, Hogg Rock) or rhyolite (Three Creek Butte). The tallest domes are (Shasta) Black Butte (730 m), Lassen Peak (~800 m), and Burney Mountain (900 m), and two or more ice-mantled eroded domes atop Mount Meager are probably of comparable size. For comparison, Ptarmigan dome at Kulshan caldera is 300 m high, Butte Camp dome at the southwest toe of Mount St. Helens is 430 m, Goat Mountain (10 km southwest of Mount St. Helens) is ~550 m, Spiral Butte is ~520 m, the 1980-86 dome in the crater of Mount St. Helens is 267 m, and Crater Rock dome near the top of Mount Hood is less than 200 m. Volumetrically, very few domes exceed 0.5 km^3, and some are smaller than 0.01 km^3. Among the largest, Spiral Butte approaches 2 km^3, Lassen Peak dome and

(Shasta) Black Butte are each ~2.5 km^3, and ice-mantled Pali dome north of Mount Cayley may be of comparable volume. By far the largest Quaternary dome in the Cascades is dacitic Burney Mountain, at ~9 km^3 (Frontispiece).

Most domes are clustered on or around a few main centers. Of the 22 Cascade domes identified in British Columbia, 17 are closely related to the major edifices, Garibaldi, Cayley, and Meager. Of 36 in the Washington Cascades, at least 15 are on or near Mount St. Helens and six are inside Kulshan Caldera. Of ~190 domes recognized in the Oregon Cascades, at least 40 lie close to Mount Jefferson (Conrey, 1991), ~22 are scattered in the Tumalo "silicic highland" and its southward extension, 28 or more are around the Three Sisters, and no fewer than 63 are on, around, or beneath Mount Mazama. Of ~90 domes in the California Cascades**,** ~45 belong to the Lassen domefield (~14 precaldera and more than 30 postcaldera), at least 5 belong to the Maidu volcanic center, and 18 are on or around Mount Shasta. In contrast to such concentrations, relatively few domes are isolated, clearly separated from major clusters or evolved centers. Examples include Spiral Butte in Washington and Frog Lake Buttes, Hayrick Butte, and Bench Mark Butte in Oregon. In not being related to any major edifice, the early Quaternary array of 18 dacite domes that extends 15 km southeastward from Barkley Mountain at the south end of the Lassen segment (fig. 21) is unparalleled in the Cascades. Another anomaly is the absence of lava domes for 140 km along the Cascade arc between Mount Mazama and the base of Mount Shasta.

Setting aside the 37 stratovolcanoes and major silicic dome complexes, the 110 shield volcanoes, and the 340 lava domes, more than 1850 additional Quaternary vents are recognized in the Cascades, nearly all of them monogenetic (as are most domes and some shields). A majority of these lesser vents are marked by scoria, spatter, or lava cones, but several fissure-fed lava flows, lava fields, and lava fans left no conspicuous edifice or crater at all. Monogenetic tuyas and comparable near-vent piles of englacial mafic lava and hyaloclastite are recognized in the Bridge River, Cayley, Garibaldi Lake, Baker, Indian Heaven, Jefferson, Mazama, and Caribou Volcanic Fields (and ice-contact lava flows are present at most of the main stratocones). Maars and tuff cones are rare in the Cascades; the few examples include Battle Ground, Carp, and Pothole Lakes in southern Washington, clusters of maars in central Oregon north of Wickiup Reservoir and east of Lookout Mountain, and tuff rings near the lakes in Newberry Caldera. Deep Hole is a mid-Pleistocene phreatic explosion crater ~800 m wide that lies 8 km west-northwest of Lassen Peak. Some monogenetic vents produced lava fields as voluminous as 1-5 km^3, but most erupted less than 1 km^3 of lava or ejecta, and several yielded less than 0.01 km^3. Among them, however, are vents for nearly all the relatively primitive magmas erupted in the Cascades.

Lengths of lava flows are influenced by magma discharge rate, viscosity, and external factors such as slope, water and ice, topographic channeling, and ponding. Walker (1973) argued that the first is often the most important. Most of the longest lava flows recognized in the Cascades are partly or exclusively HAOT: the Spring Creek (>35 km) and Ice Caves (43 km) basalts near Mount Adams; Plutos Cave basalt northwest of Mount Shasta (>30 km); Hat Creek Basalt (fig. 2*A*; 20 km); an intracanyon flow along Deer Creek southwest of the Lassen volcanic center (~45 km), and several more in the Lassen segment (30 to 55 km). Likewise, HAOT or eruptive units zoned to HAOT extend 45 km from Giant Crater (Medicine Lake) and ~50 km northward from the slopes of Newberry. Among the few arc basalts and basaltic andesites as long as 15 km (most of them intracanyon flows) are the Elaho Valley flow (~25 km) south of Mount Meager, the Cheakamus Valley basalts (>35 km) northwest of Mount Garibaldi, the Glaciate Butte flow (25 km) at Mount Adams, the Cave Basalt (15 km) at Mount St. Helens, the Big Lava Bed (15 km) at Indian Heaven, the late Holocene McKenzie River flow (15 km) from Belknap shield, several mafic flows of the Bachelor chain (15 to 22 km), the Hootman Ranch flows west of Lassen Peak, and a remarkable intracanyon flow along the Sacramento River from Everitt Hill south of Mount Shasta (~60 km). The few comparably long lava flows of andesite or dacite were (like many of the lengthy basalts) channeled along canyons or along the margins of glaciers occupying the canyons (Lescinsky and Sisson, 1998)—for example, the Ring Creek dacite flow south of Mount Garibaldi (18 km), the Glacier Creek andesite flow northwest of Mount Baker (>8 km), a thick intracanyon andesite (>20 km) along the Klickitat River east of Mount Adams, an intracanyon dacite (>22 km) along Cascade Creek southwest of Mount Adams, and several thick ice-marginal andesite-dacite flows (now forming ridges) radial to Mount Rainier, of which some were as long as 15 to 22 km (Fiske and others, 1964; Lescinsky and Sisson, 1998). In a class by itself is the 1-Ma Tieton Andesite, which flowed 80 km eastward from the Goat Rocks (Swanson, 1978). Few rhyolite or rhyodacite lava flows in the Cascades surpass 3 km in length, exceptions being the Glass Mountain zoned dacite-rhyolite flow (>5 km) at Medicine Lake and the gigantic Blue Ridge rhyolitic coulee (14 km) at Maidu. Not surprisingly, many (not all) of the longest units, whether principally mafic, intermediate, or silicic, are compositionally zoned (Eichelberger, 1975; Green, 1988; Donnelly-Nolan and others, 1991, 2005; Schick, 1994; Swanson, 1994; Grove and others, 1997; Stockstill and others, 2002).

Among the hundreds of Cascade scoria cones that are uneroded or only modestly so, most are 50 to 150 m high, only about 20 exceed 200 m, and only Border Mountain southeast of Medicine Lake is higher than 300 m. Of those that exceed 200 m, nearly all are in the Lassen region, the Caribou Volcanic Field, and the Mazama and Sisters reaches of Oregon. Only two of the many Simcoe Mountains scoria cones reach 200 m, and none of the superabundant scoria cones at Newberry is that high. Remarkably, one of the highest ejecta cones (210 m) in the region—the Central Pumice Cone at Newberry Caldera—is not mafic, consisting instead of Holocene rhyolite. Irrespective of composition and volume, global data compilations show that the original height of scoria cones is close

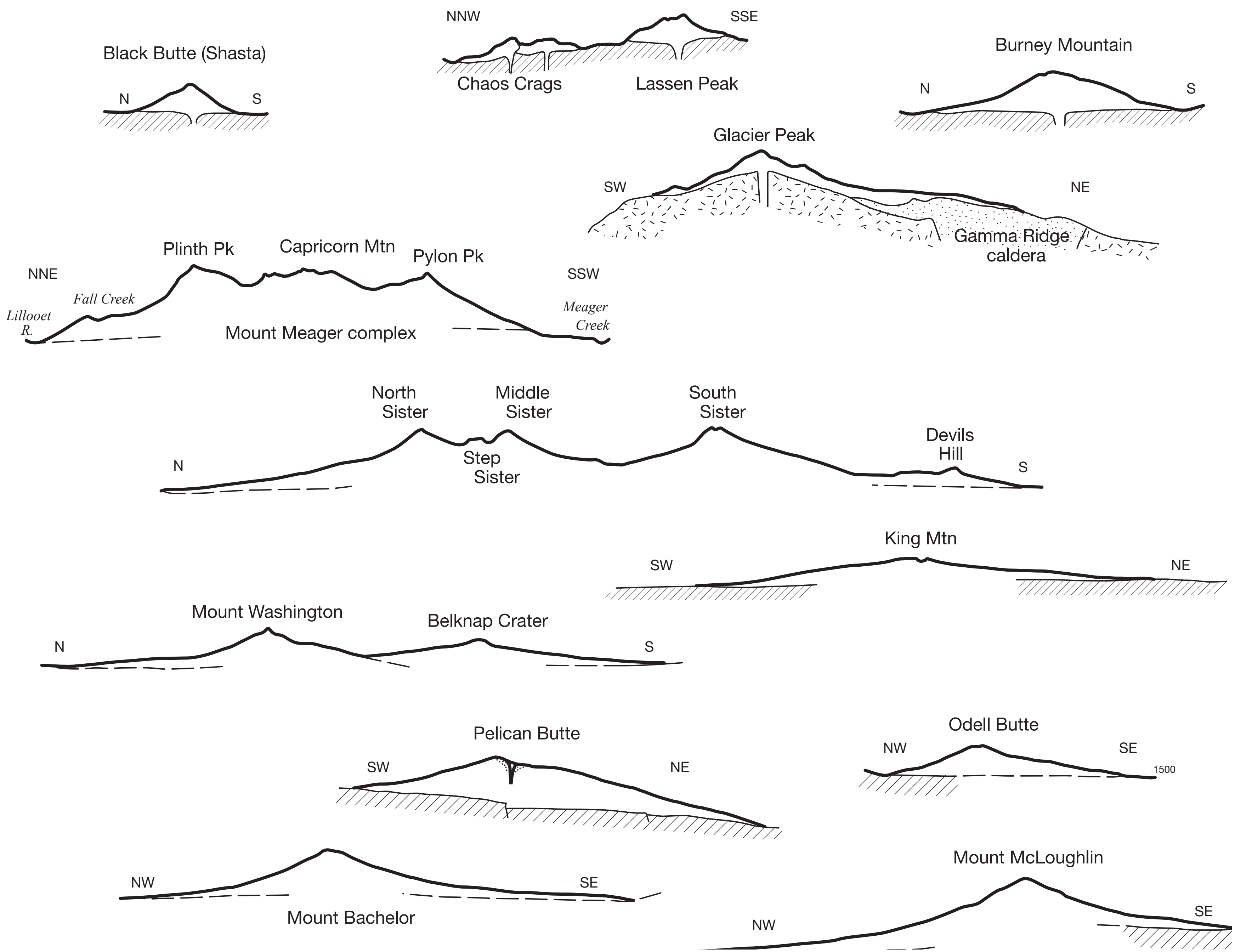
Black Butte (Shasta)
N
S
NNW
SSE
Chaos Crags
Lassen Peak
Burney Mountain
N
S
Glacier Peak
SW
NE
Gamma Ridge
caldera
Plinth Pk
Capricorn Mtn
Pylon Pk
NNE
SSW
Fall Creek
Lillooet
R.
Meager
Creek
Mount Meager complex
North
Sister
Middle
Sister
South
Sister
Devils
Hill
N
Step
Sister
S
King Mtn
SW
NE
Mount Washington
Belknap Crater
N
S
Pelican Butte
SW
NE
Odell Butte
NW
SE
1500
NW
SE
Mount Bachelor
Mount McLoughlin
NW
SE

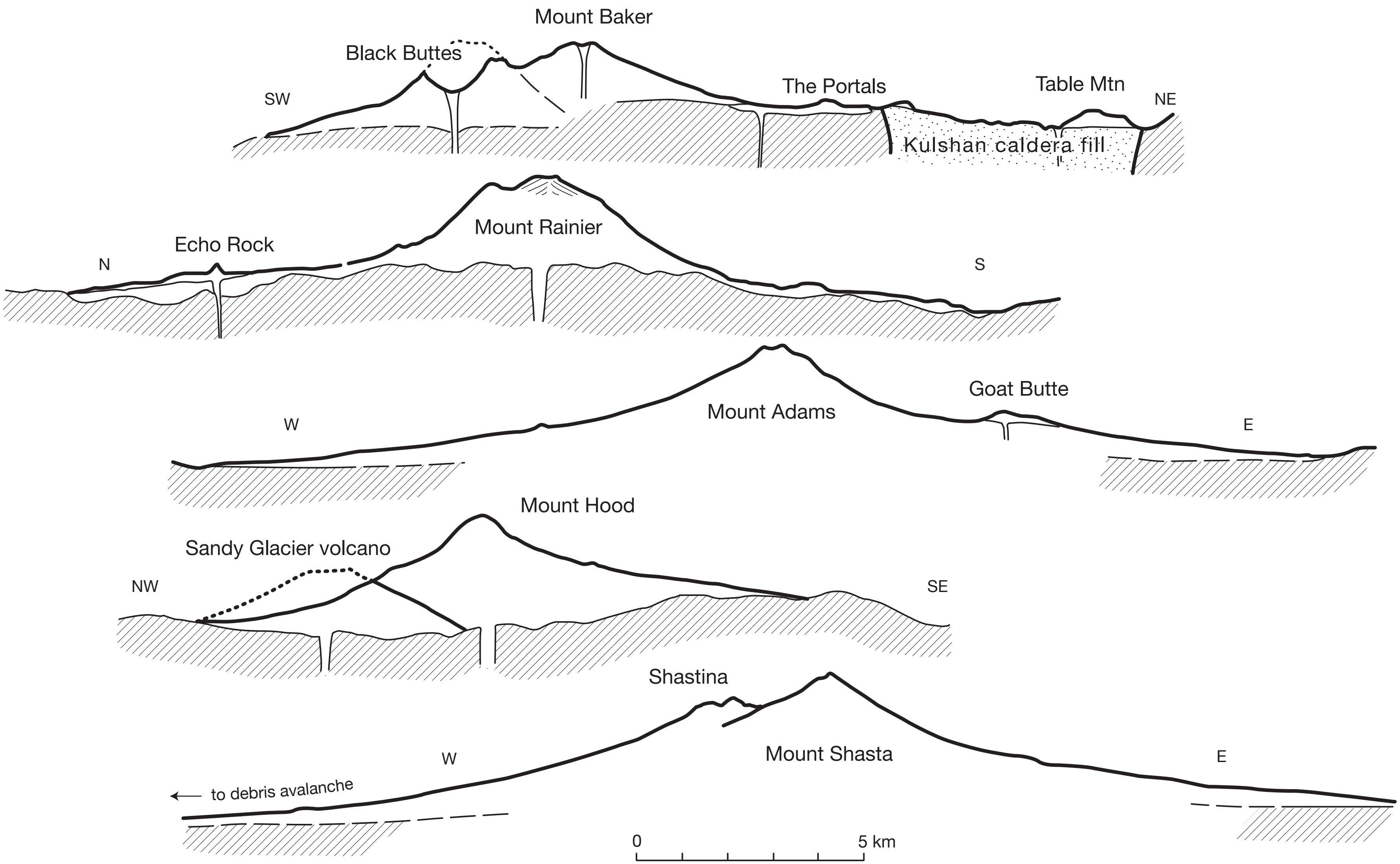

Figure 23. Profiles of selected Cascades volcanoes, all at the same scale, illustrating a variety of sizes and slopes. For only a few is the configuration of subedifice basement (hachures) well known. Free-standing **lava domes** shown are Lassen Peak and adjacent Chaos Crags, Black Butte (Shasta), and Burney Mountain, the largest Quaternary dome in the Cascades. Major **stratovolcanoes** shown are Rainier, Adams, Hood, and Shasta, which is the most voluminous in the Cascades. Although such edifices as Hood and Shasta also have vent domes, Glacier Peak is transitional in being dominated by a prominent summit dome complex that feeds an extensive apron of lavas and pyroclastic flows. **Clusters** of contiguous edifices shown are Meager, Baker, and the Three Sisters. **Mafic cones and shields** intergrade morphologically: King Mountain and Belknap are broad low-angle shields; Odell and Pelican Buttes are steep shields; Mount Bachelor has been called a mafic cone atop a shield (of similar composition); Mounts McLoughlin and Washington (and Thielsen; fig. 20) are steep and high enough to be called mafic cones with proportionally important pyroclastic and intrusive core facies.

to 0.18 × basal diameter, that nearly all such eruptions last between a week and a year, that most scoria cones include layers, lenses, or rim facies of agglutinate, and that most produce lava flows (Wood, 1980).

Pyroclastic deposits in the Quaternary Cascades are varied, superabundant, and (with only a few exceptions) small. Mafic scoria and spatter cones are most common, but only a few are known to be associated with large downwind ashfall blankets—for example, Collier Cone (Oregon), Smith Butte (Adams), Blue Lake crater (Oregon), and Cinder Cone (Lassen) (Taylor, 1987; Hildreth and Fierstein, 1997; Sherrod and others, 2004; Clynne and others, 2000); erosion of such ash is rapid, and the preservation potential poor. Crudely stratified phreatic and phreatomagmatic deposits surround the summit vents of ice-capped andesitic stratocones including Baker, Rainier, and Adams. Block-and-ash-flows (poorly pumiceous pyroclastic flows) have commonly been deposited around many Cascade stratovolcanoes and preserved most prominently at Glacier Peak, St. Helens, Hood, and Shasta, but such deposits have been rapidly scoured from the radial drainages surrounding Mount Rainier and Mount Adams. Pumiceous pyroclastic flow deposits (ignimbrites) of small to moderate scale are recognized at Lassen, Shastina and Black Butte (Shasta), Jefferson, St. Helens, Glacier Peak, Garibaldi, and Meager, but large-scale Quaternary ignimbrites (>10 km^3) are recognized only at Lassen, Crater Lake, Tumalo, and Kulshan.

Far-flung silicic fallout sheets, many of them resulting from plinian eruptions, are listed in table 3, which also gives estimates of age and volume. Absence from the list of any tephras predating the Last Glacial Maximum that issued from the silicic Canadian centers surely reflects removal by the Cordilleran ice sheet rather than incapacity to produce explosive eruptions. The great number of plinian eruptions from Mount St. Helens (table 3; Mullineaux, 1996) probably reflects major contributions from crustal sources, low temperatures, and high magmatic water contents, which also promoted crystallization of cummingtonite in many units (a mineral unknown elsewhere in the Cascades). Adams, Rainier, Hood, and Shasta have each erupted numerous dacite lavas, many as silicic as the pyroclastic products of Mount St. Helens, but none of these volcanoes has a significant record of plinian eruptions.

Vent Redundancy

Every lava dome and scoria cone marks a discrete volcanic vent and thus represents, in the broadest sense, a separate volcano. Of greater interest, however, is whether each one has its own conduit system from some magma reservoir in the crust or mantle and thus represents a truly independent volcano. Owing to the obsolete but once widespread view that most small volcanoes reflect lateral magma leakage from big ones, it may be useful to expand here on distinguishing independent volcanoes from redundant ones. Four main types of vent redundancy can be envisaged—(1) flank vents (of stratovolcanoes and some shields) fed laterally by shallow breakouts of the magma supplying the central conduit system, (2) secondary rootless vents fed by lava tubes or other breakouts on surfaces of lava-flow fields and shields, (3) chains of domes or pyroclastic cones fed concurrently from a common dike, and (4) clustered overlapping lava domes central to a large edifice or inside a caldera, fed in succession from a common reservoir of similar magma through essentially the same conduit, fissure, or ring-fracture system.

Cascade examples of type 1 (lava flows fed from authentic flank vents) are the Lava Park flow at Shastina (Williams, 1932a; Miller, 1980) and several postglacial andesite flows around Mount Adams (Hildreth and Fierstein, 1995, 1997). Flank vents at Adams, Shasta, and Mount St. Helens and abundant dikes at (deeply eroded) North Sister reflect the tendency of a high edifice to develop its own gravity-driven stressfield, favoring radial fracturing. Such edifice effects may likewise have influenced emplacement of caldera-wall dikes and preclimactic rhyodacite vents around Mount Mazama (Bacon, 1983, 1985). The relative scarcity of authentic flank vents elsewhere in the Cascades may reflect the importance of regional deviatoric stress. Throughout much of the arc, an along-arc north-south direction of maximum horizontal compression may rule against edifice dominance and in favor of somewhat deeper control of the abundant north-south vent alignments.

Examples of type 2 redundancy are present on the King Mountain shield in Washington (Hildreth and Fierstein, 1995), along the Bachelor chain in Oregon (Scott and Gardner, 1992), and on the Plutos Cave HAOT apron northwest of Mount Shasta. Examples of type 3 include the Devils Chain of rhyolite domes near South Sister (Scott, 1987), the Sharp Peak rhyodacite dome chain near Mount Mazama (Bacon, 1983), the spatter-cone vent chain for the Hat Creek Basalt (Muffler and others, 1994), the Red Crater scoria-cone chain west of Mount Bachelor (Scott and Gardner, 1992), and the Smith Butte chain of scoria and spatter cones south of Mount Adams (Hildreth and Fierstein, 1995, 1997). Cascade examples of type 4 redundancy are the succession of 1980-2006 intra-crater domes at Mount St. Helens and the summit-dome clusters at Shastina, Glacier Peak, and Mount Garibaldi. In contrast to such tight clusters, however, most domes in the distributed Lassen and pre-Mazama domefields probably had independent vents, because they were emplaced over protracted time intervals through separate conduits from secularly evolving reservoirs (although within such domefields, a few chains like the eight rhyodacite domes of Sunflower Flat north of Lassen Peak may well be examples of type-3 redundancy).

In counting Cascade volcanoes, I tried to identify all cases of vent redundancy, demonstrated or likely. Tube-fed secondary vents on the flanks of mafic shields were not included at all. Keeping track of type-4 redundancy is relatively simple, because the only Cascade examples of summit-dome clusters are Meager, Cayley, Garibaldi, Glacier Peak, Hood, Shastina, and pre-1980 St. Helens. Solitary multipulse domes such as Burney Mountain and (Shasta) Black Butte are treated as single volcanoes. Type-1 redundancy (authentic

Table 3. Major fall units from the Quaternary Cascades.

[Many additional fall units exist, either small and local, or old, eroded, and poorly documented. Mineral abbreviations: bi, biotite; cm, cummingtonite; hb, hornblende; opx, orthopyroxene; cpx, clinopyroxene. S, south; S-C; south central]

Volcano	Unit	Age	Magma (km^3)	Notes	Reference
Meager	Bridge River tephra	2.4 ka	2	Broad easterly dispersal (British Columbia, Alberta)	29, 34, 37, 49
Kulshan	Lake Tapps tephra	1.15 Ma	~30	Intracaldera tuff also ~30 km^3; outflow eroded away	23, 24
Glacier Peak	GP layer A	2 ka	<0.01	Phreatomagmatic ash associated with dome collapse	4, 17
	GP Dusty Creek tephras	5.8 ka	<0.01	Four thin fall layers; ash clouds from pyroclastic flows	4, 17
	GP layer D	6.1 ka	<0.01	Ash cloud associated with dome collapse	4, 17
	GP layer B	13 ka	2	Plinian pumice fall; dispersal axis to east-southeast	4, 19, 36
	GP layer M	13 ka	0.4	Plinian pumice fall; southeast dispersal axis	4, 19, 36
	GP layer G	13 ka	2	Plinian pumice fall; easterly dispersal axis	4, 19, 36
Rainier	MR layer C	2.2 ka	0.1	Biggest of 10 postglacial vesicular falls; mixed andesite-dacite	32, 46
	MR layer D	~6.8 ka	0.01	Subplinian pumice showers east of the edifice	32
	MR layer L	~7.2 ka	0.01	Subplinian pumice shower southeast of the edifice	32
	MR layer R	~9.7 ka	0.01	Subplinian pumice and scoria fall	32
	Biotite-bearing pumice fall	380 ka	>1	2 m thick at Sourdough Ridge; sole biotite-rich unit at Rainier	47
	White pumice fall	190 ka	>1	20 m thick at Sunset Amphitheater	47
St. Helens	MSH 18 May 80	1980 CE	0.3	Composite of plinian and coignimbrite ash contributions	7, 12, 39, 48
	MSH layer T	1800 CE	0.4	Narrow lobe to NE. Goat Rocks period; layer has opx>hb>cpx	7, 33
	MSH layer We	1482 CE	0.4	Broad easterly dispersal. Kalama period; Set W has opx+hb	7, 33
	MSH layer Wn	1480 CE	2	Narrow lobe to northeast	7, 33
	MSH layer Pu	~2.6 ka	0.2	Subplinian; dispersal to east. Pine Creek period; Set P has opx+hb	7, 33
	MSH layer Ps	~2.9 ka	0.1	Subplinian; dispersed to northeast.	7, 33
	MSH layer Ye	~3.5 ka	0.9	Strong easterly dispersal. Smith Creek period, Set Y has cm+hb	7, 33
	MSH layer Yn	~3.5 ka	4	Most voluminous eruption at MSH. Dispersal to north-northeast	7, 33
	MSH layer Yb	~3.9 ka	0.3	Dispersal to north and east. Has minor biotite (+cm+hb)	7, 33
	MSH layer Jg	~12 ka	~0.3	Subplinian; thickest to WSW. Andesitic (58% SiO_2; hb+opx+cpx)	33
	MSH layer Jb	~12 ka	~0.5	Swift Creek stage, Set J has hb+opx. Jb only to east and southeast	33
	MSH layer Jy	~12 ka	~1	Discrete lobes to southeast and northeast	33
	MSH layer So	~14 ka	~0.5	Thickest to NE and east. Swift Creek stage; Set S has cm+hb±opx	33
	MSH layer Sg	~14 ka	~1	Most voluminous layer in Set S	33
	MSH layer Mm	~20 ka	<0.3	Thickest layer of Set M on east side. Cougar stage; cm, hb, opx	33
	MSH layer Mp	~20 ka	<0.1	Subplinian. This (or another M layer) may = Summer Lake ash D	14, 33
	MSH layer Mc	~20 ka	<0.3	Coarsest layer in Set M; thickest to southeast	33
	MSH layer Mo	~20 ka	<0.05	Subplinian; limited to east and southeast	33
	MSH layer Mg	~20 ka	~0.1	Subplinian or plinian; limited to east and southeast	33

Table 3. Major fall units from the Quaternary Cascades.—Continued

[Many additional fall units exist, either small and local, or old, eroded, and poorly documented. Mineral abbreviations: bi, biotite; cm, cummingtonite; hb, hornblende; opx, orthopyroxene; cpx, clinopyroxene. S, south; S-C; south central]

Volcano	Unit	Age	Magma (km^3)	Notes	Reference
	MSH layer Cs	35-50 ka	>1	Ape Canyon stage, Set C has cm, bi, hb. Cs is thickest to south	33
	MSH layer Cy	35-50 ka	>1	Thickest to E. Cy may = Cs and both may = Summer Lake ash	12, 13, 14, 33
	MSH layer Cm	35-50 ka	~1	Thickest to east and southeast	33
	MSH layer Cw	35-50 ka	~1	Coarsest layer in Set C	6, 33
	MSH layer Ct	35-50 ka	<0.3	Subplinian. Restricted to southeast	33
	MSH pre-Set C	80±20 ka	<1	Cummingtonite-dacite ash in eastern Washington	6
	MSH pre-Set C	~300 ka	>1	Biotite-bearing ash layer OO at Summer Lake	10, 14
Jefferson	MJ layer E	50-100 ka	~1	Older than last major glaciation. Accompanied by ash flows	3, 50
	MJ layer U	50-100 ka	~0.1?	Slightly older than layer E. Accompanied by ash flows	3, 50
Tumalo	Shevlin Park Tuff	260 ka	>5	Ignimbrite near Bend, Oregon. May = Summer Lake ash JJ	11, 18, 43, 45
	Pumice of Columbia Canal	~300 ka?	~1?	Plinian fall near Bend, Oregon. May = Summer L. ash NN	11, 43, 45
	Loleta ash	440 ka	>5?	Bend pumice fall and Tumalo Tuff; = ash 6 at Clear Lake	41, 42, 43
	Rye Patch Dam ash	~650 ka	>1	Matches Desert Spring Tuff and ash T321 in Tulelake core	13, 38, 43
South Sister	Devils Chain tephra	2.0 ka	0.02	Accompanied by ash flows; followed by rhyolite domes	44
	Rock Mesa tephra	2.2 ka	0.03	Accompanied by ash flows; followed by rhyolite coulee	44
Mazama	Cloudcap Road pumice fall	>85 ka?	~1?	May = ash T2382 in Tulelake core and ash 4 at Summer Lake	1, 2, 14, 38
	Pumice Castle ash	~72 ka	>0.5	Caldera wall to Summer Lake ash 6 (and to Palouse?)	1, 2, 6, 14
	Wono ash	31 ka	>0.1	Preclimactic rhyodacite; ash F at Summer Lake.	5, 13, 14
	Preclimactic rhyodacite	~30 ka	>0.1	Ash E1 at Summer L.; ash T2438 at Tulelake.	14, 38
	Trego Hot Springs ash	27 ka	>0.1	Preclimactic rhyodacite; ash 18 at Summer L.; T2307 at Tulelake	5, 38
	Llao Rock plinian	7.9 ka	2	Tsoyawata ash in NV; ash T2309 at Tulelake	1, 5, 13, 14,38
	Mazama ash	7.7 ka	33	Caldera-forming eruption; accompanied by large ignimbrite	1, 51
Shasta	Red Banks pumice	11 ka	>1	Predates Shastina edifice; fallout sheet extends NE, NW, and east	8, 31
Lassen	Rockland ash	610 ka	>30	Caldera-forming eruption; accompanied by large ignimbrite	28, 40
	Chaos Crags fallout	1.1 ka	<0.01?	Fall deposit associated with domes identified for 30 km east	9
Rear-arc centers					
Newberry	Big Obsidian plinian	1.3 ka	0.1	Followed by ash flows and rhyolite coulee	19, 30
	Olema ash	~75 ka	>5?	May = youngest caldera-forming eruption at Newberry	15, 25, 35, 38
	Older plinian pumice falls	>75 ka	?	Several plinian deposits not well dated or correlated.	25, 26
	Tuff of Tepee Draw	280-300 ka	~10?	Caldera-forming (?) rhyolite ignimbrite; fall equivalent uncertain	15, 25, 30
Medicine Lake	Glass Mountain plinian	0.9 ka	0.03	Followed by domes and flows of rhyolite and dacite	20
	Tuff of Antelope Well	~180 ka	>3?	May = Tulelake ash T2023. [Does not = Summer Lake ash KK]	14, 16, 38

pre-Medicine Lake	Tulelake pumice T2119L	~600 ka	?	Pumice (glass 76.7% SiO_2) correlates to Clear Lake ash 7	38, 42
	Tuff of Box Canyon	1.0 Ma	>1?	May correlate to rhyolitic ash at 110.5 m in Tulelake core	16, 38
	Tuff of Gillems Bluff	2.0 Ma	>1?	May correlate to silicic ash sequence at 181-174 m, Tulelake core	16, 38
Orphan ashes (sources uncertain)					
S Cascades	Summer Lake tephra V	~140 ka	?	Rhyodacite ash (glass 73% SiO_2) = Tulelake T1193	14, 38
S Cascades	Rio Dell ash	~1.45 Ma	>5?	Ash in Humboldt Basin and DSDP cores	42
S-C Cascades	Summer Lake ash 2	~75 ka	?	4-cm rhyolitic ash; may be from Newberry?	14, 25
	Wadsworth ash	~160 ka	?	May = Summer L. ash KK and Tulelake ash T261	13, 14, 38
	Pringle Falls ash D	~218 ka	?	30-cm pumice fall; may be from Sisters reach or Newberry	21
S-C Cascades	Dibekulewe ash	~630 ka	>5?	Rhyolitic ash (glass 77% SiO_2) widespread in California, Nevada, and Oregon	13, 38

Note: In addition to these, many uncorrelated Quaternary tephras potentially derived from the Cascades, Newberry, or Medicine Lake have been found in nearby drill cores. Because only a few are >2 cm thick or contain coarse ash or lapilli, few are likely to represent plinian falls of more than local dispersal. Of 54 tephra layers logged (14) in exposures and cores at Summer Lake (southern Oregon), only 12 have been assigned to source volcanoes; 19 are unstudied because they are too wispy, reworked, or mixed; and 23 have been subjected to microprobe analysis of glass shards but remain of uncertain provenance. In the 331-m Tulelake (northern California) core (38), at least 12 uncorrelated tephras beneath the 610-ka Rockland ash are well distributed through the age range 1.97 Ma to ~620 ka; about half have high-silica glass potentially related to rhyolite eruptions near Medicine Lake, whereas half have rhyodacite glass, as likely to be related to units at Mazama, Shasta, or Lassen as to the nearby Medicine Lake area. Higher in the Tulelake core, ~28 ash layers (all but four with high-silica glass) are clustered in the age range ~360 to 140 ka; half of these are 3-8 cm thick, and six contain small pumice lapilli (38), suggesting nearby sources. Five more unassigned tephras in the top 17 m of the Tulelake core are intercalated with several from Mazama and are likely to come from there as well. In addition, at least 22 middle and late Pleistocene tephras were logged in lake-sediment cores at six sites between Mount Shasta and Klamath Lake, of which more than half are uncorrelated. On and near the Newberry edifice, many pumice-fall deposits have been identified in isolated excavations (25); some are plinian, others may be subplinian or lesser falls related to domes or pumice cones, and several are compositionally zoned or mixed and appear to be complexly lobate; although some are likely to have reached Summer Lake, ages and convincing correlations are not yet available.

No widespread fall units have been identified from Hood, Adams, Rainier, Baker, Garibaldi, or Cayley, though each of these major centers has erupted dacitic or rhyodacitic lavas and block-and-ash flows. Deposition atop (and erosion by) the Continental ice sheet may account for absence of Pleistocene fall deposits from Meager to Baker. Despite proximity of lake cores, only one widespread fall unit is identified from Shasta.

References: **1.** Bacon, 1983. **2.** Bacon and Lanphere, 2006. **3.** Beget, 19 81. **4.** Beget, 1984. **5.** Benson and others, 1997. **6.** Busacca and others, 1992. **7.** Carey and others, 1995. **8.** Christiansen, 1990. **9.** Christiansen and others, 2002. **10.** Clynne and others, 2007. **11.** Conrey, Donnelly-Nolan, and others, 2001. **12.** Criswell, 1987. **13.** Davis, 1978. **14.** Davis, 1985. **15.** Donnelly-Nolan and others, 2004. **16.** Donnelly-Nolan, in press. **17.** Foit and others, 2004. **18.** Gardner and others, 1992. **19.** Gardner and others, 1998. **20.** Heiken, 1978. **21.** Herrero-Bervera and others, 1994. **22.** Herrero-Bervera and Helsley, 1993. **23.** Hildreth, 1996. **24.** Hildreth, Lanphere, and others, 2004. **25.** Kuehn, 2002. **26.** Kuehn and Preppernau, 2005. **27.** Lanphere and others, 1999. **28.** Lanphere and others, 2004. **29.** Leonard, 1995. **30.** MacLeod and others, 1995. **31.** Miller, 1980. **32.** Mullineaux, 1974. **33.** Mullineaux, 1996. **34.** Nasmith and others, 1967. **35.** Negrini and others, 2000. **36.** Porter, 1978. **37.** Read, 1990. **38.** Rieck and others, 1992. **39.** Sarna-Wojcicki and others, 1981. **40.** Sarna-Wojcicki and others, 1985. **41.** Sarna-Wojcicki and others, 1987. **42.** Sarna-Wojcicki and others, 1988. **43.** Sarna-Wojcicki and others, 1989. **44.** Scott, 1987. **45.** Sherrod and others, 2004. **46.** Sisson and Vallance, 2005. **47.** Sisson and Lanphere, work in progress, 2007. **48.** Sparks and others, 1986. **49.** Stasiuk and Russell, 1990. **50.** Yogodzinski and others, 1983. **51.** Young, 1990.

flank vents) can be hard to identify on long-lived or deeply eroded edifices, but (perhaps surprisingly) it appears to be common at only a few centers in the Cascades. Ten unequivocal flank vents well up on the slopes of Mount Adams (fig. 24) erupted andesite-dacite lavas compositionally similar to the magma supplied centrally to the summit vent, and at least 15 similar but generally older eruptive units (30-400 ka) issued from vents (now covered by younger lavas) that could either have been central or on the upper-to-medial flanks of the stratocone. Elsewhere, there may be a few authentic flank vents on each of the following stratovolcanoes—St. Helens, Jefferson, Middle Sister, South Sister, Mazama, and Shasta—but none has been identified at Baker, Rainier, or Hood (at each of which relatively mafic peripheral vents are considered independent). In like manner, peripheral rhyolite lavas that erupted around such intermediate cones as Maidu and Middle Sister are treated as independent, because they issued either from a separate reservoir or from one at a far different evolutionary stage than when the central cone was constructed. The total number of authentic flank vents in the Quaternary Cascades is therefore not known to exceed 50.

Relatively mafic small volcanoes on or near the flanks of andesite-dacite stratocones exemplify the class of peripheral vents that were fed from deep in the crust by independent magma batches that avoided entrapment by the complex crustal reservoir and conduit bundle that supplied the central edifice. The products of such small peripheral volcanoes are commonly more primitive than anything erupted from the main central volcanoes themselves (fig. 24). Far from being mere flank vents “parasitic” upon the major stratovolcanoes, small peripheral mafic cones are actually the more fundamental volcanoes magmatically, in that they erupt magma drawn more directly from the mantle or deep crust than do the stratovolcanoes, beneath which interception, mixing, and production of evolved hybrids is the magmatic norm (Hildreth, 1981a; Hildreth and Moorbath, 1988).

Type-3 redundancy (synchronously erupted vent chains) is the hardest to prove, a strong case requiring flow-by-flow mapping, paleomagnetic, chemical, and petrographic data, and (optimally) tephra stratigraphy. Alignment alone does not signify that vents are either comagmatic or contemporaneous (Conway and others, 1997). This point is illustrated, for example, by the linear vent zones (22 to 50 km long) that strike northerly through Bachelor, Shasta, Adams, Caribou, and Indian Heaven, along each of which compositionally varied products erupted recurrently over thousands (or hundreds of thousands) of years (Christiansen and others, 1977; Korosec, 1989; Gardner, 1994; Hildreth and Fierstein, 1995; Guffanti and others, 1996; Clynne and Muffler, in press). Within the Mount Bachelor area, however, several local subchains of scoria cones and maars (the Red Crater, Siah, Sheridan, and Wuksi alignments) probably do contain redundant vents, which could total as many as 35 of the 80-odd postglacial vents mapped along and near the Bachelor chain by Scott and Gardner (1992). Likewise, among the several chains of scoria cones in the Sand Mountain-Nash Crater area (southwest of Three Fingered Jack), as many as 10 vents could be redundant (Taylor, 1968, 1990b; Sherrod and others, 2000). Five scoria cones are redundant near Mount Adams (Hildreth and Fierstein, 1995), and elsewhere in southwestern Washington another handful are likely to be so (Smith, 1993). In the periphery of Mount Mazama, as many as eight mafic to intermediate vents appear to be redundant (Bacon, 2006), and among the 476 Quaternary vents recognized in the Lassen segment about 50 are likely to be redundant—judging by the alignments, close spacing, and compositional data portrayed by Guffanti and others (1990) and Clynne and Muffler (in press). However, no mafic-vent redundancy is recognized in the Garibaldi Volcanic Belt and little in the Shasta segment (except along the Garner Mountain and Fisk Ridge chains and in the rear-arc Medicine Lake Volcanic Field). Although future work may add more examples of redundancy among the mafic monogenetic vents of the Cascade arc, the number now considered plausible is smaller than 180.

Redundancy among silicic domes warrants additional comment. Clustered summit domes (as atop Glacier Peak and Mount Garibaldi) may well be of several ages but, because they vented repeatedly within a limited area, they were presumably fed by a spatially restricted conduit system. Distributed summit domes (and intrusive equivalents) separated by 3 to 5 km (as for Mount Meager) and flank domes high on an edifice but only a few kilometers outboard of a central vent, as for Mount Cayley and pre-1980 Mount St. Helens (fig. 12) are less clearly redundant. They could have been supplied either by shallow branches of a central conduit or by independent conduits from a crustal magma reservoir. Where a large upper-crustal silicic magma body develops, derivative lava domes are commonly distributed in space and time, and each typically has its own conduit, as, for example, many of the preclimactic rhyodacites around Crater Lake (Bacon and Druitt, 1988). Dike-fed chains of contemporaneously emplaced domes like the Sharp Peak (Bacon and Druitt, 1988) and Devils Chain (Scott, 1987) alignments seem to be exceptional. Intracaldera domes can be solitary and central (as beneath Crater Lake), arcuately controlled by ring faults (as at Valles Caldera in New Mexico), or partly dike-aligned and partly scattered (as in the Lassen domefield). Nearly all Cascade domes except the dike-linked chains and summit clusters are thought to have independent conduits, although such conduits generally issue only from mid- or upper-crustal reservoirs (in contrast to deeper reservoirs for many of the monogenetic mafic volcanoes). With these qualifications, then, I consider redundant only about 60 of the nearly 340 lava domes recognized in the Cascades.

Of the 2,339 Quaternary vents identified, therefore, fewer than 50 are redundant by being authentic flank vents of stratovolcanoes, and only ~60 domes and ~180 scoria cones are redundant by having been supplied either sequentially by the same conduit or synchronously with a neighbor along a single dike. This leaves the Cascade arc with about 2,050 independent Quaternary volcanoes, roughly two volcanoes for each kilometer of arc length.

Distribution Patterns of 2,050 Independent Volcanoes

The approximately 2,050 independent Quaternary volcanoes in the Cascade arc include ~1,630 small mafic to intermediate volcanoes, ~275 domes, ~110 substantial shield volcanoes, 11 mafic stratocones, and 26 major evolved centers (of which 19 are andesite-dacite stratovolcanoes and seven are silicic dome complexes).

Virtually all of the 2,050 volcanoes are indicated on map figures 3, 8, 14, 15, and 21 (although a few vent symbols obscure each other at this scale). The map patterns illustrate several noteworthy features: (1) the concentrated clusters of volcanoes in the Garibaldi Volcanic Belt contrast with the diffuse but more continuous distribution elsewhere; (2) the close spacing of mafic volcanoes contrasts with the exceedingly irregular spacing of large evolved volcanoes; (3) the volcanic front is ragged or ill-defined and is not generally defined by stratovolcanoes or other major centers (except in the Garibaldi Volcanic Belt); (4) the breadth of the vent belt from Mount Rainier to California is extremely variable along the arc and of extraordinary width in southern Washington and California; (5) closely spaced mafic volcanoes form a belt of remarkable continuity along much of the Oregon segment; (6) dense concentrations of small volcanoes cluster tightly into several mafic volcanic fields (Indian Heaven, Mount Adams, Port-

Figure 24. Northeast side of 3,742-m Mount Adams stratovolcano, showing one late-glacial and two postglacial peripheral vents, in the foreground at 2,100 to 2,250 m. Red Butte scoria cone (at left bottom) produced slightly alkalic basaltic lavas (49-50% SiO_2) unrelated to Mount Adams that flowed as far as 13 km northeast ~14 ka. To the right of Red Butte, a 2-km-long fissure vent that strikes toward Mount Adams is marked by black lavas, agglutinate, and a scoria ridge. Erupting in the middle Holocene, it represents a lateral flank vent of the stratocone that produced lava flows of pyroxene andesite (59-60% SiO_2) that extend as far as 10 km northward. The complex of lava-flow levees at left center is a pyroxene-andesite shield (58-59% SiO_2) that erupted at 37±8 ka and is only lightly ice-scoured (proximally); likewise a lateral flank vent, its lavas are compositionally similar to contemporaneous products of the central-vent stratocone. Upper end of shield is overlain by a Holocene debris-avalanche deposit (Devils Gardens), which in turn is overlain by a Little Ice Age moraine. Summit icecap of Mount Adams feeds several radial glaciers, separated by cleavers consisting of andesitic lavas and scoria (55-60% SiO_2) that erupted between 40 and 15 ka. For detailed eruptive history, see Hildreth and Fierstein (1995, 1997). High spur left of summit is “The Castle” (Rusk, 1924), which is also visible in figure 10 (where seen from the southeast).
(Copyrighted photo by and courtesy of Darryl Lloyd, 2006.)

land, Bachelor, Caribou, and the big rear-arc fields); (7) a few gaps along the arc virtually lack Quaternary volcanoes despite contiguity with extensive segments having high vent-density; (8) forearc volcanoes are irregularly distributed, abundant in southern Washington and around Portland, sprinkled sparsely along the Oregon Cascades, absent in the Garibaldi Volcanic Belt, and common in California; (9) the arc volcanic belt overlaps eastward with three major contemporaneous rear-arc volcanic fields, which are discrete areas of high vent density that contrast with the sparsity of Quaternary rear-arc volcanism elsewhere; and (10) rhyodacite has limited local distribution in the Cascades, true rhyolite is rare except in the Lassen segment, central Oregon, and the rear-arc, and (by global arc standards) Quaternary calderas are remarkably uncommon.

Breadth of the Cascade Arc

In contrast to some single-file chains of variably spaced arc volcanoes elsewhere (for example, Alaska Peninsula, Aleutian, Lesser Antilles, and South Sandwich arcs), the belt of Quaternary volcanic vents is 25 to 100 km across in Oregon and wider still in the southern Washington and Lassen segments. Because the magma fed to most of the 2,050 independent arc volcanoes is mafic and that fed to many of the others is thought to have evolved from basalt by fractionation and hybridism within the crust (Hildreth, 1981a; Hildreth and Moorbath, 1988), such breadth implies at least equally widespread (across-arc) penetration of mantle-derived basalt into the arc crust. How such magma subsequently evolves and rises through the crust are issues addressed later, but the critical point here is that basaltic magma is contemporaneously available from partially molten sub-arc mantle across an east-west belt 25-160 km wide from Lassen to Rainier (though apparently narrower beneath the GVB).

The question is seldom addressed whether the conduit system that feeds any particular mafic volcano taps (1) a circumscribed mantle melting column; (2) a family of melting (or magma-aggregation) loci, as within an upwelling region; (3) a trunk stream that blends tributary contributions (fed by porous, networked, or channelized flow) from various mantle melting loci; or (4) a storage reservoir (collection zone in the lower crust or upper mantle) capable of blending magma contributions from many domains. If long-lived and areally extensive enough, an upwelling domain or a collection zone could each be tapped at different times by more than one conduit and might thus conceivably feed more than one apparently independent volcano. Across the Quaternary Cascade arc, however, the great compositional variety of mafic volcanoes closely interspersed in space and time, including many of fairly primitive but diverse compositions (Bacon, 1990; Leeman and others, 1990, 2005; Hildreth and Fierstein, 1995; Bacon and others, 1994, 1997; Clynne and Borg, 1997; Borg and others, 1997), suggests that given magma bodies seldom supply more than one (nonredundant) mafic volcano. Compositional contrasts among neighboring mafic scoria cones and shields, adjacent to each other on 1-to-10-km scales, illustrate a general failure of mantle-derived arc magmas to homogenize during collection and storage (except beneath large evolved centers), thereby indicating that "underplated" basaltic reservoirs are distributed, numerous, discrete, short-lived, and rarely extensive beneath arcs. Diffuse penetration of the crust by diverse mafic magmas from heterogeneous mantle sources thus maps out the surface projection, not of some vast underplated reservoir, but of the minimum region underlain by arc mantle sufficiently molten for magmas to segregate and ascend.

Production of arc magma beneath a volcanic belt as wide as 25 to 100 km (figs. 8, 14, 15, and 21) thus provides a picture of subduction-induced magma generation somewhat different from that of conventional models. Throughout the Quaternary, subcrustally derived magma has penetrated the Cascade arc crust in thousands of small batches distributed across this wide zone. During the Miocene and Pliocene, there was a gross westward drift of the arc volcanic belt in the Lassen segment and in northern Washington and British Columbia, antithetic to a broadly contemporaneous (Tertiary) eastward drift in Oregon and southern Washington. No systematic migration of activity, however, is recognized across the arc for the last 2 Myr, indicating that the unusual breadth of the magma-production zone has existed throughout much or all of the Quaternary. Areas of greatest eruptive volume are scattered, showing no preferred distribution toward the trenchward side of the arc (as implicit in some arc models). Apart from the narrow Garibaldi Volcanic Belt (fig. 3), the only major centers on the volcanic front are St. Helens, Rainier, and Shasta (and arguably Mazama; figs. 8, 15, 21). Voluminous centers like Adams, Hood, and Lassen are remote from the volcanic front. Overall, therefore, there is no evidence for a slab-derived narrow fluid curtain, for a linear belt of diapirs, for a sharp wedge corner, or for a constant depth of dehydration melting of downdragged (or complexly recirculated) hydrated peridotite; that is, there is no evidence for a narrowly linear zone of mantle melting, for which such mechanisms have been proposed to produce simple chains of arc volcanoes. Instead, basaltic magma ascends from a wide across-arc domain of the Cascadian mantle, and its eruptive distribution is scattered rather unsystematically in both volume and composition.

In studies of some arcs, parallel chains of arc volcanoes have been postulated, generally as a means of rationalizing arc breadth in terms of conceptual models of successively deeper but discontinuous zones of melting or of fluid release. Where postulated, however, such double or multiple chains seldom bear scrutiny. As in the Cascades, volcano distributions in the Japanese, Indonesian, Mexican, South American, Kurile, and Izu-Bonin arcs are better viewed as broad scatterings of hundreds of volcanoes, large and small. Imaginary parallel chains may appeal to wishful modellers or inveterate lineament-drawers, but they are generally concocted only on the basis of selectively emphasizing large evolved centers and ignoring the many small, more primitive ones. A recent example is the set of arc maps presented by Tatsumi and Eggins (1995, p. 29-41), wherein delineation of parallel volcanic chains variously entails neglecting many volcanoes, accepting one or two inboard centers as "chains," or headlong assertion of imagined alignments using the eye of faith. Although local alignments of volcanoes (some of them oblique to the strike of the arc) certainly exist, contemporaneous arc-parallel chains extending side by side for hundreds of kilometers are nowhere plausible. It is clear that mantle-wedge melting is distributed across a broad inboard swath and not limited to one or two narrow strips that overlie some fixed pressure-sensitive reaction in the subducting plate.

Because slab dehydration and plate interaction begin in the shallow forearc (Peacock, 1993; Schmidt and Poli, 1998), the megathrust zone is likely to start out as a thick brittle shear zone full of lenses, lozenges, and "knockers" of varied ultramafic, mafic, and metasedimentary rocks that remains heterogeneous into the deeper ductile regime. Such primary lithologic heterogeneity, along with spatially variable shear heating (Peacock, 1996), steep thermal gradients through the slab, uneven domainal serpentinization of lower-plate mantle peridotite, survival of serpentine and chlorite in the cooler slab interior to depths greater than in the downdragged base of the wedge (Ulmer and Trommsdorff, 1995; Peacock, 2001), persistence of diverse minor hydrous phases in slab eclogite and downdragged wedge peridotite, and solid-solution effects on progressive decomposition of such hydrous phases (Schmidt and Poli, 1998) all suggest that both initial slab release and later boundary-layer reliberation of the hydrous slab contribution into the mantle-wedge interior are likely to be smeared out unevenly over a considerable depth range beneath and beyond the volcanic front. Protracted down-dip release of hydrous fluid to the upper plate would be further enhanced if the blueschist-eclogite transition were kinetically delayed until the slab reaches depths of 100 to 170 km (Kirby and others, 1996) or if a trapped fluid phase were to persist in the downdragged peridotite layer to sub-arc depths (Davies and Stevenson, 1992; Mibe and others, 1999). Heterogeneous but roughly continuous, polybaric fluid release, typically declining but persisting well behind the volcanic front, is more congruent with the world's variety of broadly scattered across-arc and rear-arc volcanism than is a model envisaging decomposition of particular hydrous phases that release fluid curtains only at fixed depths beneath fictively circumscribed frontal and rear-arc chains. The broad Cascade arc is one of the prime examples.

Volcanic Front and Forearc Volcanoes

The volcanic-front concept originated with Sugimura (1960), who characterised it as the trenchward limit of arc volcanoes—typically a line of polygenetic cones and usually (as in Japan and Alaska) the main chain of large centers. Application of the term has been quite uneven, however, even contradictory, as some use it for the main chain of stratocones (ignoring small forearc volcanoes) and others for the array of most trenchward vents (ignoring volume and duration). Behind volcanic fronts (of many arcs), extensive fields of mafic and intermediate volcanoes carrying unequivocal arc-geochemical signatures (that is, not including alkalic intraplate basalts) show that magma-generating processes influenced by contributions from the subducting slab also persist far inboard. Less common globally but abundant in the Cascades are scatterings of forearc volcanoes, trenchward of the most productive volcanic belt. Their distribution challenges the very concept of a linear volcanic front for the Cascades and, together with the many rear-arc volcanoes, provides evidence that the processes promoting arc magmatism remain effective, though perhaps less robust, across a broad belt fore and aft of the main chain of stratovolcanoes.

Mechanisms advocated as contributing to the concentration of magmatism beneath volcanic fronts include: (1) pressure-dependent breakdown of amphibole and chlorite at ~30 kb from a viscously coupled (downdragged) layer of hydrated mantle-wedge peridotite superjacent to the subducting slab, releasing a "hydrous curtain" that fluxes mantle melting most intensely beneath the front (Tatsumi, 1986); (2) subduction-induced corner convection that sweeps the high-temperature core of the wedge to its shallowest level beneath the front (inboard of the wedge corner), thereby promoting highest melt fractions there, enhancing buoyant ascent and melt segregation (Kushiro, 1987; Davies and Stevenson, 1992; Furukawa, 1993; Tatsumi and Eggins, 1995; Schmidt and Poli, 1998); (3) ablation of the base of the lithosphere beneath the volcanic front by impingement of the inclined ascending limb of the corner convection, a process enhanced by slab sinking and rollback (Hasegawa and Zhao, 1994); (4) gradients in orientation and magnitude of the deviatoric stress field within the upper part of the ascending limb (Furukawa, 1993), favoring subvertical fracturing, melt segregation, and transition from porous flow to channelized magma ascent, preferentially beneath the arc front; and (5) existence of a P-T threshold beneath the front for grain-boundary connectivity (dihedral angle <60°) of interstitial aqueous fluid in peridotite, governing abrupt release of fluid previously trapped in the hydrated downdragged basal layer and its ascent into the hotter wedge interior (Mibe and others, 1999; Grove and others, 2002). Such mechanisms might all help focus magmatism beneath the front, but, to be realistic, their effectiveness must be spatially gradational, contributing also to arc-magma production in the rear arc (and less commonly or less robustly in the forearc). The abruptness of many arc fronts may in part reflect slab-promoted cooling of the wedge corner, freezing out a stagnant, cool (but buoyant and weak) viscous nose of serpentinized wedge peridotite just outboard of the front (Kincaid and Sacks, 1997; Hyndman and Peacock, 2003; Brocher and others, 2003), consistent with sharp increases in heat flow and seismic attenuation from forearc to volcanic front.

Contrary to lingering myth, depth to the top of the inclined seismic zone beneath volcanic fronts is far from constant. Present-day range is about 80 to 150 km, plus a few deeper examples in the tectonically complex SW Pacific (Gill, 1981). For the Cascades, the ragged and arbitrary nature of what might constitute the volcanic front renders the depth question unresolvable but, more generally, it is clear that slab depth ranges greatly beneath so broad an arc (see section entitled "Tectonic and Geophysical Insights", below). From such variability, I infer that fluid release by pressure-dependent decomposition of particular hydrous phases is only part of the volcanic-front story. An important role for mantle-wedge kinematics seems required.

In the classic Japanese model, the volcanic front is abrupt and linear, and both the total eruptive volume and the spatial density of volcanoes are greatest along the front, decreasing inboard (Sugimura, 1960; Aramaki and Ui, 1982). Of these four key features, none characterizes the Cascades south of Mount Rainier (figs. 8, 14, 15, 21). If the volcanic front were taken to be the seaward limit of Quaternary volcanoes, it would amount to an irregular zigzag of scattered centers of low volumetric output. If taken to be a line of large polygenetic stratovolcanoes, any line chosen would be arbitrary, irregularly nonlinear, and flanked on the west by scores of volcanoes trenchward of the front so defined. Accordingly, for the Cascades, the supposedly global model of a volcanic front seems inapplicable and inappropriate. Generally more meaningful may be the concept of a "Cascade volcanic axis", a belt of higher than average vent density and eruptive output that grades both east and west into flanking areas of lesser productivity. Difficulties with this viewpoint, however, include locations of the voluminous Rainier, St. Helens, and Shasta loci west of the apparent axis and the poor definition of any such axial belt in a few reaches of the Cascades (figs. 14, 15, 21).

Both the axial and frontal frameworks, however, beg the question of why so many volcanoes, large and small, are scattered far trenchward along the western side. If they are considered "forearc volcanoes" spatially, it needs to be noted that only a few of them consist of high-magnesian andesite from refractory mantle sources (for example, Clynne and Borg, 1997; Borg and others, 1997; Leeman and others, 1990, 2005) and even fewer are tholeiitic. Many are typical calcalkaline arc basalt and basaltic andesite, while a few others are HAOT, andesite, dacite, shoshonite, or alkalic basalt. Unlike the classic model, no systematic across-arc compositional distribution is apparent; the varied compositions are closely interscattered in both axial and forearc regions. Irrespective of composition or volume, however, the existence of more than 250 independent Quaternary volcanoes irregularly distributed as far as 30 to 70 km seaward of the main volcanic axis implies mantle melt production far into what is usually considered the forearc. It may be that a broad across-arc swath of the sub-arc mantle bearing partial melt is actually characteristic of most arcs but that such melt can coalesce and erupt widely only under extensional or transtensional upper-plate conditions. In more compressive arcs like the Alaska Peninsula or the Garibaldi Volcanic Belt, apparently only the most intense magmatic foci penetrate the arc crust.

The Garibaldi Volcanic Belt conforms better to the volcanic-front model than do the other Cascade segments, although (unlike Japan) it has little breadth, representing what is essentially a discontinuous chain of vent clusters (fig. 3). Most small volcanoes in the GVB (all of its mafic ones) are peripheral to the five long-lived centers, which consist largely of andesite to rhyodacite. It is not clear whether the GVB cluster pattern reflects restriction of mantle melting to discontinuous domains or whether the foci of crustal melting and storage manifested by the main edifices provide localized stress fields that enable peripheral ascent of mantle magmas that may be more widely available beneath the arc but are elsewhere muffled. The Bridge River basaltic cluster lacks any focal edifice, however. Located at the termination of the arc, the more alkalic compositions and small eruptive volumes of the Bridge River-Salal Creek volcanoes (fig. 3) may reflect attenuation of subduction-related processes, with slab-absent mantle upwelling promoting lower degrees of mantle melting, little influenced by slab-derived fluid contributions.

The largest concentrations of forearc volcanoes are in the Portland-to-St. Helens and Lassen regions, beneath both of which the slab may be torn, distorted, or unusually stressed (Michaelson and Weaver, 1986; Benz and others, 1992; Wilson, 1989, 2002). Anomalous slab geometry in these two regions might distort wedge corner convection or induce mantle upwelling more vigorous than elsewhere along the arc. Induced upwelling might be especially effective in the Lassen segment adjacent to the southern margin of the (northward-retreating) slab. The uncommonly warm thermal structure of the Cascadia subduction zone (Oleskevich and others, 1999) might favor partial melting of the mantle wedge farther trenchward than in most arcs, but this could be expected to be a general feature along the arc rather than pronounced principally in the Portland and Lassen regions. Impingement of the northward-migrating Oregon coastal block against the compressional backstop of Puget Sound, at the south margin of the region underlain by an arch in the slab, may induce upper-plate stresses conducive to forearc magma ascent (see section entitled "Translation and Rotation of the Forearc", below). Confounding the search for a unifying explanation of forearc magmatism is the close association of water-poor and water-rich mafic magmas in both the Portland and Lassen regions. Appeal to anomalous slab-edge processes is also complicated by the prominence of high-Mg andesite and HAOT in the Lassen segment (at the south edge), the dominance of alkali basalt along Bridge River (at the north edge), and the great variety of mafic magma types around Portland and across southern Washington (where there may be a torn edge).

Spacing of Major Volcanic Loci

The oft-repeated old myth of evenly spaced arc volcanoes 40 to 70 km apart, sometimes employed in idealized models, doesn't bear scrutiny in any arc, but it would verge on absurdity if advanced for the Cascades (table 4; figs. 3, 8, 14, 15, 21). Even if we neglect the fact that the most primitive mantle-derived eruptive products issue from small monogenetic vents scattered all over the volcanic belt and focus instead on the major long-lived eruptive centers, there is clearly no systematic, even roughly periodic, spacing. Table 4 (column 1) shows that the main Cascade edifices exhibit spacings that range from 35 to 170 km, with a mean of 87 km, and a standard deviation of 45 km (with spacings for off-axis variations listed parenthetically). The middle column (table 4) augments the list of main centers with nine second-rank centers that also consist wholly or in part of andesite-dacite, yielding a range of spacings from 5 to 150 km, a mean of 54 km, and a standard deviation of 38 km. The right-hand column (table 4) similarly augments the list of main centers (left-hand column) with nine large mafic centers, yielding a range from 7 to 150 km, a mean spacing of 56 km, and a standard deviation of 44 km. No manipulation of centers included or statistical contrivance can produce systematic spacing.

Vent Density

It can be calculated from table 1 that the mean spacing for all 2,339 Quaternary vents is actually less than 5 km, that is, an hour's walk between vents. It was explained above that as many as 2,050 of these vents are independent volcanoes with their own conduits from the deep crust or mantle. Measuring the areas enclosing about 25 empirically selected vent fields (not including the surrounding areas of lava flows or of other outflow deposits) permits tabulation of vent densities for the constituent segments or reaches of the entire Cascade arc and its rear-arc volcanic fields (table 1). Vent density thus approximated ranges from 3 km^2 per vent in the Caribou Volcanic Field to 6 km^2 per vent for Indian Heaven to 32 km^2 per vent for the Portland forearc. Note that a vent density of 16 km^2 per vent would signify an orthogonal vent spacing of 4 km. The vent densities given for the GVB apply only to the several individual clusters (fig. 3), but from Bumping Lake (Washington) to Mount McLaughlin (Oregon) the values tabulated in table 1 represent a continuous swath 515 km long of closely neighboring volcanoes (figs. 8, 14, 15). Inspection of figures 3, 8, 14, 15, and 21 shows that vent density reaches maxima around Mount Adams, in Indian Heaven, in several parts of the Oregon Cascades, in the axial strip east of Mount Shasta, and in the Lassen-Caribou region, as well as in the three rear-arc volcanic fields. The dense clusters around Jefferson, Mazama, and Lassen Peak are dominated by vents for dacitic and silicic products, whereas most other areas of high vent density are predominantly mafic, marked by numerous vent alignments but including few or no evolved products.

A realistic model of arc magmatism needs to encompass, in addition to the major centers, the densely but irregularly distributed sites of eruption of the mafic magmas that come most cleanly from the mantle. Spatially restricted fields of mafic monogenetic vents (scoria cones, small shields, fissure-fed lavas) have sometimes been attributed to localized mantle upwellings (diapirs), but the regional scale and along-arc continuity of monogenetic vent distribution in the Cascades cast doubt on such a model. The 515-km-long swath in Oregon and southern Washington, as well as the size and complexity of the Lassen, Shasta, and three major rear-arc vent fields, suggest instead that partially molten mantle is a general condition beneath the entire Quaternary volcanic region. Variation in relative penetrability of the lithosphere, not in the availability of basaltic magma, apparently limits and governs the distribution of volcanism.

Along-arc Gaps

Despite the unusually high vent density and breadth of so much of the Quaternary Cascade arc, its continuity is nonetheless interrupted by several long gaps containing few or no Quaternary volcanoes (table 5). Ostensibly, the contrast between extensive reaches of high vent density and intervening nonvolcanic gaps would seem to be in conflict with the standard model of arc magmatism, which presumes secular fluxing of continuously convecting sub-arc mantle by contributions from a subducting slab continuous along the strike of the arc.

Major gaps north and south of the Shasta segment are especially anomalous in view of the high vent density in adjacent areas (fig. 21). A 64-km-long reach to the north is blanketed by Tertiary arc volcanics, and the small low-K HAOT scoria cones near Copco Dam are the only known Quaternary volcanic rocks. Similarly, a 50-km-long reach south of the Shasta segment exposes Mesozoic basement rocks partly overlapped by Tertiary volcanics, and a young cluster of undated HAOT vents (Timbered Crater and Brushy Butte; fig. 21) at the eastern extremity of the gap produced the only volcanic rocks known to be of Quaternary age. The gap would be slightly wider if Chalk Mountain and other undated vents at the north end of the Lassen segment prove actually to be of Pliocene age.

A third reach ~17 km long, between Pelican Butte and Big Bunchgrass shield (fig. 15), has relatively low vent density and may or may not amount to a Quaternary gap in the present context. The reach has ~10 undated mafic vents, most of which are either Pliocene or early Quaternary. From here north, however, the Quaternary vent belt is uninterrupted for 500 km until, at the latitude of Mount Rainier and Bumping Lake (fig. 8), the continuous belt of close-set vents ends abruptly.

The Glacier Peak vent cluster, which overlies the slab arch that accommodates the change in trend of the convergent-margin system, is isolated by two major vent-free gaps. To the south, the 150-km separation of Rainier and Glacier Peak is shortened to a gap of 105 km by inclusion of two isolated mafic vents north of Rainier and a mafic vent cluster just southwest of Glacier Peak (figs. 3, 8). To the northwest, a 74-km gap separates Glacier Peak from the basaltic vents peripheral to Mount Baker. Finally, the longest vent-free gap of all extends 136 km from the Baker locus to Watts Point (fig. 3). As so delineated (table 5), the gaps in Washington and Canada consist of pre-Cenozoic basement terranes, with a fraction of Tertiary volcanic and plutonic rocks that increases southward toward Mount Rainier, but with no Quaternary vents, dikes, or other remnants.

Persistence for at least 2 Myr of these vent-free reaches along a Quaternary volcanic belt otherwise virtually continuous raises some fundamental questions about arc magmatism. If subduction is continuous along the length of the arc, and if some combination of slab-fluid flux, mantle-wedge convection, and extensional decompression promotes melting (and magma coalescence and ascent) beneath a volcanic belt 1,250 km long (and generally many tens of kilometers wide), then is the failure of magma to erupt within the gaps attributable

Table 4. Spacing of Main Quaternary Volcanoes.

Large Andesitic-to-Silicic Centers				Basalt and Basaltic Andesite	
km	**Major Pairs***	**Include 9 Lesser Centers***	**km**	**Include 9 Large Mafic Centers***	**km**
118	Lassen-Shasta	Lassen-Burney	38		
		Burney-Shasta	82		
170	Shasta-Mazama	Shasta-Goosenest	35	Shasta-McLoughlin	115
		Goosenest-Pelican	88	McLoughlin-Mazama	58
		Pelican-Mazama	47		
43	Mazama-Cappy Mtn	Mazama-Bailey	25	Mazama-Thielsen	24
		Bailey-Cappy Mtn	26	Thielsen-Cappy Mtn	18
		Cappy Mtn-Diamond Pk	28		
89	Cappy-S. Sister	Diamond Pk-S. Sister	71	Cappy-Bachelor	78
		S. Sister-M. Sister	5	Bachelor-S. Sister	15
64	S. Sister-Jefferson	M. Sister-Jefferson	59	S. Sister-N. Sister	7
(7)	(S. Sister-Broken Top)			N. Sister-Washington	19
				Washington-Three Fingered Jack	17
(67)	(Broken Top-Jefferson)			Three Fingered Jack-Jefferson	22
78	Jefferson-Hood	Jefferson-Frog Lake Buttes	61	Jefferson-Olallie Butte	16
		Frog Lake Buttes-Hood	17	Olallie-Hood	62
94	Hood-Adams			Hood-King Mtn	78
(99)	(Hood-St Helens)	Hood-Defiance	32	King Mtn-Adams	18
(54)	(Adams-St Helens)	Defiance-Adams	62	Hood-Indian Heaven (Lemei Rock)	72
35	Adams-Goat Rocks			Indian Heaven (Lemei Rock)-Rainier	93
(75)	(Adams-Rainier)				
(80)	(St Helens-Rainier)				
47	Goat Rocks-Rainier				
150	Rainier-Glacier Pk				
91	Glacier Pk-Baker				
147	Baker-Garibaldi				
35	Garibaldi-Cayley	Garibaldi-Price	7		
59	Cayley-Meager	Price-Cayley	29		

Summary of Calculated Spacings for the Cascade Arc

14	Number of Pairs	23	22	20
35–170 km	Range of Spacings	5–150 km	7–150 km	7–150 km
87 km	Mean Spacing	54 km	56 km	61 km
45 km	Standard Deviation	38 km	44 km (via Mount Adams)*	46 km via Lemei Rock)*

* Left column gives spacings among 17 large, compositionally evolved, Quaternary volcanic centers in the Cascade arc. Central column augments these with 9 lesser centers that are also composed all or partly of silicic andesite or more evolved products. Right column augments the left (not the central) column by including 9 of the largest Quaternary mafic centers. Combining all 3 columns (not shown) would yield 30 pairs having a mean spacing of 42±37 km and a spacing range of 2-150 km.

Mounts Thielsen and Bailey lie directly across-arc from each other, as do South Sister and Broken Top (Tumalo), and likewise Mount Adams, Indian Heaven, and Mount St. Helens; for consistency, therefore, only one of each group is used in calculating the along-arc mean spacings. In the left column, parenthetical entries are not included in the spacing calculations. In the right column, spacing was calculated along alternative north-south paths, by way of Mount Adams or by way of Indian Heaven (Lemei Rock).

Table 5. Gaps along the Quaternary Cascade arc.

[HAOT is high-alumina olivine tholeiite, as elaborated in the text]

Gap Length	Region	Latitude	Details
44-52 km	South of Mount Shasta	41.0—41.3	Chalk Mtn to Signal Butte. Gap is wider if Chalk Mtn is Pliocene. Young HAOT vent cluster lies at east side of gap
64 km	North of Mount Shasta	41.7—42.3	Goosenest to Little Aspen Butte. Copco HAOT scoria cone cluster is lone Quaternary exception in gap
17 km	North of Pelican Butte	42.5—42.7	Pelican Butte to Big Bunchgrass shield. Eroded mafic vents within this potential Quaternary gap are undated; probably either Pliocene or early Quaternary
105 km	North of Mount Rainier	47.1—48.0	Dalles Ridge (Greenwater) to Wards Pass (N. Fork Skykomish River)
74 km	Northwest of Glacier Peak	48.1—48.6	Glacier Peak to Bear Creek cone near Lake Shannon (southeast of Mount Baker).
136 km	Northwest of Mount Baker	48.8—49.7	Cougar Divide to Watts Point.

to (1) locally reduced slab-derived contributions, inadequate to promote robust mantle melting; (2) locally cooler thermal structure or more refractory composition of the mantle wedge; or (3) lithospheric impedance of mantle magma ascent? No discontinuity, asperity, or fracture zone on the oceanic Juan de Fuca Plate system (Wilson, 2002) is recognized to coincide with or project beneath the gaps. For the two Washington gaps, a case for mantle control might postulate that the slab arch hinders mantle-wedge convection—except that the Glacier Peak locus lies right on the arch crest where it projects eastward from beneath the Olympic Peninsula (fig. 3). No lithospheric structures are recognized that might impede magma ascent differentially beneath any of the gaps, and indeed mid-or-late Tertiary magmas had penetrated four of the gaps. For the two gaps north of Glacier Peak and Mount Baker, the Tertiary (Chilliwack-Pemberton) magmatic belt had lain far inboard, well east of the Quaternary alignment (fig. 3).

Altogether, it seems unlikely that the gaps reflect along-strike reaches of the mantle wedge that are poorly fluxed, stagnant, refractory, or otherwise deficient in partial melt. More plausible is that the slab dehydrates and the wedge convects and melts along the whole subduction margin from Lassen to Meager, but that the arc lithosphere (including a 40-km crust) is capable of stalling, suppressing, and locally completely defeating mantle melts that intrude it, within large domains, along and across arc, for millions of years at a time. The intra-arc tectonic extension expressed as vent alignments and faulting, virtually continuous from Lassen to Adams, terminates at the latitude of Bumping Lake and Mount Rainier, implicating a compressive (or at least nonextensional) lithospheric stress regime as a possible explanation of the gaps farther north, in and adjacent to the GVB. As for the gaps in Quaternary volcanism north and south of the Shasta segment, it was pointed out by Blakely and others (1997) that the gaps are dominated by northwest-southeast dextral shear but each of the adjacent volcanic segments by extensional north-south normal faults. Because the Lassen and Shasta segments have in common widespread abundances of both arc basalt and HAOT, the mantle and its melt-generating behavior beneath them are probably similar, rendering it doubtful that the 50-km-long reach of mantle separating them should be very different. These observations suggest again that extension favors magmatic penetration of the lithosphere and that its absence suppresses such penetration.

Why are Rear-Arc Volcanic Fields Few and Clustered?

The three large rear-arc volcanic fields are likewise separated by long gaps that lack rear-arc volcanic rocks of Quaternary age. The 200-km reach separating the Simcoe Mountains and Newberry Volcanic Fields contains a few Pliocene vents in the south but otherwise lacks volcanic rocks younger than the Miocene flood basalts. Similarly, the 180-km reach separating the Newberry and Medicine Lake Volcanic Fields contains numerous late Miocene and Pliocene vents but virtually none of Quaternary age (Luedke and others, 1983; Sherrod and Smith, 2000).

In the Lassen segment, the Caribou Volcanic Field and the many Quaternary vents scattered eastward to Eagle Lake (fig. 21) might well be treated as another rear-arc volcanic field, largely basaltic. During the Pliocene, the field had extended farther north as well as an additional 50 km east of Eagle Lake (Luedke and Smith, 1981; Guffanti and others, 1990). During the Quaternary, however, this inboard mafic vent field has been separated by a 50-km north-south gap from the rear-arc Medicine Lake and Hackamore fields (fig. 21).

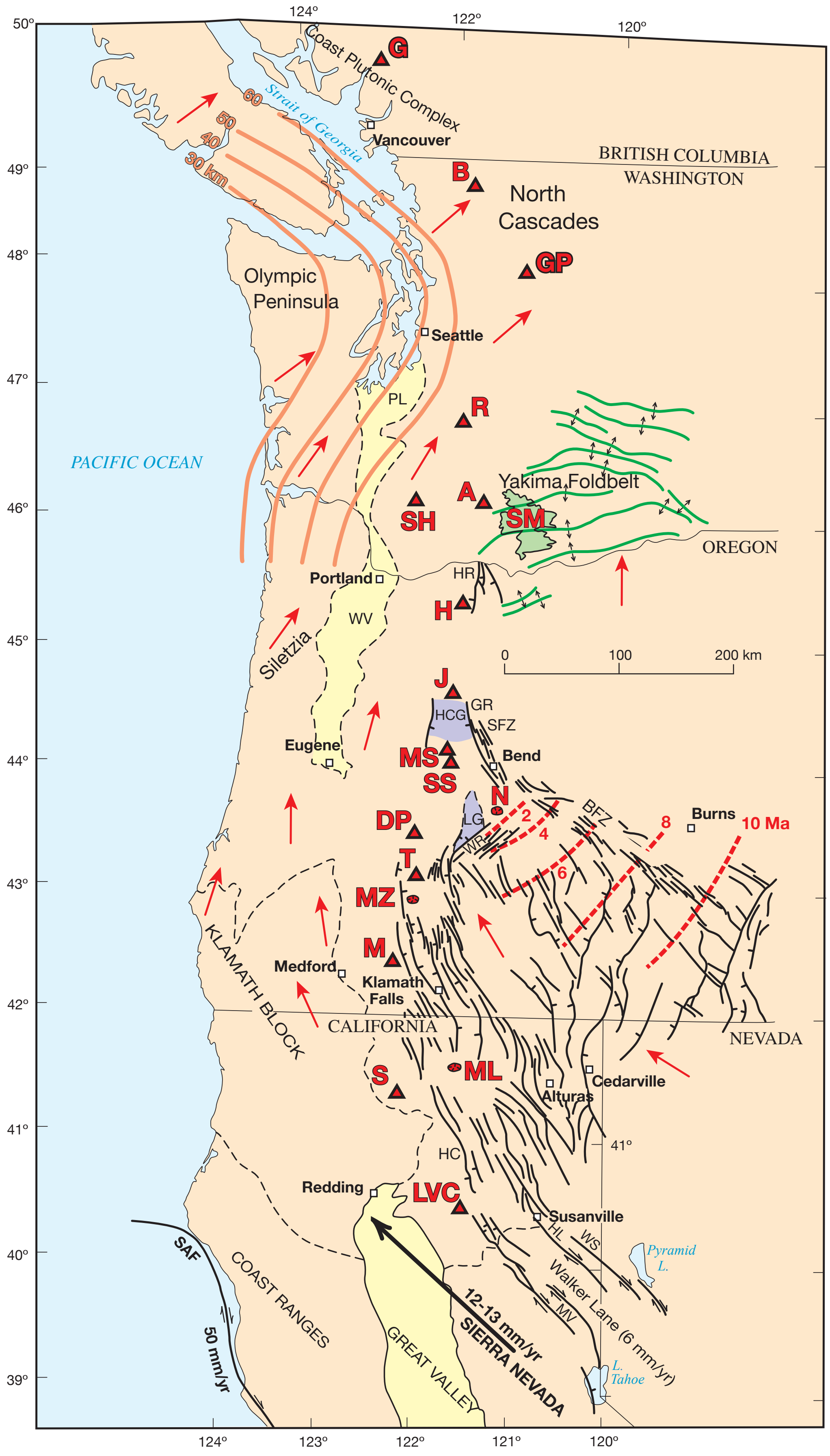
50°
49°
48°
47°
46°
45°
44°
43°
42°
41°
40°
39°
124°
122°
120°
123°
121°
G
Coast Plutonic Complex
Strait of Georgia
60
50
40
30 km
Vancouver
BRITISH COLUMBIA
WASHINGTON
B
North
Cascades
GP
Olympic
Peninsula
Seattle
PL
R
PACIFIC OCEAN
Yakima Foldbelt
A
SH
SM
OREGON
Portland
HR
H
WV
Siletzia
0
100
200 km
J
HCG
GR
SFZ
Bend
Eugene
MS
SS
N
BFZ
LG
WR
2
4
6
8
Burns
10 Ma
DP
T
MZ
M
Medford
Klamath
Falls
KLAMATH BLOCK
CALIFORNIA
NEVADA
ML
S
Alturas
Cedarville
41°
HC
Redding
LVC
Susanville
HL
WS
Pyramid
L.
SAF
COAST RANGES
50 mm/yr
12-13 mm/yr
SIERRA NEVADA
GREAT VALLEY
MV
Walker Lane (6 mm/yr)
L.
Tahoe

Behind the northern part of the arc, a 400-km-long rear-arc gap separates the Simcoe Mountains Volcanic Field from a contemporaneous (Pliocene to Quaternary) diffuse scattering of alkali basalt scoria cones in south-central British Columbia (Canil and Scarfe, 1989). The southernmost concentrated Quaternary back-arc volcanic field in Canada is the Clearwater/Wells Gray field of alkali basalts (Hickson and Souther, 1984), mostly younger than 500 ka and about 600 km north of the Simcoe field. Except for the Bridge River-Salal Creek cones at the north end of the Quaternary arc (fig. 3), however, the Canadian alkali basalt fields lie more than 200 km inboard of the arc, in contrast to the arc-adjacent rear-arc fields of Simcoe, Newberry, Medicine Lake, and Caribou-Eagle Lake.

Why do only four reaches of the Cascade arc have adjacent Quaternary rear-arc vent fields? Although widely separated from one other, each field protrudes ~50 km inboard from the main volcanic belt, each extends ~50 km north-south, each is fundamentally basaltic, and each has a reduced proportion (relative to the arc) of basalts that have arc geochemical signatures, suggesting attenuated slab flux inboard. If slab contributions were a controlling factor, it seems unlikely that their effectiveness would extend inboard of the main volcanic belt at only a few discrete loci. The following discussion thus addresses the tectonic elements (fig. 25) that may uniquely control the siting of each of these rear-arc anomalies.

The mafic rear-arc vent field in the eastern part of the Lassen segment occupies a tectonic singularity where the main outboard faults of the northern Walker Lane dextral shear zone (which bounds the northwest-translating Sierran microplate) end abruptly. From the Reno/Lake Tahoe area, the Walker Lane follows the trend of the Miocene-Pliocene Cascade arc, cutting into the otherwise rigid Sierra Nevada batholith where its crust may have been thermally weakened by the Tertiary arc magmatism. The major dextral strands here, the Mohawk Valley and Honey Lake Fault Zones (fig. 25), strike west-northwest toward Lake Almanor and Susanville, where the dextral shear terminates and merges diffusely into a system of north-to-northwest-striking normal faults that transect the Caribou/Eagle Lake rear-arc vent field (Blakely and others, 1997; Dixon and others, 2000). Farther north, the Medicine Lake and Hackamore rear-arc fields

← **Figure 25.** Tectonic setting of the Quaternary Cascade arc. Selected large volcanoes indicated in red. For complete Quaternary vent distribution, see figures 3, 8, 14, 15, and 21; for offshore plate system, see figure 1. Main features are the following: (1) Basin and Range extensional region has expanded westward since the late Miocene to overlap the subduction-induced magmatic arc in California and Oregon; black lines (with ticks on downthrown sides) indicate main faults. (2) Plate-boundary shear traction principally drives northwestward translation of rigid Sierra Nevada/Great Valley microplate, accounting for ~25 percent of relative motion between Pacific Plate and stable North America (Dixon and others, 2000), most of which takes place along San Andreas Fault (SAF). Dextral shear on Walker Lane (belt of rheologically weak lithosphere) accounts for about half the microplate translation and merges diffusely northwest into region of intra-arc normal faulting. (3) Microplate compression through Klamath block helps (along with oblique plate convergence) to drive northward translation and clockwise rotation of Oregon forearc block, contributing to intra-arc extension along its trailing edge. Oregon forearc block consists dominantly of ~30-km-thick Siletzia terrane of accreted oceanic crust; its northward motion compresses the accretionary Washington forearc against the Canadian batholithic buttress (Wells and others, 1998). North Cascades and Coast Plutonic Complex consist predominantly of crystalline basement terranes of Mesozoic and older metamorphic and plutonic rocks. Red arrows illustrate rotation of Cascadia; directions (not velocities) are generalized from hundreds of GPS sites referenced to stable North America (McCaffrey and others, 2007). (4) Seaward-concave plate margin promotes slab arch with axis plunging toward 48°N; slab depth contours (solid orange lines, 30 to 60 km) inferred from seismicity and tomography by Crosson and Owens (1987). (5) Proximal forearc depression occupied by Strait of Georgia, Puget Lowland (PL), and Willamette Valley (WV), 50 to 100 km seaward of active arc, may reflect densification of slab at eclogite transition; its absence south of Eugene may reflect upper-plate deformation by the northwest-translating Klamath block. (6) Formation of Yakima fold and thrust belt, which principally deforms lavas of the Columbia River Basalt Group, began ~15 Ma during their main eruptive interval and continues today; green lines with opposing arrows indicate anticlinal axes; Mount Adams, Mount Hood, and Simcoe Mountains Volcanic Field overlie the folds. (7) In central Oregon, isochrons (red dashed lines, 10-2 Ma) depict westward progression of initiation of rhyolitic volcanism across the High Lava Plains (MacLeod and others, 1975; Jordan and others, 2004); in the Quaternary, eruptions of true rhyolite (rare elsewhere in the Cascades) have further advanced through Newberry and as far northwest as South and Middle Sisters. Abbreviations for volcanoes (red triangles) from north to south: G, Mount Garibaldi; B, Mount Baker; GP, Glacier Peak; R, Mount Rainier; SH, Mount St. Helens; A, Mount Adams; SM, Simcoe Mountains; H, Mount Hood; J, Mount Jefferson; MS, Middle Sister; SS, South Sister; N, Newberry; DP, Diamond Peak; T, Mount Thielsen; MZ, Mount Mazama (Crater Lake); M, Mount McLoughlin; S, Mount Shasta; ML, Medicine Lake; LVC, Lassen volcanic center. Faults: HR, Hood River Fault; GR, Green Ridge Fault; SFZ, Sisters (Tumalo) Fault Zone; BFZ, Brothers Fault Zone; HCG, High Cascades Graben; LG, LaPine Graben; HC, Hat Creek Fault; WR, Walker Rim; WS, Warm Springs Fault; HL, Honey Lake Fault; MV, Mohawk Valley Fault. Purple shading in HCG and LG indicates areas of deep graben fill.

likewise lie at a structural knee where a set of more inboard northwest-striking strands of the dextral Walker Lane system end against an array of north-striking normal faults. Because the rigid Klamath and Siletzia blocks lie next northwest (fig. 25), their backstop effect requires the Walker Lane to splay out northward into a broad diffuse array of normal faults across central Oregon, where strike-slip components are subordinate until the Brothers Fault Zone east of Newberry provides a northern transform margin to the extended terrain (fig. 25). The structural knees adjacent to the Caribou/Eagle Lake and Medicine Lake rear-arc vent fields both represent zones of transfer of horizontal strain from northwest dextral shear to east-west extension. In both fields, eruption of HAOT is proportionately more common farther inboard, indicative of shallow upwelling of hot dry mantle and freer transit of basaltic magma through the extending crust.

The Newberry Volcanic Field occupies a comparably unique rear-arc tectonic position (fig. 25), where the age-progressive rhyolite trend of the High Lava Plains and the northwest corner of Basin and Range extensional faulting both impinge upon the Cascade arc (Walker and MacLeod, 1991; Jordan and others, 2004). Separating Newberry from the Cascades is the westernmost basin of the Basin and Range Province, the profound LaPine Graben, which underwent ~700 m of structural subsidence contemporaneous with growth of the Newberry edifice. The graben is bounded by the Walker Rim Fault Zone, which strikes beneath and is buried by the Newberry edifice (Walker and MacLeod, 1991; Macleod and Sherrod, 1992). An abrupt change in strike (from northwest to northeast) of the regional extensional fault swarm takes place just where it approaches the southwest toe of the edifice, against the margin of the graben. At the northwest toe of the Newberry edifice, 50 km farther north, the northwest-striking Sisters (or Tumalo) Fault Zone emerges from beneath the young volcanic pile, indicating that the edifice buries either a continuous curvilinear fault zone or (more likely) another extensional structural knee. Moreover, the northwest-striking Brothers Fault Zone, a diffuse belt of distributed oblique dextral shear that here forms the northern limit of the main extended region (Lawrence, 1976; Pezzopane and Weldon, 1993), passes Newberry adjacent to the northeast toe of the edifice.

The mid-Pleistocene to Holocene rhyolites so abundant at Newberry have numerous contemporaneous counterparts in the Three Sisters-Tumalo region just 15 to 40 km farther northwest. Because true rhyolites are elsewhere so rare in the Quaternary Cascade arc, it appears likely that the rhyolite-generating crustal-melting anomaly beneath each of these areas is attributable to the same pattern of mantle flow and decompression responsible for the 10-Myr-long westward propagation of rhyolitic volcanism across the High Lava Plains, perhaps enhanced at the present-day leading edge by pre-heated arc crust. The great Newberry edifice has thus grown over the last half-million years at the unique conjuncture of a profound and complex locus of regional extension with the advancing front of a long-lived, virtually independent, propagating mantle melting anomaly.

The rear-arc Simcoe Mountains Volcanic Field has developed in a setting no less unique. All 180-odd vents of the 1,400 km^2 field erupted through and directly onto a 2-to-3-km-thick pile of flood basalts (Columbia River Basalt Group; CRB) where they are folded into two of the major anticlines of the Yakima Foldbelt (fig. 25). The east-west-trending folds are asymmetrical north-vergent anticlinal ridges, which have sharp hingelines and oversteepened north limbs cut by high-angle reverse faults, and they are separated by broad flat-floored synclinal valleys (Reidel and others, 1989; Watters, 1989). Although they dominate the modern topography, the folds generally have less than 600 m of structural relief. Beneath the foldbelt, the CRB conceals a long-lived basin previously filled by 3 to 7 km of Eocene to mid-Miocene sediments (Campbell, 1989). Within and west of the Simcoe Mountains Volcanic Field, the folds are cut by numerous northwest-striking dextral strike-slip cross-faults of very small (1 to 30 m) displacement (Bentley and others, 1980; Walsh and others, 1987), probably accommodating curvature of the fold axes. Farther west, the folds in the CRB continue into the adjacent Cascade Range, where they are incompletely covered by late Miocene and younger arc volcanics (Walsh and others, 1987; Beeson and Tolan, 1990). The folding began by 15 Ma during outpouring of the largest CRB units, persisted into the Pliocene (thus overlapping in time the 4.5-0.6 Ma Simcoe volcanism), and is apparently still ongoing locally (Campbell and Bentley, 1981; West and others, 1996). Contemporaneously, since at least the mid-Miocene, the Oregon forearc block (principally Siletzia; fig. 25) has been moving northward and rotating clockwise with a pole of rotation northeast of the Yakima Foldbelt (Wells and others, 1998). The north-south shortening in the Puget Sound region today has its inboard counterpart in the foldbelt and in the north or north-northwest vent alignments within the Simcoe vent field.

An additional anomaly in southern Washington is the probable distortion or tearing of the subducting plate beneath the region. Its influence on mantle-wedge convection may be a factor in the unusual width of the volcanic belt here, in the abundance within the arc of HAOT and other relatively dry basalts with slab geochemical signatures weak or absent (Leeman and others, 1990), and, farthest inboard, in the dominance of water-poor alkaline intraplate basalts in the Simcoe field. In common with the alkalic basalts of British Columbia, several Simcoe scoria cones contain xenoliths of spinel peridotite (Draper, 1992; Brandon and Draper, 1996; Peslier and others, 2002), mantle cargo wholly absent among the ejecta of the Quaternary rear-arc (subalkaline) volcanic fields described farther south.

Eruption Rates and Episodicity

When dealing with rates of magmatism, one first must distinguish clearly among volumes produced, erupted, and preserved. Magma production is always greater than that erupted, whether the unerupted excess be a small fraction (as in dikes of primitive basalt) or a dominant fraction when large granitoid or gabbroic plutons crystallize. For example, fractionation to produce the 50 km^3 of climactic rhyodacite erupted at Crater Lake Caldera (7.7 ka) may have left behind three times that volume of magmatic cumulates in the upper crust (Druitt and Bacon, 1989; Bacon and Nathenson, 1996). In any system, a significant fraction of the parental magmas may stall, partially crystallize, and remain within the mantle-crust transition, or at the depth of gas saturation, or at the brittle-ductile transition, or at any discontinuity in crustal density. Furthermore, the volume of any volcanic unit erupted is always greater than that preserved. Discrepancies between volumes erupted and those preserved result from syneruptive tephra dispersal and from secular erosion. Other things being equal, pyroclastic deposits are dispersed more widely and eroded far faster than lavas, phenomena generally likely to lower the fraction of silicic products identifiable among those preserved relative to those erupted. The north-south gradient in the severity of Quaternary glaciations along the 1,250-km Cascade arc is responsible for extreme asymmetry in preservation (fig. 2). In the Lassen segment, 60 percent or more of the Quaternary eruptive products may be preserved, whereas in Canada the fraction may be less than 30 percent.

By using the term “eruption rate” here, I refer to the volumetric rate of release to the surface of volcanic products (or their equivalents recalculated as dense rock or magma), integrated over a specified time interval. Some would prefer to equate the term “eruption rate” with the magma discharge recorded during an active eruption, which is typically a brief episode of immediate interest but not one that provides a rate representative of edifice growth. Others have used the term “extrusion rate” for longer-term volcanic output (for example, Sherrod and Smith, 1990), but because the word extrusion (of lava) is widely applied in contradistinction to explosive ejection (of pyroclasts), it seems inappropriate here. Another possibility, “accumulation rate,” invites ambiguities such as erosive interference with secular accumulation and whether to count downwind ash as having accumulated. For simplicity, therefore, I think “eruption rate” best expresses the estimated total magma volume reaching the surface, regardless of the mode, form, episodicity, or irregularity of eruptive events. The context can be made clear by specifying the volcano (or volcanic region) and the interval of interest, whether integrated, for example, over 1,000 years or over the lifetime of an edifice.

Rough volume estimates for preserved sections of Tertiary arc volcanics in the Cascades of central Oregon suggested to Verplanck and Duncan (1987) that the range-wide eruption rate declined about sixfold from 32 Ma to 3 Ma, as the plate convergence rate slowed fivefold and the obliquity of subduction increased (owing in part to clockwise rotation of the Oregon forearc block). For the Quaternary Cascades, Sherrod and Smith (1990) estimated volumes preserved for about 50 centers (or along-arc reaches) and calculated volumetric rates (for the last 2 Myr) by unit linear length of various arc segments, ignoring the variations in erosion and arc breadth. They stated, in summary, that “extrusion rate” in the GVB was only 10 to 15 percent of that in the Rainier-to-Hood segment, which in turn was less than half that of the Oregon and California segments. As described above for many of the individual Cascade volcanoes, however, differences between what is erupted and preserved may be as great as twofold from the southern Oregon Cascades northward to Mount Rainier, and from twofold to fivefold in the GVB, where the volcanoes have repeatedly been torn down by advances of the Cordilleran ice sheet.

Output of Distributed Mafic Vents vis-à-vis Long-Lived Evolved Centers

It has sometimes been asserted that the magma volume erupted by the hundreds of distributed small volcanoes, mostly mafic, greatly exceeds that of the few large long-lived evolved centers. This is true for the Quaternary Cascades of central Oregon but certainly not true for the volcanic regions that include the Shasta, Mazama, Hood, Adams, Goat Rocks, or Rainier edifices, nor for any reaches of the GVB.

In the GVB, the five major polygenetic multivent andesite-to-rhyodacite edifices (fig. 3) clearly account for at least 90 percent of the volumes erupted. For the Mount Baker locus and Kulshan Caldera, the proportion exceeds 95 percent (Hildreth and others, 2003).

For the Rainier-to-Hood segment, the proportion remains above 75 percent, despite the presence of more than 400 small volcanoes (table 1) and only five large ones (fig. 8). The Indian Heaven Volcanic Field (~70 km^3) is almost entirely distributed, whereas more than 80 distributed mafic volcanoes in the adjacent Mount Adams field contributed only 15 percent of a total eruptive volume of 315±84 km^3 (Hildreth and Lanphere, 1994), about 85 percent having vented from the focal andesite-dacite edifice. Mount Rainier is virtually isolated, the central edifice having released more than 98 percent of the magma erupted in its district. Comparable focal-to-peripheral proportions can be estimated for Goat Rocks (75:25), St. Helens (75:25), and Hood (80:20), whereas the Portland forearc is entirely distributed (fig. 8). For the segment as a whole, I estimate that ~650 km^3 out of 850 km^3 (76%) erupted from the five main edifices.

The central Oregon Cascades yield the opposite proportionate relationship. Along reaches I through V (Jefferson to Mazama; figs. 14, 15) of the Oregon segment, the arc includes more than 1,000 close-set Quaternary mafic vents (table 1) and eight long-lived evolved loci. Sherrod and Smith (1990; their fig. 3) estimated that ~9 km^3 of Quaternary mafic volcanic rock is preserved for each linear kilometer along this 280-km-long stretch, yielding ~2,500 km^3. Because most of these rocks have been glaciated, the total mafic eruptive volume is likely to have been 10 to 30 percent greater. Eruptive volumes of the long-lived evolved centers, as estimated here, are as follows: Jefferson 25 km^3, Middle Sister 12 km^3, South Sister 20 km^3, Broken Top 10 km^3, Tumalo 25 km^3, Diamond Peak (andesitic upper part) 5 km^3, Cappy 20 km^3, pre-Mazama domefield 25 km^3, Mazama edifice 130 km^3, and Mazama climactic ejecta 50 km^3. The major evolved centers thus add up to ~322 km^3, which amounts to less than 12 percent of the Quaternary total output for reaches I to V, or probably less than 10 percent if erosion of the mafic lavas were taken into account.

The McLoughlin reach (VI; fig. 15; table 1) is inadequately investigated but appears to be transitional in the present context. Although none of its several andesitic centers (Pelican Butte, Brown Mountain, Devils Peak, and the Mountain Lakes cluster) is known definitively to be long-lived, their combined eruptive volume evidently exceeds that of the 20-odd mafic vents, which include Mount McLoughlin (~13 km^3) and several small distributed volcanoes.

For the Shasta segment, Sherrod and Smith (1990) estimated a present-day volume of ~120 km^3 for ~200 distributed vents (not including the Medicine Lake Volcanic Field), most but by no means all of them mafic (fig. 21). Because Mount Shasta alone is estimated to have erupted ~450 km^3 of andesite/dacite and Rainbow Mountain at least another 100 km^3, the myriad distributed vents account for less than 20 percent of the total eruptive volume of the segment—a relationship virtually antithetic to that of central Oregon.

For the Lassen segment, the Quaternary output of three long-lived evolved centers likewise volumetrically surpasses the total for 400-odd regionally distributed vents (fig. 21), though not as strikingly so as in the Shasta segment or as in Washington and Canada. Sherrod and Smith (1990) estimated at least 425 km^3 for distributed Quaternary cones and shields in the Lassen segment (of which as much as 150 to 200 km^3 may be andesitic rather than mafic). For the long-lived evolved complexes, the estimated eruptive volumes are 215 km^3 for the active Lassen volcanic center (Guffanti and others, 1996), more than 150 km^3 for the early Quaternary Dittmar volcanic center, and more than 200 km^3 for the Maidu volcanic center (of which half or more is younger than 2 Ma). Although the volume estimates are nebulous for the early Quaternary, it seems clear that more than half of the products erupted in the segment issued from the large andesite-to-rhyolite centers. Moreover, because so many of the distributed lesser vents are andesitic, the *mafic* output of the numerically dominant regional vents may amount to as little as 30-35 percent of the Quaternary eruptive volume in the Lassen segment.

Eruption Rates at Individual Loci

The volume proportion erupted from large centers vis-à-vis myriad distributed vents thus ranges widely along the Cascade arc, as does the total Quaternary volcanic production, whether integrated by segment, by reach, or by center. For a few 50-to-100-km-long reaches there has been no Quaternary volcanism at all. The common practice of estimating integrated volumetric eruption rates for particular time intervals along arcs thus seems conceptually peculiar, perhaps interesting for global comparisons of material and geochemical budgets of arcs in general but failing to provide perspectives useful for analyzing eruptive behavior within one. Even for global comparisons, the "cubic kilometers erupted per kilometer of arc length" approach is flawed by averaging the huge variations and by the enormous uncertainties in intrusive-to-extrusive proportions of the magmas emplaced along arcs in both space and time. As elaborated in studies of the volcanic fields around Mount Adams and Mount Baker (Hildreth and Lanphere, 1994; Hildreth and others, 2003), discussion of volumetric eruption rates can be somewhat misleading without conceptual clarity about scale. The time scale and spatial scale should fit the process being investigated. Appropriate scales are different for assessing slab and wedge contributions to subduction-zone magma generation, or deep-crustal heating and melting, or growth and replenishment of upper-crustal reservoirs, or eruption hazards at stratovolcanoes and calderas. For understanding volcanism, a feasible and fruitful approach is to work out the volumetric eruptive outputs of specific centers and to identify through stratigraphic and geochronologic studies any episodicities within their lifespans.

The data summarized above for the Cascades show that most of the large evolved centers have lifespans in the range 0.1 to 1 Myr and that such lifespans are sporadically punctuated by short episodes of greatly elevated volcanic output (Hildreth and Lanphere, 1994). The wider arrays of distributed vents, generally more mafic, which can sometimes be circumscribed as volcanic fields, usually have somewhat longer lifespans, but this need not always be so. The basaltic volcanic field peripheral to Mount Adams started up ~940 ka, the central stratovolcano ~520 ka, and both remain active (Hildreth and Fierstein, 1995, 1997). The mafic to intermediate distributed vent fields peripheral to Mount Hood and Mount Mazama date well back into the early Pleistocene but the focal edifices date only from the middle Pleistocene. Longevities for distributed volcanic fields that lack stratovolcanoes include ~4 Myr for the Simcoe field, ~2.5 Myr for the Portland field, ~800 kyr for Indian Heaven, and 400-500 kyr for the Caribou, Medicine Lake, and Newberry Volcanic Fields. On the other hand, for none of the central edifices of the GVB, nor for Kulshan and Hannegan Calderas (Hildreth, Lanphere, and others, 2004; Tucker and others, 2007), has a peripheral mafic volcanic field been volumetrically important. The variations are so great that the most informative approach is to estimate eruption rates for individual edifices or fields that are well defined, well studied, and well dated.

Table 6 assembles data for several Cascade systems where eruptive volumes and longevities have been reasonably well estimated, at least for growth of the present-day centers (excluding in some cases remnants of older subjacent edifices largely torn down). Averaged over the lifetime of the center, many of the better-studied evolved systems yield eruption rates of 0.1 to 0.6 cubic kilometers per 1,000 years (km^3/kyr). Exceptional are Mount Shasta (largest cone in the Cascades), which gives 0.75 km^3/kyr, and Mount St. Helens (one of the youngest), the main well-preserved parts of which yield an eruption rate of ~2 km^3/kyr. For the few long-lived distributed volcanic fields that are both well-delimited and adequately investigated, there is a marked contrast in time-integrated eruption rates between the Indian Heaven, Mount Adams, and Caribou fields (each ~0.1 km^3/kyr), on the one hand, and the

Newberry and Medicine Lake rear-arc fields (both ~1 km^3/kyr), on the other.

Stratovolcanoes tend, however, to grow in spurts (Hildreth and Lanphere, 1994), so several examples of the higher eruption rates during such episodes are given in the lower section of table 6. At Mount Adams, it was shown that four major pulses produced 80 to 85 percent of the output of the whole volcanic field; that during those four episodes (each roughly 25 kyr long) average eruption rates were 2 to 5 km^3/kyr; and that during the much longer intervals separating the pulses, the system remained active at greatly reduced eruption rates averaging ~0.05 to 0.1 km^3/kyr (1 to 5 percent of the peak rates). Because durations of major growth spurts are seldom precisely enough established, however, the real eruption rates for peak episodes are usually only loosely approximated. For example, the Bachelor, Adams, and King Mountain pulses (1 to 4 km^3/kyr) cited in table 6 might have actually represented rates twice as high if the age limits of the episodes were known more precisely. Wherever ages are somewhat better constrained—as for the Belknap shield, episode 3 at Bachelor, the last 4 kyr at Mount St. Helens, and for the preclimactic rhyodacite buildup to the Mazama caldera-forming eruption, the rates are notably higher (3 to 25 km^3/kyr). The extraordinary pulse that built the huge Shastina cone (table 6) on the side of Mount Shasta in the early Holocene could not have been recognized without radiocarbon dating of pyroclastic deposits bracketing its products (Miller, 1980; Christiansen and Miller, 1989). An ultimate peak eruption rate, of course, is a caldera-forming eruption when tens or hundreds of cubic kilometers of magma are released in hours to days; but such an event represents abrupt loss of magma that had been fed to a shallow storage reservoir over tens of millennia, as the Kulshan and Mazama precaldera and climactic records illustrate.

Volumes of particular eruptive batches are often hard to determine, owing to dispersal and erosion of pyroclastic deposits and to uncertainty whether stacks of similar lavas represent single batches or several. The most voluminous batches erupted in the Quaternary Cascades were certainly the three caldera-forming eruptions (Mazama, Kulshan, and Rockland), which each released 40 to 80 km^3 of silicic magma. Eruptive batches of dacite and andesite seldom exceed 1 km^3, with a few noteworthy exceptions. The largest Quaternary dome in the Cascades at ~9 km^3, Burney Mountain may have extruded in several pulses or lobes, but it probably represents a single dacitic magma batch. Likewise, the Shastina dacitic edifice (30 to 40 km^3) was clearly built by a series of extrusive events, but the sequence appears to be bracketed to an interval of a few centuries, suggesting that its products could have belonged to a single magma batch. Andesite edifices typically grow by incremental addition of flows and ejecta from many small eruptions (<1 km^3), but one intracanyon andesitic lava flow from the east side of Mount Adams exceeds 3 km^3, and several ridge-capping flows radial to Mount Rainier are each in the range 3 to 9 km^3. The incremental-release uncertainty as to what constitutes a coherent magma batch is still more severe for mafic lava fields, cones, and shields. Some mafic edifices as voluminous as 5 to 25 km^3 may have been constructed in centuries or less, but limiting ages are rarely precise enough to prove it. Many (not all) such cones and shields are compositionally fairly uniform, consistent with derivation from a single magma batch. Moreover, for low-viscosity basaltic magmas, modest compositional variations distinguishable in some sequences of lavas could have developed within what started as a single magma batch during its fitful ascent through the crust. The Giant Crater lava field (Medicine Lake), which erupted as a coherently zoned (basaltic andesite-to-HAOT) sequence, amounted to ~4.4 km^3 of magma—one of the largest, rapidly emplaced, mafic batches clearly identified as such (Donnelly-Nolan and others, 1990, 1991).

Postglacial Eruptions in the Cascades

Table 7 provides a compilation of some 137 postglacial eruptive episodes, of which 21 were in the GVB, 56 in the Rainier-to-Hood segment, 50 in the Oregon segment, and 10 in California. Many of those assigned to the interval 15 to 12 ka appear to have taken place during deglaciation. More refined geochronology may eventually permit subdivision of some of the listed episodes, notably the 13-ka and mid-Holocene episodes at Glacier Peak, the Polallie period at Mount Hood, the Sand Mountain chain in Oregon, the Hotlum episode at Mount Shasta, and several busy intervals at Mount St. Helens.

Volumetrically, the estimates of table 7 sum to an arc-long postglacial magma output of ~290 km^3 in the last 15 kyr, an average of 19 to 20 km^3 per 1,000 years, not including the rear-arc centers. By segment, 16 percent of this erupted in the GVB, 21 percent in the Rainier-to-Hood segment, 39 percent in the Oregon segment, 24 percent at Mount Shasta, and only 1 percent in the Lassen segment. By eruptive center, 24 percent issued from Mount Shasta, 20 percent from Mount Mazama (almost entirely between 8 and 7 ka), 17 percent from Mount St. Helens, 12 percent along the Bachelor chain, and 11 percent from Glacier Peak. Altogether, 79 percent of the 290 km^3 postglacial output was from 15 large evolved centers and only 21 percent (61 km^3) from some 63 distributed or peripheral cones, shields, or chains of mafic and intermediate products. Within the latter category, the Bachelor chain and Belknap shield complex together account for 71 percent of the 61 km^3, and the Oregon segment as a whole for 86 percent.

During the postglacial interval, there have been only three great eruptive episodes in the Cascades—(1) the early-to-mid Holocene growth spurt of Mount Shasta (~66 km^3), which included enormous effusive outputs from the Shastina and Hotlum vents, only 2 km apart; (2) the 8 to 7 ka episode centered around the caldera-forming eruption of Mount Mazama (~58 km^3); and (3) the 15 to 11 ka outpouring of mafic lavas from the main part of the Bachelor chain (~35 km^3).

Besides these three great episodes, about 30 large postglacial eruptive episodes released 1 km^3 of magma or more (table 7). These include three Holocene events in British Columbia (from Mount Meager, Clinker Peak, and Opal

Table 6. Some volumetric eruptive rates for the Quaternary Cascades.

[Compositions: A, andesite (52-63% SiO2); B, basalt; D, dacite; R, silicic products (>68% SiO2). In Compositions column, > means "exceeds" and >> means "greatly exceeds"]

Center	km^3 Erupted	Interval	km^3/kyr	Compositions	Notes	References*
Lifespans						
Mount Baker	70-100	500-0 ka	0.1-0.2	A>>B>D	Includes Black Buttes, Cougar Divide, Ptarmigan Ridge, Table Mtn andesites.	18
Kulshan Caldera	50-100	1.18-1.0 Ma	0.3-0.6	R	Ignimbrite, fallout, and lavas.	19
Mount Rainier	140-200	500-0 ka	0.3-0.4	A>D	Much lost to erosion. Omits early Pleistocene predecessor edifice, largely stripped.	10, 27, 28
Indian Heaven	60-80	800-8 ka	0.1	B>>A	Nearly 50 vents. All erupted during Brunhes Chron except core of Gifford Peak.	14, 20, 21
Mount St. Helens	40-50	23-0 ka	2	D>A>B	Severe erosive loss of pyroclastic deposits. Omits Ape Canyon stage remnants (>35 ka).	7, 22, 23, 27
Mount Adams—focal	200-330	520-4 ka	0.4-0.6	A>>D>B	Stratovolcano and its high flank vents.	15, 17
—peripheral	30-70	940-14 ka	~0.05	B>>A	Surrounding volcanic field, largely mafic.	
Mount Hood	50-100	500-0 ka	0.1-0.2	A>D	Omits older Sandy Glacier and Vista Ridge centers nearby.	26, 27, 31, 32
South Sister	20	50-2 ka	0.4	A~R~D	Includes stratocone and flank rhyolites. Omits remnants of a few mid-Pleistocene andesites.	16, 24
Mount Mazama	160-180	420-0 ka	0.3-0.4	A>R>D	Omits subjacent pre-Mazama rhyodacites. Includes climactic eruption.	1, 2
Mount Shasta	450	600-0 ka	0.75	A>D>B	Includes 45-km^3 avalanche deposit. Omits peripheral mafic shields.	3, 4, 8
Lassen volcanic center	215	825-0 ka	0.25	A~R>D	Includes Rockland caldera, Brokeoff stratocone, and postcaldera domefield.	5, 6, 13
Caribou Volcanic Field	~50	450-20 ka	0.12	A~B	Compact area east of Lassen volcanic center; includes ~140 vents for small cones and shields.	6, 13
Newberry Volcanic Field	>500	~400-1 ka	>1	B~A>R	Large uncertainties in volume and start-up time.	10
Medicine Lake V.F.	>600	500-1 ka	1.2	B>A~R	Omits remnants of early Pleistocene units that predate and are largely buried by the edifice.	9
Eruptive Pulses						
Mount St. Helens —late Holocene	>40	4-0 ka	10	D>A>B	Smith Creek eruptive period to the present.	7, 22, 23
Mount Adams —modern cone	39-52	35-15 ka	2	A	Late Pleistocene cone added 1.3 km elevation to deeply eroded older edifice.	15, 17
King Mountain chain	7-12	115-106 ka	1	B	King Mtn to Quigley Butte compound shield.	15, 17
Belknap shield	6-9	3-1.5 ka	5	B~A	Multi-vent shield only. Does not include peripheral cinder cones and lavas to S and W.	29, 30
Mount Bachelor chain	35-40	18-8 ka	4	B>A	Four main eruptive episodes along a 25-km-long chain of >35 vents.	12, 25
—Episode 3	~25	~14-13 ka	25	B>A	Main Mt Bachelor—Kwohl Butte phase probably took <1000 years.	12, 25
Mount Mazama climax	60-80	30-7 ka	3	R>A	Includes preclimactic domes and ejecta, caldera-forming ejecta, and intracaldera lavas & tuff.	1, 2
Shastina	30-40	9.7-9.4 ka	100	D>A	Growth of large cone bracketed by radiocarbon-dated pyroclastic units.	3, 4
Shasta (Hotlum cone)	25-30	9-4 ka	5	D~A	Summit cone and large fragmental ringplain.	3, 4

*References: **1.** Bacon and Druitt, 1988. **2.** Bacon and Lanphere, 2006. **3.** Christiansen, 1982, and written commun., 2006. **4.** Christiansen and others, 1977. **5.** Clynne, 1990a. **6.** Clynne and Muffler, in press. **7.** Crandell, 1987. **8.** Crandell and others, 1984. **9.** Donnelly-Nolan, in press. **10.** Donnelly-Nolan, work in progress. **11.** Fiske and others, 1964. **12.** Gardner, 1994. **13.** Guffanti and others, 1996. **14.** Hammond and Korosec, 1983. **15.** Hildreth and Fierstein, 1995. **16.** Hildreth and others, work in progress. **17.** Hildreth and Lanphere, 1994. **18.** Hildreth and others, 2003. **19.** Hildreth, Lanphere, and others, 2004. **20.** Korosec, 1989. **21.** Mitchell and others, 1989. **22.** Mullineaux, 1996. **23.** Mullineaux and Crandell, 1981. **24.** Scott, 1987. **25.** Scott and Gardner, 1992. **26.** Scott and others, 1997. **27.** Sherrod and Smith, 1990. **28.** Sisson and Lanphere, 2000. **29.** Taylor, 1968. **30.** Taylor, 1981. **31.** Wise, 1968. **32.** Wise, 1969.

Table 7. Postglacial eruptive episodes in the Cascades.

[Some of the episodes listed are likely to be subdivided after more detailed investigations. Volume estimates, adjusted to approximate the amount of magma erupted, are either from the references listed or by the present author; some are rough approximations and might be improved greatly by tighter field constraints. Dash (—) in volume column means data are inadequate for an estimate. HAOT is high-alumina olivine tholeiite, as elaborated in the text. In Composition (Comp.) column, abbreviations are as in table 6, except that M additionally separates mafic andesite (52-57% SiO_2) or refers to products zoned from basalt to andesite]

Center or reach	Eruptive episode	Age	Comp.	Volume(km^3)	References
Bridge River	•Postglacial intracanyon lava flows reported, not dated. (Most units glaciated)	<15 ka?	B	<0.1	41, 56
Meager (Plinth)	•Plinian fall (Bridge River tephra), pyroclastic flows, lava flows	2.4 ka	R	3	57, 58
Cayley	•Shovelnose dome pair and intracanyon flows (K-Ar ages older; excess Ar?)	<15 ka?	D	0.5	22, 55
Garibaldi Lake	•Clinker Peak; 2 adglacial lava flows, each 7 km long	15-12 ka	A	4	22, 34, 35
	•Price Bay scoria cone	<15 ka	A	0.04	20, 22
	•Cheakamus intracanyon lavas, youngest set of supra-till lava flows	15-12 ka	B	0.1	22, 35
Garibaldi	•Opal Cone and Ring Creek lava flow	10 ka	D	4.5	8
Baker	•Glacier Creek intracanyon lava flow; summit-derived	14 ka	A	0.1	26
	•Boulder Creek assemblage: lava flows, pyroclastic flows, and lahars	13-12 ka	A	1	26, 27
	•Tephra Set RC (^{14}C ages 10.3 to 10.7 ka)	~12 ka	A	<0.1	27, 42
	•Sulphur Creek lava flows from Schreiber Meadow scoria cone; ashfall layer SC	9.8 ka	B-A	1	21, 26
	•Subplinian ashfall layer BA; summit-derived (^{14}C age 5.8 ka)	6.5 ka	A	0.1	26
Glacier Peak	•White Chuck scoria cone	15-12 ka	B	0.2	5, 6, 59
	•Lightning Creek lava flow	15-12 ka	M	0.1	59
	•Plinian Layers G, M, and B; 6 lesser ashfalls; lava domes and pyroclastic flows	13 ka	D	15	5, 6, 40
	•Lava domes, pyroclastic flows, ashfall set D	6.1 ka	D	15	5, 6, 19
	•Lava domes, pyroclastic flows, Dusty Creek coignimbrite ashfalls	5.8 ka	D	—	5, 6, 19
	•Lava dome and pyroclastic flows	~2.8 ka	D	0.1	5, 6
	•Lava domes, pyroclastic flows, fall layer A	2.0-1.8 ka	D	0.2	5, 6, 19
	•Pyroclastic flows (and dome?)	~1.1 ka	D	0.01	5, 6
	•Small ashfall and debris flows	~0.3 ka	D	<0.01	5, 6
Rainier	•19th century period: Minor ashfalls (1820-1854; 1894); scoria fall layer X	0.15 ka	A-D	<0.01	37, 51
	•Deadman Flat period: Pyroclastic flows and thin ashfall to northeast	1.1 ka	A-D?	<0.01	51, 52
	•Summerland period: ~6 sets of thin hydromagmatic ashfalls; lava extrusions	2.6-2.2 ka	A	<0.01	51, 52
	•South Puyallup River pyroclastic flow	2.45 ka	A	<0.1	51, 52
	•Lava flows, at least two sets	2.4-2.2 ka	A	0.1	51, 52
	•Subplinian pumice fall layer C	2.2 ka	A-D	0.1	37, 65
	•growth of two small cratered summit cones	2.2-2.0 ka	A	<0.1	51, 52
	•Osceola period: •Fall layers B and H; post-Osceola lavas refill amphitheater	5.4-4.6 ka	A-D	2	37, 51

Table 7. Postglacial eruptive episodes in the Cascades.—Continued

[Some of the episodes listed are likely to be subdivided after more detailed investigations. Volume estimates, adjusted to approximate the amount of magma erupted, are either from the references listed or by the present author; some are rough approximations and might be improved greatly by tighter field constraints. Dash (—) in volume column means data are inadequate for an estimate. HAOT is high-alumina olivine tholeiite, as elaborated in the text. In Composition (Comp.) column, abbreviations are as in table 6, except that M additionally separates mafic andesite (52-57% SiO_2) or refers to products zoned from basalt to andesite]

Center or reach	Eruptive episode	Age	Comp.	Volume(km³)	References
Rainier	•Tephra layer F; phreatomagmatic blasts and pumiceous ashfall	5.6 ka	A-D	<0.01	37, 51
	•Osceola Mudflow (3.8-km³ sector collapse); during layer F	5.6 ka	—	—	37, 64
	•Tephra layer S; phreatic blast beneath Osceola Mudflow	5.6 ka	—	0	37, 64
	•Tephra layer N; pyroclastic flows and lahars	5.8 ka	A	0.001	37, 64
	•Cowlitz Park period; •Tephra layer D (subplinian hornblende-rich pumice/scoria)	7.0-6.7 ka	A-D	0.015	37, 51
	•Tephra layer L (subplinian pumice fall)	7.3-7.1 ka	A	0.01	37, 51
	•Tephra layer A	~7.5 ka	A-D	0.002	37, 51
	•Tephra layer R; pumice and scoria fall; oldest postglacial eruptive unit known	9.9-9.7 ka	A	0.01	37, 51
Adams	•Andesite of Mount Adams summit; lava flows, fragmental cone	15-5 ka	A	0.15	24, 25
	•Basalt of Trappers Creek; lava flows; Red Butte scoria cone	15-14 ka	B	0.15	24, 25
	•Andesite of Cunningham Creek; fissure/spatter vent; intracanyon lava flow	15-14 ka	A	0.05	24, 25
	•Basalt of Smith Butte; chain of scoria cones, lava-flow apron	14 ka	B	0.25	24, 25
	•Four ash and scoria falls	12-8 ka	A	<0.01	25
	•Andesite of High Camp; lava flows; vent covered	7-5 ka	A	0.01	24, 25
	•Andesite of Takh Takh Meadow; 10-km-long lava-flow field; vent covered	7-5 ka	A	0.4	24, 25
	•Andesite of Muddy Fork; fissure-fed lava flows to 8 km long	7-5 ka	A	0.3	24, 25
	•Seven ash and scoria falls; and seven hydrovolcanic crystal-lithic ashfalls	7-4 ka	A	<0.01	25
	•Andesite west of Gotchen Glacier; fissure-fed lava flow 1 km long	5-4 ka	A	0.001	24, 25
	•Aiken Lava Bed; fissure-fed flank flow 7 km long	~4 ka	A	0.1	24, 25
	•Andesite of Battlement Ridge; two spatter-fed lava flows, each ~1 km long	3-1 ka	M	0.002	24, 25
	•Four phreatic or phreatomagmatic ashfalls	2.5-1 ka	A	<0.01	25
Indian Heaven	•Big Lava Bed; scoria cone pair, 15-km-long lava field, and 0.1-km³ ashfall	9 ka	B	1	28
S. Washington	•West Crater; lava dome, 2 lava flows, each 4 km long (head of Trout Creek)	≤8 ka	A	0.2	39
	•Hackamore Creek scoria cone and short lava flow	9-8 ka	A	<0.01	23, 39
	•Puny Creek crater (S toe of Bare Mtn), scoria blanket, and (related?) lava flows	<9 ka	M	<0.01	23
	•Chinook Creek cone and intracanyon lava flows (6 km south of Swift Reservoir)	<15 ka	M	<0.01	39
St. Helens	•Swift Creek stage: •Lava domes, pyroclastic-flow fans; 5 fall layers of Set S	16-13 ka	D	10	13, 38
	•Four fall layers of Set J	~13-12 ka	D		13, 38
	•Smith Creek period: •Lava domes, pyroclastic flows; fall layers Yb, Yd	3.9-3.8 ka	D	10	13, 38
	•Pyroclastic flows & ashfalls; 5 more fall layers of Set Y	3.5-3.3 ka	D		13, 38
	•Pine Creek period: •Domes, pyroclastic-flow fans & ashfalls; 4 layers of Set P	2.9-2.6 ka	D	3	13, 38

	•Castle Creek period: •Lava flows and early ashfalls of Set B; emplaced radially	2.55-2.5 ka	A	20	13, 38
	•Lava flows on N flank; more ashfalls of Set B	~2.2 ka	A		13, 38
	•Lava domes, pyroclastic flows; ashfall layers Bd, Bi	~2.0 ka	D		13, 38
	•Lava flows: 3 radial sets of lavas; ashfall layer Bu	2.0-1.9 ka	B		13, 38
	•Cave Basalt; 14-km lava tongue down S flank; final event	1.9 ka	B	0.24	66
	•Sugar Bowl period: Domes; pyroclastic flows; lateral blasts; fall layer D	750-800 CE	R	0.1	16, 38
	•Kalama period: •Domes, pyroclastic flows; 5 fall layers of Set W	1479-1500 CE	D	5	13, 38
	•Many lava flows, pyroclastic flows; ashfall Set X	1510-1570 CE	A		13, 38
	•Summit dome, pyroclastic flows; ash layer Z	1620-1720 CE	D		13, 38
	•Goat Rocks period: •Plinian fall layer T	1800 CE	D	1	13, 38
	•Lava flow down N flank	1801 CE	A		13, 38
	•Goat Rocks lava dome with intermittent ashfall	1831-1857 CE	D		13, 38
	•1980-1986 period: Lateral blast, fallout, pyroclastic flows, lava domes	1980-1986 CE	D	0.5	7, 17, 29
	•2004-2007 period; small ash plumes and lava dome	2004-2007 CE	D	0.05	33
Hood	•Polallie period; many pyroclastic flows, domes; began during LGM	?20-12 ka	D	>5	15, 46
	•Parkdale lava flow, 6 km long, from vent in Hood River valley	7.7 ka	M	0.1	46, 67
	•Timberline period; domes and pyroclastic flows	1.5 ka	D	1	15, 46
	•Old Maid Flat period; Crater Rock dome and pyroclastic flows	0.2 ka	D	0.15	15, 46
Jefferson reach	•North Pinhead Butte; scoria cone and lava flow to E	~15 ka	M	0.1	47
	•Badger Creek flow; 2 scoria cones (12 km E of Sisi Butte)	<12 ka	M	0.03	49
	•Scoria cone at S toe of The Table	8-6 ka	M	<0.01	43
	•Horseshoe scoria cone and Jefferson Creek lava flow	~7 ka	M	0.1	43
	•Forked Butte scoria cone and two lava flows in Cabot Creek	~7 ka	M	0.1	43
	•Scoria cone at S toe of South Cinder Peak and lava flow to W	~1 ka	M	0.02	43
Sisters reach	•Sand Mtn chain; ~20 scoria cones and multi-flow lava apron	4-2.8 ka	B-M	—	60, 61, 62, 63
	•Little Nash Crater; scoria cone and lava flow	~2.6 ka	M	3.5	50, 60, 61, 62
	•Nash Crater; scoria cone and lava-flow apron	4-3 ka	B	—	50, 60, 61, 62
	•Lost Lake chain; 4 scoria cones and lava-flow apron	~2 ka	B	—	50, 60, 61, 62
	•Blue Lake crater; phreatomagmatic ejecta apron;	~3.5 ka	M	<0.01	43, 50, 60, 61
	•Spatter cone chain of 3 fissure vents (at northeast toe of Mount Washington)	<1.3 ka	M	<0.01	50, 60
	•Inaccessible Cone chain of 5 scoria cones and 2 lava aprons	~7-4 ka	B	0.03	50, 60, 61
	•Twin Craters; scoria cone pair and lava apron (southwest of Belknap shield)	~2.8 ka	M	0.02	50, 60, 61
	•Belknap Crater shield; scoria cone on top (includes South Belknap flank vent)	3-1.4 ka	B-M	6.5	50, 60, 61, 62
	•Little Belknap shield	2.9 ka	M	1.5	50, 60, 61, 62
	•Yapoah Crater; scoria cone and several lava flows as long as 13 km	~2.7 ka	M	0.25	50, 60, 61, 62
	•Four-in-One chain of 6 fissure-fed scoria cones and lava apron	2.0 ka	M-A	0.05	50, 60, 61

Table 7. Postglacial eruptive episodes in the Cascades.—Continued

[Some of the episodes listed are likely to be subdivided after more detailed investigations. Volume estimates, adjusted to approximate the amount of magma erupted, are either from the references listed or by the present author; some are rough approximations and might be improved greatly by tighter field constraints. Dash (—) in volume column means data are inadequate for an estimate. HAOT is high-alumina olivine tholeiite, as elaborated in the text. In Composition (Comp.) column, abbreviations are as in table 6, except that M additionally separates mafic andesite (52-57% SiO_2) or refers to products zoned from basalt to andesite]

Center or reach	Eruptive episode	Age	Comp.	Volume(km^3)	References
Sisters reach	•Collier Cone; scoria cone and lava flows, one as long as 13 km	<1.6 ka	M-A-D	0.3	50, 60, 61
	•Sims Butte; large scoria cone and intracanyon lava tongue as long as 14 km	~15 ka	M	0.2	50, 60, 61, 62
	•Cayuse Crater; scoria cones (one large, 2 small) and lava flows as long as 4 km	11 ka	B	0.1	45, 50
	•LeConte Crater; scoria cone and several lava flows as long as 14 km	15-10 ka	M	0.2	45
	•Katsuk and Talapus Buttes; vent chain, hyaloclastite, lava plateau, 2 scoria cones	18-15 ka	B	1.3	45
	•Chambers Lake coulee; bifurcating flow vented high on S slope of Middle Sister	14 ka	D	0.2	18
	•Rock Mesa coulee, satellite domelets, and pumice fall	2.2 ka	R	0.53	44
	•Devils chain; 20 aligned vents; small lava domes and flows and pumice fall	2.0 ka	R	0.32	44
	•Egan Cone; scoria cone and lava apron to Sparks Lake	~8 ka	B-M	0.5	45
	•Mount Bachelor summit cone and Tot Mtn flank vent	13-11 ka	M		45
	•Mount Bachelor shield; lava flows as long as 22 km; 3 scoria cones at north toe	~13 ka	B-M	25	45
	•Kwohl Butte shield; lava flows as long as 18 km; at least 7 scoria cones	15-13 ka	B-M		45
	•Siah Butte chain; 25-km-long; >30 vents; many lava flows, scoria/spatter cones	15-14 ka	B	3	45
	•Sheridan Mtn shield; many lava flows; ~8 flank scoria cones	18-15 ka	B-M	7	45
	•Red Crater chain (six vents); scoria cones and lava apron (W of Mt Bachelor)	18-12 ka	B	0.3	45
	•Wuksi Butte-Twin Lakes chain; lava apron; 6 scoria cones and 4 maars	18-15 ka	B-M	1	45
	•Sitkum Butte; fissure-fed lava apron on east flank of Pleistocene cone	<10 ka	B	<0.01	32
Wickiup reach	•Davis Lake lava flow and scoria cone	5 ka	A	0.1	32
	•Black Rock lava flow and scoria cone (south of Hamner Butte)	~5 ka	A	0.1	32
	•Black Rock Butte lava flow and scoria cone (northeast of Odell Butte)	~5 ka	A	<0.1	32
Thielsen reach	•Thirsty Point scoria cone and lava apron (11 km north of Diamond lake)	15-12 ka	M	0.15	47, 48
	•Cinnamon Butte scoria cone and lava apron (8 km north of Diamond Lake)	15-12 ka	M	0.8	47, 48
Mazama reach	•Basalt of Castle Point; 3 HAOT vents; lava flows (7 km southwest of caldera)	15-8 ka	B	0.16	2
	•Llao Rock plinian fall and lava flow, Mount Mazama	7.9 ka	R	3.5	1, 4
	•Crater Lake caldera-forming plinian fall, pyroclastic flows, and Cleetwood lava	7.7 ka	R>A	50	1
	•Wizard Island scoria cone and lava-flow apron, Crater Lake	~7 ka	A	2.62	3
	•Central Platform lava plateau (Crater Lake floor)	~7 ka	A	1.06	3
	•Merriam Cone; lava and fragmental cone on floor of Crater Lake	~7 ka	A	0.34	3
	•East Basin sediment-buried lava flow on floor of Crater Lake	~7 ka?	A?	0.03	3
	•Rhyodacite dome on floor of Crater Lake	4.8 ka	R	0.074	3
McLoughlin reach	•Imagination Peak; scoria cone and lava flows (northwest of Pelican Butte)	15-12 ka	B	0.05	53

	•Brown Mountain; postglacial lava flows at west toe of shield	15-12 ka	M-A	0.35	54
Shasta segment	•Red Banks plinian fall and pyroclastic flows	11 ka	D	>1	36
	•Shastina cone; many large lava flows, domes, and pyroclastic flows	11-10 ka	D	40	10, 36
	•Black Butte; compound lava dome with pyroclastic-flow apron	10 ka	D	2.5	36
	•Hotlum (summit) cone; many large lava flows, pfs; vulcanian ashfalls	10-0.2 ka	D-A	25	9, 36
Lassen segment	•Twin Buttes; scoria cone pair and 5-km-long lava flow (E of Burney Mtn)	15-12 ka	M	—	—
	•Andesite of hill 7416; scoria cone and 6-km-long lava flow	15-12 ka	A	0.3	14, 31
	•Devils Rock Garden; scoria cone and 4-km-long lava field	15-10 ka	A	0.35	14, 30
	•Chaos Crags; 6 lava domes, pyroclastic flows and fallout	1.1-1.0 ka	R	2	11
	•Cinder Cone; compound scoria cone, 5 lava flows, far-flung ashfall	1666 CE	M-A	0.4	12
	•Lassen Peak; lava dome, 2 short lava flows, pyroclastic flows and fallout	1915 CE	D>R~A	0.1	11

References: **1.** Bacon, 1983. **2.** Bacon and others, 1994. **3.** Bacon and others, 2002. **4.** Bacon and Druitt, 1988. **5.** Beget, 1982a. **6.** Beget, 1984. **7.** Brantley and Myers, 2000. **8.** Brooks and Friele, 1992. **9.** Christiansen, 1990. **10.** Christiansen and Miller, 1989. **11.** Christiansen and others, 2002. **12.** Clynne and others, 2000. **13.** Clynne and others, in press. **14.** Clynne and Muffler, in press. **15.** Crandell, 1980. **16.** Crandell and Hoblitt, 1986. **17.** Criswell, 1987. **18.** Fierstein and others, 2003. **19.** Foit and others, 2004. **20.** Green, 1981. **21.** Green, 1988. **22.** Green and others, 1988. **23.** Hammond, 1990. **24.** Hildreth and Fierstein, 1995. **25.** Hildreth and Fierstein, 1997. **26.** Hildreth and others, 2003. **27.** Hyde and Crandell, 1978. **28.** Korosec, 1989. **29.** Lipman and Mullineaux, 1981. **30.** Macdonald, 1963. **31.** Macdonald, 1964. **32.** Macleod and Sherrod, 1992. **33.** Major and others, 2005. **34.** Mathews, 1952b. **35.** Mathews, 1958. **36.** Miller, 1980. **37.** Mullineaux, 1974. **38.** Mullineaux, 1996. **39.** Phillips, 1987. **40.** Porter, 1978. **41.** Roddick and Souther, 1987. **42.** K.M. Scott, work in progress. **43.** Scott, 1977. **44.** Scott, 1987. **45.** Scott and Gardner, 1992. **46.** Scott and others, 1997. **47.** Sherrod, 1990b. **48.** Sherrod, 1991. **49.** Sherrod and Smith, 2000. **50.** Sherrod and others, 2004. **51.** Sisson and others, 2001. **52.** Sisson and Vallance, 2005. **53.** Smith, 1988. **54.** Smith and others, 1982. **55.** Souther, 1980. **56.** Souther, 1990. **57.** Stasiuk and Russell, 1990. **58.** Stasiuk and others, 1996. **59.** Tabor and Crowder, 1969. **60.** Taylor, 1965. **61.** Taylor, 1968. **62.** Taylor, 1981. **63.** Taylor, 1990b. **64.** Vallance and Scott, 1997. **65.** Venezky and Rutherford, 1997. **66.** Williams and others, 2004. **67.** Wise, 1969.

Cone) and two in California (Black Butte and Chaos Crags). In central Oregon, there were large mafic eruptive episodes at the Belknap shield complex, along the Sand Mountain chain, and at two chains satellitic to the Bachelor chain (Katsuk-Talapus and Wuksi-Twin Craters; table 7). The Big Lava Bed at Indian Heaven and the post-Osceola refilling of Mount Rainier's summit amphitheater also represent large outpourings of lava over limited time intervals. In addition, major pyroclastic episodes include the Polallie and Timberline periods at Mount Hood, at least four voluminous episodes at Glacier Peak, and as many as 15 from Mount St. Helens. Of the 30 large eruptive episodes, the biggest well-delimited events appear to be the Opal Cone-Ring Creek lava (4.5 km^3) and fall layer Yn from Mount St. Helens (4 km^3). However, several postglacial episodes at Glacier Peak and Mount St. Helens produced great pyroclastic-flow fans that are hard to quantify volumetrically because, when mobile, they degenerate into downstream debris flows and, after emplacement, they erode away rapidly. Many such pyroclastic episodes at Glacier Peak, St. Helens, and Hood are likely (in addition to more readily quantifiable fall deposits) to have generated fragmental flow deposits in the range 1 to 5 km^3 for each major interval.

Scott (1990), amplifying a compilation by Hoblitt and others (1987) comparable to that of table 7 (but also including phreatic events and debris flows not tied to magmatic eruptions), defined ~181 eruptive periods over the last 15 kyr. Of these, 24 were at Newberry and Medicine Lake (not dealt with here), the remainder in the Cascade arc proper. Scott called attention to the incomplete and ephemeral record left by some of the smaller events included in his count, noting that a third (60) of the eruptive periods compiled were in the past 3,000 years. The youngest, best-preserved record thus suggests a recent average of two episodes per century; and there were in fact two in the 20^{th} century—at Lassen Peak (1914-17) and Mount St. Helens (1980-86). With age, however, discerning the record and integrity of minor episodes becomes more difficult. It seems unlikely, say, 5,000 years into the future, that either the 1914-17 events atop Lassen Peak or the 2004-7 augmentation of the crater-confined St. Helens dome would be discerned as discrete eruptive episodes.

Start-up Times and Major Growth Episodes

Although an open-minded skeptic is unlikely to see any pattern of along-arc synchroneity or episodicity in the postglacial eruptive inventory of table 7, one can further examine the eruptive record on the longer timescales of edifice longevity and spurts of elevated volumetric output (tables 8, 9). Within the growth histories of many major Cascade centers, intervals of heightened eruptive output have been identified. Although the age limits of such intervals are seldom tightly defined, some of the better constrained examples are listed in table 8. They include a wide range of nominal eruption rates, between 0.2 and 10 km^3/kyr, but each represents a marked pulse at its particular volcano. Again, however, no coordinated episodicity is obvious along the Cascade arc.

The eruptive intervals selected for table 6 took place at a number of large Cascade centers where major activity appears to have begun between ~600 ka and 400 ka, an observation that might be interpreted to suggest that some tectonic-magmatic event or transition took place around that time, in the middle Pleistocene. Initiation of the Tumalo, Cappy, and Garibaldi centers may (or may not) also date from that interval. In order to examine more closely the foundations of such an inference, the start-up times for the main evolved (nonmafic) centers in the Cascades have been tabulated (table 9) along with the evidence for any older evolved predecessors, subjacent or nearby. Table 9 shows that the existing centers began growth at widely different times and that most of them overlap the eroded remnants of earlier edifices or of distributed vent fields that date from the middle or early Pleistocene.
In particular, the following points can be noted: (1) the Rainier and Hood edifices, which started up ~500 ka, are directly superimposed on remnants of predecessors as old as 1.3 Ma, and the Jefferson and Mazama edifices overlie distributed silicic volcanic fields that similarly date from the early Pleistocene; (2) the Baker, Shasta, and Lassen loci, each of which first grew large in the mid-Pleistocene, did so following shifts of the local magmatic focus by only 10 to 20 km from the sites of large evolved centers that had been active in the early Pleistocene; (3) start-up times of the South Sister, Middle Sister, and Mount St. Helens edifices are much younger (≤50 ka), as are those of evolved predecessors underlying each one (300 to 150 ka); (4) the Goat Rocks edifice started up sometime in the early Pleistocene and overlies remnants of a Pliocene center; and (5) reconnaisance K-Ar dating (Green and others, 1988) suggests that the multiphase Meager and Cayley edifices both contain components as old as 2 Ma, though this needs to be checked by current $^{40}Ar/^{39}Ar$ methods. The evident complexity is inconsistent with the suggestion that many or most Cascade edifices began growth at about the same time. After consideration of mantle processes beneath the arc, possible inferences will be addressed below concerning the contrast between shifting and stationary magmatic foci (table 9) on the 2-Myr Quaternary timescale (see the section below entitled “Shifts of Focus”).

As eruptive histories become better defined and more precisely dated, the search for along-arc coordinated episodicities should be maintained. For now, however, the data for Quaternary start-up times, subsequent episodes of high output, and the more detailed postglacial record support only skepticism concerning the existence of any pattern of synchronous magmatic behavior along the Cascades. Individual evolved centers behave independently, as does the mafic magmatism distributed along the different reaches of the arc.

Outstanding Questions

Any discussion of eruption rates or episodicities brings up many unanswered but fundamental questions about mag-

Table 8. Pulses of elevated eruptive output.

Center	Interval	Notes	References
Meager	100-2 ka	Northern half of multivent edifice built (in at least 4 stages)	8
Baker: Black Buttes	500-300 ka	Mafic to dacitic stratocone	10
Modern cone	40-12 ka	Andesitic stratocone	
Rainier	500-420 ka	Principal growth spurts of great central edifice	13
	280-190 ka		
	40-4 ka		
Adams: Early edifice	520-450 ka	Combines Hellroaring Volcano and adjacent edifice beneath modern cone	9
Modern cone	35-15 ka	Present andesitic summit cone	
St. Helens	23-0 ka	Silicic domefield concentric with young (<2.5 ka) stratocone	5,11
Jefferson	100-50 ka	Most productive interval during 280-kyr growth of modern cone	6
South Sister	50-2 ka	Growth of modern rhyolite-dacite-andesite edifice	7
Bachelor chain	18-8 ka	Multivent mafic alignment	12
Mazama	80-40 ka	Last big growth spurt of late Pleistocene edifice	1
	27-7 ka	Growth, leakage, and evacuation of climactic rhyodacite magma reservoir	
Shasta:			
Sargents Ridge	200-150 ka	Four successive overlapping cones that were built atop wreckage of larger mid-Pleistocene Sand Flat edifice eviscerated by huge debris avalanche	2
Misery Hill	40-30 ka		
Shastina and Hotlum	10-4 ka		
Lassen:			
Rockland Tuff	600 ka	Caldera-forming eruption	3,4
Brokeoff cone	590-390 ka	Postcaldera andesite-dacite stratovolcano	
Younger domefield	66-0 ka	Younger of two main intervals in growth of Lassen domefield	

References: **1**. Bacon and Lanphere, 2006. **2.** Christiansen, R.L., written commun., 2006. **3.** Clynne, 1990a. **4.** Clynne and Muffler, in press. **5.** Clynne and others, in press. **6.** Conrey, 1991. **7.** Fierstein and others, 2003. **8.** Green and others, 1988. **9.** Hildreth and Lanphere, 1994. **10.** Hildreth and others, 2003. **11.** Mullineaux, 1996. **12.** Scott and Gardner, 1992. **13.** Sisson and others, 2001.

Table 9. Start-up times, predecessors, and shifts of eruptive focus.

Center	Initiation of Present Edifice	Predecessor Edifice beneath Present Volcano?	Shift of Main Eruptive Focus?
Meager	150-100 ka	Young multi-vent silicic pile caps northern two-thirds of composite edifice. Older components crop out 3-6 km southwest.	Pylon complex (andesitic, 1-0.5 Ma), The Devastator complex (silicic, 2-1 Ma), and scraps of an andesite- dacite edifice (~2 Ma) form southern third of center.
Cayley	uncertain	None. At least 3 stages in growth of multi-vent edifice.	No. Distributed vents show no systematic migration.
Garibaldi	~260 ka	Round Mtn andesitic edifice (600±150 ka).	No. Little or no systematic vent migration.
Baker	45 ka	Remnant lava stack in Park Creek (140-80 ka) and Black Buttes cone (500-300 ka) centered 3 km southwest; overlapped by modern cone.	Kulshan caldera (1.3-1.0 Ma); 7 km northeast (fig. 26). Lake Ann stock (2.8 Ma); 13 km northeast.
Glacier Peak	600 ka	Gamma Ridge caldera (2 to 1.6 Ma) lies 4-9 km northeast of modern summit vents.	Modest (fig. 26).
Rainier	500 ka	Lily Creek volcano (1.3 to 1.0 Ma).	No
St. Helens	23 ka	Modern domefield dates from 23 ka; stratocone from 2.5 ka. Older domefield (125-35 ka) underlaps the modern complex.	Ape Canyon domefield (300-250 ka; 125-35 ka) crops out 4-10 km southwest of modern edifice.
Adams	450 ka	Hellroaring stratovolcano (520-450 ka) offset 5 km southeast of younger cone (fig. 10).	Modest (fig. 26). Distributed mafic field since ~1 Ma.
Hood	500 ka	Vista Ridge cone (1.5-0.8 Ma) buried by Hood. Sandy Glacier volcano (~1.3 Ma) crops out beneath west flank of Hood (fig. 11).	Lookout Mountain center (~3 Ma): 7-15 km east.
Jefferson	~280 ka	Distributed andesite-dacite field since 1-1.5 Ma.	Lionshead evolved center (2-3 Ma) ~10 km northeast.
Middle Sister	38 ka	Remnant lava stack at east toe (180-160 ka).	No. All older volcanoes nearby are mafic.
South Sister	50 ka	A lone dacite lava (178 ka) extends southeast from beneath toe of present edifice.	Broken Top (300-150 ka) lies 6 km southeast (fig. 26). Tumalo Volcanic Field (650-260 ka) is 12-18 km east.
Mazama	420 ka	Distributed mafic-silicic field (1.8-0.6 Ma) underlies the modern edifice.	Pre-Mazama clustered rhyodacite field (470-410 ka) underlaps edifice and extends as far as 12 km east. General drift of vents toward the west-northwest has continued during growth of the Mazama edifice.
Shasta	600 ka	None. Five successive stages were centered within 3 km of each other.	Rainbow Mountain center (~1 Ma) lies 20 km northeast (fig. 26).
Lassen domefield	300 ka	Brokeoff stratocone (590-390 ka). Rockland precaldera/caldera sequence (825-600 ka) underlaps modern domefield.	Maidu center (2.4-1.2 Ma); ~18 km south-southwest. Dittmar center (2.4-1.4 Ma); ~15 km southeast (fig. 26).

matism. The uncertainties reflect principally our nebulous understanding of mantle convection and melting and of intracrustal magma transport and multistage storage. (1) What fraction of the magma in any particular crustal column ever erupts? We don't know what proportions are deposited intra crustally as melt-depleted (cumulate) mafic and felsic intrusive rocks. (2) Why do so few eruptive loci develop into long-lived productive centers? Slab subduction is continuous along the Cascade arc for 1,250 km, but some profound modulating processes have restricted the number of large evolved Quaternary centers to fewer than 30 (table 2). (3) What causes gross differences in eruptive output along the same arc? Although of similar (andesite-dacite) composition and longevity (500 to 600 kyr), Mount Shasta has had five times the output of Mount Hood. (4) What limits longevities of most major arc volcanoes to 0.1 to 1 Myr? Possibilities include source depletion, shifts of focus, and relaxation times of mantle upwellings. (5) Why are continental-arc stratovolcanoes seldom large? Many are 10-100 km^3 but only a few erupt total volumes of 100-1000 km^3. Many intraplate shields are far more voluminous, and some intraplate extensional systems release single eruptions of silicic or mafic magma greater than 1000 km^3. Arcs never produce flood andesites. Eruptive batches are numerous and small, and even caldera-forming eruptions from shallow arc reservoirs seldom reach 100 km^3. And (6) if there is little coordinated episodicity along the arc, is it reasonable to attribute volcanic behavior (as opposed to magmatism in general) to secular, apparently steady, plate motions?

Productivity of the Cascades vis-à-vis Other Continental Arcs

It has commonly been asserted that volcanic output along the Cascade arc is low relative to that of many arcs, but the basis of the assertion has never been clear. The estimated 290 km^3 of postglacial magma erupted along the Cascade arc proper (neglecting the rear-arc centers) is equivalent to ~5 percent of the volume of oceanic crust and sediment (if together ~8 km thick) potentially subducted during any 15-kyr interval beneath the 1,250-km-long Cascadia margin at a rate of 4 cm/yr. If such an eruption rate had been steady throughout the Quaternary, this would have yielded more than 19,000 km^3 of eruptive products in 1 Myr and 38,000 km^3 in 2 Myr. Accepting estimates of Sherrod and Smith (1990) for volumetric output in California and Oregon and using my own larger estimates for the more severely glaciated volcanoes of Washington and Canada, I get a total eruptive volume of ~6,400 km^3 of Quaternary products for the Cascade arc. What is present today (or is reasonably reconstructed at well-known centers) is thus only about 17 percent of the 2-Myr eruptive volume expected based on the postglacial eruption rate. Either the postglacial rate is far greater than the Quaternary average or the erosion of early Quaternary products was far greater than anyone has estimated.

Nonetheless, even 6,400 km^3 is not low relative to the Quaternary productivity of some other continental arcs. For the 1,100-km-long Central American arc (where glacial erosion is absent), the 39 volcanic-front centers (many of them multivent edifices) yield a total volume of 3,464 km^3 (Carr and others, 2003), and in the rear-arc some 10 modest composite cones and several clusters of scoria cones and domes add no more than an additional 10 percent. For the 1,000-km-long Northeast Japan arc (Myoko to Tarumai), Aramaki and Ui (1982) conservatively estimated a total volume of 1,309 km^3 for 45 edifices or volcanic clusters plus 177 km^3 for distributed pyroclastic falls and flows. Glacial erosion in the Japanese arc has been insignificant. They stated that most of the volcanoes are younger than 0.5 Ma and very few as old as 1 Ma. Even if their estimate were quadrupled (to approximate Quaternary output for 2 Myr), the resulting volume of 5,944 km^3 would be smaller than the 6,400 km^3 estimated for the Cascades. For the 1,150-km-long Alaska Peninsula arc (including continental Unimak Island but not the oceanic Aleutian Islands chain where submarine volumes are difficult to gauge), my estimates for all 55 volcanoes yield a total volume between 2,000 and 3,000 km^3 (depending on how liberally one reconstructs erosive losses). Although glacial erosion has been severe on the Alaska Peninsula (as likewise in the northern Cascades), the observation that the accountable Quaternary volcanic volume is less than half that of the Cascade arc suggests that the latter is not particularly underproductive. Likewise, volumetric comparison with the 1,400-km-long Southern Volcanic Zone (SVZ) of the Andean arc (33-46ºS) suggests that the Quaternary volcanic output of Cascadia has been at least as vigorous. My volume estimates for all 80 large volcanoes and five distributed volcanic fields (altogether representing a total of 820 SVZ vents) yield a total of ~5,300 km^3, ~83 percent of the Quaternary volume estimated for the Cascades. Owing to a latitudinal gradient in severity of glaciation (as in the Cascades), the total volume uncertainty for the SVZ is likely to be at least ±25 percent, a value thought similar to those for the Cascadian and Alaskan estimates because the same approaches to approximation and reconstruction were used for each arc (table 10). Early Quaternary volumes are likely to be underestimated, but this is true for all the arcs just mentioned as well as the Cascades.

It thus appears that the supposedly low Quaternary productivity of the Cascade arc is another myth that can now be abandoned. This longstanding misimpression about the Cascades may have been attributable to (1) overemphasis on Cascade stratocones, which are relatively few and mostly of modest volume; (2) underappreciation of the large distributed volume in the Oregon and Lassen segments; (3) failure to account for large losses to glacial erosion in the northern half of the arc; and (4) inapt comparisons with intraoceanic arcs, where submarine edifices may well be systematically larger but the extrusive/intrusive ratios much greater than for arcs on continental crust.

Table 10. Comparison of three Quaternary continental arcs.

Characteristics	Cascade arc	Alaska Peninsula	Andean SVZ[1]
Length of Quaternary chain (km)[1]	1,250	1,150	1,400
Quaternary vents identified (arc proper only)	2,339	245	820
Major evolved centers (stratocones)[2]	26	45	65
Major mafic centers[2]	9	3	15
Large centers on volcanic front	12	45	36
Range of spacings (km) of large centers[3]	2-150	4-75	5-98
Number of pairs considered	30	44	35
Mean spacing (km)	42	27	42
Standard deviation (km)	37	23	22
Three longest Gaps without vents (km)	136, 105, 74	70, 66, 60	98, 69, 65
Distributed volcanic fields[4]	29	5	5
Total area represented (km^2)	30,700	1,680	2,150
Number of vents encompassed	3,388	127	356
Area (km^2) per vent	3-40	5-20	1.5-15
Total Quaternary volume erupted (km^3 ± 25%)	6,400	2,500	5,300

[1]Southern Volcanic Zone (SVZ) of the Andes extends from Tupungato to Hudson (33˚-46˚S); alkali-basalt fields east of the arc are excluded. Continental part of Alaskan arc extends from Hayes to Westdahl-Pogromni (152˚-165˚W). Cascade arc includes Garibaldi volcanic belt and extends from Lassen to Bridge River (40˚-51˚N; table 1); rear-arc centers are excluded here.

[2]Envolved centers have erupted andesite, dacite, or rhyolite. Major mafic centers consist of basalt and basaltic andesite; for Alaska, only Shishaldin, Westdahl, and Pogromni qualify; for the SVZ, Casimiro, Planchón, Cerro San Pedro, Aguirre, Campanario, Antuco, Carrán-Los Venados, Mencheca, Antillanca, Puntiagudo, Osorno, Hornopirén, Hualaihue (Apagado), Puyuhuapi, and Cay; for Cascade arc, see tables 2, 4.

[3]For details of Cascade spacing, see table 4. For the SVZ, where the arc is commonly broad and cluttered with vents, only the along-arc spacing of 36 volcanic-front centers is given. For Alaska, in contrast, all but 3 of the major centers lie along the front; only these three, Griggs, Amak, and Pogromni, are excluded from the spacing calculations.

[4]Multivent fields of distributed vents are the norm in the Cascade arc and are subdivided as in table 1, including the rear-arc fields. The five such fields considered in Alaska are Pogromni-Westdahl, Fisher, Shishaldin, Emmons-Pavlof, and Veniaminof. Those in the SVZ are Descabezado-Calabozos, Campanario-Laguna del Maule-Ñirales, Carrán-Los Venados, Antillanca, and Puntiagudo-Cordón Cenizas. Areas cited are those defined by vent fields, not by outflow lavas or fragmental flows.

Inferences Concerning Future Eruptive Activity

If the postglacial Cascade average of one or two eruptive episodes per century (table 7) were to be maintained, what might be anticipated next?

The likely sources of future explosive episodes that could produce widespread fallout and/or valley-sweeping flow deposits include the usual suspects—Meager, Garibaldi, Glacier Peak, St. Helens, Hood, Mazama, Shasta, and Lassen, all of which had devastating eruptions in the Holocene. On the other hand, Cayley, Goat Rocks, Jefferson, Tumalo, and Cappy, all formerly capable of such eruptions, appear to have been long moribund. The three active andesitic edifices in Washington (Baker, Rainier, and Adams) are not likely to produce major explosive events, but their relief, icecaps, and masses of hydrothermally altered rock make them especially susceptible to avalanching and to flushing of radial valleys by debris flows.

Some might be tempted to regard the Mazama system as played out owing to its 7.7-ka caldera-forming eruption and its largely andesitic postcaldera aftermath, but this would be to ignore its history of dacitic and rhyodacitic episodes recurrent for more than 500 kyr. Moreover, it should be recalled that Quaternary intracaldera eruptive activity at the Rockland and Kulshan Calderas persisted for several hundred thousand postcaldera years.

At all three Quaternary calderas, the principal caldera-producing magma had evolved at least as far as rhyodacite (each >70% SiO_2). At the Pliocene Hannegan and Devils Horns Calderas, it was rhyolite, as was the 400-ka Tumalo Tuff, which may or may not have issued from a now-buried caldera source. In contrast, none of the numerous explosive eruptions of Quaternary Cascade dacite (63-68% SiO_2) produced a caldera. There may be what amounts to a batch-size control, with dacite magma batches (seldom more voluminous than a few km^3) arising from mafic-to-andesitic parents in modest or dispersed reservoirs small enough to be susceptible to mafic recharge and convective remixing. Voluminous rhyodacite magmas, on the other hand, may typically require prior accumulation of a large reservoir of mushy dacite (granodiorite) or silicic andesite (tonalite), thick enough to buffer mafic inputs and to extract voluminous interstitial melt, while shallow enough to permit caldera subsidence. Whatever the control, the compositional correlation supports the inference that persistently dacitic volcanoes (Garibaldi, Glacier Peak, St. Helens, Hood, Shasta, and the Lassen domefield) are neither likely to have large shallow integrated reservoirs nor to undergo caldera-forming eruptions. On the contrary, Meager and Newberry have released substantial batches of Holocene rhyodacite or rhyolite, none yet voluminous enough to yield a caldera but permissive of the capacity to do so in the future.

At Mount Garibaldi, the age of the Lava Peak rhyolite (table 11) is poorly known, but if the voluminous Opal Cone-Ring Creek dacite (63% SiO_2; ~10 ka) is the youngest unit there, as is generally accepted, this suggests that any rhyolitic reservoir has been superseded.

The Mount St. Helens system generated (~1.2 ka) a small batch of rhyodacite (at 70% SiO_2, as silicic as any product known ever to have erupted there), but the numerous dacites and andesites that have subsequently erupted centrally indicate that the reservoir was since purged of any such highly evolved magma. No comparably unequivocal inference can be made about the Three Sisters magmatic system, from which several small rhyolites erupted during the interval 50-30 ka and again about 2 ka. Central eruptions of mafic, andesitic, and dacitic magmas from Middle and South Sisters during the 30 to 14 ka interval (between the rhyolitic episodes) suggest that the earlier rhyolitic reservoir(s) had been purged. However, reestablishment of a rhyolitic reservoir beneath South Sister by the late Holocene and eruption of almost 1 km^3 of phenocryst-poor rhyolitic magma in two (compositionally slightly different) batches about 2.2 and 2.0 ka provide a basis for concern; although pyroclastic phases of those eruptions were not regionally catastrophic, such modest behavior need not characterize the next one.

Although seldom (if ever) caldera-forming in the Cascades (Gamma Ridge may be an exception), dacitic pyroclastic eruptions can nonetheless devastate edifice aprons and particular drainages, and major dacitic ashclouds can be a widespread environmental nuisance, a danger to aircraft, and can cause economic damage downwind. Dacitic eruptions, however, even those as voluminous as Shastina or as explosive as the Sugar Bowl (1.2 ka) and 1980 blasts from St. Helens, seldom directly threaten lives and infrastructure farther than 20 km from vent. Andesitic eruptions pose still less of a regional threat directly, because the ashfall at 10 km downwind is seldom thicker than a few centimeters and because andesitic lava flows are typically slow-moving and valley-confined. For both andesitic and dacitic eruptions, of course, the main threat away from the edifice itself is from pyroclastic flows and, more so, from debris flows that can devastate valley floors for tens of kilometers downstream. Each of the major edifices from Meager to Hood, every one of them ice-clad, is capable of generating such valley-sweeping flows. Farther south, renewed eruptions of the Lassen domefield or summit eruptions of Shasta or South Sister can also be expected to produce radial flows, principally along existing drainages. A major eruption of Mount Mazama through its Crater Lake is capable of producing a wide range of mild through catastrophic phenomena (Bacon and others, 1997).

So irregular is the pace of magmatic processes that it would be rash, presumptuous, and misleading to forecast specific eruptions. It can be said, however, that there is no basis to expect that during the next millennium Mount St. Helens would cease to be by far the most frequently active Cascade volcano, as it has been for 4,000 years. Glacier Peak appears to have been the second most significantly active Cascade center during postglacial time, its explosive episodes recurring on a millennial timescale. The rest of the Garibaldi Volcanic Belt, from Mount Baker to Bridge River, erupts very infrequently, there being only four magmatic eruptions proven for the Holocene (table 7). Adams and

Rainier have each had at least a dozen postglacial eruptive episodes, apparently clustered into a few periods separated by thousands of years; Hood, South Sister, and Mazama have had still fewer (though more silicic and more devastating) postglacially active periods, and for none of these five volcanoes does it appear that such a pulse is currently ongoing. The same can be said for Mount Shasta, where a volumetrically enormous pulse about 10 ka was followed by sporadic summit-derived Holocene effusions (of uncertain age), none of which appear to have taken place during the last two millennia. On the other hand, although there have been few postglacial eruptive events in the Lassen segment (table 7), the two postglacial episodes inside the long-lived silicic domefield did take place in the last 1,100 years.

Attention is naturally drawn to the large polygenetic volcanoes owing to their relief, recurrent activity, potentially explosive behavior, and capacity for long-runout flows, but it needs reemphasis that the Quaternary Cascade arc has 100 times more small volcanoes than big ones. Half or more of the postglacial eruptions (table 7) have been from monogenetic vents—distributed or peripheral cones, fissure-fed chains, or short-lived shields, some andesitic but most of them mafic. The 137 postglacial episodes listed in table 7 include only 8 that were rhyolitic or rhyodacitic. Dacitic events from Mount St. Helens are likely to continue dominating Cascade volcanic activity numerically for the indefinite future, though rare explosive events at Meager, Garibaldi, Glacier Peak, Hood, South Sister, Shasta, and Lassen, and modest effusions of lava (with minor local ashfall but potentially devastating debris flows) at Adams, Baker, or Rainier are not to be discounted. The most likely and exemplary Cascadian eruptive event of the next millennium, however, would be growth of a scoria cone accompanied by mafic lava flows that block a road or river and tempt tourists to get too close.

Parental Magmas

Quaternary eruptive products in the Cascades include a vast variety of chemical compositions that range widely and continuously (at any SiO_2 or MgO content) in alkalinity, Fe/Mg, LILE/HFSE, and LREE/HREE. Isotope ratios likewise range considerably, though the absence of highly evolved values is in accord with expectation for the noncratonic setting; correlation between isotopic and chemical compositions is in general remarkably poor (see the section below entitled “Cascadian Basement and Sr-isotope Overview”). In addition to diverse mantle source compositions, much of the heterogeneity evidently results from polybaric crystal-liquid fractionation, contribution of varied crustal melts, and repeated magma mixing at different depths and scales. Intensive geochemical investigations have been undertaken by several groups attempting to identify distinctive types of relatively primitive (unevolved) eruptive products that represent distinguishably different magmatic lineages potentially parental to the heterogeneous arrays erupted (Hughes and Taylor, 1986; Hughes, 1990; Bacon, 1990; Clynne, 1990a; Bullen and Clynne, 1990; Leeman and others, 1990, 2005; Baker and others, 1994; Bacon and others, 1994, 1997; Conrey and others, 1997, 2001b; Clynne and Borg, 1997; Borg and Clynne, 1998; Borg and others, 1997; 2000, 2002; Grove and others, 2002; Hart and others, 2002, 2003; Green and Sinha, 2005; Green, 2006). A summary follows here of what appear to be primitive members of the main magmatic lineages.

High-Alumina Olivine Tholeiite (HAOT)

Also called low-K olivine tholeiite (LKOT), these fluid basalts build low shields, fissure-fed spatter ramparts, and tube-fed lava fields—some of great length. Major-element compositions are comparable to MORB, although Al_2O_3 contents (17-19%) are notably higher. The low-LILE trace-element compositions are likewise comparable, over a range from NMORB to EMORB, though most HAOT have modest relative enrichments in Ba, Sr, and Pb (± Th ± Cs), suggesting a slight slab contribution, however weak or indirect. Because such minor enrichments (relative to MORB) by a nominal subduction component also typify HAOT as far inboard of the Cascade arc as Idaho (Hart and others, 1984; Hart, 1985), it has been suggested that the component may come from the lithosphere, where it might have accumulated during Mesozoic or Tertiary arc magmatism. HAOT compositions are broadly similar but by no means uniform along the Quaternary Cascades; SiO_2 contents are in the range 47 to 50 percent, K_2O contents 0.05 to 0.5 percent, and HAOT are generally richer in Ti and Fe in Washington than in California and southern Oregon. REE patterns are nearly flat (or even LREE-depleted), and the lack of HREE depletion has been widely interpreted as consistent with low-pressure final equilibration in garnet-free uppermost mantle. If the lack of garnet influence from the source residue were primary (and not established later during magma ascent through the uppermost mantle), then the onset of melting for HAOT could be inferred as shallower than ~75 km. HAOT have been shown to be very poor in H_2O (Sisson and Layne, 1993), to have formed by 6 to 10 percent partial melting of nearly dry spinel lherzolite, and to have last equilibrated with the mantle at ~1,300ºC and 11 to 15 kb, virtually at the base of the crust (Bartels and others, 1991; Baker and others, 1994; Elkins-Tanton and others, 2001). Rapid ascent from mantle depths is commonly inferred from high abundances of compatible elements and spinel inclusions in olivine that crystallized at pressures greater than 10 kb (Clynne and Borg, 1997). It has been argued that the widespread MORB-type depleted-mantle source region of HAOT at least in part involves subcontinental lithosphere that had been secularly reenriched (notably in Al and Fe) by pyroxene addition (Clynne, 1993; Clynne and Borg, 1997), rendering the HAOT source more fertile (capable of basalt melt production) than source domains for most other Cascadian mafic magmas. Because HAOT are distributed almost entirely in areas of strong to weak lithospheric extension, along the Cascade arc from California to central Washington and inboard as far east as Idaho and Nevada, a general model of dry decompression melting of mantle domains little affected by any slab-derived flux is nicely consistent with a contribution by partial remelting of fertile mantle lithosphere during tectonic unloading.

Intraplate Basalt

Sometimes also referred to as within-plate basalt (WIP) or ocean-island basalt (OIB), primitive magmas of this type are LILE-enriched (relative to MORB and HAOT) but lack the Nb-Ta deficiency globally characteristic of the subduction component. For basalts on a continent, the term OIB seems misleading, not only for its malapropos marine insularity but owing to the diverse unresolved models for actual ocean-island basalts that variously postulate sources in deep mantle plumes, in convecting upper mantle, or in resurrected domains of old subducted lithosphere. For simplicity and clarity, therefore, I prefer the plain term "intraplate basalt," recognizing that HAOT also erupts in intraplate settings as well as in the Cascade arc.

Beneath the Cascades and the adjacent extensional interior, sources of intraplate basalts are likely to lie in convecting mantle beneath the lithosphere, either as thick sheets or as discrete domains distributed within a MORB-source matrix, little affected in either case by percolation or streaming of the slab-derived flux. Some source materials may be drawn toward the arc by wedge-corner flow from mantle domains originally inboard of the arc; others may rise into the wedge through tears or around the edges of slab segments from sub-slab asthenoshere. Compared to MORB and HAOT, primitive intraplate basalts are enriched in LILE, HFSE, and REE (except HREE), but they range widely in incompatible element abundances. They include some hypersthene-normative compositions but most are nepheline-normative, the more alkalic types generally having higher Nb/Zr ratios and other such indicators of low degrees of partial melting, probably in the range 1 to 5 percent. Most intraplate basalts have in common low Sr/Ba, steep REE patterns, and modest (not high) Ba/Nb and other LILE/HFSE ratios. They are seldom as LILE-enriched and never as HFSE-depleted as the typical arc basalts marked by an ample subduction component. Intraplate basalts are dominant in the Simcoe Mountains and Bridge River-Salal Creek Volcanic Fields, common from Mount Adams across southern Washington to Portland, sparse along the Cascades of northern and central Oregon, but unknown in the Quaternary of southern Oregon and California. Although not erupted independently there, it has been proposed that they provide a contribution to high-K arc basalts in northern California (Clynne and Borg, 1997; Borg and others, 1997). The characteristic eruptive products of Cascadian intraplate basalts are scoria cones and associated lava fields of small to modest extent.

Arc Basalt

Commonly called calcalkaline basalt (CAB) or such varieties as low-K, medium-K, and high-K calkalkaline basalt, these magmas are the paradigmatic arc suite, enriched in LILE and LREE and depleted in HFSE and HREE. They form numerous shields, scoria cones, and lava fields throughout the Cascades and are the principal parent of many (not all) basaltic andesites. The wide geochemical range embraced by this class of basalts reflects the conjunction of two broad but continuous compositional spectra—degree of enrichment in slab-derived fluid contributions (the subduction component) and wide ranges of relative enrichment in mantle-derived (non-slab) incompatible-element abundances. The two spectra of enrichment are commonly linked inversely (Hickey and others, 1986; Luhr, 1992; Borg and others, 1997); that is, more intense slab flux enriches the mantle source in Cs, Rb, Ba, Sr, Pb, U, ±Th±K±LREE, and aqueous fluid, which promotes greater degrees of partial melting of the mantle-wedge peridotite, thereby lowering (by dilution) the contribution of HFSE and REE from the convecting mantle. If mantle melting is initiated deeper than ~75 km, residual garnet in the source region could also contribute to the characteristic depletion of arc basalts in HREE, Y, and Sc. Although arc basalts bearing the hallmarks of a slab contribution (Nb-Ta troughs, LILE enrichment, and steep REE patterns) are widespread throughout the Cascades, the intensity or effectiveness of the slab flux appears to diminish irregularly (relative to the wedge contribution) in at least three regions—(1) from west to east across the Lassen segment (Clynne and Borg, 1997; Borg and others, 1997); (2) from south to north along the GVB (Green and Sinha, 2005; Green, 2006); and (3) within the broad volcanic zone from Portland across southern Washington, where numerous vents for arc and intraplate (and HAOT) basalts are scattered intimately (Leeman and others, 1990; 2005).

The term "high-alumina basalt" (HAB) should be abandoned, because it has been applied to at least two fundamentally different magmatic lineages, thus confusing generations of petrologists. It was widely applied to primitive (relatively dry) MORB-like HAOT in the Cascades and later to water-rich arc basalts globally that fractionate toward low-Mg high-Al basalt and basaltic andesite owing to delayed crystallization of plagioclase.

High-Mg Basaltic Andesite

Although most basaltic andesites evolve by fractionation and assimilation from basaltic parents, a few (noncumulative) Cascadian examples appear to be primitive, having maintained high enough Mg, Cr, and Ni abundances to have been in equilibrium with a mantle peridotite residue when the melt separated. These represent an extreme type of arc magma, enriched in the slab-derived LILE, strongly depleted in wedge-derived HFSE and HREE, and particularly water-rich (Anderson, 1974; Tatsumi, 1982; Baker and others 1994; Clynne and Borg, 1997; Grove and others, 2002). Not all high-Mg basaltic andesites (and andesites) are primitive, however; careful petrographic examination has shown at least one example from the Shasta segment (Anderson, 1974) to have resulted from basalt-dacite mixing, augmented by ultramafic crystal debris (Streck and others, 2007).

Akin to Pacific arc boninites, primitive 52 to 58 percent SiO_2 magmas appear to reflect the conjunction of an intense supply of hydrous slab fluid and a notably refractory (earlier melt-depleted) mantle-wedge peridotitic source, the high fluid contribution being necessary to initiate and sustain a high degree of partial melting, yielding atypically silicic melt and a (clinopyroxene-exhausted) harzburgitic residue. Experimental investigations of such lavas from the Shasta segment (Baker and others, 1994) indeed indicate high melt fractions (20-30%) and elevated water contents in the melt (3 to 6.5 wt% just prior to eruption). The scattered Cascadian examples of high-Mg basaltic andesite are accordingly largely in the forearc (Baker and others, 1994; Borg and others, 1997; Conrey and others, 1997; Leeman and others, 2005), where a strong flux of slab-derived fluid apparently induces melting of the most refractory part of the mantle wedge. The corner flow compelled by subduction may be accompanied by progressive east-to-west depletion (by incremental melt extraction) of the wedge peridotite dragged trenchward beneath the volcanic zone, rendering forearc domains the least fertile parts of the sublithospheric convecting mantle (Clynne and Borg, 1997; Grove and others, 2002).

Shoshonitic Arc Magma

Another uncommon but distinctive type of primitive arc magma, recognized principally in southern Washington and northern Oregon, belongs to the potassic shoshonite suite, mafic members of which (49-52% SiO_2) are sometimes called “absarokites.” Primitive examples in the Cascades (Conrey and others, 1997; Leeman and others, 2005) have Mg-numbers ≥70, MgO contents of 8 to 9 percent, and Ni contents of 160 to 200 ppm, but they also have elevated K_2O (2-3%) and P_2O_5 (0.4-0.6%). More evolved shoshonitic basaltic andesites (54-59% SiO_2) have been identified in southern Oregon (Bacon, 1990; Bacon and others, 1994). All recognized examples in the Cascades are lavas and scoria cones of small volume. The rocks have extreme slab signatures with great enrichments in LILE, especially in Ba and Sr (1,000-2,300 and 1,500-3,700 ppm, respectively), along with large LILE/HFSE ratios, deep Nb-Ta troughs, and steep REE patterns with very depleted HREE. They also have $^{87}Sr/^{86}Sr$ ratios (0.7037-0.7039) among the most radiogenic in Oregon (Bacon and others, 1994; Conrey and others, 1997). The magmas are thought to be low-degree (<5 percent) partial melts of depleted-mantle peridotite that had, earlier and deeper, been infiltrated or veined by water-rich slab-derived contributions that introduced phlogopite, amphibole, and pyroxene (± apatite ± garnet) to deep parts of the wedge (Carmichael and others, 1996; Luhr, 1997; Conrey and others, 1997; Hesse and Grove, 2003). When such shoshonitic melts ultimately separate from the peridotite matrix in the shallow mantle, they retain a more robust geochemical signature of the slab contribution than do any other magmas recognized in the Cascades, even when modified and diluted by reaction and melting of their envelope during upwelling through the hotter wedge core. It remains unclear whether the Quaternary examples are products of modern subduction-zone infiltration and upwelling or of extension-induced remelting of veined lithosphere stagnant since episodes of Tertiary arc magmatism.

Rhyolite and Dacite

Some rhyolitic, rhyodacitic, and dacitic magmas may be produced by direct partial melting of crustal rocks, with or without subsequent crystal fractionation or mixing with mafic magmas that helped heat their source. In this sense, some silicic crustal melts can be at least as primitive (near-primary) as the basaltic melts that result from the conjunction of slab- and wedge-derived contributions and undergo prolonged melt-matrix reaction during many tens of kilometers of ascent. There is broad agreement that silicic crustal melts provide persistent, varied, and substantial contributions to intermediate arc magmas that range from basaltic andesite to dacite (Hildreth and Moorbath, 1988; Bullen and Clynne, 1990; Hill, 1991; Clynne, 1993; Smith and Leeman, 1987, 1993; Green, 1994b; Borg and Clynne, 1997; Conrey, Hooper, and others, 2001), but the petrogenetic challenge has always been to identify silicic eruptive products that approach near-primary crustal melts and to infer their source materials.

For the rhyolites at Three Sisters, Tumalo, and Broken Top, Hill (1991) showed geochemically that none could have evolved by crystal fractionation from the broadly contemporaneous dacitic or rhyodacitic magmas. He inferred that the Three Sisters rhyolites resulted from 20 to 30 percent dehydration melting of basaltic amphibolite and the Broken Top-Tumalo (slightly more sodic) rhyolites from 30 to 50 percent melting of Cascadian tonalite. Both rhyolitic suites have $^{87}Sr/^{86}Sr$ in the range 0.7036 to 0.7037, favoring sources in Cenozoic Cascadian arc crust. Because both suites also have flat and relatively undepleted HREE patterns, residual garnet appears to be excluded, suggesting (Hill, 1991) that melt extraction took place in the middle crust rather than in the deepest arc crust, there as thick as 45 km. Conrey, Hooper, and others (2001) agreed that the fairly uniform suite of amphibole-bearing rhyodacites ($^{87}Sr/^{86}Sr$ ~0.7032-0.7034) around Mount Jefferson could not have descended from any of the mafic or intermediate magmas erupted nearby, concluding instead that they were partial melts of mid-crustal basaltic amphibolite at 850 to 900°C. At Mount St. Helens, the varied dacites that have dominated its explosive eruptive history (mostly 62-66% SiO_2; $^{87}Sr/^{86}Sr$ ~0.7035-0.7039) were shown by Smith and Leeman (1987) to have HFSE and REE contents similar to or lower than those of associated basalts and andesites, precluding a fractionation relationship. They inferred that there the primary crustal melt is dacitic, arising from partial melting of MORB-like amphibolite fluxed by LILE-bearing slab fluids, leaving residual amphibole, and providing the parent magma for rhyodacites by crystal fractionation and for St. Helens andesites by mixing with mafic magmas (Smith and Leeman, 1993). Indeed, partial melting experiments (Sisson and others, 2005) have verified that voluminous arc-type dacite, rhyodacite, and rhyolite melts can be generated from moderately hydrous medium-to-high-K basaltic compositions at 825 to 925°C and 7 kb (mid-crustal pressures), the melts becoming increasingly rhyolitic at higher oxygen fugacity or lower melt fraction.

Haystack, a phenocryst-poor dacite dome (64% SiO_2) at the northwest toe of Mount Shasta, is unusual in having most of the compositional characteristics of "adakite." These include high Sr (1,450 ppm), high Sr/Y (76), low K_2O/Na_2O (0.2), and remarkably unevolved isotopic ratios—$^{87}Sr/^{86}Sr$ = 0.7029 and εNd = +7.4. This small dacite batch may have been a relatively simple partial melt of low-K MORB-like oceanic crust in the accretionary terranes beneath the Shasta segment.

In modeling geochemical evolution of the diverse regional suite of arc basalts and andesites in the Lassen segment, Clynne (1993) found that the crustal contributions are rhyolitic, added as melts (not bulk assimilants), and derived from young arc crust, not principally from the pre-Cenozoic basement. For the long-lived Lassen volcanic center (LVC), Bullen and Clynne (1990) concluded that geochemical trends of several successive suites each resulted from mixing between well-homogenized silicic melts and heterogeneous mafic magmas. They showed that the most silicic LVC products have Pb-Sr-Nd isotopic compositions within the ranges defined by the mafic magmas of both the LVC and regional suites, leading them to infer partial melting of young mafic lower crust and extraction of some batches of silicic melt cleanly enough to avoid mixing with contemporaneous mafic batches. Borg and Clynne (1998) expanded the investigation to rhyolitic and rhyodacitic products scattered all across the Lassen segment, concluding much the same about young mafic deep-crustal sources—apparently free of residual garnet here (on the basis of REE patterns) where the crust is as thin as 38 km. For generating the observed spectrum of silicic magmas (65-75% SiO_2), they inferred a range of partial melting conditions for deep-crustal basaltic amphibolite intruded by basaltic magmas of varied water content. Hotter drier melting exhausts residual amphibole, yielding pyroxene rhyodacites, whereas wetter melting at ≤900°C yields hb±bi±opx rhyolites marked by a MREE deficiency characteristic of residual amphibole. Very few silicic eruptive units were identified that show evidence (such as elevated Pb and O isotope ratios or steep REE patterns) for partial melting of upper-crustal granitoids, though modest contributions of such melts can be expected wherever mafic magmas are stored or transported shallowly (for example, Grove and others, 1988; Baker and others, 1991; Green, 1994b).

Sr-Rich Andesite

Another kind of intracrustal melt was advocated by Conrey, Hooper, and others (2001) to be near-primary, as its derivation has likewise proved impossible to model geochemically by crystal fractionation (or AFC) of any mafic Cascadian magma recognized. This Sr-rich andesite (58-62% SiO_2, 800-1200 ppm Sr) has high Sr/Y and low HREE, Y, Ba/La, and $^{87}Sr/^{86}Sr$ (0.7028-0.7031). It too may arise by partial melting of mafic lower crust but under drier, hotter (~1,050°C), deeper conditions, leaving a garnet-bearing residue (Conrey, Hooper, and others, 2001). They further proposed that the MORB-like deep-crustal source domains may have underplated the arc crust during a pulse of HAOT magmatism that accompanied Pliocene extension of the High Cascades Graben (Smith and others, 1987; Conrey and others, 1997). Such rocks are scattered in the Mount Jefferson area (Conrey, Hooper, and others, 2001) and may also occur sparsely at Diamond Peak, near Mount Mazama, and in the Shasta and Lassen segments; the magma type is also thought to contribute as a mixing member to some basaltic andesites and to be related to coexisting high-Sr dacites. The thermal and material behavior of the deep crust in response to intrusion of basaltic magmas, under conditions leading to generation of rhyodacitic vis-à-vis andesitic partial melts, has been explored by Dufek and Bergantz (2005).

Inferences About Mantle Magmatism

Wherever a primitive mantle-derived magma erupts with little crustal contamination, it can be inferred that no intracrustal magma reservoir was present to impede its ascent. Because primitive basalts produce scoria cones, small shields, and discrete lava fields but virtually never erupt centrally at stratovolcanoes (or domefields), it is also presumptive that the latter sorts of systems do overlie crustal columns and reservoirs that intercept and process the mantle input.

The intimate spatial scale of vent locations for arc, intraplate, and shoshonitic basalts, HAOT, and primitive basaltic andesites—all recurrently within 5 km of each other and often very close to andesite-dacite stratocones as well—supports additional inferences about deep magmatism. The lithosphere is more widely a pincushion than a sponge. Some mantle magma batches that rise from independent source columns may, of course, merge, blend, stall, and fractionate, intensively so beneath stratovolcanoes, but many others penetrate the lithosphere independently without mutual interference. Arc magmas are often defined tectonically as evolving "above subducting lithosphere," but in the Cascades (and elsewhere) they are closely accompanied by neighboring batches of HAOT and intraplate basalts that lack a geochemical subduction signature. It has sometimes been asserted that there is"no depleted mantle beneath continental arcs" (for example, Pearce and Peate, 1995, p. 274), but the widespread MORB-like HAOT in the Cascades demonstrates the opposite. There is still no consensus, however, on the nature and distribution of the primary source regions for the HAOT and intraplate basalts, which are little affected by ascent of the slab-derived subduction component. Distributed domains (plums) within a depleted mantle-wedge matrix, layers of unfluxed convecting mantle drawn into the wedge-corner flow, deep mantle upwellings from beneath or inboard of a steep or segmented slab, and even the shallow mantle lithosphere have all been advocated as sources. Whatever the actual configuration, the following seem likely: (1) the slab-derived contribution does not permeate the entire wedge; (2) primary mantle source domains for the disparate primitive magmas, if distributed laterally, are separated by no more than a few kilometers; and (3) if sources are distributed vertically, some of the magma batches that each kind of source produces are able to pass upward through mantle domains of contrasting kind without loss of identity. It seems clear that the Cascade arc lacks a well-marked curtain of slab-fluid release governed by any major pressure-dependent downdip phase change, because (1) there is no abrupt, continuous, and voluminous volcanic front, (2) globally defined arc-type basalts are scattered across arc segments as wide as 50 to 100 km, and (3) intraplate basalts and HAOT are likewise scattered from the rear-arc to the western (trenchward) edge of the Quaternary volcanic belt.

Volcanic fields dominated by monogenetic cones and small shields are sometimes attributed to decompression melting of ascending mantle diapirs that result in clustered ascent of many small magma batches. In the Cascades, much of the arc might be considered a field of such monogenetic vents, studded locally by a handful of large long-lived evolved centers. In any case, the belt of 2,000 lesser Cascade vents is generally continuous and elongate along the arc, as are many local vent concentrations and vent alignments within it, so the principal structural influence would appear to be along-arc lithospheric extensional tectonics rather than a belt of discretely focussed, intrinsically buoyant, mantle upwellings.

Production of fundamentally contrasting types of basalt that erupt close together in space and time, whether as distributed vent fields or as arrays surrounding big andesite-dacite foci like Adams, Mazama, and Shasta, is difficult to attribute to large coherent diapiric upwellings, the more so owing to a lack of concentrically zonal compositional arrangements. Such diversity suggests, instead, coexistence of large- and small-degree melts from different depths with varied source materials and ascent paths, independently penetrating the arc crust in hundreds of small batches. The diversity of basalts reaching the surface also provides strong evidence against the existence of any regionally continuous intracrustal melt zone, an idea once boosted for the extensional parts of the Cascades on the basis of high and relatively uniform heat flow (see fig. 10 of Blackwell and others, 1990).

Intracrustal Evolution of Arc Magmas

The mantle proposes; the crust disposes. Much (not all) of the variation among intermediate arc magmas arises within the crust, which frames a unique path for every batch, interposes traps for transient storage at many depths, contributes partial melts of its varied lithologies, and modulates the ascent of basalt and its derivatives. Basaltic magma impinges widely on the base of the Cascadian arc crust, but there are countless penetration pathways for some of its descendants to reach the surface. Fundamentally different basaltic parents can produce suites that converge intracrustally by mixing, partial remelting, and assimilation of common wallrocks, while identical basalts might produce divergent suites by polybaric fractionation and assimilation of contrasting wallrocks. There is perpetual tension between attenuation of heterogeneities (homogenization) by diffusion, convection, confluence of melts extracted from heterogeneous source domains, and blending of independent magmas in crustal reservoirs *vis-à-vis* diversification (differentiation) by injection of new basalt batches, crystal-melt fractionation, interactions with the heterogeneous crustal envelope, and upward escape of melt batches extracted from mush at successive transient magma traps. The simple proposition that most intermediate arc magmas are produced by varied combinations of crustal assimilation and fractional crystallization of a range of primitive basalts has outlived a number of alternative passing fancies: (1) that andesites are primary hydrous melts of mantle peridotite; (2) that arc magmas are slab melts; (3) that low-Mg high-Al basalts are a principal primary arc magma; and (4) that MORB-like HAOT is a universal arc parent.

MASH Model

A chemical and isotopic study of the 15 northernmost stratovolcanoes along the volcanic front of the Andean Southern Volcanic Zone (SVZ) revealed large crustal contributions for all volcanoes along the transect. There was shown to be a strong northward along-arc trend toward greater, deeper, and older crustal contributions, consistent with the regional gradients in upper-plate geology and a doubling of crustal thickness. The data led to formulation of the melting-assimilation-storage-homogenization (MASH) model of Hildreth and Moorbath (1988, 1991), wherein the baseline geochemical signature of each large arc volcano is set during protracted entrapment, storage, and reprocessing of mantle-derived magma within a focussed domain of remelting and hybridism in the deep crust. Cursory reading has led some to reduce the model to little more than lower-crustal assimilation, but the discussion (Hildreth and Moorbath, 1988, p. 480-485) is far more specific. Salient points include the following. (1) In addition to partial melting of older crustal protoliths, the MASH process entails extensive partial remelting of deep-crustal mafic intrusions and their differentiates, thermally induced by renewed pulses of basaltic intrusion and crystallization. (2) A MASH zone is not a magma chamber but, rather, a plexus of tabular and mushy differentiated intrusions, where ductile deformation promotes extraction, aggregation, and blending of melts. (3) MASH zones wax and wane in response to basaltic influx and to ascent of aggregated hybrids. (4) Each major center has its own focal MASH zone, usually impenetrable by primitive basalts, whereas, peripheral to such foci, more primitive batches (not intercepted and hybridized) can ascend to produce monogenetic volcanoes. (5) Crustal thickness can be important by imparting to magmas the geochemical signature of residual garnet or amphibole and by increasing intracrustal path length, but age and composition of heterogeneous crustal lithologies are of comparable importance. (6) MASH zones intermittently feed hybrid melt to upper-crustal reservoirs, and some mobilize diapirically and segregate mush and melt to produce differentiated mid-crustal plutons. Assimilation in dikes or in subsequent mid-to upper-crustal reservoirs enriches magmas above MASH baseline ranges, enhancing diversity. Hildreth and Moorbath (1988; their fig. 6) dealt specifically with instances of important additional crustal contributions to ascending magmas, subsequent to the deep-crustal MASH process. And (7) in mature arcs, much of the arc-geochemical signature is acquired not only from proximate slab contributions but by repeated assimilative withdrawals from the secularly accumulated, deep-crustal, "arc-intrusive repository" (which is of far greater mass than the magmatic throughput).

Persistent focussing at each MASH domain promotes thermal and mechanical feedback between entrapment of basalt, enhancement of lower-crustal ductility and melting, and maintenance of a buoyancy barrier. Such long-lived focussing is especially intense beneath large arc volcanoes but likewise beneath large intracontinental centers and at the deep-crustal staging reservoirs for flood basalts (many of which evolve in expanding well-mixed reservoirs to compositions well beyond the normal basaltic range). Crustal contributions to arc magmas are hard to quantify, owing in part to wide ranges in the proportions of slab and mantle contributions and in part to poor isotopic and chemical leverage provided by the young mafic lower crust progressively accreting. Nd-Sr-Pb-O isotopic contrast between mantle-derived magma and deep arc crust can actually decrease with time, as the average age of the lower crust becomes progressively younger, diluted by intrusive underplating by the arc basalt itself. A big change along an arc in mean age or composition of its basement is thus required to yield unambiguous evidence for large contributions from reprocessed lower crust, and such a change along the Chilean volcanic front was the basis of the transect experiment that led to the MASH model. Os-isotope data later sustained application of the MASH model to volcanic centers on thinner and younger mafic crust (in both Chile and the Cascades), permitting inference of a range of deep-crustal contributions that provided radiogenic $^{187}Os/^{188}Os$ ratios as much as five times greater than mantle values (Ruiz and others, 2000; Hart and others, 2003).

The apparent paradox that basalts are uncommon at the large Cascade stratovolcanoes but abundant and widely dispersed around and between them is readily understood if MASH zones are discrete domains, not a continuous deep-crustal underplate. Because small and diverse mafic volcanoes are so densely distributed throughout much of the Cascade arc, however, the process that really needs clarification is the focusing mechanism for MASH zones beneath the major centers. The 2,000-odd mafic volcanoes show that basalt impinges on the base of the crust almost everywhere beneath the Cascade arc but with intensity sufficient to promote large-scale partial melting of crustal rocks at only a few dozen scattered loci. The contrasting heat and mass balance demands of the adjoining, contemporaneous, and areally comparable Lassen and Caribou loci (fig. 21) were modeled by Guffanti and others (1996). They calculated that the flux of primitive basalt injecting and fractionally crystallizing in the lower crust was at least five times greater beneath the Lassen volcanic center (where extensive crustal melting contributes heavily to silicic and hybrid magmatism) than beneath the persistently mafic Caribou field (where more limited crustal melting is sufficient only to raise the average volcanic output into the compositional range of basaltic andesite).

As a first-order question, then, does such locally intense focusing ultimately reflect lower-plate processes, patterns of convection and magma aggregation in the mantle wedge, or the topology of magma entrapment in the lower crust? Arc-magma dynamics probably involves a series of batch processes. Although slab subduction and wedge corner convection may be virtually continuous, fluid or melt is likely to ascend batchwise from the interfacial region into the hot core of the wedge. Even if porous magma percolation is widespread in partially molten columns within the wedge, the aggregation, ascent, and arrival of large volumes of melt at the base of the crust is probably likewise ultimately a batch process, whether partly diapiric or by channelized flow. Crustal magma transport is even more certainly a batch process, too, as indicated by the sporadic nature of eruptive phenomena and the irregular compositional fluctuations at long-lived arc volcanoes. In fact, the mismatch between typical timescales of eruptive recurrence (10^2 to 10^4 years) at stratovolcanoes and the documented longevities (10^5 to 10^6 years) for such major fixed centers weighs against the likelihood of MASH-domain focusing being fundamentally controlled by the properties or behavior of the crust, which appears to process magma throughput much more rapidly than the lifetime of the system. Such longevities are likewise difficult to reconcile with batch release of material from the subduction interface, which should be far more frequent as well as spatially more widespread than the sparsely distributed arc stratovolcanoes. It thus seems most plausible that MASH zones are fundamentally focussed by excess melt production in particular domains of the mantle wedge, speculatively where permeability and melt aggregation are enhanced by mantle upwelling or other forms of convective strain.

After an exceptional mass of basaltic melt has locally intruded the base of the crust, the modified topology of the interface may itself induce changes in the buoyancy, strain field, and permeability of the system, promoting positive feedback that stabilizes the anomaly and promotes its growth. The great volumes of basalt erupted at a few of the largest arc volcanoes (such as Fuji and Klyuchevskoi) apparently represent extreme cases where throughput is rapid and MASH-zone processing only modest; such examples provide further evidence that localized concentration of mantle-derived melt is the key process in focusing large arc systems. From the distribution patterns of surface volcanism, it can be inferred that, in plan view, the intensely injected loci that develop MASH zones are typically 10 to 30 km across. That the major volcanic centers they feed are irregularly separated by 5 to 150 km (table 4) probably mirrors spacing of the MASH domains themselves, which in turn is likely to reflect the convective upwelling structure of the mantle wedge.

Shifts of Focus

Numerous arc stratovolcanoes have died out, only to be promptly succeeded by an active neighbor, overlapping or nearby. Well-known pairs include Ixtaccihuatl/Popocatépetl and Nevado de Colima/Volcán de Colima in Mexico, and in the Andes, Sierra Velluda/Antuco, La Picada/Osorno, Pomerape/Parinacota, and San Pablo/San Pedro. Figure 26 illustrates some examples in the Cascades, several of which involve silicic domefields or calderas as well as stratocones. Seldom are such shifts of focus plausibly related to plate motions, either in terms of azimuth or timescale and distance of the jump, as seems clear for the inconsistent vectors of figure 26. The shifts are typically 5 to 20 km with no systematic directionality and, in most instances, they took place on timescales commensurate with normal longevities of the component volcanoes (fig. 27). I thus infer that some change or instability in mantle or crustal elements of the magma system itself caused it not to die out but to relocate.

The shifts of individual volcanic foci illustrated in figure 26 appear to have little or nothing to do with the migration of whole segments of the arc on longer timescales. For example, the westward jump from the Oligocene-Miocene Pemberton-Chilliwack arc to the Quaternary Garibaldi Volcanic Belt (fig. 3) and, since the late Miocene, the eastward drift of the Oregon segment and the westward drift of the Lassen segment, are all likely to reflect regional-scale plate interactions, subduction geometry, and upper-plate internal microplate motions.

If the large, long-lived, evolved systems are individually rooted in deep-crustal MASH domains, the question of what allows some of them to jump is closely linked to the question of what pins most of them at fixed locations for million-year lifetimes. On the one hand, some lateral shifts of focus might simply represent relocation of a shallow crustal reservoir owing to magmatic exploitation of an intracrustal structural discontinuity. At the other extreme, a volcanic shift might mirror a modest lateral shift in the locus of mantle upwelling and thus in the site of intensified basaltic injection of the lower crust. A third possibility is successive buoyant protrusions from different parts of a common, thermally fluctuating, MASH zone.

If a MASH domain deep beneath a major volcanic center is a mushy to ductile, polyintrusive plexus of amphibolite, gabbro, diorite, tonalite, and protolith restites, all laced with leucosomes, cumulates, ephemeral magma pods, and mafic and felsic dikes, and if some such domains attain lateral diameters of 10 to 30 km, then, during thermally prograde intervals, discrete parts might blossom as buoyant domical protrusions (protodiapirs of Hopson and Mattinson, 1994). Locally intensified pulses of basaltic injection or pulses of ductile deformation might help destabilize particular regions within the broader mushy plexus, and secular melt depletion in long-active parts of the MASH domain might eventually favor shifting the buoyancy to adjacent regions. Successive mobilizations of different parts of the deep-crustal plexus would offset the staging area for the dikes that ascend to feed upper-crustal reservoirs, perhaps by the 5 to 20 km typical of the jumps in eruptive focus shown in figure 26. There is no conceptual conflict between buoyant ductile doming of a deep-crustal migmatized MASH zone and separation from it of a vanguard of dikes of hybrid magma that helps lower the viscosity of the deep crust directly above it while ultimately supplying and expanding the upper-crustal magma reservoir that feeds a volcano.

If major evolved volcanic centers can shift positions, or wholly new centers can arise, on timescales of 10^5-10^6 years, then it might be asked how long it takes for *all reaches* along an arc to have been occupied by such edifices (and the shallow plutonic reservoirs supporting them). As suggested by the continuous composite batholiths exposed in Mesozoic arcs and by the 50-to-100-km-long plutonic reaches of Tertiary arcs exposed in the Washington Cascades (Chilliwack batholith and Snoqualmie-Index-Squire Creek batholiths), some magmatic arc chains do completely “fill in,” at least on 10 to 30 Myr timescales. The tentative answer from the volcanic Cascades appears to be more than 5 Myr, which is long enough to introduce the complication of lateral drift of whole arc segments. The axial portion of the Lassen segment could be said to have filled in between the Yana and Snow Mountain volcanic centers (fig. 21) over an interval of about 4 Myr, but no remnants of andesitic (or more silicic) centers younger than Miocene are recognized between the Lassen and Shasta segments, nor between Goosenest and the Mountain Lakes cluster, nor between Hood and Adams, nor between Rainier and Glacier Peak, nor between any of the five GVB loci. On the other hand, closely spaced *mafic* volcanoes have built a continuous strip more than 500 km long from southern Oregon to east of Mount Rainier on a timescale shorter than 1 Myr (figs. 8, 14, 15).

Basaltic Andesite

Several compositional varieties of basaltic andesite have been distinguished in the Cascades, as discussed by Hughes and Taylor (1986), Hughes (1990), Clynne (1990a), Bullen and Clynne (1990), Bacon (1990), Gardner (1994), and Conrey (1998). Although a few dozen of the thousand-odd basaltic andesite (52-57% SiO_2) cones and shields in the Cascades may represent fairly primitive descendants of primary melts of the mantle or the crust, the great majority are thought to evolve intracrustally from basaltic parents by varied combinations of crystal fractionation, remobilization of cumulates, deep-to-

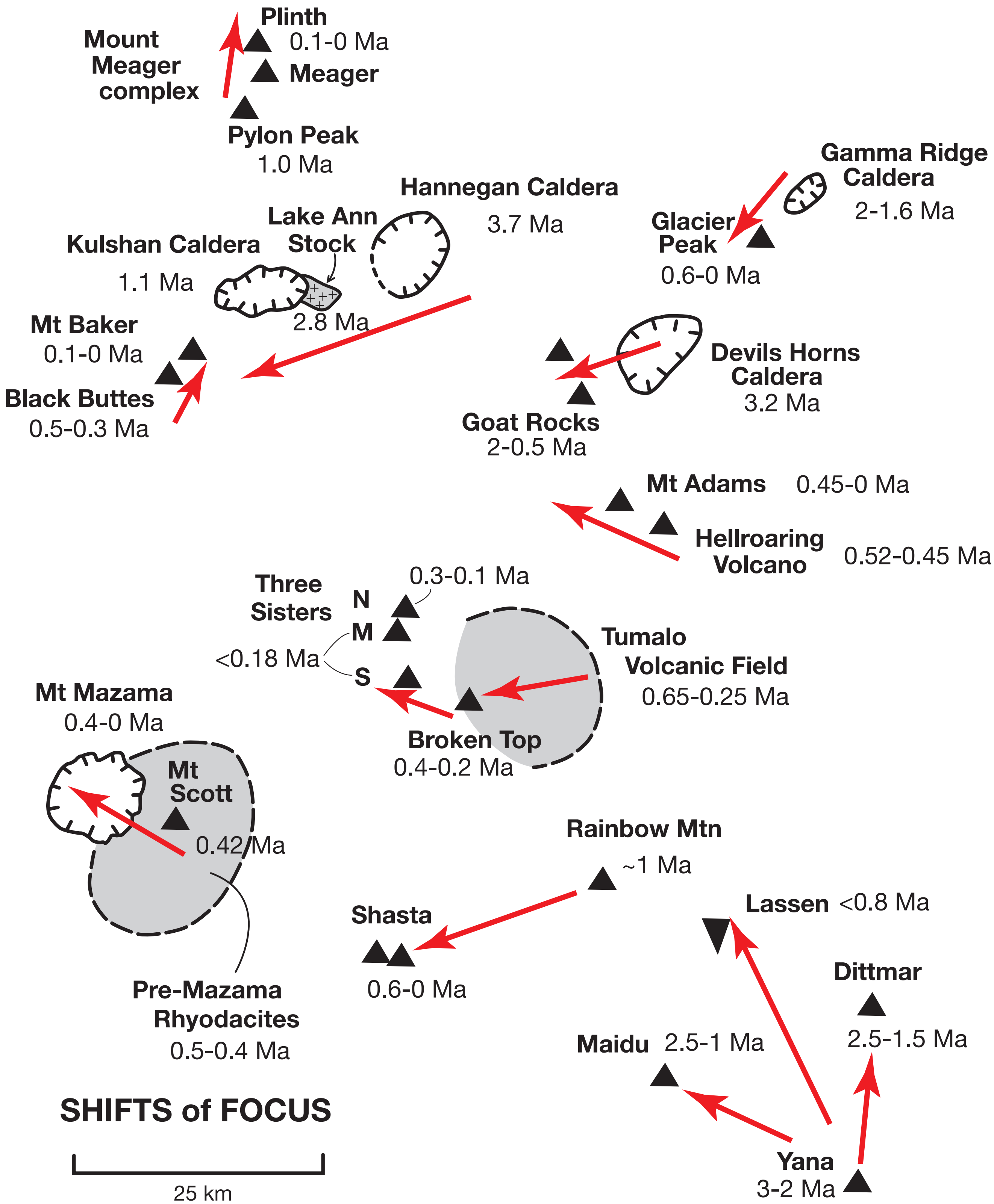

Figure 26. Shifts of eruptive focus. Examples from nine areas in the Cascade arc where the principal site of eruption of evolved (andesite to rhyolite) magma migrated substantially during the Quaternary. All sketch maps at same scale. Red arrows generalize azimuths and distances of shifts. References are cited in text discussions of each center.

shallow crustal assimilation, backmixing of related batches of evolving magma, and cross-mixing of unrelated batches. (On the scale of an eruptive batch, there is no such thing as a "pure magma" as even most HAOT or rhyolitic magmas blend parental contributions and subsequently ingest distinguishable contaminants). Much of the variability among the mafic andesites is likely to reflect batch size, thermal budget, water content, and depths of transient storage, as well as compositions of primitive magmas and compositions of wall rocks partially assimilated. Critical influences during storage and ascent, sometimes compositionally detectable in the eruptive products, include the stability of garnet, plagioclase, and amphibole (each sensitive to pressure and water content of a magma reservoir) and the wallrock envelope, which might change during ascent successively from dry mafic granulite to amphibolite to tonalite-granodiorite. Great thicknesses of arc basalt and HAOT underplated during the Tertiary as gabbro and its differentiates, and their dehydrated or hydrated metamorphosed successors, may provide major Quaternary assimilants in the deep Cascade crust.

The mechanisms of crustal assimilation by mafic magmas are no doubt varied and probably include all of the following: (1) Ductile kneading of partial melts from polylithologic deep-crustal wall rocks; (2) filter-pressing of interstitial melts by volume expansion during partial melting of (water-undersaturated) wall rocks at any depth; (3) melting and disaggregation of fragments stoped from the roofs of reservoirs or torn from the walls of dikes, thereby contributing both melts and xenocrysts; (4) fractional assimilation of melts and antecrysts from mushy mafic plutonic forerunners in the deep crust; (5) fractional assimilation of melts and antecrysts from felsic plutonic forerunners in the mid and shallow crust; and (6) reentrainment of cumulate crystals and associated melts at any depth during multibatch magma passage through long-lived mushy ascent columns (Philpotts and Asher, 1993; Green, 1994b, Nakada and others, 1994; Dungan and Davidson, 2004;

Figure 27. Example of a late Pleistocene shift of eruptive focus: Black Buttes stratovolcano (500-290 ka) adjacent to southwest side of ice-clad Mount Baker (40-12 ka), viewed northeastward from the air. For Black Buttes, andesitic lavas and breccias of the two high crags, Lincoln Peak (left, 2,770 m) and Colfax Peak (right; 2,850 m) display opposing 30° dips that frame the gutted edifice. Extending below Lincoln Peak, an arcuate rugged ridge of outward-dipping flow-breccia sheets wraps the glacier-filled bowl where erosion has removed the hydrothermally altered fragmental core of the volcano. Shift of the central vent 3 km northeastward to the site of Mount Baker may have taken place by 100 ka, but the young cone (3,286 m) has grown largely since about 40 ka. Construction was complete by about 12 ka, and the only Holocene eruption of the cone was an andesitic ashfall about 6.5 ka. Summit crater is ice-filled; right shoulder below summit is rim of Sherman Crater, a lateral hydrothermal vent still fumarolically active. For details, see Hildreth and others (2003). Black Buttes edifice had twice or more the eruptive volume of Mount Baker. Relief visible in image is about 2,000 m. (USGS photograph by Austin Post, 1999.)

Bacon and Lowenstern, 2005). Magma ascent through the 40-km-thick Cascade crust almost inevitably incurs such interactions. Because of preferential incorporation of incompatible elements during multistage assimilation, it would be rare for an erupting mafic magma to retain the trace-element ratios or concentrations of its mantle-derived parent.

Because most arc basalts and basaltic andesites have only 4 to 7 percent MgO, it is commonly unclear what their primitive mantle-derived parents had been. Zoned mafic eruptions occasionally provide a clearer view; for example, the arc eruptions of Tolbachik 1975-76 in Kamchatka (10.5 to 4% MgO), Jorullo 1759-74 in Mexico (9.3 to 4.3% MgO), and Galunggung 1982-83 in Java (11.5 to 3.2% MgO) were all zoned to low-Al high-Mg arc basalt as their most primitive product (Fedotov and Markhinin, 1983; Luhr and Carmichael, 1985; Gerbe and others, 1992). In the Cascades, however, zoned basaltic-andesite eruptive units have been shown to grade down to *either* arc basalt or HAOT. Examples of the former include the Callahan flow at Medicine Lake, parts of the Bachelor chain, and the Sulphur Creek flow near Mount Baker (Kinzler and others, 2000; Gardner, 1994; Green, 1988; Hildreth and others, 2003). The best documented example of zonation involving a HAOT end member is the Giant Crater lava field (6.6 to 10.5% MgO; 53.4 to 47.7% SiO_2; 1.1 to 0.06% K_2O), also at Medicine Lake (Donnelly-Nolan and others, 1991; Baker and others, 1991).

Investigations of mafic lavas in the Cascades additionally support the following inferences. (1) Virtual absence of mantle xenoliths in the arc basalts and basaltic andesites (and HAOT) suggests magma collection, transient storage, and settling out of the crystal cargo in crustal reservoirs. In contrast, many rear-arc alkalic basalts of the Simcoe Mountains Volcanic Field (some with as little as 6 percent MgO) carry abundant mantle xenocrysts and nodules of lherzolite, harzburgite, and dunite, from which more continuous passage through the crust can be inferred. (2) Mafic shields in the Cascades probably remain active for something between 10 and 10^4 years, and most have volumes of 1 to 5 km^3 (rarely to 15 km^3 or more). Such longevities and volumes may suggest characteristic limits on the sizes of batches departing the mantle and fractionally crystallizing within the crust. (3) Most shields are constructed of mafic andesite and nonprimitive basalt, and although their lavas are seldom strictly homogeneous, they usually (not always) lack evidence for an upper-crustal contribution, leading to the inference that their proximate reservoirs typically lie in deep mafic crust. Clear exceptions marked by granitoid assimilants are well documented among the mafic products in the rear-arc Medicine Lake Volcanic Field (Grove and others, 1988; Donnelly-Nolan and others, 1991; Baker and others, 1991; Kinzler and others, 2000). And (4) although there are some fairly homogeneous mafic shields where one might infer rapid tapping of a single reservoir, there may in general be too much conceptual emphasis on “chambers” for holding mafic magmas in the crust. Widespread evidence for heterogeneity and mixing suggests that the crustal columns supplying mafic shields on millennial timescales may often consist of swarms of dikes (with a high combined surface area exposed to wall-rock assimilation), as well as numerous transient magma pods that experience quasi-independent fractionation/assimilation histories. The basalts and basaltic andesites of the Bachelor chain, where Gardner (1994) distinguished ten different chemical groups (49 to 57% SiO_2, 8 to 3% MgO, 170 to 20 ppm Ni; 0.5 to 1.25% K_2O), erupted from vents along or adjacent to the same alignment within an episode only a few thousand years long, providing a well-documented illustration of the effects of such plumbing complexity.

Andesite and Dacite

Many silicic andesites (57-63% SiO_2) evolved by rapid crystallization differentiation when their mafic parents reached water saturation in the upper crust, but most apparently also reflect continuation of hybridizing processes, having still more complicated downstream mixing histories. For every intermediate eruptive unit, basic questions concern the depths and wall-rock lithologies of preeruptive storage in single or successive intracrustal reservoirs, the mechanisms by which crustal contributions are added, and the extent to which the crystal cargo of numerous successive batches are mixed, partially resorbed, or re-entrained. One should beware the shoehorn of “end-member” oversimplification, because identifying coherent AFC trends (which may be occasionally feasible for a compact upper-crustal chamber with one dominant wall rock) is unrealistic for an intermediate magma batch traversing a 40-km column of varied crustal lithologies, distributed pods of cumulates, and mushy differentiates of forerunning batches.

Tonalitic-to-dioritic plutons are the leftovers of andesitic magma bodies and demonstrate the reality of intermediate magma storage in the mid-to-upper crust. Granodiorite plutons likewise are evidence for shallow storage of dacitic magma. Because such granitoids usually lose interstitial silicic melt (to dikes, leucogranitoid bodies, and eruptions) during mushy stages of advancing crystallization, they end up somewhat less silicic than their former integrated bulk compositions. The relatively uncommon batches of crystal-poor silicic andesite sometimes erupted are likely to have been extracts of melt from comparably mushy bodies of crystallizing mafic magma.

Although intermediate plutons can grow large by incremental aggregation of numerous batches of water-rich andesitic magma (which crystallize extensively when water-saturating in the upper crust), the dike or lens of eruptible magma at any stage is likely always to be small relative to the accreting mush body. Andesitic eruptive units are typically modest in volume, crystal-rich, and carry several generations of antecrysts and phenocrysts. That so many of them also carry chilled enclaves of more mafic magma suggests that their preeruptive holding cells within the larger crystallizing reservoir (pluton) had been fairly small when invaded by the enclave-generating batch, thus permitting convective dispersal of the disaggregated blobs throughout the cell and eruptive response to the invasion on a timescale faster than settling of the blobs. Because rhyolites and rhyodacites typically carry few such enclaves (or lack them entirely), the preeruptive melt-rich lenses from which they erupt are likely to be well buffered by thicker mush reservoirs that protect them from such invasion. The equivalent storage cells (layers, lenses) from which dacite magma batches erupt would, following this logic, have crystallizing envelopes with a wider range of buffering capacity, since dacite lavas range from enclave-rich (as at Lassen) to aphyric and enclave-free (as at Adams). Great eruptions of flood rhyolite and flood basalt are widely documented, so the lack of flood andesites is yet another indication of the intimate nature of andesitic hybridism in complexly intricate plumbing systems.

If andesites were generally straightforward fractionation daughters of mafic magmas, it would seem a striking anomaly that so few of the numerous mafic shields in the Cascades grade into andesite. The few known to do so are Mount Defiance, Diamond Peak, Mount Bailey, Devils Peak, and Prospect Peak. At least 90 percent of the Quaternary andesite in the Cascades was erupted from 22 major evolved centers (Meager, Cayley, Garibaldi Lake, Garibaldi, Baker, Glacier Peak, Rainier, Goat Rocks, Adams, St. Helens, Hood, Jefferson, Middle Sister, South Sister, Broken Top, Cappy, Mazama, Rainbow, Shasta, Maidu, Dittmar, and Lassen). The remaining 10 percent resides in nine substantial shields (Jennies Butte in Washington; Badger Butte, Timber Crater, Pelican Butte, and Brown Mountain in Oregon; Goosenest, West Prospect Peak, Badger Mountain, and Table Mountain in California) and in about 75 minor off-edifice units that include small shields, domes, cones, chains of cones, lava fields, and isolated flows. The 75 minor units of silicic andesite (57-63% SiO_2) include eight north of Goat Rocks, five in southern Washington, 15 scattered from Frog Lakes Buttes to the area around Summit Butte, five near Santiam and McKenzie Passes, six near Wickiup Reservoir, six south of Mazama, four in the Mountain Lakes cluster, six near Whaleback and Garner Mountain, and as many as 30 in the Lassen segment. It may be worth stressing the point again that in this reputedly "andesitic arc," fewer than 10 percent of the 2,000-odd Cascade vents have erupted andesite. That most of the andesite is concentrated at only 22 loci is taken to indicate that deep-crustal MASH processes are focussed in discrete domains.

Many ordinary Cascade dacites are simply andesites further evolved, whereas the somewhat less common class of phenocryst-poor dacites is likely to have been interstitial melt that escaped from mafic-to-andesitic crystal mush. On the other hand, some crystal-rich dacites are mixtures of rhyodacite with various mafic-to-intermediate magmas, as in the Lassen domefield (Clynne, 1990a, 1999), and a few may be near-primary partial melts of mafic crust, as at Mount St. Helens (Smith and Leeman, 1987). At least 90 percent of the Quaternary dacite (63-68% SiO_2) in the Cascades erupted from the same 22 major volcanic centers that account for most of the silicic andesite. This is no surprise if most dacites descended from andesites that had been either fractionating parents or mixing members (with rhyodacite). If phenocryst-poor dacites represent interstitial melt extracted from crystal mush, the proximate parent may commonly be somewhat more mafic than silicic andesite, accounting for the not-uncommon bimodal arc association of dacite with basaltic andesite.

Dacite appears to be the volumetrically dominant product at Meager, Cayley, Garibaldi, Glacier Peak, St. Helens, and probably the Lassen volcanic center, where both precaldera and postcaldera dacites are especially numerous. Dacite is also a major constituent at Hood, Jefferson, and Shasta and a subordinate one at the remainder of the 22 main intermediate centers. Off-edifice domes and flows of dacite (not derived from vents within a major center) number about 35, fewer than half the number (~75) of comparably distributed andesitic units. These 35 units make up less than 10 percent of the total volume of Quaternary Cascade dacite; they include the Watts Point remnant in Canada, and Spiral Butte and the Snowden flow (which may be Pliocene) in southern Washington. In Oregon, there are at least 24 off-edifice dacites—a dozen separate domes and flows peripheral to Mount Jefferson, flows along First Creek (southeast of Three Fingered Jack), the Todd Lake Volcano and Kokostick Butte south of South Sister, a fraction of the zoned Shevlin Park Tuff in the Tumalo Volcanic Field, three small domes near Wickiup Reservoir, Mule Peak lavas (south of Cappy Mountain), and three pre-Mazama units just southeast of the Mazama edifice. Dacites in California include seven off-edifice domes west of Mount Shasta, the huge composite dome of Burney Mountain, lavas of Huckleberry Mountain (20 km northwest of Lassen Peak), and the Barkley Mountain chain (40 km southwest of it; fig. 21).

What accounts for the great volume excess of andesite and dacite at just a few centers along the arc may best be understood in terms of discrete long-lived MASH domains at the base of the crust. Longevities of the big intermediate centers are typically at least two orders of magnitude greater than those of the mafic shields that dominate eruptive output along the reaches between them. Scrutiny of tables 2 and 4 reveals no correlation between andesite-dacite edifice volume and spacing, so it seems clear that here (as in other arcs) there is no organized or periodic system of along-arc intracrustal upwelling instabilities. Because so many, small and varied, mafic volcanoes closely neighbor the major intermediate centers (table 1; figs. 3, 8, 14, 15, 21), it is also unlikely that an attractive process is involved, whereby some mantle columns suck in melt from a wide periphery. Instead, because mafic vent density is often elevated in the immediate periphery of the large intermediate centers (even in the GVB; fig. 3), one can infer the opposite—that the spatial density and intensity of independent basaltic magma batches reaching the base of the crust increase laterally toward the major foci that underlie MASH zones and the long-lived hybrid-intermediate volcanic centers they support. As for the productive mantle columns that power the foci, there is no evidence in the Cascades for any systematic spatial distribution that would suggest a regionally organized mantle structure of major convective upwellings or focussed melt channelization. Within the broad belt of subduction-influenced Cascade volcanism, 1,250 km long and locally as wide as 100 km, the major (and minor) andesite-dacite centers are scattered, with no systematic pattern to their mutual relative locations.

At risk of over-generalizing, many basalts and basaltic andesites are fairly phenocryst poor because relatively unimpeded ascent from the lower crust means that much of their preeruptive crystallization history took place in deep reservoirs where low melt viscosity allowed rapid removal of crystals. Arc andesites are typically rich enough in water that they exsolve an aqueous gas phase on ascent to the upper crust, which then compels extensive crystallization. Most andesites erupt rich in crystals because higher viscosity retards crystal removal and multi-batch recharge and mixing keeps crystals in circulation as well as sweeping up those of forerunning batches. Some andesite batches less disturbed by recharge may zone to dacite by gradual crystallization, while others that crystallize extensively may expel dacitic or even rhyodacitic melt from crystal mush. The widespread phenocryst-poor dacites are more likely to be the latter, whereas the phenocryst-rich dacites may either be andesite-rhyodacite mixtures or simply evolving andesites that erupted during advancing crystallization.

Rhyodacite and Rhyolite

Quaternary volcanic rocks more silicic than dacite are sparsely and irregularly distributed in the Cascades. None is present between the Jefferson and St. Helens loci, and except for a poorly exposed rhyodacite lava at the foot of McKenzie Butte (south of Mount Shasta), they are also lacking along the main chain between Mount Mazama and the Lassen segment. In contrast, the rear-arc Medicine Lake and Newberry centers have numerous rhyolites, including some in western peripheral areas transitional to the main arc. In the Washington Cascades south of Kulshan Caldera, no Quaternary rhyolites or rhyodacites are reported at Glacier Peak, and only one or two small units of rhyodacite are known at each of three other major centers, Adams, Rainier, and Goat Rocks (where the Devils Horns rhyolites are pre-Quaternary). At Mount St. Helens, only a handful of the many eruptive units had evolved as far as 68 to 70 percent SiO_2, probably by fractionation of the volumetrically dominant crystal-rich dacites.

Stratocones seldom erupt rhyolite or rhyodacite centrally, though Magee Volcano and South Sister (at 50-30 ka) provide apparent exceptions. More commonly, such silicic magmas issue from flank vents or independent peripheral vents (as at Shasta, Middle Sister, Jefferson, Adams, Baker, and the 2.4-ka Bridge River assemblage at Mount Meager), or, when shallow chambers grow large, they erupt as aligned dome chains or distributed domefields with or without calderas (as at Lassen, pre-Mazama, Mazama pre-climactic, Holocene South Sister, Tumalo, early St. Helens, and Kulshan). All three rear-arc (extensional) volcanic fields (Simcoe Mountains, Newberry, and Medicine Lake), however, built central rhyolitic complexes that began early in development of the three large shield-like edifices. The only rhyodacite or rhyolite units not clearly related to a major center are a few lavas as far as 8 km north of Mount Jefferson, the scattered Tumalo domes, and a few domes around the periphery of the Newberry edifice. The latter two sets of rhyolitic lavas lie near the leading edge of the age-progressive rhyolite trend of the High Lava Plains.

Table 11 gives the SiO_2 content of the most silicic eruptive product reported for each of the main evolved Cascade centers and for several minor ones. Of the 34 arc volcanoes listed, only 14 have SiO_2 limits of 72 percent or higher; that is, only these have rhyolite (rather than rhyodacite or dacite) as the most evolved product erupted. High-silica rhyolite (75-77% SiO_2) is especially rare, limited to the Lassen segment, the Obsidian Cliffs lava flow near Middle Sister, and a single dome at Mount Garibaldi, but several lavas and pyroclastic units at each of the three large rear-arc centers are rhyolitic. Similarly, very few high-silica rhyolites are recognized in the Aleutian, Andean, and Japanese arcs, although the few include some voluminous pyroclastic units. Such scarcity is actually a global phenomenon for volcanic arcs, the upper SiO_2 limit at each evolved arc volcano being typically in the range 69 to 74 percent, in contrast to rear-arc and continental-interior centers where high-silica (75-77%) rhyolite is widespread. The scarcity might reflect a need for either minimum melting of a quartz-bearing plutonic protolith or for expulsion of interstitial melt from already-evolved (dacite-to-rhyodacite) crystal mush. In the Cascades, rationalization of the scarcity of rhyolitic magmas in terms of a possible lack of continental basement might be advanced for northern Oregon but certainly not for the North Cascades or the Klamath-Shasta regions, where pre-Cenozoic crystalline rocks are widespread.

Many pyroclastic-flow deposits and far-flung tephras in the Cascades are dacitic, with rhyolitic, rhyodacitic, and andesitic units being common but subordinate. Table 3 lists more than 70 Quaternary fall units from Cascadian arc or rear-arc centers. In bulk (pumice) composition, about a dozen are rhyolitic, about 25 rhyodacitic, and most of the rest dacitic (though the glass phase that volumetrically dominates downwind ash is more silicic than dacite for all but the most phenocryst-poor dacitic fall units). Pyroclastic flows in the Cascades, whether pumiceous or the denser block-and-ash flows generally associated with dome collapse, are most commonly dacite (or silicic andesite) in bulk composition. Rhyodacitic pyroclastic flows are present, however, at Meager, Cayley, Garibaldi, Kulshan, Jefferson, Tumalo, and Mazama, whereas rhyolitic ones are identified only at South Sister, Tumalo, Lassen, and the three big rear-arc centers. Pyroclastic flows voluminous enough to be widely devastating (0.1 to 5 km^3) have erupted at Meager, Cayley, Garibaldi, Glacier Peak, St. Helens, Adams, Hood, Jefferson, South Sister, Tumalo, Shasta, and the three rear-arc centers, but Quaternary ignimbrite eruptions great enough to be caldera-forming (>10 km^3) have been limited to Kulshan, Mazama, Lassen, Newberry, and (perhaps) Tumalo. Only a few Quaternary pyroclastic eruptions in the Cascades have been voluminous enough to reveal compositional zoning. At Tumalo, the Shevlin Park Tuff (260±15 ka) is compositionally bimodal, containing

Table 11. Silicic products at Cascade volcanoes.

[Listed is the weight percent SiO_2 of the most silicic eruptive product recognized at each volcano, all the analytical totals having been normalized to 100 percent, volatile-free. The percent (%) values given in the Notes column likewise refer to SiO_2. At most centers, the most silicic product belongs to a compositional continuum shared by less evolved products. At other volcanoes, however, rhyolites are separated from the main compositional array by a pronounced compositional gap. This pertains principally to high-silica rhyolites (75-77% SiO_2) and is most conspicuous at Garibaldi, Middle Sister, and the three large rear-arc centers]

Volcano	Highest % SiO_2	Notes	References
Meager	70	Bridge River 2.4-ka assemblage from Plinth subedifice	26
Cayley	69	Rhyodacites largely at Mount Cayley proper	12
Garibaldi Lake	65	Black Tusk. (Clinker Peak to 64%; Mount Price to 63%)	9, 10
Garibaldi	77	Lava Peak obsidian. (Silicic rocks here mostly dacite)	12
Watts Point	66	Lavas, tuffs, and dikes	11
Kulshan Caldera	73	Ignimbrite pumice and postcaldera lavas 65-73%	16
Baker	68.5	Boulder Ridge. (No other units >65%)	15
Glacier Peak	67	Domes and pyroclastic flows (mostly dacite)	17, 27
Rainier	68.5	Edifice mainly andesite-dacite; few rocks >66.	5
Spiral Butte	66	Large dome 4 km northeast of White Pass	3
Goat Rocks	68	Andesite-dacite stratocone cluster (Adjacent Pliocene rhyolites up to 75%)	3
Adams	68.5	Many dacite lavas from main stratocone	13, 14
St. Helens	70	Sugar Bowl dome (and mid-Pleistocene domes)	25
Indian Heaven	59	Forlorn Lakes. (Volcanic field mostly basalt)	19, 24
Hood	65	Postglacial pyroclastic flows 62-64%	23, 28, 29
Jefferson	72	Rhyodacites peripheral to andesite-dacite edifice	6, 7
Middle Sister	76.5	Obsidian Cliffs. (A dome at south toe has 74%)	17
South Sister	74	Many 50 to 30-ka rhyolites. (Holocene lavas 72-73.5%)	17
Broken Top	69.5	Coulees at Squaw Creek Falls and Tam McArthur Rim	17
Tumalo	74.5	Bend pumice fall and several lava domes	17, 18
Edison Butte	74.5	Dome 8 km southeast of Mount Bachelor	18
Benham Falls dome	71.5	Dome/flow 10 km southwest of Bend, Oregon	17
Bench Mark Butte	65.5	Coulee 16 km southwest of Mount Bachelor	17
Cappy Mountain center	71	Clover Butte. (Nearby Burn and Hemlock Buttes and Mule Mtn all 69-70%)	17
Mazama	72	Llao Rock episode. (Climactic pumice ≤71%)	1
Pre-Mazama domefield	73	Many dacite to rhyodacite lavas	22
Shasta	72	Lava south of McKenzie Butte. (Black Butte 65.7%; Haystack 65%; main andesite-dacite edifice up to 67.5%)	5, 17
Burney Mountain	65	Large composite dome 35 km north of Lassen Peak	21
Magee	72	Late rhyodacite lava from mafic-to-andesitic cone	2
Lassen domefield	71.5	Many domes 64-70%	4
Brokeoff	68	Edifice dominantly andesitic 55-63%	4
Rockland caldera	74.5	Ignimbrite pumice zoned 71-74.5%	4
Maidu	76	Rhyolite coulees peripheral to andesite cone	4
Dittmar	75	Rhyolite lavas peripheral to andesite cone	4
Rear-arc centers			
Simcoe	76	Ignimbrite pumice and lava flows (Pliocene)	17
Newberry	75	Pleistocene McKay Butte. (Holocene rhyolites 72-74%)	20
Medicine Lake	77	Pleistocene lavas. (Holocene rhyolites up to 74.5%)	8

References: 1. Bacon and Druitt, 1988. 2. Borg and Clynne, 1998. 3. Clayton, 1983. 4. Clynne and Muffler, in press. 5. Condie and Swenson, 1973. 6. Conrey, 1991. 7. Conrey, Hooper, and others, 2001. 8. Donnelly-Nolan, 1998. 9. Green, 1981. 10. Green, 1982. 11. Green, 1994b. 12. Green, N.L., unpubl. data, 2005. 13. Hildreth and Lanphere, 1994. 14. Hildreth and Fierstein, 1995. 15. Hildreth and others, 2003. 16. Hildreth, Lanphere, and others, 2004. 17. Hildreth and Fierstein, work in progress. 18. Hill, 1991. 19. Leeman and others, 1990. 20. MacLeod and others, 1995. 21. Muffler, L.J.P., unpubl. data, 1981. 22. Nakada and others, 1994. 23. Scott and others, 1997. 24. Smith, 1984. 25. Smith and Leeman, 1987. 26. Stasiuk and Russell, 1989. 27. Tabor and Crowder, 1969. 28. White, 1980. 29. Wise, 1969.

black pumice (55-62% SiO_2) and pale silicic pumice (64-68% SiO_2) (Conrey and others, 2001); and at Medicine Lake, pumice in the Tuff of Antelope Well ranges from 63 to 67 percent SiO_2 (Donnelly-Nolan, 2006). Even in the voluminous Kulshan and Rockland (Lassen) pyroclastic units, the silicic pumice ranged through only 3 to 4 percent SiO_2. The great volume of rhyodacite magma released in the caldera-forming eruption of Mount Mazama was nearly homogeneous, but the intermediate scoria and cumulate mush that closed the eruptive sequence provide important insights concerning magmatic parentage and intrachamber fractionation processes (Bacon and Druitt, 1988) that may be applicable to many intracrustal arc-magma systems.

The phenocryst mineralogy of Cascadian rhyolites and rhyodacites is fairly simple, with plagioclase, orthopyroxene, and FeTi oxides ubiquitous and amphibole also present in many units. Clinopyroxene is commonly absent in these silicic rocks, although sparsely present in a few, especially within clots and enclaves. Quartz is common at Lassen and Meager and occurs sparsely at Kulshan, Maidu, Dittmar, and in many early eruptive units at St. Helens. Biotite occurs in a single pumice fall at Rainier, is present but uncommon at Kulshan, Maidu, Dittmar, and in the quartz-bearing early St. Helens units, and is common at Meager, Cayley, Garibaldi, and in many units of the Lassen domefield. Uniquely at Mount St. Helens, the Ca-poor ferromagnesian amphibole, cummingtonite, occurs in many units (mostly dacites) older than 3,000 years and commonly coexists with hornblende. No sanidine has been reported in the Quaternary Cascades.

There are many roads to rhyolite, so summarizing the magmatic origins of the Cascadian silicic rocks is not straightforward. The following processes have been advocated: (1) Serial escape of silicic interstitial liquid from numerous successive batches of crystallizing intermediate magma that thereby contribute to concurrent accumulation of zones of crystal-poor melt and melt-depleted cumulate mush; (2) percolation of such interstitial silicic melt to the top of large upper-crustal reservoirs (plutons) of dacitic/granodioritic mush; (3) fractionation of parental dacitic magmas, many of which may have originated by intracrustal partial melting of mafic rocks; (4) fractionation from hybrid parents that are mixtures of basalt, andesite, and partial melts of granitoids, young or old; and (5) direct intracrustal partial melting of mafic rocks. No Cascade rhyolites have been identified that might be straightforward partial melts of metasedimentary or granitoid rocks, though the relatively elevated Sr-isotope ratios of some California rhyolites (as high as 0.7045) suggest contributions from such sources (see section below entitled "Cascadian Basement and Sr-isotope Overview"). A simple liquid line of descent, by which rhyolite fractionates continuously from a basaltic parent, is seldom plausible, volumetrically or volcanologically.

While anticipating complexity, a first-order question for any rhyolite is whether it arose principally by crustal melting or represented melt separated from a crystallizing reservoir of intermediate magma. Small batches of crustal melt might sometimes escape hybridization, but no large upper-crustal silicic magma body is likely to have been fed directly by melting of a lithologically simple source. Even where crustal melting may have begun within a fairly homogeneous, deep-crustal gabbroic underplate, growth of an upper-crustal chamber would integrate contributions from all along the crustal column as well as from its own envelope. A long-lived melting column is inevitably self-hybridizing, and the coalescence of partial melts of varied protoliths is intrinsically a mixing process. Moreover, beneath a large evolved volcanic center that lasts a million years, basaltic injection and crustal melting would be spasmodically fluctuating processes, waxing and waning, such that episodic fractionation would provide a range of partially remeltable deep-crustal rocks, from gabbros (with or without amphibole) to tonalite and lesser fractions of more silicic differentiates. Growth of large upper-crustal silicic magma bodies may involve at least three (conceptually discrete) major magma-transfer mechanisms—(1) incremental addition of mafic-to-andesitic magmas that ascend batchwise from the deep crust, then fractionate within the shallow reservoir itself; (2) separation and coalescence of broadly dacitic melt batches in deep mafic crust, followed by ascent and addition to the shallow reservoir; and (3) buoyant mobilization of partially molten MASH complexes that, during upwelling through the lower-to-middle crust, physically segregate into dike swarms and melt-rich silicic fractionates at the top, passing down through hybrid cumulate mush into cumulate and refractory dregs. Each and all may contribute to some upper-crustal magma reservoirs, and there are probably transitions among them.

Much of the compositional variation among andesite-dacite magmas parental to rhyolites is likely to reflect fH_2O and fO_2 conditions prevalent at sites of deep-crustal melting (Tepper and others, 1993; Sisson and others, 2005), which in turn may principally reflect the flux and water contents of mantle-derived basaltic intrusions that range in the Cascades from dry to water-rich (Sisson and Layne, 1993; Grove and others, 2002). Isotopic studies, particularly Nd-isotope systematics, have demonstrated repeatedly that most metaluminous (arc and intracontinental) rhyolites descend from hybrid parents that blend local crustal contributions with proportionately greater immature mantle inputs supplied either directly as contemporaneous basaltic magma or, second-hand, by partial remelting of Cenozoic gabbros and their differentiates in the deep crust (Mahood and Halliday, 1988; Hildreth and Moorbath, 1988; Hildreth and others, 1991; Johnson, 1991). Few arc rhyolites are likely to be direct, unfractionated, crustal melts, and most probably represent melts that separated from intermediate parents with complex antecedence. The strongly peraluminous intracrustal magmas (for example, Andean macusanite and Himalayan leucogranite) are distinctive exceptions that prove the hybrid norm for silicic magmatism. Intracrustal melting is no doubt massive beneath arcs (and more so in areas of intracontinental extension), but partial melting of the predominantly mafic sub-arc protoliths generally yields not rhyolitic but intermediate magmas, from which most rhyolites subsequently evolve. If rhyolitic melt batches are sometimes produced directly, such as by partial remelting of deep-crustal tonalites or their differentiates, few such batches are likely to be large enough to avoid hybridization in complex long-lived systems. Over a million-year timescale, crustal melting and crystal-melt fractionation, of course, both contribute to production of rhyodacites and rhyolites. The polarized interpretive dichotomy that contraposes melting vis-à-vis fractionation becomes moot when applied to a long-lived crustal column that fluctuates thermally in response to successive mantle inputs.

At some centers, rhyodacites are part of an unbroken compositional array with dacites and andesites, suggesting continuous fractionation (and/or back-mixing), whereas elsewhere some rhyodacites and many rhyolites are set apart from intermediate members by wide compositional gaps, suggesting that the silicic melt had evolved not progressively but by batchwise extraction from crystal mush. That most rhyolites are phenocryst-poor weighs in favor of melt extraction from pluton-scale mush reservoirs but weighs against both (1) conventional fractionation models of progressive compositional evolution by subtraction of crystals from a melt-dominant magma and (2) extraction of viscous rhyolitic minimum melts from restite-rich migmatites. The abundance of mafic and andesitic enclaves in andesite-dacite extrusions (and in tonalite-granodiorite plutons) contrasts with their rarity in phenocryst-poor rhyolites, further supporting the notion that rhyolitic melt lenses accumulate at the top of thick granitoid mush reservoirs that buffer the upper levels from new mafic inputs. A comparable inference can be drawn from the withdrawal sequences of many ignimbrite sheets that start with low-temperature gas-saturated crystal-poor rhyolite and end with higher-temperature crystal-rich intermediates (Hildreth, 1981a). Entrainment by many rhyolitic magmas of subpopulations of refractory zircon antecrysts as much as 50 to 250 kyr older than the eruption attests further to the generality of thermally waxing-waning, incrementally accumulating, mush reservoirs (Reid and others, 1997; Brown and Fletcher, 1999; Vazquez and Reid, 2002; Bacon and Lowenstern, 2005; Charlier and others, 2005). The "mush model" of rhyolitic magmatism was elaborated by Hildreth (2004) and discussed in detail by Hildreth and Wilson (2007).

Some high-silica rhyolites exhibit such extreme contrasts in trace-element abundances and ratios as compared with associated dacites and andesites (notably in REE, Y, and HFSE) that explanations of their origin are driven to invoke either fractionation of sparse accessory phases or direct low-degree melting of crustal rocks (Miller and Mittlefehldt, 1984; Hildreth and Wilson, 2007). Such rhyolites are abundant intracontinentally, uncommon in arcs, and unrecognized in the Quaternary Cascades.

Arc Plutons and Upper Crustal Magma Chambers

Granitoid plutons of Quaternary age are rarely exposed, the lone Cascadian example recognized being the small Bar Creek stock (~0.7 Ma) in a deep glacial trough at the margin of Kulshan Caldera (Hildreth and others, 2003; Hildreth, Lanphere, and others 2004). Granitoid xenoliths quarried by several different eruptions of Mount Mazama and of Medicine Lake Volcanic Field, however, indicate Quaternary growth of extensive composite plutons beneath both centers; U-Pb and U-Th dating of zircons from the xenoliths (and drillcore) yields several discrete clusters of Pleistocene crystallization ages (320-20 ka), some of which coincide with silicic eruptive intervals (Bacon and others, 2000; Lowenstern and others, 2000, 2003; Bacon and Lowenstern, 2005; Bacon and others, 2005). There can be little doubt that many other Cascadian volcanic centers with histories of episodic silicic-to-intermediate eruptive activity extending over 10^5 to 10^6 years have likewise built multiphase composite plutons (of diorite to granite) in the upper crust beneath them. That Pleistocene granitoids underlie Meager, Cayley, Garibaldi, Kulshan, Glacier Peak, Rainier, St, Helens, Hood, Jefferson, South Sister, Broken Top, Newberry, Cappy, Shasta, Dittmar, Maidu, and Lassen seems inescapable. More interesting, but generally unknown, are the size and compositional-lithologic variability of the upper-crustal plutonic complexes now under construction.

Many plutons of Tertiary age, however, have been unroofed in the Cascades and may provide insights into those now forming, considering that they grew in an arc system and basement terranes much like those of the present. Owing to the northward increase in severity of glacial erosion, exposure of Tertiary plutons is much better in Washington and British Columbia than in Oregon, where the few Miocene stocks partly unroofed (Walker and Macleod, 1991) may in some cases represent windows into larger granitoid batholiths. No Tertiary granitoids are yet unroofed in the California Cascades. In the Cascades of central Washington where preservation of Tertiary volcanics and unroofing of Tertiary plutons are *both* good, most of the numerous dacitic to rhyolitic ignimbrites were doubtlessly derived from magma bodies that helped construct some of the 27 to 13 Ma granitoid plutons, several of which are 10 to 40 km across (for example, Snoqualmie, Grotto, Cloudy Pass, Bumping Lake, Tatoosh, and Spirit Lake plutons; Tabor and others, 1993, 2000, 2002; Walsh and others, 1987). Most Cascade plutons consist of granodiorite and tonalite (or monzonitic equivalents) with lesser representation of granite and gabbro-diorite. Rhyolite-equivalent leucogranites (70-74% SiO_2) are few, and the sparse intrusives with 75 to 77 percent SiO_2 are mostly dikes or small masses of aplite or alaskite. Because of secular upward fractionation of the melt phase at all stages of crustal magmatism, eruptive losses result in many plutons being melt-depleted quasi-cumulates that on average are a few percent less silicic than either their net volcanic output or the integrated bulk composition that intruded the upper crust.

One of the best-exposed Tertiary plutonic complexes is the long-lived Chilliwack composite batholith, which is compared at equivalent scales in figure 28 with the series of Pliocene-to-recent andesitic-to-rhyolitic volcanic centers in the Lassen region. From the Chilliwack pattern, one can infer that (1) most volcanic deposits are rapidly stripped in glaciated mountainous terrain, with intracaldera fill being preferentially preserved; (2) calderas are commonly similar in size to some plutons but smaller than many; (3) some plutons are nested, others consist of several transitional phases or lobes, and still others sharply crosscut older ones; and (4) the mass of mafic magma that rose through the mushy crustal column to produce shallow gabbro-diorite bodies is a trivial fraction (1-5%) of the upper-crustal batholith. In the Lassen sketch (fig. 28), each of the volcanic centers outlined stayed active for ~1 Myr and embraces dozens of vents for products that range from andesite to rhyolite. At least one caldera (Rockland) and possibly three or more are buried by younger volcanic rocks of the Lassen region. The upper-crustal plutonic roots of many long-lived volcanic centers are likely to be as complex as that depicted for equivalent areas of the Chilliwack batholith. If the 55 plutons distinguished along the 60-km-long Chilliwack exposure are representative of the upper arc crust, there could be more than 1,000 plutons (40-0 Ma) along the present-day Cascade arc and still more along its Tertiary continuation southeast into Nevada (Christiansen and Yeats, 1992). To the many substantial plutons (1-to-40-km across) must be added countless smaller plugs, dikes, and irregular intrusions, mostly gabbro-diorite or dacite-granodiorite.

Lower crustal domains, if preheated (as implicit in a long history of pluton growth), can be expected to be more responsive to renewed mantle input in generating new batches of hybrid to silicic magma, helping account for the longevity and recurrent rejuvenation of some magmatic loci. On a shorter timescale (10^4 to 10^5 years), gradual preheating of the upper crust during an extended period of emplacement of intermediate magma batches could prepare the shallow system for eventual coalescence of a large reservoir of crystal mush, extraction of rhyolitic melt, and a caldera-forming eruption. A well-documented example is the 7.7-ka climactic eruption of Mount Mazama, where a shallow body of rhyodacite magma only began to segregate ~30 ka, following several hundred thousand years of distributed andesite-dacite injections (Bacon and Lanphere, 2006). Granitoid plutons should not be thought of solely as a magmatic dying stage but a culmination in productivity of the crustal column. A thick mass of crystal mush can for a time suppress eruption of all but its own silicic differentiates. As the upper end of a partially molten crustal column, such a mush reservoir can long remain susceptible to rejuvenation by amplification of the mantle-derived basaltic power supply.

Many upper-crustal plutonic complexes appear to be products of piecemeal assembly spread out over the 10^5-to-10^6 -year lifetimes of systems that wax and wane thermally. Some granitoid reservoirs grow large and fast enough to absorb and homogenize numerous ascending magma batches, whereas others (when batch addition is slow relative to crystallization) end up as composite assemblages of discrete intrusive bodies, related but distinguishable phases that may be contiguous, overlapping, or nested (fig. 28). Compositionally “andesitic” plutons (quartz diorite) are usually small, probably because such batches seldom crystallize independently but are instead typically blended into larger reservoirs that undergo secular fractionation into gabbroic cumulates and more silicic melts. The scarcity of large gabbro-diorite plutons in the upper arc crust must also reflect their inability to penetrate upward through the more buoyant granitoid mush that their thermal contribution helped engender. Large plutons of tonalite and granodiorite are commonly intruded by mafic sheets, dikes, and swarms of distributed derivative enclaves. Thick mushy plutons preferentially restrict penetration of mafic inputs to deeper levels, accounting for the relative scarcity of mafic enclaves in their felsic upper zones, as well as in voluminous rhyolites. Large pyroclastic eruptions of crystal-poor silicic magma sometimes end by tapping into viscous crystal mush (as at Mazama and Katmai), whereas small ones are commonly bimodal, reflecting mafic injection of small silicic chambers more susceptible to eruption-triggering invasion. There are hierarchies of input intensity and reservoir growth; upper-crustal chambers are but one manifestation of the magma processing along a column penetrating the whole crust.

Eruptive leakage from a tonalite-granodiorite pluton accumulating in the upper crust might for long intervals feed a limited range (58-65% SiO_2) of andesite-dacite magma to a growing stratocone (Baker, Glacier Peak, Rainier, Adams, Hood, Jefferson, Rainbow, Shasta). When such a reservoir grows large and mushy enough to separate a substantial roof zone of silicic melt (buoyantly resistant to convective remixing), leakage might variously feed central plinian eruptions (Llao Rock, Bridge River), central dome clusters (Meager, Garibaldi, Glacier Peak, St. Helens), dome chains (South Sister, Sharp Peak, Mono Craters), distributed domefields (Lassen, Tumalo, Kulshan), or pyroclastic withdrawals large enough to initiate caldera subsidence. In arcs, as elsewhere, caldera-forming eruptions typically follow lengthy intervals of andesite-dacite (or more silicic) eruptive activity, which provides the thermal conditioning of the upper crust leading to coalescence and growth of a large shallow magma reservoir. The precaldera volcanism may or may not construct an edifice (like Mount Mazama), but it usually does include extrusion of silicic lava domes. In northern Washington and Canada, however, recurrent glaciation has obliterated all but scraps of precaldera volcanic products and virtually all extracaldera pyroclastic deposits resulting from caldera-forming eruptions (for example, Berman and Armstrong, 1980; Clayton, 1983; Hildreth, Lanphere, and others, 2004; Tucker and others, 2007).

Coalescence of large shallow bodies of evolved magma, whether beneath arcs or intracontinentally, is apparently favored by tectonic extension. Intra-arc extensional caldera belts are well described in Kyushu, Guatemala, and the Taupo Volcanic Zone. The great Toba caldera complex in Sumatra formed along a major transtensional fault zone, and many of the big calderas in Mexico and the Andes are in weakly extensional rear-arc settings, behind the chains of stratovolcanoes. In the extensional interior of the western USA, there are more than 100 large calderas of Oligocene and younger age. Extensional unloading evidently favors mantle melt production, focusing of magma ascent, buoyant mobilization of deep-crustal MASH zones, and formation of magma traps for mid-to-upper-crustal pluton growth. In the brittle upper crust, extension naturally favors magma ascent, though at deeper crustal levels, ductile stretching might promote sill formation. Extension, however, is not the only factor influencing growth of large shallow crustal magma systems, which are scattered along the Quaternary arc from Lassen to Meager (that is, from its most to its least extensional segment), and some caldera-forming reservoirs do develop along non-extensional volcanic fronts (for example, Kulshan and several along the Alaska Peninsula). The long persistence of mafic volcanic fields (Caribou, Hackamore, Indian Heaven, and reaches of the central Oregon Cascades) in areas of strong to weak tectonic extension, accompanied by little or no silicic volcanism, suggests that intensely localized crustal focusing of the basaltic magma flux from the mantle, not the extension itself, is the main prerequisite for growth of large reservoirs of silicic magma.

Tectonic and Geophysical Insights

Numerous geophysical and tectonic observations provide a variety of insights that help rationalize some of the varied patterns of volcano distribution in the Cascades (figs. 1, 25).

Concave Curvature of the Margin

The Cascadia subduction zone is unusual in that its northern half exhibits trenchward-concave curvature (fig. 1). Accordingly, northeast-directed subduction of the small oceanic plates of the Juan de Fuca system (Riddihough, 1984) results in nearly arc-normal convergence along the Garibaldi Volcanic Belt but oblique convergence elsewhere, which is apparently one of the factors that imparts a transtensional component to the Quaternary volcanic arc from

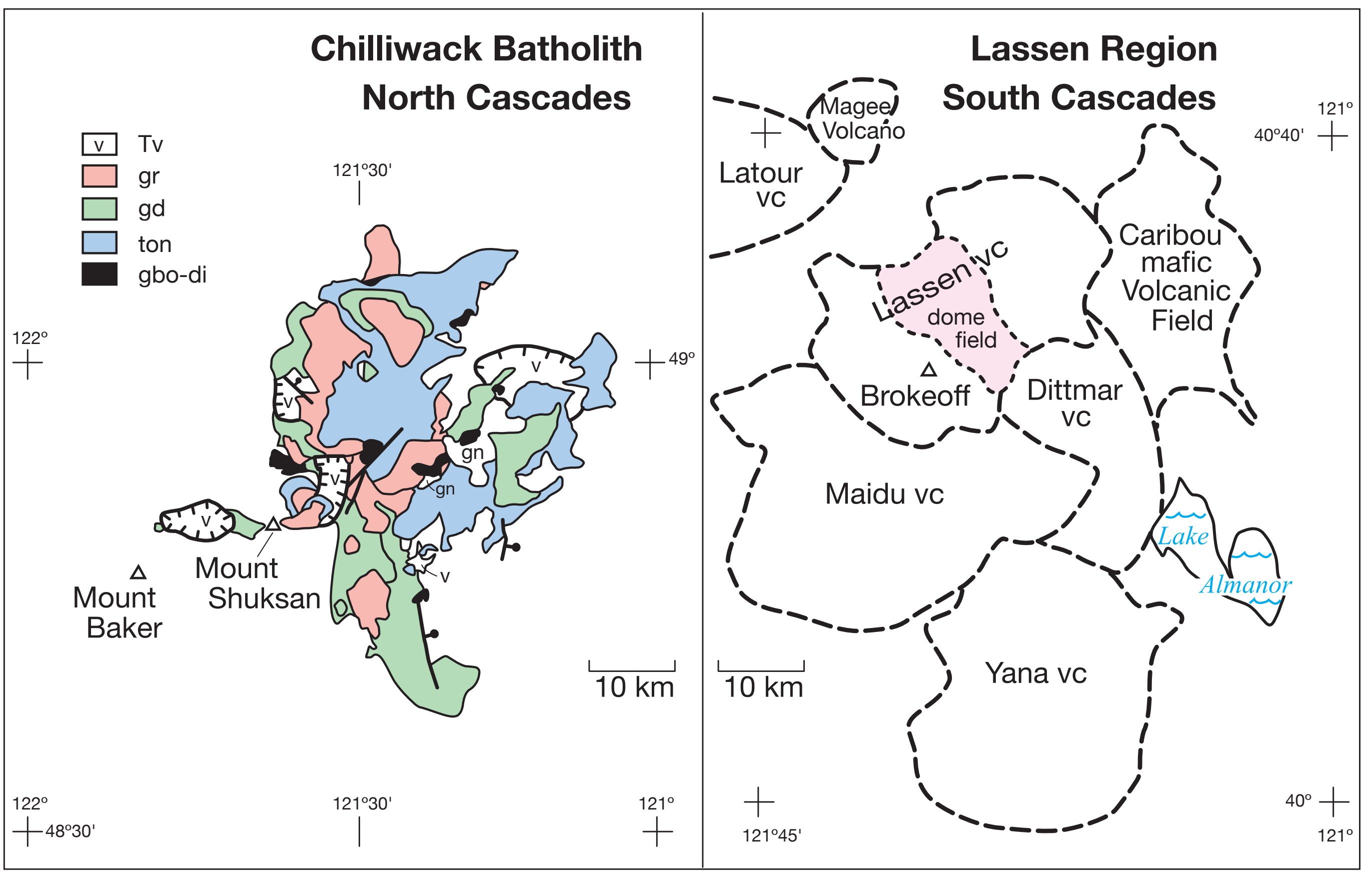

Figure 28. Examples of long-lived clustering of Cascadian magmatism, comparing at the same scale shallow plutonic and volcanic levels of exposure—Chilliwack composite batholith in the glaciated North Cascades and major volcanic components of the Lassen region, all of which except Caribou are evolved (andesite to rhyolite) volcanic centers (vc). About 55 separate Chilliwack plutons (not all separable at this scale) range in age from 32 to 0.7 Ma, whereas all volcanic rocks in the Lassen regional sketch are younger than 4 Ma (the Lassen domefield being still active). Principal lithology of each Chilliwack pluton is given in map key: gr, granite; gd, granodiorite; ton, tonalite; gbo-di, gabbro and diorite; Tv, volcanic remnants in the roof of the batholith, largely pyroclastic, including at least three caldera fills (hachures); gn, inliers of basement gneiss. Compiled principally from Tabor and others (2003), Tepper and others (1993), Macdonald (1963), and Clynne and Muffler, in press.

central Washington to California, probably contributing to its unusual breadth.

Because the concave-seaward margin of northern Cascadia is contrary to the natural convex curvature of a plate subducting into a sphere, the Juan de Fuca slab accommodates by bending into an apparently smooth arch (fig. 25), the crest of which plunges east (at about 48°N), as imaged by both seismicity and seismic tomography, beneath the Olympic Peninsula and Glacier Peak (Crosson and Owens, 1987; Weaver and Baker, 1988; Bostock and VanDecar, 1995). The relatively shallower slab over the crest of the arch implies a thinner mantle wedge there, which might reduce magma generation and thus provide an influence in limiting Quaternary volcanism along the 200-km reach between Rainier and Baker to the single locus around Glacier Peak. Moreover, if the slab beneath Glacier Peak were shallower, cooler, and wetter than to the north or south, that might help explain why that isolated volcano contrasts with its nearest neighbors in its abundance of explosive hornblende dacites.

Translation and Rotation of the Forearc

Tectonic deformation of Cascadia and adjacent areas is fundamentally driven by dextral shear between the Pacific and North American plates (Atwater, 1970) and by extension promoted by buoyant mantle beneath the western Basin and Range Province (Jones and others, 1996). Opposite the Cascade arc, most of the relative motion between the two megaplates is accommodated by spreading on the Juan de Fuca Ridge and subduction beneath Cascadia, but some 25 percent of the relative motion is distributed far inboard as block rotations and translations (Pezzopane and Weldon, 1993; Walcott, 1993; Wells and others, 1998; McCaffrey and others, 2007).

In response to the dextral shear couple, and in concert with northwestward motion of the nearly rigid Sierra Nevada-Great Valley-Klamath microplate (Dixon and others, 2000; Hammond and Thatcher, 2004) and with Basin and Range extension inboard (fig. 25), the Oregon forearc has undergone clockwise rotation since at least the mid-Miocene (Wells and Heller, 1988; Wells, 1990; Wells and others, 1998). Along its trailing margin, rotation of the forearc block apparently contributes to the intra-arc and rear-arc east-west extension prominent along the Oregon Cascades, from the Klamath Graben (fig. 15) to the Columbia River (fig. 25). On the decadal timescale of GPS measurements, however, intra-arc extension there is currently limited to about 1 mm/yr or less (McCaffrey and others, 2007). Oblique subduction of the Juan de Fuca Plate probably also contributes by basal traction to northward motion of the Cascadia forearc. The transition from predominantly dextral shear in California to block rotation in Oregon lies between the Lassen and Shasta segments of the arc, coinciding with the transition offshore from a strike-slip to a subducting plate boundary (figs. 1, 25).

Northward motion of the forearc microplate promotes north-south shortening in the Washington forearc, may promote transpression along the arc north of Mount Rainier, and enhances compression along the Garibaldi Volcanic Belt, north of the restraining bend where the Coast Plutonic Complex forms a stable buttress. As shown by the GPS vectors of McCaffrey and others (2007), clockwise rotation of the Cascadia forearc is apparently coordinated with and merges smoothly into the nearly orthogonal plate convergence in northwest Washington and British Columbia. Northeasterly motion of the Mount Baker region may help account for the magmatic age progression of the Hannegan-to-Baker locus (figs. 3, 26; Hildreth, 1996).

Northwestward translation of the Sierra Nevada-Great Valley microplate involves a broad dextral inboard shear zone that extends from southern Nevada to northeastern California, where the northwest-trending strike-slip belt merges diffusely into an array of north-striking normal faults that reach northward through Mount Mazama. Faults of the dextral shear zone (Walker Lane belt) strike into the Lassen segment, and others may impinge on the Medicine Lake and Hackamore Volcanic Fields. In this region, Blakely and others (1997) outlined three right-stepping offsets where nonmagmatic gaps containing northwest-southeast dextral faults alternate with the Lassen, Shasta, and McLoughlin volcanic segments, within which north-south normal faults are more prominent. The pattern suggests that, where the regional belt of dextral shear overlaps the volcanic arc, east-west extension is capable of establishing the dominant structures principally within the crustal segments most weakened by magmatism.

Farther north, a belt of weaker northwest-trending dextral shear, the Brothers Fault Zone (fig. 25), provides a diffuse northern margin for the Basin and Range extended region (Lawrence, 1976). The Brothers Fault Zone likewise terminates diffusely against the Cascade arc, first stepping left (west) to form the northwest-trending Sisters (Tumalo) Fault Zone, which in turn merges with the north-striking High Cascades Graben (HCG in fig. 25; Taylor, 1981, 1990a; Smith and Taylor, 1983; Smith and others, 1987; Sherrod and others, 2004). Elements of this intra-arc belt of modest east-west extension, structurally active at least since ~5 Ma, may or may not follow the Cascade axis from Green Ridge (44.5ºN) northward through the Jefferson reach to join the Hood River Fault (fig. 25) near the Columbia River (Conrey and others, 1997; Walker and MacLeod, 1991), where discernible extension apparently peters out.

Inboard of both the Cascade arc and the Oregon Basin and Range, most of eastern Oregon and southern Idaho appear to be rotating clockwise as a large coherent block. As shown by the GPS vectors of McCaffrey and others (2007), the northwest end of this block moves directly northward against the Yakima Foldbelt and adjacent Mount Adams area. North-directed compression there, with a small clockwise rotational component, is consistent with the east-west fold axes, minor dextral faults that crosscut the axes, north-vergent reverse faults, and several northerly vent alignments.

Differential extension and block rotation of the lithosphere may play a more important role than subduction geometry in controlling segmentation of the volcanic belt, in defining its several distinguishable reaches in Oregon (figs. 14, 15), and in promoting its exceptional width in California and southern Washington. The Cascade arc has been a well-defined continuous belt since the Eocene, but the dextral shear, block rotations, and Basin and Range extension were not imposed on the arc until the mid-Miocene. Had none of these external tectonic processes been superimposed on the Cascades, there would nonetheless still be a Cascade arc today, owing to the slab-derived contribution to mantle-wedge melt production. In all likelihood, however, there would be no HAOT, no rear-arc Simcoe, Newberry, Medicine Lake, nor Hackamore Volcanic Fields, and the volcanic belt in the Lassen segment would be much narrower.

Slab Depths and Discontinuities

Slab depths beneath the Quaternary volcanic belt are not well known, though the slab does appear to be segmented (Guffanti and Weaver, 1988; Bostock and VanDecar, 1995). Except along the nearly aseismic Oregon subduction zone, seismicity within the slab is well recorded beneath the forearc, where it extends continuously to depths of about 60 km in British Columbia, Washington, and California (Taber and Smith, 1985; Walter, 1986; Crosson and Owens, 1987; Weaver and Baker, 1988). Earthquakes within or along the slab at 60 to 80 km depths are rare and still deeper events absent. Imaging the slab by seismic tomography, however, suggests that slab dip increases abruptly from 5° to 20° beneath the outer forearc to 50° to 70° beneath the Willamette-Puget-Georgia forearc trough (fig. 25), the flexure (and breakaway?) typically lying 50 to 100 km seaward of the arc. The slab flexure and the topographic trough probably both reflect slab densification owing to basalt-to-eclogite phase changes at slab depths of 50 to 60 km (shallower than in older colder slabs). This pattern pertains from British Columbia to California (Michaelson and Weaver, 1986; Rasmussen and Humphreys, 1988; Harris and others, 1991; Benz and others, 1992; Bostock and VanDecar, 1995; Zhao and others, 2001). In contrast to the tomographic analyses just cited, however, that of Bostock and others (2002) suggests a lesser (30°) slab dip east of the flexure in central Oregon, so the actual shape of the seismically silent slab beneath Oregon evidently remains unresolved (McCrory and others, 2004).

If the steep, tomographically inferred, dips are real, then a 60° dip implies a slab-depth difference of 87 km across a 50-km-wide volcanic belt (as in Oregon) or a 173-km difference across a 100-km-wide belt (as in southern Washington or the Lassen segment). For example, if a slab dipping 60° lies ~75 km beneath the Portland-St. Helens forearc, then it might be 160 km below Mount Adams or as deep as 250 km beneath the Quaternary volcanoes farthest inboard near Goldendale (fig. 8). Moreover, if the slab were that steep beneath parts of the arc, then its vertical fall component might contribute to hingeline rollback, intra-arc extension, upwelling of mantle material little influenced by slab-derived fluid, and consequent production of some of the observed mantle magmas atypical of arcs (principally HAOT and alkali basalt).

On the south limb of the slab arch in southern Washington (fig. 25), there is likely to be some kind of structural discontinuity in the slab. In northern and central Washington, the deep slab is tomographically imaged to depths of 400 to 500 km but only to 300 km in southern Washington and to only 150-200 km beneath Oregon (Michaelson and Weaver, 1986; Rasmussen and Humphreys, 1988; Harris and others, 1991; Bostock and VanDecar, 1995). The discontinuity might take the form of an east-trending tear, fold, or monocline, and such a structure could be expected to distort mantle-wedge flow, which might in turn influence the compositional diversity and extraordinary width of the volcanic belt from Portland across southern Washington. On the basis of a linear trend in deep slab earthquakes beneath southwest Washington, McCrory and others (2003) indeed proposed just such a tear. Another possibility, an arc-parallel (north-south) tear, breakaway, or sharp hingeline where the Oregon slab steepens abruptly, would still require some kind of east-west disruption of the transition zone between the Oregon slab and that beneath the Rainier-to-Hood segment.

Reconstruction of 7-to-0-Ma motion of the Juan de Fuca microplate system (Riddihough, 1984; Wilson, 1989, 2002; Oppenheimer and others, 1993) indicates (1) slowing of its northeast-directed convergence from ~70 mm/yr to ~30 to 45 mm/yr today, owing to the growing resistance to subduction of progressively younger (more buoyant) oceanic lithosphere, resulting in (2) detachment of the youngest (slowest) portion at ~3.5 Ma, creating an independent Explorer microplate that then virtually ceased subducting, and (3) subsequent stressing of the young buoyant southernmost portion of the plate, leading after 3 Ma to deformation, independence, further slowing (to 2 to 3 cm/yr), and potential locking of the so-called Gorda plate. Slowing and eventual Pliocene shrinkage of the Juan de Fuca Plate system at both ends may have influenced, over the same time interval, the westward jump of arc magmatism from the Pemberton-Chilliwack belt (fig. 3) to the Garibaldi belt in the north (Souther and Yorath, 1991) and the westward drift of volcanism in the Lassen segment in the south (Guffanti and others, 1990). In both areas, slowing of subduction may further have permitted a larger role for upwelling of poorly fluxed mantle, leading to production of alkali basalts in the north and abundant HAOT in the south, each impoverished in subduction components. Enhanced mantle upwelling past the edges (Lewis and others, 1997; Beaudoin and others, 1998) of the shrinking slab might also contribute to the crustal melting anomalies near the ends of the arc, expressed in the silicic Meager and Maidu centers and the Barkley Mountain dacite chain (figs. 3, 21).

Hingeline rollback and/or sinking of recently detached slab segments might well account for westerly arc drift at the north and south ends of the Cascades, but arc drift has been antithetically eastward in the center. From central Washington to southernmost Oregon, the Quaternary volcanic axis lies just east of the broad Miocene belt, the apparent crossovers (where Quaternary and Miocene arcs coincide) being near Glacier Peak and the California border. In between, the eastward migration of Cascade magmatism is more likely to reflect the trenchward component of western Oregon's upper-plate clockwise rotation than any shallowing of the steep sub-Oregon slab. In the Oregon Cascades, there is substantial overlap between the broad belts of Pliocene and Quaternary volcanism, so it appears that the last significant eastward shift of the Cascade volcanic axis took place around 7 to 5 Ma, at the onset of intra-arc extension, which is linked to the rotation and has maintained the position of the axial magmatic belt ever since.

Young Warm Slab and Influences on Magmatism

The main part of the Juan de Fuca slab itself is, by global comparison, relatively young, warm, and buoyant, and its convergence with North America is relatively slow (30-45 mm/yr) and initially (beneath the outer forearc) shallowly dipping (5-20°). Plate age at the deformation front (trench) is only 6-8 Ma, contributing (along with an unusually thick 3-km blanket of sediments on the incoming oceanic plate) to a high initial temperature (225-260ºC) on the megathrust at the (filled) trench (Oleskevich and others, 1999). Those investigators model downdip temperatures to reach 350ºC at 12 km depth, 450ºC at 25 km, and 550ºC at ~40 km, where the thrust plane dips below the forearc Moho. Slow subduction of hot young oceanic lithosphere might well influence mantle-wedge rheology and lessen cooling of the wedge nose, but it is hard to see how elevation of slab temperature by even as much as 100ºC above normal could alone account for the unusual abundance of forearc volcanism (with eruption temperatures as high as ~1,200ºC) in parts of the Cascades.

Isochrons of Juan de Fuca sea-floor age (Wilson, 1988, 1989, 2002) suggest subducting slab ages of 14 to 15 Ma beneath Puget Sound, 10 to 12 Ma beneath the Strait of Georgia (facing the Canadian volcanoes), 11 to 12 Ma beneath the coastline of southern Washington and northern Oregon, and 8 to 10 Ma beneath the coastline of southern Oregon and northern California, where deformation has made the sea-floor magnetic pattern especially complex. Owing to along-strike variation in the longitude and dip of apparently abrupt slab steepening farther inboard (presumably at the phase changes to eclogite) and to uncertainties in tomographic imaging of steep silent slab segments under the volcanic belt itself, slab depths directly beneath the Cascade arc remain poorly known (but revisit the slab-depth discussion, above; and see the slab-depth extrapolation of Harry and Green, 1999, discussed below).

Because the Juan de Fuca slab is young and thus unusually warm, several studies have sought linkages between Cascadian thermal structure, slab dehydration, and compositions of magmas erupted. Widespread production of primitive H_2O-poor HAOT, from Lassen to Glacier Peak, is interpreted to indicate especially high temperatures (1,300-1,450ºC) in parts of the mantle wedge (Bartels and others, 1991; Bacon and others, 1997; Elkins-Tanton and others, 2001). Since fairly primitive arc basalts that had contained several percent H_2O at upper-mantle temperatures of 1,100-1,200ºC (Baker and others, 1994; Sisson and Grove, 1993; Grove and others, 2002) have erupted from vents situated close in space and time to those of HAOT, the thermal structure of the wedge cannot be simple.

Largely on the basis of Li and B depletions, which they identified in basalts of all types and attributed to atypically early devolatilization of the hot Juan de Fuca slab beneath the forearc, Leeman and others (1990, 2004, 2005) argued that the slab contribution is weak or absent beneath all of the southern Washington Cascades. Assigning great weight to loss of these light volatile trace elements, they went so far as to propose virtually complete forearc dehydration of the slab, thus challenging the very model of arc magma generation fluxed by ongoing ascent of slab-derived fluids and proposing instead that the abundant arc basalts in southern Washington that do carry a typical slab signature had acquired it during passage through pre-Quaternary arc lithosphere. Problems with such proposals include (1) that advanced forearc dehydration of slabs (warm or cold) is a global phenomenon; (2) that the subduction-component geochemical signatures for Cascadian arc basalts are well within the normal range found for arcs above slabs of all ages; and (3) that the many HAOT and intraplate alkalic basalts that are closely interspersed with normal arc basalts in the Washington Cascades had traversed the same lithosphere without acquiring a comparable geochemical overprint. Slab dehydration always takes place predominantly beneath the forearc (Peacock, 1993; Schmidt and Poli, 1998; Bostock and others, 2002; Hacker and others, 2003; Hyndman and Peacock, 2003; Brocher and others, 2003). Most of the Li and B depletion of the subducting plate is expected to occur by collapse of porosity and dehydration of zeolites at 300 to 500ºC, therefore at slab depths shallower than 40 km. Globally, only a small fraction of the original slab water can ever reach the ~100-km depths beneath an arc, but the fraction remaining is obviously adequate to induce wedge melting and to yield hydrous magmas in all arcs. Many experimental and theoretical studies (summarized in Hildreth, Fierstein, and others, 2004) indicate that diverse minor hydrous phases persist—in slab eclogite, in serpentinized lower-plate mantle peridotite, and in downdragged hydrated wedge peridotite—to depths of 100 to 250 km. Progressive down-dip reliberation of hydrous fluid upward into the mantle wedge, smeared out over a great depth range owing to solid-solution effects on breakdown of several hydrous phases, helps account for the breadth of the Cascade arc, for crude across-arc gradients in intensity of the slab contribution identified in some reaches (Borg and others, 1997; Bacon and others, 1997), and for production of some subduction-signature basalts even at the rear-arc Newberry and Medicine Lake Volcanic Fields (where HAOT is the dominant primitive magma).

Opposite the Garibaldi Volcanic Belt, the slab youngs northwestward at the onset of its subduction beneath the forearc, because the convergent plate margin is oblique to isochrons on the oceanic plate (Wilson, 1988). Thermal modeling, accordingly, suggests that the initial temperature of the downgoing slab is as much as 75ºC hotter opposite Mount Meager than opposite Glacier Peak (Harry and Green, 1999; Green, 2006). The obliquity likewise suggests that, downdip beneath the volcanoes, the slab youngs from 22 Ma beneath Glacier Peak to 19 Ma under Mount Baker to 15 to 14 Ma beneath the Mount Garibaldi to Bridge River reach (Green and Harry, 1999; Green and Sinha, 2005; Green, 2006). Arguing that the hotter younger (more north-westerly) oceanic lithosphere would dehydrate earlier and more thoroughly, Green and coworkers made a case for an along-arc correlation with basalt compositions. When the hot and drying subducting slab reaches a position beneath the arc, their logic continued, its fluid contribution would be relatively weaker to the northwest, where any fluid-induced melting of the mantle wedge would there be deferred to greater depths and would result in weaker slab geochemical signatures, lower melt fractions, and thus more alkalic magmas. The gradient in basalt geochemistry that they correlate with a younger hotter drier slab northwestward along the GVB depends heavily, however, on the two ends of the segment, as most of the basalts in between carry normal arc-type signatures (Green and Sinha, 2005; Green, 2006). At the southeast end, the lone HAOT-like low-K basalt in the GVB (White Chuck scoria cone) is accompanied nearby by normal arc basalts; and it seems hard to fit a hot dry HAOT into the cooler wetter end of the model. At the northwest end of the segment, the alkalic basalts of Bridge River and Salal Creek support the model, but they are likely to represent poorly fluxed intraplate upwellings beyond the edge of the slab rather than products of hot dry subduction.

Some intensification of forearc dehydration is reasonable for a slab younger and hotter than most, but total elimination of hydrous phases that could remain stable to slab depths and temperatures beneath the arc and rear-arc is unrealistic (Schmidt and Poli, 1998; Hacker and others, 2003). Moreover, even the hottest slab is a heat sink relative to the interior of the convecting mantle wedge, which may exceed 1,400ºC (Tatsumi and others, 1983; Kushiro, 1987; Ulmer, 2001; Grove and others, 2002). An arc-magma generation model for the Cascades must account for intimately scattered eruption sites for relatively wet arc basalts and dry HAOT, and locally for H_2O-poor, low-melt-fraction, intraplate alkali basalts as well. It appears likely that once a slab-derived fluid batch induces partial melting of wedge peridotite, intrinsic buoyancy of the affected region induces domainal upwelling and/or porous upward flow of interstitial melt athwart the main corner convection of the wedge. Decompression and percolation through the high-temperature core of the wedge should both enhance melt fraction (and thus ascent rate) and, by progressive addition of melt at shallower levels, should gradually reduce initially high slab-derived water contents of the melt (Grove and others, 2002). HAOT generation, on the other hand, is probably related to dry decompression melting within the hot upper limb of the wedge corner convection, perhaps enhanced by extension and local entrainment of the (partially remelting) base of the overlying mantle lithosphere. Modelling of such corner flow suggests that the upper limb should shallow gently trenchward (Furukawa, 1993; Currie and others, 2004), as also suggested petrologically by an east-to-west traverse of HAOT generation depths across northern California (Elkins-Tanton and others, 2001). Because all the HAOT units investigated were thought to have first crystallized olivine and plagioclase virtually *at the base of the crust* (Bartels and others, 1991; Elkins-Tanton and others, 2001), each must either have originated by partial melting of mantle lithosphere or (more likely) have arisen from the hot convecting wedge and penetrated the lithosphere as a discrete batch of modest volume. Subsequent progress to the surface must have been rapid, because protracted storage of hot crystallizing HAOT in or adjacent to the lower crust (unless the envelope were refractory cumulates) would inevitably promote voluminous crustal melts, which might be expected to contaminate or suppress further ascent of the HAOT magma.

If the trenchward-flowing upper limb of the convecting mantle wedge (with or without contributions from superjacent mantle lithosphere) is the principal source of HAOT, and the slab-fluxed deeper part of the wedge is the starting point for arc basalts, then batches of the latter must penetrate the upper limb in discrete columns, whether as upwellings, percolation columns of porous flow, fracture networks of channelized flow, or all of these sequentially. With such a discretely columnar configuration, the slab-derived geochemical signature should not overprint the whole wedge but only the ascent columns, at least where traversing the upper limb and lithosphere. In modeling wedge corner flow beneath Cascadia, Currie and others (2004) concluded that forced convection by slab traction (coupled downdrag) was insufficient to account for the high temperatures observed across the arc and rear arc. They suggested that an additional component of free convection by small-scale thermally buoyant upwellings is required to produce the across-arc thermal structure, consistent with my inference based on the closely spaced ascent paths of geochemically contrasting primitive basalts.

As for the intraplate alkalic basalts, those of the Simcoe Mountains Volcanic Field and the Bridge River-Salal Creek field may result from low-fraction partial melting of unfluxed mantle upwellings, respectively just inboard of and just off the edge of the extensive wedge domain affected by contributions arising from the steeply subducting slab. The alkalic basalts interspersed with HAOT and arc basalt across southern Washington (and rarely elsewhere in the Cascades), however, are probably low-fraction partial melts of domains within the upper limb of the convecting wedge that remain uncontaminated by the nearby columns of slab-fluxed melt ascending through the wedge core. Alternatively, if the slab is broken or distorted into adjacent segments of different dip beneath southern Washington, the intraplate alkalic basalts might arise from columns of sub-slab asthenospheric mantle upwelling past the segment margins.

Cascadian Basement and Sr-Isotope Overview

Geophysical investigations summarized by Mooney and Weaver (1989) show the crust beneath the Cascade arc in the USA to range only modestly in thickness (42±4 km), to reach an apparent minimum (~38 km) in the (incipiently extended) Lassen segment, and to be underlain by upper mantle having P-wave velocities of 7.7 to 7.8 km/s. Seismic refraction and reflection surveys (Cook, 1995; Clowes and others, 1995; Zelt and others, 1996) show the GVB volcanoes of southern British Columbia to overlie slightly thinner crust (35-38 km) and slightly faster upper mantle (~7.8-7.9 km/s).

Despite only modest differences in total crustal thickness, the along-strike variation in upper-crustal basement lithologies is substantial. The Lassen segment (Berge and Stauber, 1987), Medicine Lake (Fuis and others, 1987), and the volcanoes in British Columbia (Wheeler and McFeeley, 1991) overlie Mesozoic batholiths with varied proportions of metamorphic wall rocks. In the Northwest Cascades, Mount Baker overlies a stack of nappes consisting of Mesozoic and Paleozoic metavolcanic and marine metasedimentary rocks (Tabor and others, 2003), whereas Glacier Peak overlies a terrane boundary between distinct packages of amphibolite-grade Mesozoic metasedimentary rocks intruded by discrete tonalitic plutons of late Cretaceous age (Tabor and others, 2002). From the Mount Rainier area for 500 km south to the Oregon-California border, basement rocks are wholly concealed (in the so-called Columbia Embayment) beneath Cascadian arc rocks of Eocene to Holocene age. A large window of basement rocks 20 km southeast of Mount Rainier (Miller, 1989) has age and lithologic affinities to the thrust sheets and mélange belts of both the Klamath Mountains and the Northwest Cascades. Consisting of tectonic slices and accretionary mélange of submarine fan deposits, hemipelagic sea-floor deposits, pillowed MORB greenstones, and tonalitic and mafic metaigneous K-poor arc rocks, all of Mesozoic age, the assemblage may be representative of the thick crust concealed beneath much of the "embayment." Although it has been speculated that Mesozoic or Tertiary sea floor might underlie the "embayment," a thick stack of varied accretionary rocks, thrust or underplated inboard and translated dextrally northward along the Mesozoic continental margin, is more consonant with the 44-km-thick sub-arc crust and with the absence of any discontinuity in the seismic-velocity structure along a refraction profile up the Oregon Cascade axis (Leaver and others, 1984), notably where the profile crosses the postulated Klamath-Blue Mountain lineament (Riddihough and others, 1986). Mount Shasta overlies the transition between the Mesozoic batholith inboard and a stack of thrust sheets of Paleozoic and Mesozoic, accretionary and ophiolitic, metasedimentary and metaigneous rocks that include the Trinity ultramafic sheet (Fuis and others, 1987). If undocumented Precambrian rocks are present anywhere in the structurally complex sub-Cascadian crust, they are likely to be metamorphosed marine sediments and proportionally trivial.

Crustal contributions to Cascadian magmas are unusually hard to quantify owing to the basement being mostly Mesozoic and Tertiary, much of it consisting of accretionary arc and oceanic terranes that provide (at best) modest isotopic and chemical contrasts with the mantle-derived magmas penetrating them. Such contrasts can actually diminish with time as the mean age of the lower arc crust becomes progressively younger owing to secular intrusive underplating by the arc basalt itself. Figure 29 presents a compilation of $^{87}Sr/^{86}Sr$ determinations for more than 660 samples of Quaternary eruptive products along the Cascade arc, illustrating a fairly limited range of values (0.7027-0.7046), a generally poor correlation between $^{87}Sr/^{86}Sr$ and bulk composition, and the largest isotopic diversity in California (where the basement includes Mesozoic granitoids) and in southern Washington (where the basement is not exposed but probably accretionary). Although more Sr-isotope data are needed for northern Washington and parts of Oregon, the along-arc coverage is far better than for Nd, Pb, O, or Os isotope data, which are adequate only locally.

Scrutiny of figure 29 shows the following. (1) Sr-isotope ratios for HAOT (47-50% SiO_2) in the Cascades range widely—0.7027 to 0.7037 in Washington, 0.7028 to 0.7036 in Oregon, and 0.7031 to 0.7044 in California, suggesting routine Sr-isotopic contamination of these low-Sr basalts in the arc crust and mantle lithosphere. (2) Arc basalts, basaltic andesites, and andesites all span wide and comparable ranges of $^{87}Sr/^{86}Sr$ in all segments, suggesting that assimilation of crustal Sr is unsystematic and certainly not a simple AFC process. In the Mazama and Jefferson areas, andesites show a wider range and extend to lower ratios than the mafic arc rocks. (3) Ratios for rhyodacites and rhyolites generally fall in the upper (more radiogenic) half of the range in each area investigated. This should be no surprise, since partial melts of crustal rocks are expected to be a leading contaminant across the whole range of compositions erupted and a proportionately larger one in the more silicic rocks. Values of $^{87}Sr/^{86}Sr$ for rhyolites are as high as 0.7046 in the Lassen segment but reach only 0.7036 in Canada, though in both areas the magmas erupted through Mesozoic crystalline basement. (4) Ratios for dacites range remarkably widely, from 0.7028 to 0.7044 in California alone, supporting inferences discussed previously that Cascadian dacites include varieties that originated as andesite-rhyodacite mixtures, as near-primary partial melts of mafic crustal rocks, as straightforward fractionates of andesite, and as interstitial melts extracted from a range of mushy mafic to andesitic parents. And (5) whatever proportion of the Sr-isotopic diversity in the Cascades may have been inherited from mantle sources is at best obscure.

Vent Distribution and Basement Influences

Although the Juan de Fuca Plate subducts northeast at 3 to 4.5 cm/yr beneath the North American Plate (fig. 1), the maximum principal horizontal stress direction in the upper plate is margin-parallel, not in the convergence direction (Spence, 1989; Zoback, 1992; Ma and others, 1996; Hyndman and others, 2003). Owing presumably to the combination of oblique convergence and northward push of the Sierra Nevada-Klamath block, the direction of compression is north-south in Washington and Oregon and as far south as Mount Shasta, within the arc, forearc, and parts of the rear-arc such as the Yakima Foldbelt and Simcoe Mountains Volcanic Field. This stress orientation is reflected in north-south vent alignments from Shasta to Mount Adams. Impingement of the inboard dextral shear system no doubt influences the many northwest-southeast vent alignments in the Lassen segment, and local changes in strike of extensional faulting in the rear-arc Medicine Lake and Newberry Volcanic Fields evidently contribute to varied vent alignments.

The unusual forearc location of Mount St. Helens and its low-K compositions and recurrently explosive behavior may reflect in part the structure of the crustal basement. Weaver and others (1987) proposed that the volcano is located above a right-stepping offset in the north-northwest-striking St. Helens seismic zone (inferred to be dextral on the basis of focal mechanisms), permissive of a local extensional domain focusing the upper-crustal magma reservoir. A second belt of persistent seismicity strikes east-northeast, perpendicularly crossing the first beneath the volcano, which appears to have grown within a small pull-apart basin. Moreover, Parsons and others (1998) interpret a discontinuity in seismic velocity structure beneath the St. Helens seismic zone to represent the inboard margin of Siletzia (fig. 25), an accreted Eocene basaltic seamount terrane as thick as 30 km that forms much of the Oregon-Washington forearc basement. Trace-element systematics (Smith and Leeman, 1987) indicate that the dacitic magmas so characteristic of Mount St. Helens are not fractionated from basaltic magma

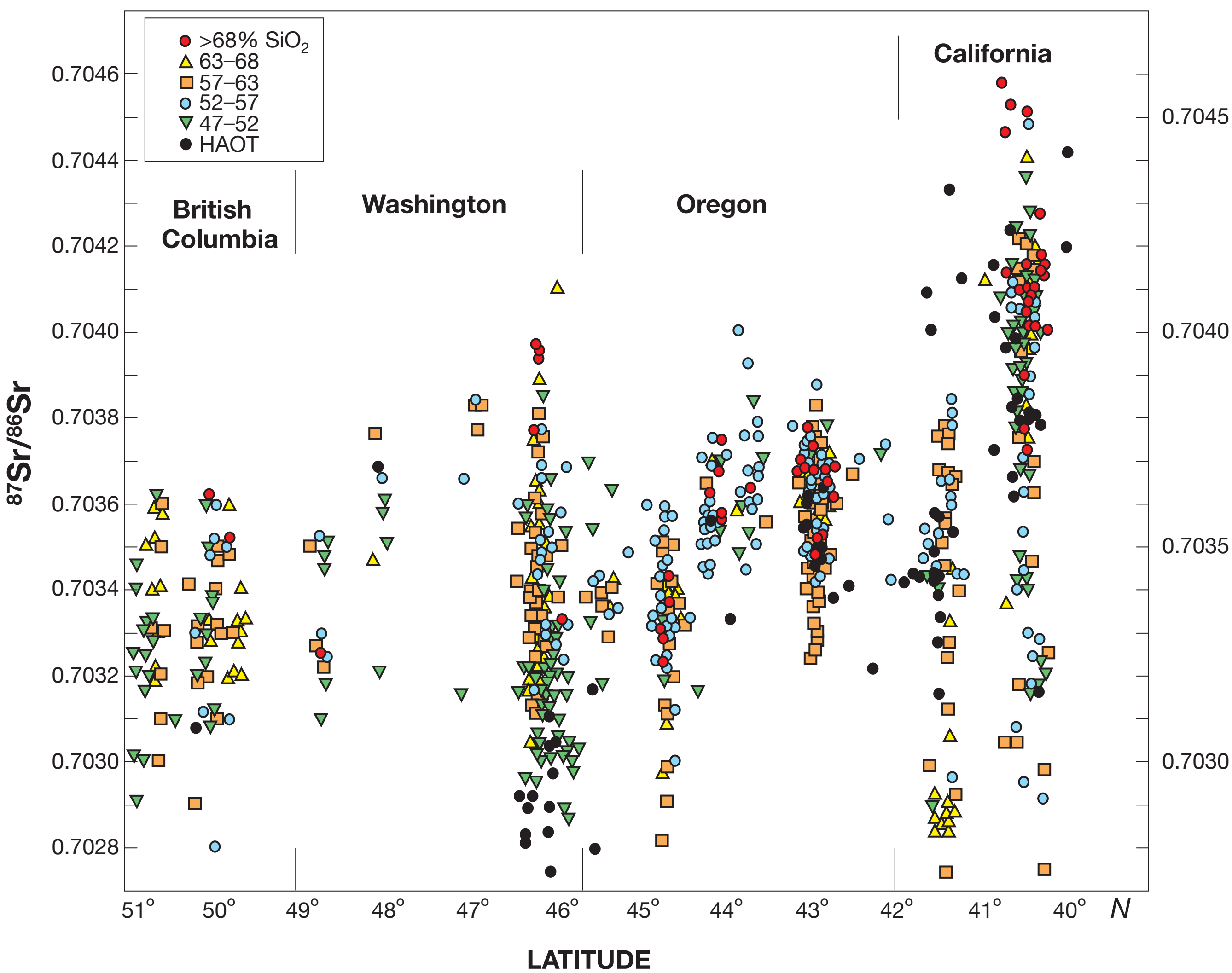

Figure 29. Sr isotope data plotted versus latitude for the Quaternary Cascades. Explanation of symbols in inset: HAOT (LKOT) 47-50 percent SiO_2; other basalts 47-52 percent SiO_2; basaltic andesite 52-57 percent SiO_2; andesite 57-63 percent SiO_2; dacite 63-68 percent SiO_2; rhyodacite and rhyolite >68 percent SiO_2. Data sources: Bacon and others, 1994, 1997; Borg and others, 1997; Borg and Clynne, 1998; Bullen and Clynne, 1990; Conrey, Hooper, and others, 2001; Green and Sinha, 2005; Grove and others, 2002; Halliday and others, 1983; G.L. Hart and Hildreth, unpub. data; Hildreth and S. Moorbath, unpub. data; W.P. Leeman and Hildreth, unpub. data; Leeman and others, 1990; Schmidt, 2005; Smith, 1984.

but are produced by partial melting of hydrated basalt or gabbro in the deep crust. If a lower-plate influence is additionally important, such as some distortion or tearing of the slab that intensifies the flux of slab-derived fluid and/or wedge-derived wet basaltic magma into the lower forearc crust of Portland and southern Washington, then such effects do not extend 50 km east of Mount St. Helens, where the andesite-dacite products of Mount Adams lack hydrous phenocrysts, generally erupt effusively, and are surrounded by an array of peripheral vents that include HAOT and alkalic basalt.

The area close to Mount Jefferson is one of the narrowest reaches in the Cascade arc, as defined by Quaternary vent distribution (fig. 14). An axial strip that includes the stratocone has maintained throughout the Quaternary what is probably the lowest proportion of mafic volcanic rocks in the Oregon Cascades (Conrey, 1991). Eruption of intermediate and silicic products along a high-vent-density (table 1) strip narrower than it is long (10x20 km; fig. 14), almost to the exclusion of mafic products for 2 Myr or more, supports the notion of tightly focussed mantle input engendering a long-lived, partially molten, MASH domain virtually impenetrable by basalt.

The regional "fabric" of volcanism—vent distribution, vent density, and the time-volume-compositional record of eruptions—encourages certain inferences about deeper magmatic processes beneath the Cascades. (1) Vent alignments, where not edifice-influenced, are largely controlled by stress orientation and structure in the brittle upper crust. (2) Magmatic shadow zones operate at two levels—in the deep crust, where MASH domains intercept basalts at the base of long-lived magma columns, and in the upper crust, where intermediate magma reservoirs prevent throughput of all but their own differentiates. (3) Within mafic volcanic fields in and adjacent to the Cascades (Caribou, Medicine Lake, Bachelor, Belknap, Newberry, Indian Heaven, Adams periphery, Simcoe), no secular patterns or stages of compositional evolution are recognized (as, say, in Hawaii); typically, instead, reversals and alternations occur among tholeiitic, alkalic, and arc basalts, primitive basalts and mafic andesites, and even sporadic eruptions of silicic magmas. Batches from separate sources and with different paths of hybridization and fractionation remain concurrently available. (4) Most magmatism is local. Each volcanic field evolves independently of others along the arc. If a field is subjected to long-term extension or focussed mantle upwelling, some secular shift in source compositions or differentiation processes can be expected to modify the suite of magma types being erupted there. (5) There is no secular evolution at major stratovolcanoes from andesite to dacite; both recur throughout edifice lifetimes. (6) There is no systematic drift toward rhyolite production, which instead depends on establishment of large fractionating reservoirs of intermediate magma that in turn reflect fluctuations in the basaltic power supply. Rhyodacite or rhyolite appeared *early* at Lassen (Rockland), Baker (Kulshan), and Simcoe; *late* at Maidu, Garibaldi, and Meager; *both* early and late at Mazama, Newberry, Medicine Lake, and St. Helens; and recurrently during the so-far short history of South Sister. (7) Most of the true rhyolite (≥72% SiO_2) in the Cascades erupted either in the rear-arc centers or along an extension of the across-Oregon progression beyond Newberry to Tumalo, South Sister, and Obsidian Cliffs. (8) Mafic vent density is lowest in the compressional GVB and greatest in patently extensional areas, notably Indian Heaven, the Bachelor-Belknap region, Caribou, and the three big rear-arc volcanic fields. (9) Lack of extension in the GVB reduces also the number of evolved volcanic loci, both along and across the arc (fig. 3). And (10) the greater proportion of basalts across southern Washington (and Portland) and across the Lassen segment contrasts with the dominance of basaltic andesite among the Quaternary mafic rocks of the Oregon Cascades. It seems unlikely that a significantly more fusible crustal column would be responsible for diluting the mantle input preferentially beneath Oregon, because dacitic and silicic volcanic rocks are plentiful at the major centers in all three regions. Tectonically influenced vent alignments are also prominent in all three regions, though the observation that the proportion of basalt attains a maximum for Oregon in the Bachelor area, where such vent alignments are best developed, lends plausibility to the expectation that tectonic extension can favor unimpeded ascent of basaltic magma. The broader vent belts of southern Washington and northern California may simply reflect more widely distributed extension that provides more paths for basalt to the surface than does the more narrowly constrained extensional vent belt of the Oregon Cascades, where more concentrated basaltic flux may increase deep-crustal melting and impede magma transit, causing greater degrees of fractionation and reprocessing to be the norm.

K_2O Asymmetry Across the Cascade Arc?

Ever since the suggestion that the potassium content (K) of arc magma suites might correlate with depth (h) of the subducting slab beneath their volcanic centers (Dickinson and Hatherton, 1967), the search for across-arc patterns in concentrations of K (and other LILE and isotope ratios) has been pursued by many investigators (for example, Hickey and others, 1986; Luhr, 1992; Stern and others, 1993; Ryan and others, 1995; Tatsumi and Eggins, 1995; Patino and others, 1997; Hildreth, Fierstein, and others, 2004). In the Cascades, the search might seem futile because of the widespread distribution of low-K HAOT along, across, and inboard of the arc and because of the great range of K contents among the diverse basalts at several individual loci. For example, in the area close to Mount Adams, the K_2O content of fairly primitive basalts (at 48 percent SiO_2) ranges from 0.1 to 1.6 percent (Hildreth and Lanphere, 1994).

If a cross-arc K-h correlation were held to originate with the basaltic members of suites starting in the mantle, then processes potentially responsible could include, first, a set of those that are linked to slab depth itself—(1) progressively smaller melt fractions inboard from the volcanic front owing to a diminishing flux of slab-derived fluid with slab depth; (2) greater secular depletion of the wedge source below the volcanic front where the slab flux is most intensive; and (3) pressure-dependent breakdown of K-poor hydrous phases at shallower slab depths and K-richer ones (phengite, phlogopite) at greater depths. Second, a set of influences *independent* of slab depth could contribute across-arc geochemical asymmetries to the magmas—(1) the sub-arc mantle wedge might inherit an initial lateral gradient from subcontinental inboard to more oceanic outboard; (2) the sub-arc lithosphere might similarly inherit a gradient from more potassic and thicker inboard to thinner oceanic or accreted terranes outboard; (3) the inboard mantle lithosphere might be older than that beneath the front and thus more enriched by secular veining from below; (4) rear-arc extension might promote decompression melting of a secularly enriched mantle lithosphere that contributes less to magmas that penetrate unextended parts of the arc; (5) rear-arc extension might promote separation of low-melt-fraction alkalic magmas from mantle upwellings unfluxed by slab contributions; and (6) the upper limb of the mantle-wedge convective counterflow might draw more potassic inboard mantle toward rear-arc and sub-arc melting domains, where melt extraction would then impose progressive depletion trenchward. All nine possibilities are feasible, so geochemical asymmetries across broad arcs should not be unexpected, but the second set of six involves conditions or processes not tied to slab depth; and intraplate alkali basalts (on which many supposed K-h correlations depend) are not arc magmas at all. In some arcs the nine potentially contributing factors are assembled more systematically than in the Cascades, where accretionary lithosphere, varied basement terranes, a warm warped slab, highly heterogeneous mantle, and latitudinally uneven rear-arc and intra-arc extension severely complicate the relative influences.

We need to recall, however, that the original K-h observation by Dickinson and Hatherton (1967) emphasized K contents of *andesitic* suites (normalized at 55 or 60% SiO_2), not basalts, as in those early years of the subduction paradigm many investigators thought that andesitic magmas were primary. If, instead, most andesites are hybrids that have assimilated crustal contributions, the possibility of across-arc gradients in age and composition of the crustal assimilants should be added to the list of factors potentially producing geochemical asymmetry.

In the Cascades, the segments where any pattern of across-arc asymmetry might be best discerned (through the confusion of mixed magmas and fields of interspersed vents for arc and non-arc basalts) could be expected to be the broadest ones, southern Washington and the Lassen segment. Indeed, ignoring HAOT, the mafic arc lavas of a 60-km-wide transect of the Quaternary Lassen segment show a rough tendency for K, Fe, P, HFSE, REE, Ba, and Th to increase eastward (Borg and others, 1997; Clynne and Borg, 1997). These investigators emphasized the dual importance of increasingly fertile (less depleted) mantle inboard and diminishing intensity of the slab-fluid flux inboard. On the other hand, for the southern Washington-to-Portland transect, where HAOT and alkali-basalt vents are closely interspersed with those for arc basalts across the entire 160-km width of the volcanic belt, Leeman and others (1990, 2004, 2005) found among the arc basalts only random scattering of K_2O contents and no systematic across-arc pattern at all in incompatible elements or radiogenic isotope ratios. Moreover, for the eruptive suites in southern Washington, a K_2O-SiO_2 plot (fig. 30) shows large-scale overlap among the four west-to-east volcanic fields and a great range of K_2O among the basalts of each suite. In the basaltic-to-silicic andesite range (52-63% SiO_2), it can generally be argued that the K_2O arrays increase inboard (fig. 30), but one needs statistics to affirm it.

Continuing Quest for Clarity

A great variety of investigations into convergent-margin processes has contributed over recent decades to improving our understanding of arc magmatism globally, as in the Cascades. In contrast to a generation ago, there is now considerable agreement (though seldom unanimity) that the following points are fairly well established. (1) The fundamental basis of plate-margin arc magmatism is mobilization from a subducting plate of a water-rich contribution that ascends into a convecting mantle wedge, where it enhances partial melting and buoyancy. (2) Because the wedge is cooler above, below, and at its outboard corner than within its core, melting paths are influenced by reversal of the thermal gradient as well as by decompression and by lateral and temporal variations in concentration of the slab-derived contribution. (3) Decompression melting of drier mantle domains (little influenced by proximate slab contributions) takes place concurrently, more so in the Cascades than in other continental-margin arcs, presumably in response to pressure release by intra-arc and rear-arc tectonic extension. (4) Several primitive mantle-derived magmas coexist. Most are Mg-rich basalts, but a few Mg-rich andesites may also be near-primary partial melts of mantle peridotite (harzburgite) previously melt-depleted but strongly refluxed by water-rich slab-derived contributions. (5) When hot mantle magmas penetrate the crust, crustal contributions are inevitable and ubiquitous, but they range widely in magnitude. Basaltic magma intrudes the base of the crust all along and across the arc, but the crust modulates its transit and traps most of it. (6) The deep-crustal melting caused by injection of batches of basaltic magma might sometimes involve ancient rocks but principally entails remelting arc gabbros and their differentiates—the arc plutonic rocks that constructed the deep Cascadian arc crust during the past 40 Myr. A few arc andesites and dacites may be near-primary partial melts of such (relatively young) mafic crust, but most are complexly hybrid blends of crustal and juvenile basaltic contributions. Deep-crustal HAOT gabbro may likewise have begun to play such a role after the onset of intra-arc extension around 7 to 5 Ma, perhaps contributing partial remelts to the LILE-deficient basaltic andesites common in the Oregon Cascades (Hughes, 1990; Schmidt, 2005). (7) The few large mafic volcanoes as well as the myriad small ones are fed from deep-crustal reservoirs that incorporate only modest crustal contributions. And (8) the large long-lived andesite-dacite stratocones and domefields are supplied by crustal columns rooted in major deep-crustal domains of melting, fractionation, and hybridization that fluctuate thermally with variations in intensity of focussed mantle input. Most such columns also accumulate upper-crustal reservoirs, in which crystallization-differentiation is extensive when

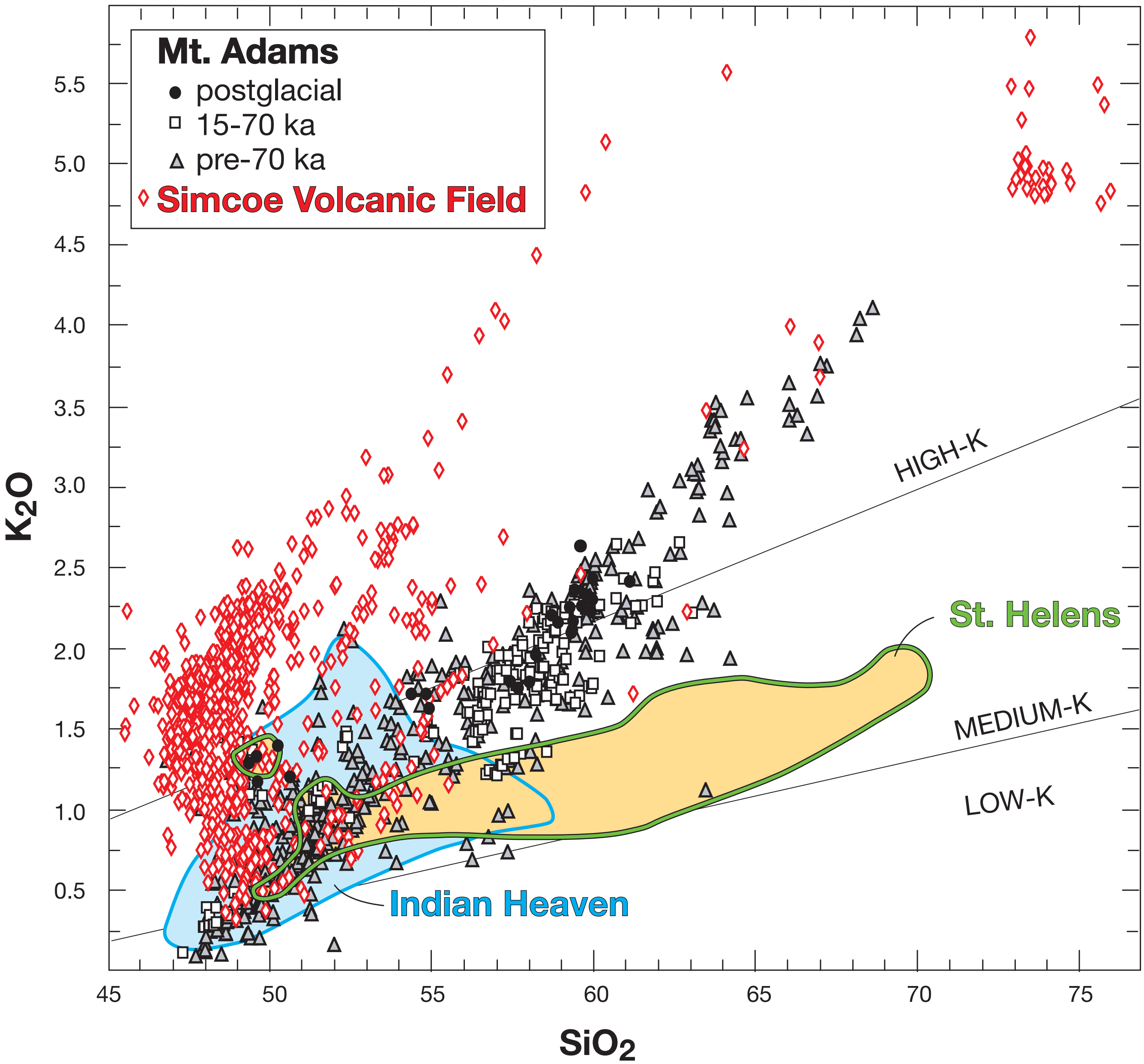

Figure 30. K_2O versus SiO_2 contents (in weight percent, normalized to 100 percent volatile-free) of products of vents distributed across southern Washington (fig. 8), grouped by volcanic field—from west to east, Mount St. Helens (n>300), Indian Heaven (n>100), Mount Adams (n>700), and Simcoe Mountains Volcanic Field (n>700). K_2O contents of andesites (at 58 pecent SiO_2) are 0.8 to 1.4 percent at St. Helens, ~1.0 percent at Indian Heaven, 1.3 to 2.4 percent at Adams, and 2.2 to 4.4 percent in the Simcoe field. Data sources: Clynne and others (in press); Hammond and Korosec (1983); Hildreth and J. Fierstein, unpub. data; Hildreth and Lanphere (1994); Korosec (1989); Leeman and others (1990, 2005); Smith and Leeman (1987, 1993). Higher-K set of St. Helens basalts erupted centrally during the interval 2.5-1.9 ka, as did many of the lower-K basalts at that volcano.

magmas attain water saturation; they build plutons and may or may not fractionate melt-rich caps of rhyodacite or rhyolite.

In contrast, understanding of the following matters could be said to range from limited clarity to downright poor; all deserve continued investigation. (1) What is the composition of the slab-derived contribution? If its release into the wedge is pulsed rather than continuous, how compositionally varied are the batches? (2) How widely is partial melt present in the sub-arc mantle wedge? Is wedge convection continuous or pulsed and how does its motion affect melting and melt coalescence? What causes melt-ascent paths that reach the lithosphere to be locally focussed or intensified? (3) Prior to melting or ascent, what were the spatial relations among the mantle domains that yielded contrasting HAOT, alkalic, and arc basalts? Were they dispersed randomly (like plums in pudding), layers at different depths, melting columns contrasting with ambient host mantle, or convecting asthenospheric mantle vis-à-vis remobilized lithosphere? How might the rheology of dry and wet upwellings differ? (4) How much pre-arc lithospheric mantle survives as such beneath a long-lived magmatic arc? Where partially melted and remobilized during arc magmatism, does such former lithosphere then participate in wedge convection and to what extent does it contribute to arc magmas? (5) Why is the intensely focussed basaltic flux that pins MASH domains (and the derivative crustal ascent columns that feed upper-crustal reservoirs and stratovolcanoes) maintained for million-year intervals but limited at a given time to only a few sites along an arc? (6) Why do so many mafic volcanic fields and intermediate stratovolcanoes alike have apparent longevities in the range 0.5 to 1.5 Myr? (7) Away from the basalt-entrapping MASH domains, what controls the rates of crustal throughput for batches of basalt? Why do a few erupt with still-primitive compositions while most stall, fractionate, and assimilate their envelope, evolving to low-Mg basalt or basaltic andesite during transient intra crustal storage? (8) What causes a few long-lived andesite-dacite centers to initiate episodes of voluminous rhyodacite or rhyolite melt production while most do not? (9) Do the lengthy gaps along the arc (table 5) that lack volcanic activity for millions of years at a time reflect muffling of magmatism (as favored here) by a tight lithosphere? Or is there some property or behavior of the slab or wedge that temporarily reduces melt production or coalescence along such reaches? And (10) what proportion of the intracrustal magma system beneath a long-lived volcanic center fails to erupt? Is the eruptive/intrusive ratio far greater for a mafic stratocone or shield than for a major andesite-dacite center (as favored here)? Or does the former leave behind a proportionally large mafic-ultramafic intrusion in the lower crust? For a big evolved system, how is the total intrusive mass partitioned among deep-crustal cumulates, varied hybrid restites, deep to shallow plutons, and leftovers distributed as sheets, pods, and conduit-fills along the whole crustal column?

There are many uncertainties and interesting questions to be worked out by the next generation. Promising investigations include not only new theoretical, geochemical, and geophysical approaches to convergent-margin processes but detailed field studies to work out the time-volume-compositional evolution of Cascadian magmas, in systems large and small, mafic and evolved, volcanic and plutonic, Tertiary and Quaternary, and (whenever possible) with attention to measurable rates of concurrent tectonic and magmatic processes. The progress report and overview presented here nonetheless makes clear that modeling the Cascades as consisting of a few big andesite-dacite centers misses the essence of the arc, which is better expressed by the 2000 mafic vents that map out the wide distribution of sub-arc magmatism.

Acknowledgments

This overview was initiated at the invitation of George Bergantz, organizer of the Cascadia keynote symposium of the 1994 GSA Annual Meeting in Seattle (Hildreth, 1994), and it was resurrected a decade later at the behest of Jeff Wynn, chief of the USGS Volcano Hazards Team. Reviews and comments that improved the clarity and accuracy of the long manuscript were provided by Bob Christiansen, Mike Clynne, Julie Donnelly-Nolan, Judy Fierstein, Don Swanson, and Willie Scott, to all of whom I am truly grateful. Meticulous scrutiny by USGS editor Jim Hendley polished the presentation and achieved suitable accommodation between stylistic convention and the author's eccentricities. I also thank Kelly Russell, Melanie Kelman, Patrick Muffler, and Willie Scott for providing fine photographs, and especially my friend and lifelong champion of Mount Adams, Darryl Lloyd, for his fine images of the Guardians of the Columbia. My perspectives elaborated in this paper are an outgrowth of three decades of authentic geologic mapping in the Cascades, principally by my colleagues in the USGS Geothermal Research and Volcano Hazards Programs, spearheaded and spurred foremost by L.J. Patrick Muffler. Major contributors have been Charlie Bacon, Duane Champion, Bob Christiansen, Mike Clynne, Rocky Crandell, Julie Donnelly-Nolan, Russ Evarts, Judy Fierstein, Cynthia Gardner, Norm MacLeod, Dan Miller, Patrick Muffler, Don Mullineaux, Kevin Scott, Willie Scott, Dave Sherrod, Jim Smith, Tom Sisson, Don Swanson, and Ed Wolfe. The perspectives, however, are my own, and those colleagues are not responsible for any errors, omissions, or misinterpretations. As new data come in, ideas will inevitably and properly change; all geologic studies are progress reports. The high-precision geochronology of Marvin Lanphere and Andy Calvert, particularly in dating late Pleistocene eruptive products, has been crucial in advancing our understanding of the rates of magmatic processes. Outside the USGS, the contributions of Rick Conrey, Nathan Green, Paul Hammond, Cathie Hickson, Cliff Hopson, Bill Mathews, Kelly Russell, Jack Souther, and Ed Taylor have been especially important. Howel Williams, of course, got it all started and covered more of the Cascades than most of us. During my 27 summers in the Cascades, scarcely a week went by when I didn't muse on the vitality, insight, and promise of my long-lost field pardner, Dave Johnston, who was swept away in the blast of May 18th, 1980 (see Hildreth, 1981b). In one sense, my field investigations in the Cascades and Alaska have always, I think, been dedicated to the recognition that I was privileged to carry on and Dave wasn't.

References

Allen, J.E., 1975, Volcanoes of the Portland area, Oregon: Oregon Department of Geology and Mineral Industries, The Ore Bin, v. 37, no. 9, p. 145-157.

Anderson, A.T., 1971, Alkali-rich SiO_2-deficient glasses in high-alumina olivine tholeiite, Hat Creek Valley, California: American Journal of Science, v. 271, p. 293-303.

Anderson, A.T., 1974, Evidence for a picritic volatile-rich magma beneath Mt. Shasta, California: Journal of Petrology, v. 15, p. 243-267.

Anderson, A.T., and Gottfried, D., 1971, Contrasting behavior of P, Ti, and Nb in a differentiated high-aluminum olivine tholeiite and a calc-alkaline andesitic suite: Geological Society of America Bulletin, v. 82, p. 1929-1942.

Anderson, C.A., 1940, Hat Creek lava flow: American Journal of Science, v. 238, p. 477-492.

Anderson, C.A., 1941, Volcanoes of the Medicine Lake Highland, California: University of California Publications, Bulletin of the Department of Geological Sciences, v. 25, no. 7, p. 347-422.

Aramaki, S, and Ui, T., 1982, Japan, *in* Thorpe, R.S., ed., Andesites: John Wiley & Sons, p. 259-292.

Atwater, T., 1970, Implications of plate tectonics for the Cenozoic evolution of western North America: Geological Society of America Bulletin, v. 81. p. 3513-3536.

Bacon, C.R., 1983, Eruptive history of Mount Mazama and Crater Lake caldera, Cascade Range, U.S.A.: Journal of Volcanology and Geothermal Research, v. 18, p. 57-115.

Bacon, C.R., 1985, Implications of silicic vent patterns for the presence of large crustal magma chambers: Journal of Geophysical Research, v. 90, p. 11243-11252.

Bacon, C.R., 1990, Calc-alkaline, shoshonitic, and primitive tholeiitic lavas from monogenetic volcanoes near Crater Lake, Oregon: Journal of Petrology, v. 31, p. 135-166.

Bacon, C.R., 1992, Partially melted granodiorite and related rocks ejected from Crater Lake caldera, Oregon: Transactions of the Royal Society of Edinburgh, v. 83, p. 27-47.

Bacon, C.R., 2005, Magma sheets and other contributions to the Quaternary pluton under Crater Lake caldera, Oregon: Geological Society of America Abstracts with Programs, abstract 254-11.

Bacon, C.R., 2007, Geologic map of Mount Mazama and Crater Lake caldera, Oregon: U.S. Geological Survey Scientific Investigations Map SIM-2382, scale 1:24,000.

Bacon, C.R., Bruggman, P.E., Christiansen, R.L., Clynne, M.A., Donnelly-Nolan, J.M., and Hildreth, W., 1997, Primitive magmas at five Cascade volcanic fields: Melts from hot, heterogeneous sub-arc mantle: Canadian Mineralogist, v. 35, p. 397-423.

Bacon, C.R., and Druitt, T.H., 1988, Compositional evolution of the zoned calcalkaline magma chamber of Mount Mazama, Crater Lake, Oregon: Contributions to Mineralogy and Petrology, v. 98, p. 224-256.

Bacon, C.R., Gardner, J.V., Mayer, L.A., Buktenica, M.W., Dartnell, P., Ramsey, D.W., and Robinson, J.E., 2002, Morphology, volcanism, and mass wasting in Crater Lake, Oregon: Geological Society of America Bulletin, v. 114, p. 675-692.

Bacon, C.R., Gunn, S.H., Lanphere, M.A., and Wooden, J.L., 1994, Multiple isotopic components in Quaternary volcanic rocks of the Cascade arc near Crater Lake, Oregon: Journal of Petrology, v. 35, p. 1521-1556.

Bacon, C.R., and Lanphere, M.A., 1990, The geologic setting of Crater Lake, Oregon, *in* Drake, E.T., Larson, G.L., Dymond, J., and Collier, R., eds., Crater Lake—An ecosystem study: San Francisco, Pacific Division of the American Association for the Advancement of Science, p. 19-27.

Bacon, C.R., and Lanphere, M.A., 2006, Eruptive history of Mount Mazama and the Crater Lake region, Oregon: Geological Society of America Bulletin, v. 118, p. 1331-1359.

Bacon, C.R., Lanphere, M.A., and Champion, D.E., 1999, Late Quaternary slip rate and seismic hazards of the West Klamath Lake fault zone near Crater Lake, Oregon Cascades: Geology, v. 27, p. 43-46.

Bacon, C.R., Lanphere, M.A., and Lowenstern, J.B., 2005, Eruptive and intrusive history of Mount Mazama explains growth of a young silicic magma body: Eos, Joint Assembly Supplement, v. 86, no. 18, abstract V22A-02.

Bacon, C.R., and Lowenstern, J.B., 2005, Late Pleistocene granodiorite source for recycled zircon and phenocrysts in rhyodacite lava at Crater Lake, Oregon: Earth and Planetary Science Letters, v. 233, p. 277-293.

Bacon, C.R., and Nathenson, M., 1996, Geothermal resources in the Crater Lake area, Oregon: U.S. Geological Survey Open-File Report 96-663, 34 p.

Bacon, C.R., Persing, H.M., Wooden, J.L., and Ireland, 2000, Late Pleistocene granodiorite beneath Crater Lake caldera, Oregon, dated by ion microprobe: Geology, v. 28, no. 5, p. 467-470.

Baker, M.B., Grove, T.L., Kinzler, R.J., Donnelly-Nolan, J.N., and Wandless, G.A., 1991, Origin of compositional zonation (high-alumina basalt to basaltic andesite) in the Giant Crater Lava Field, Medicine Lake volcano, northern California: Journal of Geophysical Research, v. 96, p. 21819-21842.

Baker, M.B., Grove, T.L., and Price, R., 1994, Primitive basalts and andesites from the Mt. Shasta region, N. California—Products of varying melt fraction and water content: Contributions to Mineralogy and Petrology, v. 118, p. 111-119.

Barnes, C.G., 1992, Petrology of monogenetic volcanoes, Mount Bailey area, Cascade Range, Oregon: Journal of Volcanology and Geothermal Research, v. 52, p. 141-156.

Bartels, K.S., Kinzler, R.J., and Grove, T.L., 1991, High pressure phase relations of primitive high-alumina basalts from Medicine Lake volcano, northern California: Contributions to Mineralogy and Petrology, v. 108, p. 253-270.

Beaudoin, B.C., Hole, J.A., Klemperer, S.L., and Tréhu, A.M., 1998, Location of the southern edge of the Gorda slab and evidence for an adjacent asthenospheric window: Results from seismic profiling and gravity: Journal of Geophysical Research, v. 103, p. 30101-30115.

Beeson, M.H., and Tolan, T.L., 1990, The Columbia River Basalt Group in the Cascade Range: A Middle Miocene reference datum for structural analysis: Journal of Geophysical Research, v. 95, p. 19547-19559.

Beget, J.E., 1981, Evidence of Pleistocene explosive eruptions of Mount Jefferson, Oregon: Eos, Transactions American Geophysical Union, v. 62, p. 1089.

Beget, J.E., 1982a, Postglacial volcanic deposits at Glacier Peak, Washington, and potential hazards from future eruptions: U.S. Geological Survey Open-File Report 82-830, 77 p.

Beget, J.E., 1982b, Recent volcanic activity at Glacier Peak: Science, v. 215, p. 1389-1390.

Beget, J.E., 1984, Tephrochronology of late Wisconsin deglaciation and Holocene glacier fluctuations near Glacier Peak, North Cascade Range, Washington: Quaternary Research, v. 21, p. 304-316.

Benson, L.V., Smoot, J.P., Kashgarian, M., Sarna-Wojcicki, A., and Burdett, J.W., 1997, Radiocarbon ages and environments of deposition of the Wono and Trego Hot Springs tephra layers in the Pyramid Lake subbasin, Nevada: Quaternary Research, v. 47, p. 251-260.

Bentley, R.D., Anderson, J.L., Campbell, N.P., and Swanson, D.A., 1980, Stratigraphy and structure of the Yakima Indian Reservation, with emphasis on the Columbia River Basalt Group: U.S. Geological Survey Open-File Report 80-200, 83 p.

Benz, H.M., Zandt, G., and Oppenheimer, D.H., 1992, Lithospheric structure of northern California from teleseismic images of the upper mantle: Journal of Geophysical Research, v. 97, p. 4791-4807.

Berge, P.A., and Stauber, D.A., 1987, Seismic refraction study of upper crustal structure in the Lassen Peak area, northern California: Journal of Geophysical Research, v. 92, p. 10571- 10579.

Berman, R.G., and Armstrong, R.L., 1980, Geology of the Coquihalla volcanic complex, southwestern British Columbia: Canadian Journal of Earth Sciences, v. 17, p. 985-995.

Black, G.L., Woller, N.M., and Ferns, M.L., 1987, Geologic map of the Crescent Mountain area, Linn County, Oregon: Oregon Department of Geology and Mineral Industries, Geologic Map Series, GMS-47, scale 1:62,000.

Blackwell, D.D., Steele, J.L., and Kelley, S., 1990, Heat flow in the state of Washington and thermal conditions in the Cascade Range: Journal of Geophysical Research, v. 95,p. 19495-19516.

Blakely, R.J., Christiansen, R.L., Guffanti, M., Wells, R.E., Donnelly-Nolan, J.M., Muffler, L.J.P., Clynne, M.A., and Smith, J.G., 1997, Gravity anomalies, Quaternary vents, and Quaternary faults in the southern Cascade Range, Oregon and California: Implications for arc and backarc evolution: Journal of Geophysical Research, v. 102, p. 22513-22527.

Borg, L.E., 1989, Petrogenesis of Magee composite volcano, northern California: University of Texas at Austin, M.A. Thesis, 128 p.

Borg, L.E., Blichert-Toft, J., and Clynne, M.A., 2002, Ancient and modern subduction zone contributions to the mantle sources of lavas from the Lassen region of California inferred from Lu-Hf isotopic systematics: Journal of Petrology, v. 43, p. 705-723.

Borg, L.E., Brandon, A.D., Clynne, M.A., and Walker, R.J., 2000, Re-Os isotopic systematics of primitive lavas from the Lassen region of the Cascade arc, California: Earth and Planetary Science Letters, v. 177, p. 301-317.

Borg, L.E., and Clynne, M.A., 1998, The petrogenesis of felsic calc-alkaline magmas from the southernmost Cascades, California—Origin by partial melting of basaltic lower crust: Journal of Petrology, v. 39, p. 1197-1222.

Borg, L.E., Clynne, M.A., and Bullen, T.D., 1997, The variable role of slab-derived fluids in the generation of a suite of primitive calc-alkaline lavas from the southernmost Cascades, Calfornia: Canadian Mineralogist, v. 35, p. 425-452.

Bostock, M.G., and VanDecar, J.C., 1995, Upper mantle structure of the northern Cascadia subduction zone: Canadian Journal of Earth Sciences, v. 32, p. 1-12.

Bostock, M.G., Hyndman, R.D., Rondenay, S., and Peacock, S.M., 2002, An inverted continental Moho and serpentinization of the forearc mantle: Nature, v. 417, p. 536-538.

Brandon, A.D., and Draper, D.S., 1996, Constraints on the origin of the oxidation state of mantle overlying subduction zones: An example from Simcoe, Washington, USA: Geochimica et Cosmochimica Acta, v. 60, p. 1739-1749.

Brantley, S.R., and Myers, B., 2000, Mount St. Helens—From the 1980 eruption to 2000: U.S. Geological Survey Fact Sheet 036-00, 2 p. [http://pubs.usgs.gov/fs/2000/fs036-00/].

Brocher, T.M., Parsons, T.E., Tréhu, A.M., Snelson, C.M., and Fisher, M.A., 2003, Seismic evidence for widespread serpentinized forearc upper mantle along the Cascadia margin: Geology, v. 31, p. 267-270.

Brooks, G.R., and Friele, P.A., 1992, Bracketing ages for the formation of the Ring Creek lava flow, Mount Garibaldi volcanic field, southwestern British Columbia: Canadian Journal of Earth Sciences, v. 29, p. 2425-2428.

Brown, S.J.A., and Fletcher, I.R., 1999, SHRIMP U-Pb dating of the preeruption growth history of zircons from the 340 ka Whakamaru Ignimbrite, New Zealand—Evidence for >250 k.y. magma residence times: Geology, v. 27, p. 1035-1038.

Bullen, T.D., and Clynne, M.A., 1990, Trace element and isotopic constraints on magmatic evolution at Lassen volcanic center: Journal of Geophysical Research, v. 95, p. 19671-19691.

Busacca, A.J., Nelstead, K.T., McDonald, E.V., and Purser, M.D., 1992, Correlation of distal tephra layers in loess in the Channeled Scabland and Palouse of Washington state: Quaternary Research, v. 37, p. 281-303.

Bye, A., Edwards, B.R., and Hickson, C.J., 2000, Preliminary field, petrographic, and geochemical analysis of possible subglacial, dacitic volcanism at the Watts Point volcanic centre, southwestern British Columbia: Geological Survey of Canada Current Research 2000-A20, p. 1-9.

Campbell, N.P., 1989, Structural and stratigraphic interpretation of rocks under the Yakima fold belt, Columbia Basin, based on recent surface mapping and well data: Geological Society of America Special Paper 239, p. 209-222.

Campbell, N.P., and Bentley, R.D., 1981, Late Quaternary deformation of the Toppenish Ridge uplift in south-central Washington: Geology, v. 9, p. 519-524.

Canil, D., and Scarfe, C.M., 1989, Origin of phlogopite in mantle xenoliths from Kostal Lake, Wells Gray Park, British Columbia: Journal of Petrology, v. 30, p. 1159-1179.

Carey, S., Gardner, J., and Sigurdsson, H., 1995, The intensity and magnitude of Holocene plinian eruptions from Mount St. Helens volcano: Journal of Volcanology and Geothermal Research, v. 66, p. 185-202.

Carmichael, I.S.E., Lange, R.A., and Luhr, J.F., 1996, Quaternary minettes and associated volcanic rocks of Mascota, western Mexico—A consequence of plate extension above a subduction modified mantle wedge: Contributions to Mineralogy and Petrology, v. 124, p. 302-333.

Carmichael, I.S.E., Lange, R.A., Hall, C.M., and Renne, P.R., 2006, Faulted and tilted Pliocene olivine-tholeiite lavas near Alturas, NE California, and their bearing on the uplift of the Warner Range: Geological Society of America Bulletin, v. 118, p. 1196-1211.

Carr, M.J., Feigenson, M.D., Patino, L.C., and Walker, J.A., 2003, Volcanism and geochemistry in Central America—Progress and problems, *in* Eiler, J., ed, Inside the Subduction Factory: American Geophysical Union, Geophysical Monograph 138, p. 153-174.

Chadwick, W.W., Jr., and Howard, K.A., 1991, The pattern of circumferential and radial eruptive fissures on the volcanoes of Fernandina and Isabela Islands, Galápagos: Bulletin of Volcanology, v. 53, p. 259-275.

Charlier, B.L.A., Wilson, C.J.N., Lowenstern, J.B., Blake, S., Van Calsteren, P.W., and Davidson, J.P., 2005, Magma generation at a large, hyperactive silicic volcano (Taupo, New Zealand) revealed by U-Th and U-Pb systematics in zircons: Journal of Petrology, v. 46, p. 3-32.

Christiansen, R.L., 1982, Volcanic hazard potential in the California Cascades, *in* Martin, R.C., and Davis, J.F., eds., Status of volcanic prediction and emergency response capabilities in volcanic hazard zones of California: California Division of Mines and Geology Special Publication 63, p. 41-59.

Christiansen, R.L., 1985, The Mount Shasta magmatic system, *in* Guffanti, M., and Muffler, L.J.P., eds., Proceedings of the Workshop on Geothermal Resources of the Cascade Range: U.S. Geological Survey Open-File Report 85-521, p. 31-33.

Christiansen, R.L., 1990, Shasta, p. 214-216 *in* Wood, C.A., and Kienle, J., Volcanoes of North America: Cambridge University Press, 354 p.

Christiansen, R.L., 1996, Reorientation of crustal stress between Mount Shasta and Medicine Lake volcanoes, northern California Cascades: Eos, Transactions American Geophysical Union, v. 77, no. 46, p. F642-F643.

Christiansen, R.L., Clynne, M.A., and Muffler, L.J.P., 2002, Geologic map of the Lassen Peak, Chaos Crags, and upper Hat Creek area, California: U.S. Geological Survey Map I-2723, scales 1:24,000 and 1:2500; pamphlet 17 p.

Christiansen, R.L., and Miller, C.D., 1989, Mount Shasta and vicinity, *in* Muffler, L.J.P., leader, South Cascades arc volcanism, California and southern Oregon—Field Trip Guidebook T312, 28th International Geological Congress: Washington, D.C., American Geophysical Union, p. 42-52.

Christiansen, R.L., Kleinhampl, F.W., Blakely, R.J., Tuchek, E.T., Johnson, F.L., and Conyac, M.D., 1977, Resource appraisal of the Mt. Shasta Wilderness Study Area, Siskiyou County, California: U.S. Geological Survey Open-File Report 77-250, 53 p.

Christiansen, R.L., and Yeats, R.S., 1992, Post-Laramide geology of the U.S. Cordilleran region, *in* Burchfiel, B.C., Lipman, P.W., and Zoback, M.L., eds., The Cordilleran Orogen—Conterminous U.S.: Geological Society of America, The Geology of North America, v. G-3, p. 261-406.

Clague, J.J., and Souther, J.G., 1982, The Dusty Creek landslide on Mount Cayley, British Columbia: Canadian Journal of Earth Sciences, v. 19, p. 524-539.

Clark, J.G., 1983, Geology and petrology of South Sister volcano, High Cascade Range, Oregon: Ph.D. thesis, University of Oregon, Eugene, 235 p.

Clayton, G., 1980, Geology of White Pass—Tumac Mountain area, Washington: Washington Division of Geology and Earth Resources Open-File Report 80-8, scale 1:24,000.

Clayton, G., 1983, Geology of the White Pass area, south-central Cascade Range, Washington: Seattle, University of Washington, M.S. thesis, 212 p.

Clowes, R.M., Zelt, C.A., Amor, J.R., and Ellis, R.M., 1995, Lithospheric structure in the southern Canadian Cordillera from a network of seismic refraction lines: Canadian Journal of Earth Sciences, v. 32, p. 1485-1513.

Clynne, M.A., 1984, Stratigraphy and major element geochemistry of the Lassen Volcanic Center, California: U.S. Geological Survey Open-File Report 84-224, 168 p.

Clynne, M.A., 1989, Dissagregation of quenched magmatic inclusions contributes to chemical diversity in silicic lavas of Lassen Peak, California: New Mexico Bureau of Mines and Mineral Resources, Bulletin 131, p. 54.

Clynne, M.A., 1990a, Stratigraphic, lithologic, and major element geochemical constraints on magmatic evolution at Lassen volcanic center, California: Journal of Geophysical Research, v. 95, p. 19651-19669.

Clynne, M.A., 1990b, Lassen; Pre-Lassen Centers; and Lassen—Other Cones, *in* Wood, C.A., and Kienle, J., eds., Volcanoes of North America: Cambridge University Press, p. 216-222.

Clynne, M.A., 1993, Geologic studies of the Lassen volcanic center, Cascade Range, California: Ph.D dissertation, University of California, Santa Cruz, 404 p.

Clynne, M.A., 1999, Complex magma mixing origin for rocks erupted in 1915, Lassen Peak, California: Journal of Petrology, v. 40, p. 105-132,

Clynne, M.A., and Borg, L.E., 1997, Olivine and chromian spinel in primitive calc-alkaline and tholeiitic lavas from the southernmost Cascade Range, California—A reflection of relative source fertility: Canadian Mineralogist, v. 35, p. 453-472.

Clynne, M.A., Calvert, A.T., Wolfe, E.W., Evarts, R.C., Fleck, R.J., and Lanphere, M.A., in press, The Pleistocene eruptive history of Mount St. Helens, Washington, from 300,000 to 12,800 years before present, chap. 28 *of* Sherrod, D.R., Scott, W.E., and Stauffer, P.H., A volcano rekindled; the renewed eruption of Mount St. Helens, 2004-2006: U.S. Geological Survey Professional Paper 1750.

Clynne, M.A., Champion, D.E., Trimble, D.A., Hendley, J.W., II, and Stauffer, P.H., 2000, How old is "Cinder Cone"?—Solving a mystery in Lassen Volcanic National Park, California: U.S. Geological Survey Fact Sheet 023-00, 4 p.

Clynne, M.A., Christiansen, R.L., Trimble, D.A., and McGeehin, J.P., 2002, Radiocarbon dates from volcanic deposits of the Chaos Crags and Cinder Cone eruptive sequences and other deposits, Lassen Volcanic National Park, California: U.S. Geological Survey Open-File Report 2002-290, 21 p.

Clynne, M.A., and Muffler, L.J.P., 1989, Lassen Volcanic National Park and vicinity, *in* Muffler, L.J.P., leader, South Cascades arc volcanism, California and southern Oregon—Field Trip Guidebook T312, 28th International Geological Congress: Washington, D.C., American Geophysical Union, p. 2-15.

Clynne, M.A., and Muffler, L.J.P., 1990, Geologic map of the Lassen region, Cascade Range, USA: Geothermal Resources Council Transactions, v. 14, part 2, p. 1387-1389.

Clynne, M.A., and Muffler, L.J.P., in press, Geologic map of Lassen Volcanic National Park and vicinity, California: U.S. Geological Survey Map I-2899, scale 1:50,000.

Clynne, M.A., Ramsey, D.W., and Wolfe, E.W., 2005, Pre-1980 eruptive history of Mount St. Helens, Washington: U.S. Geological Survey Fact Sheet 2005-3045, 4 p.

Condie, K.C., and Swenson, D.H., 1973, Compositional variation in three Cascade stratovolcanoes: Jefferson, Rainier, and Shasta: Bulletin of Volcanology, v. 37, p. 205-230.

Conrey, R.M., 1991, Geology and petrology of the Mount Jefferson area, High Cascade region, Oregon: Washington State University, Pullman, Ph.D. dissertation, 357 p.

Conrey, R.M., 1998, Basaltic andesite volcanoes in the north-central Oregon High Cascade Range—Products of three component mixing: Eos, Transactions American Geophysical Union, v. 79, p. F968.

Conrey, R.M., 2002, Adakites—A review of slab melting over the past decade and the case for a slab-melt component in arcs: comment and reply: Eos, Transactions American Geophysical Union, v. 83, no. 23, p. 256-257.

Conrey, R.M., Donnelly-Nolan, J., Taylor, E.M., Champion, D., and Bullen, T., 2001, The Shevlin Park Tuff, central Oregon Cascades Range—Magmatic processes recorded in an arc-related ash-flow tuff: Eos, Transactions American Geophysical Union, v. 82, no. 47, Fall Meeting Supplement, Abstract V32D-0994.

Conrey, R.M., Hooper, P.R., Larson, P.B., Chesley, J., and Ruiz, J., 2001, Trace element and isotopic evidence for two types of crustal melting beneath a High Cascade volcanic center, Mt. Jefferson, Oregon: Contributions to Mineralogy and Petrology, v. 141, p. 710-732.

Conrey, R.M., Sherrod, D.R., Hooper, P.R., and Swanson, D.A., 1997, Diverse primitive magmas in the Cascade arc, northern Oregon and southern Washington: Canadian Mineralogist, v. 35, p. 367-396.

Conrey, R.M., Taylor, E.M., Donnelly-Nolan, J.M., and Sherrod, D.R., 2002, North-central Oregon Cascades: Exploring petrologic and tectonic intimacy in a propagating intra-arc rift, *in* Moore, G.W., ed., Field Guide to Geologic Processes in Cascadia: Oregon Department of Geology and Mineral Industries, Special Paper 36, p. 47-90.

Conrey, R.M., Uto, K., Uchiumi, S., Beeson, M.H., Madin, I.P., Tolan, T.L., and Swanson, D.A., 1996, Potassium-Argon ages of Boring Lava, northwest Oregon and southwest Washington: Isochron/West, no. 63, p. 3-9.

Conway, F.M., Ferrill, D.A., Hall, C.M., Morris, A.P., Stamatakos, J.A., Connor, C.B., Halliday, A.N., and Condit, C., 1997, Timing of basaltic volcanism along the Mesa Butte Fault in the San Francisco Volcanic Field, Arizona, from $^{40}Ar/^{39}Ar$ dates—Implications for longevity of cinder cone alignments: Journal of Geophysical Research, v. 102, p. 815-824.

Cook, F.A., 1995, The reflection Moho beneath the southern Canadian Cordillera: Canadian Journal of Earth Sciences, v. 32, p. 1520-1530.

Crandell, D.R., 1963, Surficial geology and geomorphology of the Lake Tapps quadrangle, Washington: U.S. Geological Survey Professional Paper 388-A, 84 p.

Crandell, D.R., 1971, Postglacial lahars from Mount Rainier volcano, Washington: U.S. Geological Survey Professional Paper 677, 75 p.

Crandell, D.R., 1980, Recent eruptive history of Mount Hood, Oregon, and potential hazards from future eruptions: U.S. Geological Survey Bulletin 1492, 81 p.

Crandell, D.R., 1987, Deposits of pre-1980 pyroclastic flows and lahars from Mount St. Helens volcano, Washington: U.S. Geological Survey Professional Paper 1444, 91 p.

Crandell, D.R., 1989, Gigantic debris avalanche of Pleistocene age from ancestral Mount Shasta volcano, California, and debris-avalanche hazard zonation: U.S. Geological Survey Bulletin 1861, 32 p.

Crandell, D.R., and Hoblitt, R.P., 1986, Lateral blasts at Mount St. Helens and hazard zonation: Bulletin of Volcanology, v. 48, p. 27-37.

Crandell, D.R., Miller, C.D., Glicken, H.X., Christiansen, R.L., and Newhall, C.G., 1984, Catastrophic debris avalanche from ancestral Mount Shasta volcano, California: Geology, v. 12, p. 143-146.

Crandell, D.R., Mullineaux, D.R., Sigafoos, R.S., and Rubin, M., 1974, Chaos Crags eruptions and rockfall avalanches, Lassen Volcanic National Park, California: Journal of Research, U.S. Geological Survey, v. 2, p. 49-59.

Criswell, C.W., 1987, Chronology and pyroclastic stratigraphy of the May 18, 1980, eruption of Mount St. Helens, Washington: Journal of Geophysical Research, v. 92, p. 10,237-10,266.

Crosson, R.S., and Owens, T.J., 1987, Slab geometry of the Cascadia subduction zone beneath Washington from earthquake hypocenters and teleseismic converted waves: Geophysical Research Letters, v. 14, p. 824-827.

Currie, C.A., Wang, K., Hyndman, R.D., and He, J., 2004, The thermal effects of steady-state slab-driven mantle flow above a subducting plate—The Cascadia subduction zone and back-arc: Earth and Planetary Science Letters, v. 223, p. 35-48.

Davies, J.H., and Stephenson, D.J., 1992, Physical model of source region of subduction zone volcanics: Journal of Geophysical Research, v. 97, p. 2037-2070.

Davis, J.O., 1978, Quaternary tephrochronology of the Lake Lahontan area, Nevada and California: University of Nevada, Reno, Nevada Archeological Survey, Research Paper 7.

Davis, J.O., 1985, Correlation of late Quaternary tephra layers in a long pluvial sequence near Summer Lake, Oregon: Quaternary Research, v. 23, p. 38-53.

Dawes, R.L., 1994, Mount St. Helens—Potential example of the partial melting of the subducted lithosphere in a volcanic arc; comments and reply: Geology, v. 22, p. 187-190.

Dickinson, W.R., and Hatherton, T., 1967, Andesitic volcanism and seismicity around the Pacific: Science, v. 157, p. 801-803.

Dieterich, J.H., 1988, Growth and persistence of Hawaiian volcanic rift zones: Journal of Geophysical Research, v. 93, p. 4258-4270.

Dixon, T.H., Miller, M., Farina, F., Wang, H., and Johnson, D., 2000, Present-day motion of the Sierra Nevada block and some tectonic implications for the Basin and Range province, North American Cordillera: Tectonics, v. 19, p. 1-24.

Donnelly-Nolan, J.M., 1988, A magmatic model of Medicine Lake volcano, California: Journal of Geophysical Research, v. 93, p. 4412-4420.

Donnelly-Nolan, J.M., 1998, Abrupt shift in $\delta^{18}O$ values at Medicine Lake volcano (California, USA): Bulletin of Volcanology, v. 59, p. 529-536.

Donnelly-Nolan, J.M., 2006, Chemical analyses and K-Ar ages of samples from 13 drill holes, Medicine Lake volcano, California: U.S. Geological Survey Open-File Report 2006-1041, 20 p. [http://pubs.usgs.gov/of/2006/1041].

Donnelly-Nolan, J.M., in press, Geologic map of Medicine Lake volcano, northern California: U.S. Geological Survey Scientific Information Map 2927, scale 1:50,000.

Donnelly-Nolan, J.M., and Champion, D.E., 1987, Geologic map of Lava Beds National Monument: U.S. Geological Survey Map I-1804, scale 1:24,000.

Donnelly-Nolan, J.M., and Lanphere, M.A., 2005, Argon dating at and near Medicine Lake volcano, California: Results and data: U.S. Geological Survey Open-File Report 2005-1416, 37 p. [http://pubs.usgs.gov/of/2005/1416].

Donnelly-Nolan, J.M., Lanphere, M.A., and Ramsey, D.W., 2003, Medicine Lake volcano—results of geologic mapping and argon dating: Geological Society of America Abstracts with Programs, v. 35, no. 6, p. 563.

Donnelly-Nolan, J.M., Champion, D.E., Grove, T.L., Baker, M.B., Taggart, J.E., Jr., and Bruggman, P.E., 1991, The Giant Crater Lava Field: Geology and geochemistry of a compositionally zoned, high-alumina basalt to basaltic andesite eruption at Medicine Lake volcano, California: Journal of Geophysical Research, v. 96, p. 21843-21863.

Donnelly-Nolan, J.M., Champion, D.E., Ramsey, D.W., and Lanphere, M.A., 2005, The basalt of Yellowjacket Butte, another large and interesting lava flow at Medicine Lake volcano, N. California, USA: Eos, Transactions American Geophysical Union, v. 86, no. 52, Fall Meeting Supplement, Abstract V53B-1562.

Donnelly-Nolan, J.M., and Nolan, K.M., 1986, Catastrophic flooding and eruption of ash-flow tuff at Medicine Lake volcano, California: Geology, v. 14, p. 875-878.

Donnelly-Nolan, J.M., Champion, D.E., Lanphere, M.A., and Ramsey, D.W., 2004, New thoughts about Newberry volcano, central Oregon, USA: Eos, Transactions American Geophysical Union, v. 85, no. 47, Fall Meeting Supplement, Abstract V43E-1452.

Donnelly-Nolan, J.M., Champion, D.E., Miller, C.D., Grove, T.L., and Trimble, D.A., 1990, Post-11,000-year volcanism at Medicine Lake volcano, Cascade Range, northern California: Journal of Geophysical Research, v. 95, p. 19,693-19,704.

Donnelly-Nolan, J.M., Smith, J.G., Champion, D.E., and Lanphere, M.A., 1996, A Pleistocene back-arc basalt center, northeastern CA: Geological Society of America Abstracts with Programs, v. 28, no. 5, p. 62.

Draper, D.S., 1992, Spinel lherzolite xenoliths from Lorena Butte, Simcoe Mountains, southern Washington (USA): Journal of Geology, v. 100, p. 766-776.

Druitt, T.H., and Bacon, C.R., 1989, Petrology of the zoned calcalkaline magma chamber of Mount Mazama, Crater Lake, Oregon: Contributions to Mineralogy and Petrology, v. 101, p. 245-259.

Dufek, J., and Bergantz, G.W., 2005, Lower crustal magma genesis and preservation—A stochastic framework for the evaluation of basalt-crust interaction: Journal of Petrology, v. 46, p. 2167-2195.

Dungan, M.A., and Davidson, J., 2004, Partial assimilative recycling of the mafic plutonic roots of arc volcanoes—An example from the Chilean Andes: Geology, v. 32, p. 773-776.

Eaton, J.P., and Murata, K.J., 1960, How volcanoes grow: Science, v. 132, p. 925-938.

Eichelberger, J.C., 1975, Origin of andesite and dacite—Evidence of mixing at Glass Mountain in California and at other circum-Pacific volcanoes: Geological Society of America Bulletin, v. 86, p. 1381-1391.

Ellingson, J.A., 1972, The rocks and structure of the White Pass area, Washington: Northwest Science, v. 46, p. 9-24.

Elkins-Tanton, L.T., Grove, T.L., and Donnelly-Nolan, J., 2001, Hot, shallow mantle melting under the Cascades volcanic arc: Geology, v. 29, p. 631-634.

Evans, S.G., and Brooks, G.R., 1991, Prehistoric debris avalanches from Mount Cayley volcano, British Columbia: Canadian Journal of Earth Sciences, v. 28, p. 1365-1374.

Evarts, R.C., and Swanson, D.A., 1994, Geologic transect across the Tertiary Cascade Range, southern Washington, ch. 2H *in* D.A. Swanson and R.A. Haugerud, eds., Geologic field trips in the Pacific Northwest: Dept. of Geological Sciences, University of Washington, in conjunction with 1994 Annual Meeting of the Geological Society of America, Seattle, v. 2, p. 2H-1-31.

Ewert, J.W., Guffanti, M., and Murray, T.L., 2005, An assessment of volcanic threat and monitoring capabilities in the United States—Framework for a National Volcano Early Warning System (NVEWS): U.S. Geological Survey Open-File Report 2005-1164, 62 p.

Fedotov, S.A., and Markhinin, E.K., eds., 1983, The Great Tolbachik fissure eruption: Geological and geophysical data, 1975-1976: Cambridge University Press, 341 p.

Feeley, T.C., and Hacker, M.D., 1995, Intracrustal derivation of Na-rich andesitic and dacitic magmas: An example from Volcán Ollagüe, Andean Central Volcanic Zone: Journal of Geology, v. 103, p. 213-225.

Fierstein, J., Calvert, A., and Hildreth, W., 2003, Two young silicic sisters at Three Sisters Volcanic Field, Oregon: Geological Society of America, Annual Meeting (Seattle) Abstracts with Programs, v. 34, no.7, p. 563.

Fiske, R.S., Hopson, C.A., and Waters, A.C., 1963, Geology of Mount Rainier National Park, Washington: U.S. Geological Survey Professional Paper 444, 93 p.

Fiske, R.S., Hopson, C.A., and Waters, A.C., 1964, Geologic map and section of Mount Rainier National Park, Washington: U.S. Geological Survey Map I-432.

Foit, F.F., Jr., Gavin, D.G., and Hu, F.S., 2004, The tephra stratigraphy of two lakes in south-central British Columbia, Canada, and its implications for mid-late Holocene volcanic activity at Glacier Peak and Mount St. Helens, Washington, USA: Canadian Journal of Earth Sciences, v. 41, p. 1401-1410.

Fuis, G.S., Zucca, J.J., Mooney, W.D., and Milkereit, B., 1987, A geologic interpretation of seismic-refraction results in northeastern California: Geological Society of America Bulletin, v. 98, p. 53-65.

Furukawa, Y., 1993, Magmatic processes under arcs and formation of the volcanic front: Journal of Geophysical Research, v. 98, p. 8309-8319.

Gardner, C.A., 1994, Temporal, spatial, and petrologic variations of lava flows from the Mount Bachelor volcanic chain, central Oregon High Cascades: U.S. Geological Survey Open-File Report 94-261, 100 p.

Gardner, C.A., Hill, B.E., Negrini, R.M., and Sarna-Wojcicki, A.M., 1992, Paleomagnetic correlation of middle Pleistocene ignimbrites from the Bend, Oregon, area with distal tephra beds: Geological Society of America Abstracts with Programs, v. 24, no. 5, p. 26.

Gardner, J.E., Carey, S., and Sigurdsson, H., 1998, Plinian eruptions at Glacier Peak and Newberry volcanoes, United States: Implications for volcanic hazards in the Cascade Range: Geological Society of America Bulletin, v. 110, p. 173-187.

Gardner, J.E., Rutherford, M., Carey, S., and Sigurdsson, H., 1995, Experimental constraints on pre-eruptive water contents and changing magma storage prior to explosive eruptions of Mount St. Helens volcano: Bulletin of Volcanology, v. 57, p. 1-17.

Gerbe, M.-C., Gourgaud, A., Sigmarsson, O., Harmon, R.S., Joron, J.-L., and Provost, A., 1992, Mineralogical and geochemical evolution of the 1982-1983 Galunggung eruption (Indonesia): Bulletin of Volcanology, v. 54, p. 284-298.

Geschwind, C.-H., and Rutherford, M.J., 1992, Cummingtonite and the evolution of the Mount St. Helens (Washington) magma system—An experimental study: Geology, v. 20, p. 1011-1014.

Gilbert, N.J., 1969, Chronology of post-Tuscan volcanism in the Manton area, California: University of California, Berkeley, M.A. thesis, 79 p.

Gill, J., 1981, Orogenic Andesites and Plate Tectonics: Springer Verlag, Berlin, 390 p.

Gill, J., and Condomines, M., 1992, Short-lived radioactivity and magma genesis: Science, v. 257, p. 1368-1376.

Gradstein, F.M., Ogg, J.G., Smith, A.G., Bleeker, W., and Lourens, L.J., 2004, A new geologic time scale, with special reference to Precambrian and Neogene: Episodes, v. 27, p. 83-100.

Green, N.L., 1981, Geology and petrology of Quaternary volcanic rocks, Garibaldi Lake area, southwestern British Columbia—Summary: Geological Society of America Bulletin, part I, v. 92, p. 697-702.

Green, N.L., 1982, Co-existing calcic amphiboles in calc-alkaline andesites—Possible evidence of a zoned magma chamber: Journal of Volcanology and Geothermal Research, v. 12, p. 57-76.

Green, N.L., 1988, Basalt-basaltic andesite mixing at Mount Baker volcano, Washington—I, Estimation of mixing conditions: Journal of Volcanology and Geothermal Research, v. 34, p. 251-265.

Green, N.L., 1990, Late Cenozoic volcanism in the Mount Garibaldi and Garibaldi Lake volcanic fields, Garibaldi Volcanic Belt, southwestern British Columbia: Geoscience Canada, v. 17, no. 3, p. 171-175.

Green, N.L., 1994a, Mount St. Helens—Potential example of the partial melting of the subducted lithosphere in a volcanic arc; comments and reply: Geology, v. 22, p. 187-190.

Green, N.L., 1994b, Mechanism for middle to upper crustal contamination: Geology, v. 22, p. 231-234.

Green, N.L., 2006, Influence of slab thermal structure on basalt source regions and melting conditions: REE and HFSE constraints from the Garibaldi volcanic belt, northern Cascadia subduction system: Lithos, v. 87, p. 213-249.

Green, N.L., Armstrong, R.L., Harakal, J.E., Souther, J.G., and Read, P.B., 1988, Eruptive history and K-Ar geochronology of the late Cenozoic Garibaldi volcanic belt, southwestern British Columbia: Geological Society of America Bulletin, v. 100, p. 563-579.

Green, N.L., and Harry, D.L., 1999, On the relationship between subducted slab age and arc basalt petrogenesis, Cascadia subduction system, North America: Earth and Planetary Science Letters, v. 171, p. 367-381.

Green, N.L., and Sinha, A.K., 2005, Consequences of varied slab age and thermal structure on enrichment processes in the sub-arc mantle of the northern Cascadia subduction system: Journal of Volcanology and Geothermal Research, v. 140, p. 107-132.

Grose, T.L.T., and McKee, E.H., 1986, Potassium-argon ages of late Miocene to late Quaternary volcanic rocks in the Susanville-Eagle Lake area, Lassen County, California: Isochron West, no. 45, p. 5-11.

Grose, T.L.T., Saucedo, G.J., and Wagner, D.L., 1990, Geologic map of the Susanville quadrangle, Lassen and Plumas Counties, California: California Department of Conservation, Division of Mines and Geology, Open-File Report 91-1, scale 1:100,000; pamphlet 26 p.

Grose, T.L.T., Saucedo, G.J., and Wagner, D.L., 1992, Geologic map of the Eagle Lake quadrangle, Lassen County, California: California Department of Conservation, Division of Mines and Geology, Open-File Report 92-14, scale 1:100,000; pamphlet 33 p.

Grove, T.L., Donnelly-Nolan, J.M., and Housh, T, 1997, Magmatic processes that generated the rhyolite of Glass Mountain, Medicine Lake volcano, California: Contributions to Mineralogy and Petrology, v. 127, p. 205-223.

Grove, T.L., Kinzler, R.J., Baker, M.B., Donnelly-Nolan, J.M., and Lesher, C.E., 1988, Assimilation of granite by basaltic magma at Burnt Lava Flow, Medicine Lake volcano, northern California: Contributions to Mineralogy and Petrology, v. 99, p. 320-343.

Grove, T.L., Parman, S.W., Bowring, S.A., Price, R.C., and Baker, M.B., 2002, The role of an H_2O-rich fluid in the generation of primitive basaltic andesites and andesites from the Mount Shasta region, N. California: Contributions to Mineralogy and Petrology, v. 142, p. 375-396.

Grubensky, M.J., Smith, G.A., and Geissman, J.W., 1998, Field and paleomagnetic characterization of lithic and scoriaceous breccias at Pleistocene Broken Top volcano, Oregon Cascades: Journal of Volcanology and Geothermal Research, v. 83, p. 93-114.

Guffanti, M., Blakely, R.J., Christiansen, R.L., Clynne, M.A., Donnelly-Nolan, J.M., Muffler, L.J.P., and Smith, J.G., 1994, Spatial correlation of gravity anomalies, volcanic vents, and young faulting in the Cascade Range, California, and implications for crustal stress and structure: Geological Society of America Abstracts with Programs, v. 26, p. A-145.

Guffanti, M., Clynne, M.A., and Muffler, L.J.P., 1996, Thermal and mass implications of magmatic evolution in the Lassen volcanic region, California, and constraints on basalt influx to the lower crust: Journal of Geophysical Research, v. 101, p. 3001-3013.

Guffanti, M., Clynne, M.A., Smith, J.G., Muffler, L.J.P., and Bullen, T.D., 1990, Late Cenozoic volcanism, subduction, and extension in the Lassen region of California, southern Cascade Range: Journal of Geophysical Research, v. 95, p. 19453-19464.

Guffanti, M., and Weaver, C.S., 1988, Distribution of Late Cenozoic volcanic vents in the Cascade Range—Volcanic arc segmentation and regional tectonic considerations: Journal of Geophysical Research, v. 93, p. 6513-6529.

Hacker, B.R., Abers, G.A., and Peacock, S.M., 2003, Subduction factory 1—Theoretical mineralogy, densities, seismic wave speeds, and H_2O contents: Journal of Geophysical Research, v. 108, no. B1, 2029; p. ESE 10: 1-26.

Halliday, A.N., Fallick, A.E., Dickin, A.P., Mackenzie, A.B., Stephens, W.E., and Hildreth, W., 1983, The isotopic and chemical evolution of Mount St. Helens: Earth and Planetary Science Letters, v. 63, p. 241-256.

Hammond, P.E., 1980, Reconnaissance geologic map and cross sections of southern Washington Cascade Range: Publications of the Department of Earth Sciences, Portland State University, Portland, Oregon; 31 p., 2 sheets, scale 1:125,000.

Hammond, P.E., 1983, Volcanic formations along the Klamath River near Copco Lake: California Geology, v. 36, no. 5, p. 99-109.

Hammond, P.E., 1990, Marble Mountain—Trout Creek Hill zone, Washington, *in* C.A. Wood and J. Kienle, eds., Volcanoes of North America: Cambridge University Press, p. 167-168.

Hammond, P.E., and Korosec, M.A., 1983, Geochemical analyses, age dates, and flow-volume estimates for Quaternary volcanic rocks, southern Cascade Mountains, Washington: Washington Division of Geology and Earth Resources Open-File Report 83-13, 36 p.,1 plate.

Hammond, W.C., and Thatcher, W., 2004, Contemporary tectonic deformation of the Basin and Range province, western United States—10 years of observation with the Global positioning System: Journal of Geophysical Research, v. 109, B08403, 21 p.

Harris, R.A., Iyer, H.M., and Dawson, P.B., 1991, Imaging the Juan de Fuca plate beneath southern Oregon using teleseismic P wave residuals: Journal of Geophysical Research, v. 96, p. 19879-19889.

Harry, D.L., and Green, N.L., 1999, Slab dehydration and basalt petrogenesis in subduction systems involving very young oceanic lithosphere: Chemical Geology, v. 160, p. 309-333.

Hart, G.L., Johnson, C.M., Shirey, S.B., and Clynne, M.A., 2002, Osmium isotope constraints on lower crustal recycling and pluton preservation at Lassen Volcanic Center, CA: Earth and Planetary Science Letters, v. 199, p. 269-285.

Hart, G.L., Johnson, C.M., Hildreth, W., and Shirey, S.B., 2003, New osmium isotope evidence for intracrustal recycling of crustal domains with discrete ages: Geology, v. 31, p. 427-430.

Hart, W.K., 1985, Chemical and isotopic evidence for mixing between depleted and enriched mantle, northwestern U.S.A.: Geochimica et Cosmochimica Acta, v. 49, p. 131-144.

Hart, W.K., Aronson, J.L., and Mertzman, S.A., 1984, Areal distribution and age of low-K, high-alumina olivine tholeiite magmatism in the northwestern Great Basin: Geological Society of America Bulletin, v. 95, p. 186-195.

Hart, W.K., Mertzman, S.A., and Weaver, S., 1979, The volcanic geology of the Tennant area, eastern Siskiyou County, California: Northwest Geology, v. 8, p. 10-17.

Hasegawa, A., and Zhao, D., 1994, Deep structure of island arc magmatic regions as inferred from seismic observations, *in* Ryan, M.P., ed., Magmatic Systems: San Diego, Academic Press, p. 179-195.

Hasenaka, T., 1994, Size, distribution, and magma output rate for shield volcanoes of the Michoacán-Guanajuato volcanic field, central Mexico: Journal of Volcanology and Geothermal Research, v. 63, p. 13-31.

Hasenaka, T., and Carmichael, I.S.E., 1985, The cinder cones of Michoacán-Guanajuato, central Mexico—Their age, volume and distribution, and magma discharge rate: Journal of Volcanology and Geothermal Research, v. 25, p. 105-124.

Heiken, G., 1978, Plinian-type eruptions in the Medicine Lake Highland, California, and the nature of the underlying magma: Journal of Volcanology and Geothermal Research, v. 2, p. 1-16.

Heiken, G., and Eichelberger, J.C., 1980, Eruptions at Chaos Crags, Lassen Volcanic National Park, California: Journal of Volcanology and Geothermal Research, v. 7, p. 443-481.

Heliker, C., 1995, Inclusions in Mount St. Helens dacite erupted from 1980 through 1983: Journal of Volcanology and Geothermal Research, v. 66, p. 115-135.

Helley, E.J., Harwood, D.S., Barker, J.A., and Griffin, E.A., 1981, Geologic map of the Battle Creek fault zone and adjacent parts of the northern Sacramento Valley, California: U.S. Geological Survey Map MF-1298, scale 1:62,500; pamphlet 12 p.

Helley, E.J., and Harwood, D.S., 1985, Geologic map of the late Cenozoic deposits of the Sacramento Valley and northern Sierran foothills, California: U.S. Geological Survey Map MF-1790, scale 1:62500, pamphlet 24 p.

Herrero-Bervera, and E., Helsley, C.E., 1993, Global paleomagnetic correlation of the Blake geomagnetic polarity episode: Society of Economic Paleontologists and Mineralogists, Special Publication no. 49, p. 71-82.

Herrero-Bervera, E., Helsley, C.E., Sarna-Wojcicki, A.M., Lajoie, K.R., Meyer, C.E., McWilliams, M.O., Negrini, R.M., Turrin, B.D., Donnelly-Nolan, J.M., and Liddicoat, J.C., 1994, Age and correlation of a paleomagnetic episode in the western United States by $^{40}Ar/^{39}Ar$ dating and tephrochronology—The Jamaica, Blake, or a new polarity episode: Journal of Geophysical Research, v. 99, p. 24091-24103.

Hesse, M., and Grove, T.L., 2003, Absarokites from the western Mexican Volcanic Belt—Constraints on mantle wedge conditions: Contributions to Mineralogy and Petrology, v. 146, p. 10-27.

Hickey, R. L., Frey, F.A., and Gerlach, D.C., 1986, Multiple sources for basaltic arc rocks from the Southern Volcanic Zone of the Andes (34º-41ºS) —Trace element and isotopic evidence for contributions from subducted oceanic crust, mantle, and continental crust: Journal of Geophysical Research, v. 91, p. 5963-5983.

Hickson, C.J., Russell, J.K., and Stasiuk, M.V., 1999, Volcanology of the 2350 B.P. eruption of Mount Meager volcanic complex, British Columbia, Canada—Implications for hazards from eruptions in topographically complex terrain: Bulletin of Volcanology, v. 60, p. 489-507.

Hickson, C.J., and Souther, J.G., 1984, Late Cenozoic volcanic rocks of the Clearwater—Wells Gray area, British Columbia: Canadian Journal of Earth Sciences, v. 21, p. 267-277.

Hildreth, W., 1981a, Gradients in silicic magma chambers—Implications for lithospheric magmatism: Journal of Geophysical Research, v. 86, p. 10153-10192.

Hildreth, W., 1981b, David Alexander Johnston 1949-1980, *in* Johnston, D.A., and Donnelly-Nolan, J., eds., Guides to some volcanic terranes in Washington, Idaho, Oregon, and northern California: U.S. Geological Survey Circular 838, p. viii-x.

Hildreth, W., 1994, Quaternary magmatism in the Cascades—Some geologic perspectives: Geological Society of America Abstracts with Programs, v. 26, no. 7, p. A-30.

Hildreth, W., 1996, Kulshan caldera—A Quaternary subglacial caldera in the North Cascades, Washington: Geological Society of America Bulletin, v. 108, no. 7, p. 794-814.

Hildreth, W., 2004, Volcanological perspectives on Long Valley, Mammoth Mountain, and Mono Craters—Several contiguous but discrete systems: Journal of Volcanology and Geothermal Research, v. 136, p. 169-198.

Hildreth, W., and Fierstein, J., 1995, Geologic map of the Mount Adams volcanic field, Cascade Range of southern Washington: U.S. Geological Survey Map I-2460, scale 1:50,000.

Hildreth, W., and Fierstein, J., 1997, Recent eruptions of Mount Adams, Washington Cascades, USA: Bulletin of Volcanology, v. 58, p. 472-490.

Hildreth, W., Fierstein, J., and Lanphere, M., 2003, Eruptive history and geochronology of the Mount Baker volcanic field, Washington: Geological Society of America Bulletin, v. 115, p. 729-764.

Hildreth, W., Fierstein, J., Siems, D.F., Budahn, J.R., and Ruiz, J., 2004, Rear-arc vs. arc-front volcanoes in the Katmai reach of the Alaska Peninsula: A critical appraisal of across-arc compositional variation: Contributions to Mineralogy and Petrology, v. 147, p. 243-275.

Hildreth, W., Halliday, A.N., and Christiansen, R.L., 1991, Isotopic and chemical evidence concerning the genesis and contamination of basaltic and rhyolitic magma beneath the Yellowstone Plateau volcanic field: Journal of Petrology, v. 32, p. 63-138.

Hildreth, W., Lanphere, M.A., Champion, D.E., and Fierstein, J., 2004, Rhyodacites of Kulshan caldera, North Cascades of Washington: Postcaldera lavas that span the Jaramillo: Journal of Volcanology and Geothermal Research, v. 130, p. 227-264.

Hildreth, W., and Lanphere, M.A., 1994, Potassium-argon geochronology of a basalt-andesite-dacite arc system: The Mount Adams volcanic field, Cascade Range of southern Washington: Geological Society of America Bulletin, v. 106, p. 1413-1429.

Hildreth, W., and Moorbath, S., 1988, Crustal contributions to arc magmatism in the Andes of central Chile: Contributions to Mineralogy and Petrology, v. 98, p. 455-489.

Hildreth, W., and Moorbath, S., 1991, Reply to comment on "Crustal contributions to arc magmatism in the Andes of central Chile" by W. Hildreth and S. Moorbath: Contributions to Mineralogy and Petrology, v. 108, p. 247-252.

Hildreth, W., and Wilson, C.J.N., 2007, Compositional zoning of the Bishop Tuff: Journal of Petrology, v. 48, p. 951-999.

Hill, B.E., 1991, Petrogenesis of compositionally distinct silicic volcanoes in the Three Sisters region of the Oregon Cascade Range—Effects of crustal extension on the development of continental arc silicic magmatism: Ph.D. dissertation, Oregon State University, Corvallis, 247 p.

Hill, B.E., and Priest, G.R., 1992, Geologic setting of the Santiam Pass area, central Cascade Range, Oregon: Oregon Department of Geology and Mineral Industries Open-File Report 0-92-3, p. 5-18.

Hill, B.E., and Taylor, E.M., 1989, Oregon central High Cascade pyroclastic units in the vicinity of Bend, Oregon: U.S. Geological Survey Open-File Report 89-645, p. 51-54.

Hill, B.E., and Taylor, E.M., 1990, Oregon central High Cascade pyroclastic units in the vicinity of Bend, Oregon: Oregon Geology, v. 52, no. 6, p. 125-126, 139-140.

Hoblitt, R.P., Miller, C.D., and Scott, W.E., 1987, Volcanic hazards with regard to siting nuclear-power plants in the Pacific Northwest: U.S. Geological Survey Open-File Report 87-297, 196 p.

Hopson, C.A., and Mattinson, J.M., 1994, Chelan Migmatite Complex—Field evidence for mafic magmatism, crustal anatexis, mixing and protodiapiric emplacement, *in* Swanson, D.A., and Haugerud, R.A., eds., Geologic Field Trips in the Pacific Northwest: Guides to Field Trips, 1994 Geological Society of America Annual Meeting, Seattle, v. 2, chapter 2K, 21 p.

Hopson, C.A., and Melson, W.G., 1990, Compositional trends and eruptive cycles at Mount St. Helens: Geoscience Canada, v. 17, p. 131-141.

Hughes, J.M., and Mertzman, S.A., 1976, Geology and petrology of the Garner Mountain area, northern California: Northwest Geology, v. 5, p. 10-20.

Hughes, S.S., 1990, Mafic magmatism and associated tectonism of the central High Cascade Range, Oregon: Journal of Geophysical Research, v. 95, p. 19623-19638.

Hughes, S.S., and Taylor, E.M., 1986, Geochemistry, petrogenesis, and tectonic implications of central High Cascade mafic platform lavas: Geological Society of America Bulletin, v. 97, p. 1024-1036.

Hyde, J.H., 1975, Upper Pleistocene pyroclastic-flow deposits and lahars south of Mount St. Helens volcano, Washington: U.S. Geological Survey Bulletin 1383-B, 20 p.

Hyde, J.H., and Crandell, D.R., 1978, Postglacial volcanic deposits at Mount Baker, Washington, and potential hazards from future eruptions: U.S. Geological Survey Professional Paper 1022-C, 17 p.

Hyndman, R.D., Mazzotti, S., Weichert, D., and Rogers, G.C., 2003, Frequency of large crustal earthquakes in Puget Sound-Southern Georgia Strait predicted from geodetic and geological deformation rates: Journal of Geophysical Research, v. 108, no. B1, 2033, doi:10.1029/2001JB001710, p. ESE 12: 1-12.

Hyndman, R.D., and Peacock, S.M., 2003, Serpentinization of the forearc mantle: Earth and Planetary Science Letters, v. 212, p. 417-432.

Jarrard, R.D., 1986, Relations among subduction parameters: Reviews of Geophysics, v. 24, p. 217-284.

Jensen, R, 2006, Roadside guide to the geology and history of Newberry Volcano (Fourth edition): Bend, Oregon, CenOreGeo Pub, 182 p. Available from bjensen@bendnet.com

Johnson, C.M., 1991, Large-scale crust formation and lithosphere modification beneath middle to late Cenozoic calderas and volcanic fields, western North America: Journal of Geophysical Research, v. 96, p. 13485-13507.

Jones, C.H., Unruh, J.R., and Sonder, L.J., 1996, The role of gravitational potential energy in active deformation in the southwestern United States: Nature, v. 381, p. 37-41.

Jordan, B.T., Grunder, A.L., Duncan, R.A., and Deino, A.L., 2004, Geochronology of age-progressive volcanism of the Oregon High Lava Plains: Implications for the plume interpretation of Yellowstone: Journal of Geophysical Research, v. 109, no. B10202, doi:10.1029/2003JB002776, p. 1-19.

Kay, S.M., and Kay, R.W., 1994, Aleutian magmas in space and time, ch. 22 *in* Plafker, G., and Berg, H.C., eds., The Geology of Alaska: Boulder, Colorado, Geological Society of America, The Geology of North America, v. G-1, p. 687-722.

Kay, S.M., Ramos, V.A., and Marquez, M., 1993, Evidence in Cerro Pampa volcanic rocks for slab-melting prior to ridge-trench collision in southern South America: Journal of Geology, v. 101, p. 703-714.

Keith, T.E.C., Donnelly-Nolan, J.M., Markman, J.L., and Beeson, M.H., 1985, K-Ar ages of rocks in the Mount Hood area, Oregon: Isochron West, no. 42, p. 12-16.

Kelman, M.C., Russell, J.K., and Hickson, C.J., 2002, Effusive intermediate glaciovolcanism in the Garibaldi Volcanic Belt, southwestern British Columbia, Canada, *in* Smellie, J.L., and Chapman, M.G., eds., Volcano-ice interaction on Earth and Mars: Geological Society, London, Special Publication 202, p. 195-211.

Kincaid, C., and Sacks, I.S., 1997, Thermal and dynamical evolution of the upper mantle in subduction zones: Journal of Geophysical Research, v. 102, p. 12295-12315.

Kinzler, R.J., Donnelly-Nolan, J.M., and Grove, T.L., 2000, Late Holocene hydrous mafic magmatism at the Paint Pot Crater and Callahan flows, Medicine Lake volcano, N. California, and the influence of H_2O in the generation of silicic magmas: Contributions to Mineralogy and Petrology, v. 138, p. 1-16.

Kirby, S., Engdahl, E.R., and Denlinger, R., 1996, Intermediate-depth intraslab earthquakes and arc volcanism as physical expressions of crustal and uppermost mantle metamorphism in subducting slabs, *in* Bebout, G.E., and others, eds., Subduction—Top to bottom: American Geophysical Union Monograph 96, p. 195-214.

Korosec, M.A., 1989, New K-Ar age dates, geochemistry, and stratigraphic data for the Indian Heaven Quaternary volcanic field, south Cascade Range, Washington: Washington Division of Geology and Earth Resources Open-File Report 89-3, 42 p.

Kuehn, S.C., 2002, Stratigraphy, distribution, and geochemistry of the Newberry volcano tephras: Washington State University, Pullman, PhD dissertation, 701 p.

Kuehn, S.C., and Preppernau, C.A., 2005, Pumice Flat tephra of Newberry volcano, Oregon: Deposit of a mixed-magma plinian eruption: Geological Society of America Abstracts with Programs, v. 37, no. 4.

Kushiro, I., 1987, A petrological model of the mantle wedge and lower crust in the Japanese island arcs, *in* Mysen, B.O., ed., Magmatic processes—Physicochemical principles: Geochemical Society Special Publication 1, p. 165-181.

Lanphere, M.A., Champion, D.E., Christiansen, R.L., Donnelly-Nolan, J.M., Fleck, R.J., and Sarna-Wojcicki, A.M., 1999, Evolution of tephra dating in the western United States: Geological Society of America Abstracts with Programs, v. 31, no. 6, p. A-73.

Lanphere, M.A., Champion, D.E., Clynne, M.A., Lowenstern, J.B., Sarna-Wojcicki, A.M., and Wooden, J.L., 2004, Age of the Rockland tephra, western USA: Quaternary Research, v. 62, p. 94-104.

Lanphere, M.A., and Sisson, T.W., 1995, K-Ar ages of Mount Rainier volcanics: Eos, Transactions American Geophysical Union, v. 76, no. 46 (supplement), p. F651.

Lawrence, R.B., Armstrong, R.L., and Berman, R.G., 1984, Garibaldi Group volcanic rocks of the Salal Creek area, southwestern British Columbia—Alkaline lavas on the fringe of the predominantly calcalkaline Garibaldi (Cascade) volcanic arc: Journal of Volcanology and Geothermal Research, v. 21, p. 255-276.

Lawrence, R.D., 1976, Strike-slip faulting terminates the Basin and Range province in Oregon: Geological Society of America Bulletin, v. 87, p. 846-850.

Leaver, D.S., Mooney, W.D., and Kohler, W.M., 1984, A seismic refraction study of the Oregon Cascades: Journal of Geophysical Research, v. 89, p. 3121-3134.

Leeman, W.P., Lewis, J.F., Evarts, R.C., Conrey, R.M., and Streck, M.J., 2005, Petrologic constraints on the thermal structure of the Cascade arc: Journal of Volcanology and Geothermal Research, v. 140, p. 67-105.

Leeman, W.P., Smith, D.R., Hildreth, W., Palacz, Z., and Rogers, N., 1990, Compositional diversity of late Cenozoic basalts in a transect across the southern Washington Cascades: Implications for subduction zone magmatism: Journal of Geophysical Research, v. 95, p. 19561-19582.

Leeman, W.P., Tonarini, S., Chan, L.H., and Borg, L.E., 2004, Boron and lithium isotopic variations in a hot subduction zone—the southern Washington Cascades: Chemical Geology, v. 212, p. 101-124.

Leonard, E.M., 1995, A varve-based calibration of the Bridge River tephra fall: Canadian Journal of Earth Sciences, v. 32, p. 2098-2102.

Lescinsky, D.T., and Sisson, T.W., 1998, Ridge-forming, ice-bounded lava flows at Mount Rainier, Washington: Geology, v. 26, p. 351-354.

Lewis, T.J., Lowe, C., and Hamilton, T.S., 1997, Continental signature of a ridge-trench triple junction: Northern Vancouver Island: Journal of Geophysical Research, v. 102, p. 7767-7781.

Lipman, P.W., and Mullineaux, D.R., eds., 1981, The 1980 eruptions of Mount St. Helens, Washington: U.S. Geological Survey Professional Paper 1250, 844 p.

Lowenstern, J.B., Persing, H.M., Wooden, J.L., Lanphere, M., Donnelly-Nolan, J., and Grove, T.L., 2000, U-Th dating of single zircons from young granitoid xenoliths—New tools for understanding volcanic processes: Earth and Planetary Science Letters, v. 183, p. 291-302.

Lowenstern, J.B., Donnelly-Nolan, J., Wooden, J.L., and Charlier, B.L.A., 2003, Volcanism, plutonism and hydrothermal alteration at Medicine Lake volcano, California: Proceedings, Twenty-eighth Workshop on Geothermal Reservoir Engineering, Stanford University, January 27-29, 2003, SGP-TR-173, p. 1-8.

Luedke, R.G., and Smith R.L., 1981, Map showing distribution, composition, and age of Late Cenozoic volcanic centers in California and Nevada: U.S. Geological Survey Map I-1091-C.

Luedke, R.G., Smith, R.L., and Russell-Robinson, S.L., 1983, Map showing distribution, composition, and age of Late Cenozoic volcanoes and volcanic rocks of the Cascade Range and vicinity, northwestern United States: U.S. Geological Survey Map I-1507, scale 1:500,000.

Luhr, J.F., 1992, Slab-derived fluids and partial melting in subduction zones: Insights from two contrasting Mexican volcanoes (Colima and Ceboruco): Journal of Volcanology and Geothermal Research, v. 54, p. 1-18.

Luhr, J.F., 1997, Extensional tectonics and the diverse primitive volcanic rocks in the western Mexican Volcanic Belt: Canadian Mineralogist, v. 35, p. 473-500.

Luhr, J.F., and Carmichael, I.S.E., 1985, Jorullo Volcano, Michoacán, Mexico (1759-1774)—The earliest stages of fractionation in calc-alkaline magmas: Contributions to Mineralogy and Petrology, v. 90, p. 142-161.

Ma, L., Crosson, R., and Ludwin, R., 1996, Western Washington earthquake focal mechanisms and their relationship to regional tectonic stress: U.S. Geological Survey Professional Paper 1560, p. 257-284.

Macdonald, G.A., 1963, Geology of the Manzanita Lake quadrangle, California: U.S. Geological Survey Map GQ-248, scale 1:62,500.

Macdonald, G.A., 1964, Geology of the Prospect Peak quadrangle, California: U.S. Geological Survey Map GQ-345, scale 1:62,500.

MacLeod, N.S., and Sammel, E.A., 1982, Newberry volcano, Oregon: A Cascade Range geothermal prospect: Oregon Geology, v. 44, no. 11, p. 123-131.

MacLeod, N.S., and Sherrod, D.R., 1988, Geologic evidence for a magma chamber beneath Newberry volcano, Oregon: Journal of Geophysical Research, v. 93, p. 10067-10079.

MacLeod, N.S., and Sherrod, D.R., 1992, Reconnaissance geologic map of the west half of the Crescent 1° by 2° quadrangle, central Oregon: U.S. Geological Survey Map I-2215, scale 1:250,000.

MacLeod, N.S., Sherrod, D.R., Chitwood, L.A., and Jensen, R.A., 1995, Geologic map of Newberry volcano, Deschutes, Klamath, and Lake Counties, Oregon: U.S. Geological Survey Map I-2455, scales 1:62,500 and 1:24,000.

MacLeod, N.S., Walker, G.W., and McKee, E.H., 1975, Geothermal significance of eastward increase in age of Upper Cenozoic rhyolite domes in southeastern Oregon: U.S. Geological Survey Open-File Report 75-348, 22 p.

Mahood, G.A., and Halliday, A.N., 1988, Generation of high-silica rhyolite: a Nd, Sr, and O isotopic study of Sierra La Primavera, Mexican Neovolcanic Belt: Contributions to Mineralogy and Petrology, v. 100, p. 183-191.

Major, J.J., Scott, W.E., Driedger, C., and Dzurisin, D., 2005, Mount St. Helens erupts again: U.S. Geological Survey Fact Sheet 2005-3036, 4 p.

Mallin, K., and Hart, W.K., 1991, New K-Ar ages of mafic lavas from the Basin and Range—Cascade transition zone in northeastern California and southern Oregon: Isochron West, no. 57, p. 8-11.

Mathews, W.H., 1951, The Table, a flat-topped volcano in southern British Columbia: American Journal of Science, v. 249, p. 830-841.

Mathews, W.H., 1952a, Mount Garibaldi, a supraglacial Pleistocene volcano in southwestern British Columbia: American Journal of Science, v. 250, p. 81-103.

Mathews, W.H., 1952b, Ice-dammed lavas from Clinker Mountain, southwestern British Columbia: American Journal of Science, v. 250, p. 553-565.

Mathews, W.H., 1957, Petrology of Quaternary volcanics of the Mount Garibaldi map-area, southwestern British Columbia: American Journal of Science, v. 255, p. 400-415.

Mathews, W.H., 1958, Geology of the Mount Garibaldi map-area, southwestern British Columbia, Canada, part II —Geomorphology and Quaternary volcanic rocks: Geological Society of America Bulletin, v. 69, p. 179-198.

Maynard, L.C., 1974, Geology of Mount McLoughlin: University of Oregon, Eugene, M.S. thesis, 139 p.

McCaffrey, R., Qamar, A.I., King, R.W., Wells, R., Khazaradze, G., Williams, C.A., Stevens, C.W., Vollick, J.J., and Zwick, P.C., 2007, Fault locking, block rotation and crustal deformation in the Pacific Northwest: Geophysical Journal International, v. 169, p. 1315-1340.

McCrory, P.A., Blair, J.L., Oppenheimer, D.H., and Walter, S.R., 2004, Depth to the Juan de Fuca slab beneath the Cascadia subduction margin—A 3-D model for sorting earthquakes: U.S. Geological Survey Data Series 91, CD-ROM [http://pubs.usgs.gov/ds/91/].

McCrory, P.A., Pollitz, F.F., and Blair, J.L., 2003, Evidence for a tear in the Juan de Fuca plate in the vicinity of the 2001 Nisqually earthquake: Geological Society of America Abstracts with Programs, v. 35, no. 6, p. 309 [paper no. 113-10].

McKee, E.H., Duffield, W.A., and Stern, R.J., 1983, Late Miocene and early Pliocene basaltic rocks and their implications for crustal structure, northeastern California and south-central Oregon: Geological Society of America Bulletin, v. 94, p. 292-304.

McKenna, J.M., 1994, Summit versus flank-vent eruptions and implications for the magma system of Mount Rainier volcano, Cascade arc, Washington: Geological Society of America Abstracts with Programs, v. 26, no. 7, p. A-332.

Mertzman, S.A., 1982, K-Ar results for silicic volcanics from the Medicine Lake Highland, northeastern California—A summary: Isochron/West, no. 34, p. 3-7.

Mertzman, S.A., Hazlett, R., and Weaver, S.G., 1992, The geology of the Mt. McLoughlin—Brown Mountain region, southern Oregon: Geological Society of America Abstracts with Programs, v. 24, no. 5, p. 70.

Meyer, C.E., Sarna-Wojcicki, A.M., Hillhouse, J.W., Woodward, M.J., Slate, J.L., and Sorg, D.H., 1991, Fission-track age (400,000 yr) of the Rockland tephra, based on inclusion of zircon grains lacking fossil fission tracks: Quaternary Research, v. 35, p. 367-382.

Mibe, K., Fujii, T., and Yasuda, A., 1999, Control of the location of the volcanic front in island arcs by aqueous fluid connectivity in the mantle wedge: Nature, v. 401, p. 259-262.

Michaelson, C.A., and Weaver, C.S., 1986, Upper mantle structure from teleseismic P wave arrivals in Washington and northern Oregon: Journal of Geophysical Research, v. 91, p. 2077-2094.

Miller, C.D., 1978, Holocene pyroclastic-flow deposits from Shastina and Black Butte, west of Mount Shasta, California: Journal of Research, U.S. Geological Survey, v. 6, p. 611-624.

Miller, C.D., 1980, Potential hazards from future eruptions in the vicinity of Mount Shasta volcano, northern California: U.S. Geological Survey Bulletin 1503, 43 p.

Miller, C.F., and Mittlefehldt, D.W., 1984, Extreme fractionation in felsic magma chambers—A product of liquid-state diffusion or fractional crystallization?: Earth and Planetary Science Letters, v. 68, p. 151-158.

Miller, R.B., 1989, The Mesozoic Rimrock Lake inlier, southern Washington Cascades: Implications for the basement to the Columbia Embayment: Geological Society of America Bulletin, v. 101, p. 1289-1305.

Mimura, K., 1992, Reconnaissance geologic map of the west half of the Bend and the east half of the Shevlin Park 7 1/2' quadrangles, Deschutes County, Oregon: U.S. Geological Survey Map MF-2189, scale 1:24,000.

Mitchell, R.J., Jaeger, D.J., Diehl, J.F., and Hammond, P.E., 1989, Paleomagnetic results from the Indian Heaven volcanic field, south-central Washington: Geophysical Journal, v. 97, p. 381-390.

Mooney, W.D., and Weaver, C.S., 1989, Regional crustal structure and tectonics of the Pacific coastal states, California, Oregon, and Washington: Geological Society of America Memoir 172, p. 129-161.

Moreno-Roa, H., 1976, The upper Cenozoic volcanism in the Andes of Southern Chile (from 40˚00' to 41˚30' S.L.), *in* González-Ferrán, O., ed., Symposium on Andean and Antarctic Volcanology Problems, International Association of Volcanology and Chemistry of the Earth's Interior, Proceedings (Santiago, Sept. 1974), p. 143-171.

Morrison, R., and Kukla, G., 1998, The Pliocene-Pleistocene (Tertiary-Quaternary) boundary should be placed at about 2.6 Ma, not at 1.8 Ma!: GSA Today, v. 8, no. 8, p. 9.

Muffler, L.J.P., Clynne, M.A., and Champion, D.E., 1994, Late Quaternary normal faulting of the Hat Creek Basalt, northern California: Geological Society of America Bulletin, v. 106, p. 195-200.

Mullineaux, D.R., 1974, Pumice and other pyroclastic deposits in Mount Rainier National Park, Washington: U.S. Geological Survey Bulletin 1326, 83 p.

Mullineaux, D.R., 1996, Pre-1980 tephra-fall deposits erupted from Mount St. Helens, Washington: U.S. Geological Survey Professional Paper 1563, 99 p.

Mullineaux, D.R., and Crandell, D.R., 1962, Recent lahars from Mount St. Helens, Washington: Geological Society of America Bulletin, v. 73, p. 855-869.

Mullineaux, D.R., and Crandell, D.R., 1981, The eruptive history of Mount St. Helens, *in* Lipman, P.W., and Mullineaux, D.R., eds., The 1980 eruptions of Mount St. Helens, Washington: U.S. Geological Survey Professional Paper 1250, p. 3-15.

Mundorff, M.J., and Eggers, A.A., 1988, Tumtum Mountain, a late Pleistocene volcanic dome in southwestern Washington: Northwest Science, v. 62, p. 10-15.

Nakada, S., Bacon, C.R., and Gartner, A.E., 1994, Origin of phenocrysts and compositional diversity in pre-Mazama rhyodacite lavas, Crater Lake, Oregon: Journal of Petrology, v. 35, p. 127-162.

Nasmith, H., Matthews, W.H., and Rouse, G.E., 1967, Bridge River ash and some other Recent ash beds in British Columbia: Canadian Journal of Earth Sciences, v. 4, p. 163-170.

Negrini, R.M., Erbes, D.B., Faber, K., Herrera, A.M., Roberts, A.P., Cohen, A.S., Wigand, P.E., and Foit, F.F., 2000, A paleoclimate record for the past 250,000 years from Summer Lake, Oregon, USA: I. Chronology and magnetic proxies for lake level: Journal of Paleolimnology, v. 24, p. 125-149.

Ogg, J., 2004, Introduction to concepts and proposed standardization of the term "Quaternary": Episodes, v. 27, p. 125-126.

Oleskevich, D.A., Hyndman, R.D., and Wang, K., 1999, The updip and downdip limits to great subduction earthquakes: Thermal and structural models of Cascadia, south Alaska, SW Japan, and Chile: Journal of Geophysical Research, v. 104, p. 14965-14991.

Oppenheimer, D., and 19 others, 1993, The Cape Mendocino, California, earthquakes of April 1992—Subduction at the triple junction: Science, v. 261, p. 433-438.

Pallister, J.S., Hoblitt, R.P., Crandell, D.R., and Mullineaux, D.R., 1992, Mount St. Helens a decade after the 1980 eruptions: magmatic models, chemical cycles, and a revised hazards assessment: Bulletin of Volcanology, v. 54, p. 126-146.

Parsons, T., Trehu, A.M., Luetgert, J.H., Miller, K., Kilbride, F., Wells, R.E., Fisher, M.A., Flueh, E., ten Brink, U.S., and Christensen, N.I., 1998, A new view into the Cascadia subduction zone and volcanic arc: Implications for earthquake hazards along the Washington margin: Geology, v. 26, p. 199-202.

Patino, L.C., Carr, M.J., and Feigenson, M.D., 1997, Cross-arc geochemical variations in volcanic fields in Honduras C.A.—Progressive changes in source with distance from the volcanic front: Contributions to Mineralogy and Petrology, v. 129, p. 341-351.

Peacock, S.M., 1991, Numerical simulation of subduction zone pressure-temperature-time paths: Constraints on fluid production and arc magmatism: Philosophical Transactions Royal Society of London, v. A335, p. 341-353.

Peacock, S.M., 1993, Large-scale hydration of the lithosphere above subducting slabs: Chemical Geology, v. 108, p. 49-59.

Peacock, S.M., 1996, Thermal and petrologic structure of subduction zones, *in* Bebout, G.E., and others, eds., Subduction: Top to Bottom: American Geophysical Union, Geophysical Monograph 96, p. 119-133.

Peacock, S.M., 2001, Are the lower plates of double seismic zones caused by serpentine dehydration in subducting oceanic mantle? Geology, v. 29, p. 299-302.

Peacock, S.M., 2003, Thermal structure and metamorphic evolution of subducting slabs, *in* Eiler, J., ed., Inside the Subduction Factory: American Geophysical Union, Geophysical Monograph 138, p. 7-22.

Pearce, J.A., and Parkinson, I.J., 1993, Trace element models for mantle melting: Application to volcanic arc petrogenesis, p. 373-403 *in* H.M.Prichard, T. Alabaster, N.B.W. Harris, and C.R. Neary, eds., Magmatic Processes and Plate Tectonics: Geological Society Special Publication No. 76.

Pearce, J.A., and Peate, D.W., 1995, Tectonic implications of the composition of volcanic arc magmas: Annual Reviews of Earth and Planetary Sciences, v. 23, p. 251-285.

Peslier, A.H., Luhr, J.F., and Post, J., 2002, Low water contents in pyroxenes from spinel-peridotites of the oxidized, sub-arc mantle wedge: Earth and Planetary Science Letters, v. 201, p. 69-86.

Pezzopane, S.K., and Weldon, R.J., 1993, Tectonic role of active faulting in central Oregon: Tectonics, v. 12, p. 1140-1169.

Phillips, W.M., 1987, Geologic map of the Vancouver quadrangle, Washington and Oregon: Washington Division of Geology and Earth Resources Open File Report 87-10; scale 1;100,000; pamphlet 32 p.

Philpotts, A.R., and Asher, P.M., 1993, Wallrock melting and reaction effects along the Higganum Diabase Dike in Connecticut—Contamination of a continental flood basalt feeder: Journal of Petrology, v. 34, p. 1029-1058.

Pillans, B., 2004, Proposal to redefine the Quaternary: Episodes, v. 27, p. 127.

Plank, T., and Langmuir, C.H., 1998, The chemical composition of subducting sediment and its consequences for the crust and mantle: Chemical Geology, v. 145, p. 325-394.

Porter, S.C., 1978, Glacier Peak tephra in the North Cascade Range, Washington: Stratigraphy, distribution, and relationship to late-glacial events: Quaternary Research, v. 10, p. 30-41.

Rasmussen, J., and Humphreys, E., 1988, Tomographic image of the Juan de Fuca plate beneath Washington and western Oregon using teleseismic P-wave travel times: Geophysical Research Letters, v. 15, p. 1417-1420.

Read, P.B., 1978, Geology, Meager Creek geothermal area, British Columbia: Geological Survey of Canada Open File 603; scale 1:20,000.

Read, P.B., 1990, Mount Meager complex, Garibaldi belt, southwestern British Columbia: Geoscience Canada, v. 17, no. 3, p. 167-170.

Reid, M.R., Coath, C.D., Harrison, T.M., and McKeegan, K.D., 1997, Prolonged residence times for the youngest rhyolites associated with Long Valley caldera— ^{230}Th-^{238}U ion microprobe dating of young zircon: Earth and Planetary Science Letters, v. 150, p. 27-39.

Reidel, S.P., Fecht, K.R., Hagood, M.C., and Tolan, T.L., 1989, The geologic evolution of the central Columbia Plateau: Geological Society of America Special Paper 239, p. 247-264.

Reiners, P.W., Hammond, P.E., McKenna, J.M., and Duncan, R.A., 2000, Young basalts of the central Washington Cascades, flux melting of the mantle, and trace element signatures of primary arc magmas: Contributions to Mineralogy and Petrology, v. 138, p. 249-264.

Richmond, G.M., and Fullerton, D.S., 1985, Introduction to Quaternary glaciations in the United States of America: Quaternary Science Reviews, v. 5, p. 3-10.

Riddihough, R., 1984, Recent movements of the Juan de Fuca plate system: Journal of Geophysical Research, v. 89, p. 6980-6994.

Riddihough, R., Finn, C., and Couch, R., 1986, Klamath-Blue Mountain lineament, Oregon: Geology, v. 14, p. 528-531.

Rieck, H.J., Sarna-Wojcicki, A.M., Meyer, C.E., and Adam, D.P., 1992, Magnetostratigraphy and tephrochronology of an upper Pliocene to Holocene record in lake sediments at Tulelake, northern California: Geological Society of America Bulletin, v. 104, p. 409-428.

Roddick, J.C., and Souther, J.G., 1987, Geochronology of Neogene volcanic rocks in the northern Garibaldi Belt, British Columbia: Geological Survey of Canada, Paper 87-2, p. 21-24.

Ruiz, J., Chesley, J.T., and Hildreth, W., 2000, The Os isotopic record of Andean MASH zone magmas: Eos, Transactions American Geophysical Union, v. 81, p. 1268-1269.

Rusk, C.E., 1924, Tales of a Western Mountaineer: Boston, Houghton Mifflin Company, 309 p.

Rutherford, M., Sigurdsson, H., Carey, S., and Davis, A., 1985, The May 18, 1980 eruption of Mount St. Helens 1. Melt composition and experimental phase equilibria: Journal of Geophysical Research, v. 90, p. 2929-2947.

Ryan, J.G., Morris, J., Tera, F., Leeman, W.P., and Tsvetkov, A., 1995, Cross-arc geochemical variations in the Kurile arc as a function of slab depth: Science, v. 270, p. 625-627.

Sarna-Wojcicki, A.M., Meyer, C.E., Bowman, H.R., Hall, N.T., Russell, P.C., Woodward, M.J., and Slate, J.L., 1985, Correlation of the Rockland ash bed, a 400,000-year old stratigraphic marker in northern California and western Nevada, and implications for middle Pleistocene paleogeography of central California: Quaternary Research, v. 23, p. 236-257.

Sarna-Wojcicki, A.M., Meyer, C.E., Adam, D.P., and Sims, J.D., 1988, Correlations and age estimates of ash beds in late Quaternary sediments of Clear Lake, California: Geological Society of America Special Paper 214, p. 141-150.

Sarna-Wojcicki, A.M., Morrison, S.D., Meyer, C.E., and Hillhouse, J.W., 1987, Correlation of upper Cenozoic tephra layers between sediments of the western United States and eastern Pacific Ocean and comparison with biostratigraphic and magnetostratigraphic age data: Geological Society of America Bulletin, v. 98, p. 207-223.

Sarna-Wojcicki, A.M., Meyer, C.E., Nakata, J.K., Scott, W.E., Hill, B.E., Slate, J.L., and Russell, P.C., 1989, Age and correlation of mid-Quaternary ash beds and tuffs in the vicinity of Bend, Oregon: U.S. Geological Survey Open-File Report 89-645, p. 55-66.

Sarna-Wojcicki, A.M., Shipley, S., Waitt, R.B., Dzurisin, D., and Wood, S.H., 1981, Areal distribution, thickness, mass, volume, and grainsize of air-fall ash from the six major eruptions of 1980: U.S. Geological Survey Professional Paper 1250, p. 577-600.

Schick, J.D., 1994, Origin of compositional variability of the lavas at Collier Cone, High Cascades, Oregon: Eugene, University of Oregon, M.S. thesis, 142 p.

Schmidt, M.E., 2005, Deep crustal and mantle inputs to North Sister volcano, Oregon High Cascade Range: Oregon State University, Corvallis, PhD dissertation, 185 p.

Schmidt, M.E., and Grunder, A.L., 2003, The persistence of North Sister basaltic andesite and implications for deep crustal processes in the central Oregon High Cascades: Geological Society of America Abstracts with Programs, v. 35, no. 6, p. 563.

Schmidt, M.W., and Poli, S., 1998, Experimentally based water budgets for dehydrating slabs and consequences for arc magma generation: Earth and Planetary Science Letters, v. 163, p. 361-379.

Scott, K.M., 1988, Origins, behavior, and sedimentology of lahars and lahar-runout flows in the Toutle-Cowlitz River system: U.S. Geological Survey Professional Paper 1447-A, 76 p.

Scott, K.M., 1989, Magnitude and frequency of lahars and lahar-runout flows in the Toutle-Cowlitz River system: U.S. Geological Survey Professional Paper 1447-B, 33 p.

Scott, K.M., Vallance, J.W., and Pringle, P.T., 1995, Sedimentology, behavior, and hazards of debris flows at Mount Rainier, Washington: U.S. Geological Survey Professional Paper 1547, 56 p.

Scott, W.E., 1977, Quaternary glaciation and volcanism, Metolius River area, Oregon: Geological Society of America Bulletin, v. 88, p. 113-124.

Scott, W.E., 1987, Holocene rhyodacite eruptions on the flanks of South Sister volcano, Oregon, *in* J.H. Fink, ed., Geological Society of America Special Paper 212, p. 35-53.

Scott, W.E., 1990, Patterns of volcanism in the Cascade arc during the past 15,000 years: Geoscience Canada, v. 17, p. 179-183.

Scott, W.E., and Gardner, C.A., 1990, Field trip guide to the central Oregon High Cascades, Part 1: Mount Bachelor—South Sister area: Oregon Geology, v. 52, no. 5, p. 99-114.

Scott, W.E., and Gardner, C.A., 1992, Geologic map of the Mount Bachelor volcanic chain and surrounding area, Cascade Range, Oregon: U.S. Geological Survey Map I-1967, scale 1:50,000.

Scott, W.E., Gardner, C.A., and Sarna-Wojcicki, A.M., 1989, Guidebook for field trip to the Mount Bachelor-South Sister-Bend area, central Oregon High Cascades: U.S. Geological Survey Open-File Report 89-645, 66 p.

Scott, W.E., Gardner, C.A., Sherrod, D.R., Tilling, R.I., Lanphere, M.A., and Conrey, R.M., 1997, Geologic history of Mount Hood volcano, Oregon—A field-trip guidebook: U.S. Geological Survey Open-File Report 97-263, 39 p.

Servicio Nacional de Geología y Minería, 1982, Mapa Geológica de Chile, scale 1:1,000,000, six sheets.

Sheppard, R.A., 1967, Geology of the Simcoe Mountains volcanic area, Washington: Washington Division of Mines and Geology, Geologic Map GM-3.

Sherrod, D.R., 1990a, Western Cascades, Oregon, *in* Wood, C.A., and Kienle, J., eds., Volcanoes of North America: Cambridge University Press, p. 169-170.

Sherrod, D.R., 1990b, High Cascades, Oregon, *in* Wood, C.A., and Kienle, J., eds. Volcanoes of North America: Cambridge University Press, p. 175-180, 187-191.

Sherrod, D.R., 1991, Geologic map of a part of the Cascade Range between latitude 43°-44°, central Oregon: U.S. Geological Survey Map I-1891, scale 1:125,000; pamphlet 14 p.

Sherrod, D.R., and Pickthorn, L.B.G., 1992, Geologic map of the west half of the Klamath Falls 1° by 2° quadrangle, south-central Oregon: U.S. Geological Survey Map I-2182, scale 1:250,000.

Sherrod, D.R., and Scott, W.E., 1995, Preliminary geologic map of the Mount Hood 30-by-60-minute quadrangle, northern Cascade Range, Oregon: U.S. Geological Survey Open-File Report 95-219, scale 1:100,000, pamphlet 35 p.

Sherrod, D.R., and Smith, J.G., 1990, Quaternary extrusion rates of the Cascade Range, northwestern United States and southern British Columbia: Journal of Geophysical Research, v. 95, p. 19465-19474.

Sherrod, D.R., and Smith, J.G., 2000, Geologic map of upper Eocene to Holocene volcanic and related rocks of the Cascade Range, Oregon: U.S. Geological Survey Map I-2569, scale 1:500,000; pamphlet 17 p.

Sherrod, D.R., Benham, J.R., and MacLeod, N.S., 1983a, Geology and mineral resource potential map of the Windigo-Thielsen Roadless Area, Douglas and Klamath Counties, Oregon: U.S. Geological Survey Open-File Report no. 83-660, 22 p.

Sherrod, D.R., Moyle, P.R., Rumsey, C.M., and MacLeod, N.S., 1983b, Geology and mineral resource potential map of the Diamond Peak Wilderness, Lane and Klamath Counties, Oregon: U.S. Geological Survey Open-File Report no. 83-661, 20 p.

Sherrod, D.R., Taylor, E.M., Ferns, M.L., Scott, W.E., Conrey, R.M., and Smith, G.A., 2004, Geologic map of the Bend 30- x 60-minute quadrangle, central Oregon: U.S. Geological Survey Map I-2683, scale 1:100,000; pamphlet 48 p.

Sisson, T.W., 1995, An overview of the geology of Mount Rainier's volcanic edifice: Eos, Transactions American Geophysical Union, v. 76, no. 46 (supplement), p. F643.

Sisson, T.W., and Bronto, S., 1998, Evidence for pressure-release melting beneath magmatic arcs from basalt at Galunggung, Indonesia: Nature, v. 391, p. 883-886.

Sisson, T.W., and Grove, T.L., 1993, Temperatures and H_2O contents of low-MgO high-alumina basalts: Contributions to Mineralogy and Petrology, v. 113, p. 167-184.

Sisson, T.W., and Lanphere, M.A., 2000, The geologic history of Mount Rainier volcano, Washington: Washington Geology, v. 28, p. 28.

Sisson, T.W., and Layne, G.D., 1993, H_2O in basalt and basaltic andesite glass inclusions from four subduction-related volcanoes: Earth and Planetary Science Letters, v. 117, p. 619-635.

Sisson, T.W., Ratajeski, K., Hankins, W.B., and Glazner, A.F., 2005, Voluminous granitic magmas from common basaltic sources: Contributions to Mineralogy and Petrology, v. 148, p. 635-661.

Sisson, T.W., and Vallance, J.W., 2005, Late Holocene andesitic eruptions at Mount Rainier: Eos, Transactions American Geophysical Union, v. 86, no. 52, Fall Meeting Supplement, Abstract V53B-1561.

Sisson, T.W., Vallance, J.W., and Pringle, P.T., 2001, Progress made in understanding Mount Rainier's hazards: Eos, v. 82, p. 113-120.

Smith, D.R., 1984, The petrology and geochemistry of High Cascade volcanics in southern Washington: Mount St. Helens volcano and the Indian Heaven volcanic field: Rice University, Houston, PhD dissertation, 409 p.

Smith, D.R., and Leeman, W.P. 1987, Petrogenesis of Mount St. Helens dacitic magmas: Journal of Geophysical Research, v. 92, p. 10313-10334.

Smith, D.R., and Leeman, W.P., 1993, The origin of Mount St. Helens andesites: Journal of Volcanology and Geothermal Research, v. 55, p. 271-303.

Smith, G.A., Snee, L.W., and Taylor, E.M., 1987, Stratigraphic, sedimentologic, and petrologic record of late Miocene subsidence of the central Oregon High Cascades: Geology, v. 15, p. 389-392.

Smith, G.A., and Taylor, E.M., 1983, The central Oregon High Cascade graben—What? Where? When?: Geothermal Resources Council Transactions, v. 7, p. 275-279.

Smith, J.G., 1983, Geologic map of the Sky Lakes Roadless Area and Mountain Lakes Wilderness, Jackson and Klamath Counties, Oregon: U.S. Geological Survey Map MF-1507-A, scale 1:62,500.

Smith, J.G., 1988, Geologic map of the Pelican Butte quadrangle, Klamath County, Oregon: U.S. Geological Survey Map GQ-1653, scale 1:62,500.

Smith, J.G., 1993, Geologic map of upper Eocene to Holocene volcanic and related rocks in the Cascade Range, Washington: U.S. Geological Survey Map I-2005, scale 1:500,000, pamphlet 19 p.

Smith, J.G., and Donnelly-Nolan, J.M., 2005, Quantitative analysis of 0-2 Ma volcanic vent distribution in space, time, and composition centered on Medicine Lake volcano, northern California, USA: Eos, Transactions American Geophysical Union, v. 86, no. 52, Fall Meeting Supplement, Abstract V53B-1563.

Smith, J.G., Page, N.J., Johnson, M.G., Moring, B.C. and Gray, F., 1982, Preliminary geologic map of the Medford 1ºx2º quadrangle, Oregon and California: U.S. Geological Survey Open-File Report 82-955; scale 1:250,000.

Souther, J.G., 1980, Geothermal reconnaissance in the central Garibaldi belt, British Columbia: Current Research, Part A, Geological Survey of Canada, Paper 80-1A, p. 1-11.

Souther, J.G., 1990, Bridge River Cones, Canada, p. 139-141 *in* C.A. Wood and J. Kienle, eds., Volcanoes of North America: Cambridge University Press, 354 p.

Souther, J.G., and Dellechaie, F., 1984, Geothermal exploration at Mt. Cayley—A Quaternary volcano in southwestern British Columbia: Geothermal Resources Council, Transactions, v. 8, p. 463-468.

Souther, J.G., and Yorath, C.J., 1991, Neogene Assemblages, ch. 10 *in* H. Gabrielse and C.J. Yorath, eds., Geology of the Cordilleran Orogen in Canada: Geological Society of America, The Geology of North America, v. G-2, p. 375-401.

Sparks, R.S.J., Moore, J.G., and Rice, C.J., 1986, The initial giant umbrella cloud of the May 18, 1980, explosive eruption of Mount St, Helens: Journal of Volcanology and Geothermal Research, v. 28, p. 257-274.

Spence, W., 1989, Stress origins and earthquake potentials in Cascadia: Journal of Geophysical Research, v. 94, p. 3076-3088.

Stasiuk, M.V., and Russell, J.K., 1989, Petrography and chemistry of the Meager Mountain volcanic complex, southwestern British Columbia: Geological Survey of Canada, Paper 89-1E, p. 189-196.

Stasiuk, M.V., and Russell, J.K., 1990, The Bridge River Assemblage in the Meager Mountain volcanic complex, southwestern British Columbia: Geological Survey of Canada, Paper 90-1E, p. 227-233.

Stasiuk, M.V., Russell, J.K., and Hickson, C.J., 1996, Distribution, nature, and origins of the 2400 BP eruption products of Mount Meager, British Columbia: Linkages between magma chemistry and eruption behavior: Geological Survey of Canada Bulletin 486, 27 p.

Stern, R.J., Jackson, M.C., Fryer, P., and Ito, E., 1993, O, Sr, Nd and Pb isotopic composition of the Kasuga cross-chain in the Mariana arc—A new perspective on the K-h relationship: Earth and Planetary Science Letters, v. 119, p. 459-475.

Stockstill, K.R., Vogel, T.A., and Sisson, T.W., 2002, Origin and emplacement of the andesite of Burroughs Mountain, a zoned large-volume lava flow at Mount Rainier, Washington, USA: Journal of Volcanology and Geothermal Research, v. 119, p. 275-296.

Stolper, E., and Newman, S., 1994, The role of water in the petrogenesis of Mariana trough magmas: Earth and Planetary Science Letters, v. 121, p. 293-325.

Streck, M.J., Leeman, W.P., and Chesley, J., 2007, High-magnesian andesite from Mount Shasta—A product of magma mixing and contamination, not a primitive mantle melt: Geology, v. 35, p. 351-354.

Sugimura, 1960, Zonal arrangement of some geophysical and petrological features in Japan and its environs: Journal of the Faculty of Science, University of Tokyo, sec.2, v. 12, p. 133-153.

Swanson, D.A., 1978, Geologic map of the Tieton River area, Yakima County, Washington: U.S. Geological Survey Map MF-968, scale 1:62,500.

Swanson, D.A., 1989, Geologic maps of the French Butte and Greenhorn Buttes quadrangles, Washington: U.S. Geological Survey Open-File Report 89-309, 25 p., scale 1:24,000.

Swanson, D.A., 1990, Goat Rocks, Washington, *in* C.A. Wood and J. Kienle, eds., Volcanoes of North America: Cambridge University Press, p. 160-161.

Swanson, D.A., 1994, Geologic map of the East Canyon Ridge quadrangle, southern Cascade Range, Washington: U.S. Geological Survey Open-File Report 94-591, 31 p.

Swanson, D.A., 1996, Basaltic vents under and alongside a glacier in the Cispus valley, southern Washington Cascades: Geological Society of America Abstracts with Programs, v. 28, no. 5, p. 115.

Swanson, D.A., and Clayton, G.A., 1983, Generalized geologic map of the Goat Rocks Wilderness and Roadless Areas (6036, Parts A, C, and D), Lewis and Yakima Counties, Washington: U.S. Geological Survey Open-File Report 83-357, 9 p., scale 1:48,000.

Swanson, D.A., Cameron, K.A., Evarts, R.C., Pringle, P.T., and Vance, J.A., 1989, Cenozoic volcanism in the Cascade Range and Columbia Plateau, southern Washington and northernmost Oregon, excursion 1A *in* C.E. Chapin and J. Zidek, eds., Field excursions to volcanic terranes in the western United States, Vol. II: Cascades and Intermountain West: New Mexico Bureau of Mines and Mineral Resources, Memoir 47, p. 1-50.

Taber, J.J., and Smith, S.W., 1985, Seismicity and focal mechanisms associated with the subduction of the Juan de Fuca plate beneath the Olympic Peninsula, Washington: Bulletin of the Seismological Society of America, v. 75, p. 237-249.

Tabor, R.W., and Crowder, D.F., 1969, On batholiths and volcanoes—Intrusion and eruption of Late Cenozoic magmas in the Glacier Peak area, North Cascades, Washington: U.S. Geological Survey Professional Paper 604, 67 p.

Tabor, R.W., Booth, D.B., Vance, J.A., and Ford, A.B., 2002, Geologic map of the Sauk River 30- by 60-minute quadrangle, Washington: U.S. Geological Survey Map I-2592, scale 1:100,000; pamphlet 67 p. [http://pubs.usgs.gov/imap/i2592/].

Tabor, R.W., Frizzell, V.A., Jr., Booth, D.B., Waitt, R.B., 2000, Geologic map of the Snoqualmie Pass 30 x 60 minute quadrangle, Washington: U.S. Geological Survey Map I-2538, scale 1:100,000; pamphlet 57 p. [http://pubs.usgs.gov/imap/i2538/].

Tabor, R.W., Frizzell, V.A., Jr., Booth, D.B., Waitt, R.B., Whetten, J.T., and Zartman, R.E., 1993, Geologic map of the Skykomish River 30- by 60-minute quadrangle, Washington: U.S. Geological Survey Map I-1963, scale 1:100,000; pamphlet 42 p.

Tabor, R.W., Haugerud, R.A., Hildreth, W., and Brown, E.H., 2003, Geologic map of the Mount Baker 30- by 60-minute quadrangle, Washington: U.S. Geological Survey Map I-2660, scale 1:100,000; pamphlet 73 p. [http://pubs.usgs.gov/imap/i2660/].

Takahashi, E., 1986, Genesis of calc-alkali andesite magma in a hydrous mantle-crust boundary—Petrology of lherzolite xenoliths from the Ichinomegata crater, Oga Peninsula, northeast Japan, part II: Journal of Volcanology and Geothermal Research, v. 29, p. 355-395.

Tatsumi, Y., 1982, Origin of high-magnesian andesites in the Setouchi volcanic belt, southwest Japan, II—Melting phase relations at high pressures: Earth and Planetary Science Letters, v. 60, p. 305-317.

Tatsumi, Y., 1986, Formation of the volcanic front in subduction zones: Geophysical Research Letters, v. 13, p. 717-720.

Tatsumi, Y., 1991, Origin of subduction zone magmas based on experimental petrology, ch. 10 *in* L.L. Perchuk and I. Kushiro, eds., Physical Chemistry of Magmas: Berlin, Springer Verlag, Advances in Physical Geochemistry, v. 9, p. 268-301.

Tatsumi, Y., and Eggins, S., 1995, Subduction zone magmatism: Blackwell Science, 211 p.

Tatsumi, Y., Sakuyama, M., Fukuyama, H., and Kushiro, I., 1983, Generation of arc basalt magmas and thermal structure of the mantle wedge in subduction zones: Journal of Geophysical Research, v. 88, p. 5815-5825.

Taylor, E.M., 1965, Recent volcanism between Three Fingered Jack and North Sister, Oregon Cascade Range, Part I—History of volcanic activity: The Ore Bin, v. 27, no. 7, p. 121-147.

Taylor, E.M., 1968, Roadside geology, Santiam and McKenzie Pass Highways, Oregon, *in* H.M. Dole, ed., Andesite Conference Guidebook: Oregon Department of Geology and Mineral Industries Bulletin 62, p. 3-33.

Taylor, E.M., 1978, Field geology of S.W. Broken Top quadrangle, Oregon: Oregon Department of Geology and Mineral Industries Special Paper 2, 50 p.

Taylor, E.M., 1981, Central High Cascade roadside geology: Bend, Sisters, McKenzie Pass, and Santiam Pass, Oregon, *in* D.A. Johnston and J. Donnelly-Nolan, eds., Guides to some volcanic terranes in Washington, Idaho, Oregon, and northern California: U.S. Geological Survey Circular 838, p. 55-83.

Taylor, E.M., 1987, Field geology of the northwest quarter of the Broken Top 15' quadrangle, Deschutes County, Oregon: Oregon Department of Geology and Mineral Industries Special Paper 21, 20 p.

Taylor, E.M., 1990a, Volcanic history and tectonic development of the central High Cascade Range, Oregon: Journal of Geophysical Research, v. 95, p. 19611-19622.

Taylor, E.M., 1990b, Sand Mountain, Oregon, p. 180-181 *in* C.A. Wood and J. Kienle, eds., Volcanoes of North America: Cambridge University Press, 354 p.

Taylor, E.M., and Ferns, M.L., 1994, Geology and mineral resources map of the Tumalo Dam quadrangle, Deschutes County, Oregon: Oregon Department of Geology and Mineral Industries, Geological Map Series GMS-81.

Taylor, E.M., MacLeod, N.S., Sherrod, D.R., and Walker, G.W., 1987, Geologic map of the Three Sisters Wilderness, Deschutes, Lane, and Linn Counties, Oregon: U.S. Geological Survey Map MF-1952, scale 1:63,360.

Tepper, J.H., Nelson, B.K., Bergantz, G.W., and Irving, A.J., 1993, Petrology of the Chilliwack batholith, North Cascades, Washington: Generation of calc-alkaline granitoids by melting of mafic lower crust with variable water fugacity: Contributions to Mineralogy and Petrology, v. 113, p. 333-351.

Tucker, D., Hildreth, W., Ullrich, T., and Friedman, R., 2007, Geology and complex collapse mechanisms of the 3.72 Ma Hannegan caldera, North Cascades, Washington, USA: Geological Society of America Bulletin, v. 119, p. 329-342.

Turrin, B.D., Christiansen, R.L., Clynne, M.A., Champion, D.E., Gerstel, W.J., Muffler, L.J.P., and Trimble, D.A., 1998, Age of Lassen Peak, California, and implications for the ages of late Pleistocene glaciations in the southern Cascade Range: Geological Society of America Bulletin, v. 110, p. 931-945.

Turrin, B.D., Muffler, L.J.P., Clynne, M.A., and Champion, D.E., 2007, Robust 24±6 ka $^{40}Ar/^{39}Ar$ age of a low-potassium tholeiitic basalt in the Lassen Region of NE California: Quaternary Research, v. 68, p. 96-110.

Ulmer, P., 2001, Partial melting in the mantle wedge—the role of H_2O in the genesis of mantle-derived "arc-related" magmas: Physics of the Earth and Planetary Interiors, v. 127, p. 215-232.

Ulmer, P., and Trommsdorff, V., 1995, Serpentine stability to mantle depths and subduction-related magmatism: Science, v. 268, p. 858-861.

Uto, K., Hildreth, W., and Lanphere, M.A., 1991, Geology, geochemistry, and geochronology of the southern half of the Simcoe Mountains volcanic field, Washington: Eos, Transactions American Geophysical Union, v. 72, p. 521.

Vallance, J.W., and Donoghue, S., 2000, Holocene eruptive history of Mount Rainier: Washington Geology, v. 28, p. 29.

Vallance, J.W., and Scott, K.M., 1997, The Osceola Mudflow from Mount Rainier: Sedimentology and hazard implications of a huge clay-rich debris flow: Geological Society of America Bulletin, v. 109, p. 143-163.

Vazquez, J.A., and Reid, M.R., 2002, Time scales of magma storage and differentiation of voluminous high-silica rhyolites at Yellowstone caldera, Wyoming: Contributions to Mineralogy and Petrology, v. 144, p. 274-285.

Venezky, D.Y., and Rutherford, M.J., 1997, Pre-eruption conditions and timing of dacite-andesite magma mixing in the 2.2 ka eruption at Mount Rainier: Journal of Geophysical Research, v. 102, p. 20069-20086.

Verplanck, E.P., and Duncan, R.A., 1987, Temporal variations in plate convergence and eruption rates in the Western Cascades, Oregon: Tectonics, v. 6, p. 197-209.

Waddell, B., and Green, N.L., 1993, Loggers Lake volcanic complex, SW British Columbia, Canada: An example of shallow-level crustal contamination in continental margin calc-alkaline magmas: Eos, Transactions American Geophysical Union, Fall Meeting Supplement, v. 74, no. 43, p. 681.

Wagner, T.P., Donnelly-Nolan, J.M., and Grove, T.L., 1995, Evidence of hydrous differentiation and crystal accumulation in the low-MgO, high-Al_2O_3 Lake Basalt from Medicine Lake volcano, California: Contributions to Mineralogy and Petrology, v. 121, p. 201-216.

Walcott, D., 1993, Neogene tectonics and kinematics of western North America: Tectonics, v. 12, p. 326-333.

Walker, G.P.L., 1973, Lengths of lava flows: Philosophical Transactions of the Royal Society of London, ser. A, v. 274, no. 1238, p. 107-118.

Walker, G.P.L., 1993, Basaltic-volcano systems, *in* H.M. Pritchard, T. Alabaster, N.B.W. Harris, and C.R. Neary, eds., Magmatic Processes and Plate Tectonics: Geological Society Special Publication No. 76, p. 3-38.

Walker, G.W., 1974, Some implications of late Cenozoic volcanism to geothermal potential in the High Lava Plains of south-central Oregon: The Ore Bin, v. 36, no. 7, p. 109-118.

Walker, G.W., and MacLeod, N.S., 1991, Geologic Map of Oregon: U.S. Geological Survey, scale 1:500,000, 2 sheets.

Walsh, T.J., Korosec, M.A., Phillips, W.M., Logan, R.L., and Schasse, H.W., 1987, Geologic Map of Washington—southwest quadrant: Washington Division of Geology and Earth resources, Geologic Map GM-34; scale 1:250,000.

Walter, S.R., 1986, Intermediate-focus earthquakes associated with Gorda plate subduction in northern California: Bulletin of the Seismological Society of America, v. 76, p. 583-588.

Waters, A.C., Donnelly-Nolan, J.M., and Rogers, B.W., 1990, Selected caves and lava-tube systems in and near Lava Beds National Monument: U.S. Geological Survey Bulletin 1673, 102 p.

Watters, T.R., 1989, Periodically spaced anticlines of the Columbia Plateau: Geological Society of America Special Paper 239, p. 283-292.

Weaver, C.S., and Baker, G.E., 1988, Geometry of the Juan de Fuca plate beneath Washington and northern Oregon from seismicity: Bulletin of the Seismological Society of America, v. 78, p. 264-275.

Weaver, C.S., Grant, W.C., and Shemeta, J.E., 1987, Local crustal extension at Mount St. Helens, Washington: Journal of Geophysical Research, v. 92, p. 10170-10178.

Webster, J.R., 1992, Petrology of Quaternary volcanics of the Broken Top and Diamond Peak areas, central and south-central Oregon High Cascades: Evidence for varied magmatic processes from two contrasting volcanic centers: Indiana University, Bloomington, Ph.D. dissertation, 412 p.

Wells, R.E., 1990, Paleomagnetic rotations and the Cenozoic tectonics of the Cascade arc, Washington, Oregon, and California: Journal of Geophysical Research, v. 95, p. 19409-19417.

Wells, R.E., and Heller, P.L., 1988, The relative contribution of accretion, shear, and extension to Cenozoic tectonic rotation in the Pacific Northwest: Geological Society of America Bulletin, v. 100, p. 325-338.

Wells, R.E., Weaver, C.S., and Blakely, R.J., 1998, Fore-arc migration in Cascadia and its neotectonic significance: Geology, v. 26, p. 759-762.

West, M.W., Ashland, F.X., Busacca, A.J., Berger, G.W., and Shaffer, M.E., 1996, Late Quaternary deformation, Saddle Mountains anticline, south-central Washington: Geology, v. 24, p. 1123-1126.

Wheeler, J.O., and McFeeley, P, 1991, Tectonic assemblage map of the Canadian Cordillera and adjacent parts of the United States of America: Geological Survey of Canada Map 1712A, scale 1:2,000,000.

White, C.M., 1980, Geology and geochemistry of Mt. Hood volcano: Oregon Department of Geology and Mineral Industries Special Paper 8, 26 p.

White, C.M., 1992, Evolution of calc-alkaline magmas at the early Quaternary Battle Ax volcano, Western Cascade Range, Oregon: Journal of Volcanology and Geothermal Research, v. 52, p. 107-122.

Williams, D.A., Kadel, S.D., Greeley, R., Lesher, C.M., and Clynne, M.A., 2004, Erosion by flowing lava: Geochemical evidence in the Cave Basalt, Mount St. Helens, Washington: Bulletin of Volcanology, v. 66, p. 168-181.

Williams, H., 1929, The volcanic domes of Lassen Peak and vicinity, California: American Journal of Science, v. 18, p. 313-330.

Williams, H., 1932a, Mount Shasta, a Cascade volcano: Journal of Geology, v. 45, p. 417-429.

Williams, H., 1932b, Geology of the Lassen Volcanic National Park, California: University of California Publications, Bulletin of the Department of Geological Sciences, v. 21, no. 8, p. 195-385, map scale 1:48,000.

Williams, H., 1933, Mount Thielsen—a dissected Cascade volcano: University of California Publications, Bulletin of the Department of Geological Sciences, v. 23, p. 195-214.

Williams, H., 1935, Newberry volcano of central Oregon: Geological Society of America Bulletin, v. 46, p. 253-304.

Williams, H., 1942, The Geology of Crater Lake National Park, Oregon: Carnegie Institution of Washington Publication 540, 162 p.

Williams, H., 1944, Volcanoes of the Three Sisters region, Oregon Cascades: University of California Publications, Bulletin of the Department of Geological Sciences, v. 27, no. 3, p. 37-84.

Williams, H., 1949, Geology of the Macdoel Quadrangle: California Division of Mines Bulletin 151, 78 p.; map scale 1:125,000.

Williams, H., 1957, A geologic map of the Bend quadrangle, Oregon, and a reconnaissance geologic map of the central portion of the High Cascade Mountains: Oregon Department of Geology and Mineral Industries, scales 1:125,000 and 1:250,000.

Wilson, D.S., 1988, Tectonic history of the Juan de Fuca ridge over the last 40 million years: Journal of Geophysical Research, v. 93, p. 11863-11876.

Wilson, D.S., 1989, Deformation of the so-called Gorda plate: Journal of Geophysical Research, v. 94, p. 3065-3075.

Wilson, D.S., 2002, The Juan de Fuca plate and slab: Isochron structure and Cenozoic plate motions, *in* Kirby, S., Wang, K., and Dunlop, S., eds., The Cascadia subduction zone and related subduction systems: U.S.Geological Survey Open-File Report 02-328, p. 9-12.

Wise, W.S., 1968, Geology of the Mount Hood volcano, *in* H.M. Dole, ed., Andesite Conference Guidebook: Oregon Department of Geology and Mineral Industries Bulletin 62, p. 81-98.

Wise, W.S., 1969, Geology and petrology of the Mount Hood area: A study of High Cascade volcanism: Geological Society of America Bulletin, v. 80, p. 969-1006.

Wise, W.S., 1970, Cenozoic volcanism in the Cascade Mountains of southern Washington: Washington Division of Mines and Geology Bulletin 60, 45 p.

Wood, C.A., 1980, Morphometric evolution of cinder cones: Journal of Volcanology and Geothermal Research, v. 7, p. 387-413.

Woodhead, J., Eggins, S., and Gamble, J., 1993, High-field-strength and transition element systematics in island-arc and back-arc basin basalts—evidence for multiphase melt extraction and a depleted mantle wedge: Earth and Planetary Science Letters, v. 114, p. 491-504.

Wozniak, K.C., 1982, Geology of the northern part of the southeast Three Sisters quadrangle, Oregon: Oregon State University, Corvallis, M.S. thesis, 98 p.

Yogodzinski, G.M., Smith, G.A., Dill, T.E., Conrey, R.M., and Taylor, E.M., 1983, Deposits of two late Pleistocene eruptions of Mount Jefferson, Oregon: Eos, Transactions American Geophysical Union, v. 64, p. 899.

Young, S.R., 1990, Physical volcanology of Holocene airfall deposits of Mt. Mazama, Crater Lake, Oregon: University of Lancaster, Lancaster, UK, PhD dissertation, 307 p.

Zelt, B.C., Ellis, R.M., and Clowes, R.M., 1996, Inversion of three-dimensional wide-angle seismic data from the southwestern Canadian Cordillera: Journal of Geophysical Research, v. 101, p. 8503-8529.

Zhao, D., Hasegawa, A., and Kanamori, H., 1994, Deep structure of Japan subduction zone as derived from local, regional, and teleseismic events: Journal of Geophysical Research, v. 99, p. 22313-22329.

Zhao, D., Wang, K., Rogers, G.C., and Peacock, S.M., 2001, Tomographic image of low *P*-velocity anomalies above slab in northern Cascadia subduction zone: Earth, Planets, and Space, v. 53, p. 285-293.

Zoback, M.L., 1992, First- and second-order patterns of stress in the lithosphere—The World Stress Map Project: Journal of Geophysical Research, v. 97, p. 11703-11728.

Zoback, M.L., and Zoback, M., 1980, State of stress in the conterminous United States: Journal of Geophysical Research, v. 85, p. 6113-6156.

This page intentionally left blank

USGS

Hildreth—**Quaternary Magmatism in the Cascades—Geologic Perspectives**—U.S. Geological Survey Professional Paper 1744

ISBN 1-4113-1945-1

9 781411 319455